

**Effects of broad-bandwidth LED light spectra on the development and
quality of medicinal and aromatic plants including
thyme (*Thymus vulgaris* L.), peppermint (*Mentha x piperita* L.) and
basil (*Ocimum basilicum* L.)**

Inaugural-Dissertation to obtain the academic degree
Doctor rerum naturalium (Dr. rer. nat.)

Submitted to the Department of Biology, Chemistry, Pharmacy
of Freie Universität Berlin

by

JENNY MANUELA TABBERT

Berlin, May 2023

This dissertation was conducted at the Julius Kühn-Institute, Institute for Ecological Chemistry, Plant Analysis and Stored Product Protection in Berlin between March 2018 and April 2023 under the supervision of Prof. Dr. Hartwig Schulz.

1st Reviewer: Prof. Dr. Hartwig Schulz

2nd Reviewer: Prof. Dr. Matthias F. Melzig

Date of defense: 07/14/2023

As a reminder that dreams can come true after all

Acknowledgment

First and foremost, I sincerely thank Prof. Dr. Hartwig Schulz and Dr. Andrea Krähmer for their persistent support throughout the preparation of this dissertation. I am forever grateful for your guidance, support and encouragement. I also thank Prof. Dr. Matthias Melzig for formally endorsing this work and for his words of wisdom when they were needed the most.

I further extend my deepest appreciation to the members of the Julius Kühn-Institute without whom the realization of this exciting research project would not have been possible. Your commitment and willingness to approach the many and diverse tasks this ambitious research project entailed will not ever be forgotten: I genuinely thank Roland Buchhorn, Claudia Könecke, Heike Bäumer and Sabrina Pilz for their exceptional cultivation assistance; Maik Repnack and his team for their outstanding technical support; René Grünwald, Michael Glitschka, Astrid Hansen, Dr. Dieter Felgentreu, Raphael Büchner and Silvia Baas for their knowledgeable analytical assistance; Silvio Arganese, Viktoria Kappes and Leonard Golz for their never-ending provision of literature; Dominique Conrad, Mario Harke as well as Marcus Müller and Konradin Feierabend from the Humboldt University of Berlin for their assistance during the many time-consuming data collections; Gabriele Fischer and Paul Ebert for their IT support as well as Annika Fritsche, Catharina Blank, Vera Frimel and Liane Rabe for their administrative assistance.

Honest gratitude also goes to Dr. Torsten Meiners, Dr. Christoph Böttcher and Dr. David Riewe for their critical reviews and important feedback.

I would also like to thank our project partners at FUTURELED and Humboldt University as well as the members of the family-owned business Oderbruch Müller and Christine Wandke, owner of Kräuterlounge for pursuing this interdisciplinary endeavor. It was a pleasure to work with you.

I further express my sincere gratitude to Dr. Nadine Austel, Dr. Nanina Tron, Dr. Gabriela Bischoff, Dr. Nadine Herwig, Dominic Lamprecht, Dr. Marlen Heinz, Verena Ristau, Yvonne Ratzlaff and Sophie Bliedung for your genuine kindness, your positivity and emotional support throughout this endeavor.

Last but not least, I express my deepest gratitude to my husband James Alfred Tabbert III. Without your empathy and unwavering encouragement throughout these challenging years, this dissertation would have never been completed.

Affidavit

I hereby declare that I have written this dissertation independently and that I have not employed any other sources and tools than those sited in this work.

Table of content

Abbreviations	1
Short version of the results	3
Kurzfassung der Ergebnisse	5

Chapter 1

1. General Introduction	7
1.1 Significance of urban controlled-environment agriculture	7
1.1.1 Conventional agriculture under pressure	7
1.1.2 Benefits of urban controlled-environment agriculture	7
1.1.3 Challenges of urban controlled-environment agriculture	9
1.2 LEDs and conventional lighting in horticulture	10
1.3 The significance of light	13
1.3.1 The role of plant pigments for photosynthesis	13
1.3.1.1 The photosystems	14
1.3.1.2 The light reaction during photosynthesis	14
1.3.1.3 Spectral light absorption of photosynthetic plant pigments	15
1.3.1.4 Photosynthetically active radiation (PAR)	16
1.3.2 Photoreceptors	18
1.3.2.1 Spectral light absorption of photoreceptors	19
1.3.2.2 Plant responses mediated by photoreceptors	20
1.3.2.2.1 Phytochromes	20
1.3.2.2.2 Cryptochromes	23
1.3.2.2.3 Phototropins	25
1.3.2.2.4 UV resistance locus 8 (UVR8)	27
1.3.2.2.5 Putative green light-sensing photoreceptor	29
1.4 Impact of narrow-bandwidth LED lighting on plant development	30
1.4.1 From red to red/blue LED lighting strategies	30
1.4.2 Influence of ultraviolet, green and far-red wavelengths on plant development	35
1.4.2.1 Plant responses to ultraviolet radiation (λ 280-400 nm)	35
1.4.2.2 Plant responses to green light (λ 500-600 nm)	50
1.4.2.3 Plant responses to far-red light (λ 700-800 nm)	63

1.5 Towards broad-bandwidth LED light spectra to improve plant development	76
1.6 Essential oils under LED lighting	90
2. LED4Plants project	112
2.1 List of published peer-reviewed articles	113

Chapter 2

Increased plant quality, greenhouse productivity and energy efficiency with broad-spectrum LED systems: A case study for thyme (*Thymus vulgaris* L.)

Abstract	114
Keywords	114
1. Introduction	114
2. Materials and methods	117
2.1 Experimental design	117
2.2 Lighting systems and illumination conditions	117
2.3 Irradiance profile measurements	118
2.4 Plant material and growth conditions	120
2.5 Harvest and crop management	120
2.6 Energy measurements	121
2.7 Chemicals	121
2.8 Extraction of volatile organic compounds	121
2.9 GC-FID and GC-MS analysis	122
2.10 Identification and quantification of volatile organic compounds	122
2.11 Statistical analysis and calculations	122
3. Results and discussion	123
3.1 Biomass yield, partitioning, and morphology	123
3.2 Content and composition of volatile organic compounds (VOCs)	125
3.3 Productivity	130
3.4 Power consumption and biomass efficacy	131
4. Conclusion	132

Chapter 3

Investigation of LED light qualities for peppermint (*Mentha x piperita* L.) cultivation focusing on plant quality and consumer safety aspects

Abstract	134
Keywords	134
1. Introduction	134
2. Materials and methods	136
2.1 Experimental design	136
2.2 Plant material and growth conditions	136
2.3 Cultivation system	138
2.4 Lighting systems and illumination conditions	139
2.5 Irradiance measurements	139
2.6 Crop measurements and harvest	141
2.7 Essential oil isolation	141
2.8 GC-FID and GC-MS analysis	142
2.9 Identification and quantification of essential oil compounds	142
2.10 Statistical analysis	142
3. Results	143
3.1 Plant height	143
3.2 Branch length	144
3.3 Number of leaf pairs	144
3.4 Length and width of leaves	144
3.5 Biomass yields	145
3.6 Composition, content and yield of essential oil	146
4. Discussion	149
4.1 Plant height	150
4.2 Leaf growth and expansion	150
4.3 Biomass accumulation	151
4.4 Essential oil	152
5. Conclusion	154

Chapter 4

Facing energy limitations – approaches to increase basil (*Ocimum basilicum* L.) growth and quality by different increasing light intensities emitted by a broadband LED light spectrum (400-780 nm)

Abstract	155
Keywords	155
1. Introduction	156
2. Materials and methods	158
2.1 Experimental design	158
2.2 Plant material and growth conditions	158
2.3 Lighting systems and illumination conditions	159
2.4 Energy measurements	161
2.5 Extraction of volatiles	161
2.6 GC-FID and GC-MS analysis	162
2.7 Identification and quantification of volatile compounds	162
2.8 Statistics and calculations	163
3. Results and discussion	164
3.1 Cultivar-dependent morphological differences	164
3.2 Enhances basil development under I_{High} results in earlier marketability than under I_{Low}	169
3.3 I_{High} induced light avoidance responses in green basil cultivars while purple basil remained 'light-tolerant'	169
3.4 I_{Low} resulted in beneficial acclimation responses in green basil cultivars while purple basil performed insufficiently	171
3.5 Cultivar-dependent light intensity requirements under increasing light intensity conditions	172
3.6 Cultivar-specific VOC concentrations change over time	174
3.7 In contrast to purple basil, green basil cultivars use energy more efficiently under I_{Low}	184
3.8 Improvement of basil production via eustress management	185
4. Conclusion	186

Chapter 5

1. General Discussion	188
1.1 Effectiveness of the developed broadband LED lighting systems and some technological challenges to overcome.	188
1.2 Are the developed broadband LED light spectra photosynthetically efficient?	192
1.3 Broadband LED light spectra expand morphological plant trait manipulations.	195
1.4 Multidisciplinary research efforts are required to advance essential oil regulations under LED-based CEAs.	196
References	202
Appendix	248
List of figures and tables	248
Figures	248
Tables	248

Abbreviations

AOC	Antioxidant capacity
ASRM	Artificial sunlight research module
ATP	Adenosine triphosphate
B	Blue
CA	Caffeic acid
CEA	Controlled environment agriculture
Chl	Chlorophyll
CHP	Combined heat and power
CO ₂	Carbon dioxide
cv.	Cultivar
EO	Essential oil
EUE	Energy use efficiency
FL	Fluorescent lamp
FR	Far-red
FW	Fresh weight
G	Green
GH	Greenhouse
H ₂ O	Dihydrogen oxide (<i>Water</i>)
HID	High intensity discharge
HPS	High-pressure sodium
λ (<i>Lambda</i>)	Wavelength (<i>expressed in nanometers; nm</i>)
LED	Light-emitting diode
MAP	Medicinal aromatic plant
MEP	Methyl-erythritol-phosphate pathway
MH	Metal halide
NADPH	Nicotinamide adenine nucleotide phosphate
O ₂	Dioxygen (<i>Oxygen</i>)
PAR	Photosynthetically active radiation (400-700 nm)
PBAR	Photobiologically active radiation (280-800 nm)
PPE	Photosynthetic photon efficacy

PPFD	Photosynthetic photon flux density (<i>expressed in micromole per square meter and second; $\mu\text{mol m}^{-2} \text{s}^{-1}$</i>)
R	Red
ROS	Reactive oxygen species
SD	Standard deviation
SDG	Sustainable development goals
TAC	Total anthocyanin content
TFC	Total flavonoid content
TPC	Total phenolic content
UN	United Nations
UV	Ultraviolet
UVR8	Ultraviolet resistance locus

Short version of the results

Within the framework of the regional and interdisciplinary research project *LED4Plants*, broadband lighting systems via light-emitting diodes (LED) were developed, which cover the plant-receptive waveband region between ultraviolet and far-red radiation (360-780 nm). To investigate the practical feasibility of these LED-broadband spectra for horticultural productions, three different herbs from the Lamiaceae family were cultivated under practice-relevant cultivation conditions.

During the naturally low irradiated fall and winter months of Berlin, Germany, *Thymus vulgaris* L. was cultivated under semi-controlled greenhouse conditions. In direct comparison to the traditionally applied high pressure sodium lamps and fluorescent lights, the broadband LED lighting enabled an accelerated development of *Thymus vulgaris* L., which resulted in distinct yield increases. In addition, prolonged internodes and greater leaf surfaces became apparent under the broadband LED light spectrum. While the chemical compositions of the aroma compounds were similar, the contents of these volatile organic compounds (VOC) were significantly elevated by the high pressure sodium lamps and especially by the LED-systems in comparison to the fluorescent lights in thyme. In contrast to the conventional lighting systems, the broadband LED system enabled a feasible extension of greenhouse productions and allows the cultivation of a greater variety of crops with greater light requirements due to its superior photon output and greater energy efficiency.

In an automated vertical cultivation system, *Mentha x piperita* L. was exposed to a broadband LED light spectrum and two narrow LED light spectra (RB = Red/Blue, RGB = Red/Green/Blue) under initially identical light intensity conditions and under the exclusion of natural sunlight. While RB resulted in a compact growth, both green-containing light conditions induced excessive stem and side branch elongations and significant leaf expansions known as shade avoidance responses. Although peppermint plants achieved marketable appearances under all light conditions, their essential oil compositions did not meet consumer safety requirements due to high concentrations of pulegone and menthofuran. All results are discussed as a result of the specific lighting conditions and the time of harvest.

Under the exclusion of natural light, four *Ocimum basilicum* L. cultivars were illuminated with a broadband LED light spectrum with elevated blue and red light fractions and exposed to two different rising light intensities (I_{Low} and I_{High}). Cultivar-dependent differences in plant height, leaf and branch pair developments were observed over time. In comparison to the I_{Low} light conditions, I_{High} resulted in accelerated developments and greater biomass yields of all basil cultivars and expedited their marketability by 3-5 days. However, exposure to light intensities above approximately $300 \mu\text{mol m}^{-2} \text{s}^{-1}$ induced light avoidance responses in the green-leafed basil cultivars. In contrast, I_{Low} resulted in consumer-

preferred visual qualities and greater biomass efficiencies of the green-leafed basil cultivars and are discussed as a result of their ability to adapt well to low light conditions. In contrast, the purple-leafed cultivar developed insufficiently under I_{Low} , but remained light-tolerant under I_{High} , which was attributed to its high anthocyanin contents. Regardless of the light treatment applied, cultivar-specific VOC compositions changed tremendously in a developmental stage-dependent manner.

Kurzfassung der Ergebnisse

Im Rahmen des regionalen und interdisziplinären Forschungsprojekts *LED4Plants* wurden Breitbandbeleuchtungssysteme mittels Leuchtdioden (LED) entwickelt, welche den für Pflanzen wahrnehmbaren Wellenlängenbereich zwischen ultravioletter und dunkelroter Strahlung (360 bis 780 nm) abdecken. Um die Praxistauglichkeit dieser LED-Breitbandspektren für gartenbauliche Produktionen zu untersuchen, wurden drei verschiedene Kräuter aus der Familie der Lamiaceae unter praxisrelevanten Anbaubedingungen kultiviert.

Während der durch geringe natürliche Sonnenstrahlung geprägten Herbst- und Wintermonate wurde *Thymus vulgaris* L. unter semi-kontrollierten Gewächshausbedingungen in Berlin (Deutschland) kultiviert. Im direkten Vergleich zu den herkömmlichen Natriumdampfdrucklampen und Leuchtstoffröhren ermöglichte das entwickelte LED-System eine beschleunigte Entwicklung von *Thymus vulgaris* L., die sich in deutlichen Ertragssteigerungen bemerkbar machte. Zusätzlich wurden verlängerte Internodien und größere Blattflächen unter den LED-Beleuchtungssystemen beobachtet. Während sich die chemischen Profile der Aromakomponenten ähnelten, wurden die Gehalte dieser flüchtigen organischen Verbindungen (VOC) durch die Natriumdampfdrucklampen und besonders durch die LED-Systeme im Vergleich zu den Leuchtstoffröhren bei Thymian stark erhöht. Im Gegensatz zu den konventionellen Beleuchtungssystemen ermöglichte das LED-Breitbandbeleuchtungssystem aufgrund der erhöhten Photonenabgabe und der besseren Energieeffizienz eine wirtschaftliche Verlängerung der Gewächshausproduktion und erlaubt den Anbau einer größeren Vielfalt an Kulturpflanzen mit erhöhtem Lichtbedarf.

In einem automatisierten vertikalen Anbausystem wurde *Mentha x piperita* L. mit einem LED-Breitbandspektrum sowie mit zwei schmalbandigen Spektren (RB = Rot/Blau, RGB = Rot/Grün/Blau) unter anfänglich gleichen Lichtintensitätsbedingungen und unter Ausschluss des natürlichen Sonnenlichts beleuchtet. Während RB in einem kompakten Wachstum resultierte, induzierten die beiden grünhaltigen Lichtkonditionen exzessive Stängel- und Seitentriebverlängerungen sowie signifikante Blattexpansionen. Obwohl die Pfefferminzpflanzen unter allen Lichtbedingungen ein vermarktungsfähiges Erscheinungsbild erreichten, erfüllten die ätherischen Ölkonzentrationen aufgrund ihrer hohen Pulegon- und Menthofurankonzentrationen nicht die Verbraucherschutzanforderungen. Alle Ergebnisse werden vor dem Hintergrund der spezifischen Lichtkonditionen und des Erntezeitpunkts diskutiert.

Auch unter Ausschluss des natürlichen Sonnenlichts, wurden vier Basilikumkultivare mit einem LED-Breitbandspektrum mit erhöhten Blau- und Rotanteilen beleuchtet und dabei zwei unterschiedlich steigenden Lichtintensitäten ausgesetzt (I_{Low} und I_{High}). Kultivarabhängige Unterschiede in Pflanzenhöhe,

Blattpaar- und Seitentriebentwicklungen wurden über die Zeit beobachtet. Im Vergleich zu I_{Low} resultierte I_{High} in höheren Biomasseerträgen und beschleunigte deren Marktreife um 3-5 Tage. Lichtintensitäten oberhalb von etwa $300 \mu\text{mol m}^{-2} \text{s}^{-1}$ induzierten jedoch Lichtvermeidungsstrategien in den grünblättrigen Basilikumkultivaren unter I_{High} . Dagegen resultierte I_{Low} in einer von Konsumenten bevorzugten visuellen Qualität und höheren Biomasseeffizienzen der grünblättrigen Kultivare, welche als Resultat ihrer Anpassungsfähigkeit an geringe Lichtbedingungen diskutiert wird. Im Gegensatz zu den grünblättrigen Kultivaren, entwickelte sich der violettblättrige Kultivar unzureichend unter I_{Low} , erwies sich aber unter I_{High} als licht-tolerant, was auf dessen hohe Anthozyangehalte zurückzuführen ist. Unabhängig von den Lichtbedingungen veränderten sich die kultivar-spezifischen VOC-Kompositionen entwicklungsabhängig.

1. General Introduction

Growth and development of plants do not only rely on light but are also influenced by light. While plant pigments harvest the lights' energy to drive the essential light reactions of photosynthesis, photoreceptors play crucial roles in the morphogenesis of plants. Thereby, the light's quality, intensity and duration cause a plethora of anatomical, physiological, and biochemical responses in plants. Due to the adjustability of its spectral light composition, the light-emitting diode (LED) technology enables a fine-tuning of plant photosynthesis and plant physiology to improve yields and plant traits of interest. Consequently, LEDs are starting to transform controlled-environment agriculture, which is projected to play a significant role in future food production systems. Though a great amount of research has been conducted within the last 20 years to study the effects of various LED light qualities and intensities, far more exploration is necessary in order to find suitable lighting strategies for a range of crop types.

1.1 Significance of urban controlled-environment agriculture

1.1.1 Conventional agriculture under pressure

Though our agricultural sector is currently still producing enough food to feed the worlds' population - and it is only due to our inability to distribute the produced food effectively that over 800 million people are faced with hunger (Boliki, 2019) - the future availability of arable land (Zhang & Cai, 2011) and of agricultural resources such as phosphate and potassium (Heffer & Prud'homme, 2013) are under tremendous pressure. Not only the effects of climate change, including the expansion of drylands, the diminishing fresh water supplies and extreme weather conditions such as heat, droughts and floods (Zhang & Cai, 2011), but also soil depletions and degradations due to over-farming and poor production practices (Gomiero, 2016), as well as the increasing world population (Fedoroff, 2015; Döös, 2002) - which is projected to reach 9.7 billion by 2050 (USCB, 2021) - continue to reduce the amount of fertile arable land per person.

1.1.2 Benefits of urban controlled-environment agriculture

A viable approach to tackle these global megatrends that will continue to decrease the arable land stocks per person and threaten the food security for upcoming generations is urban controlled-environment agriculture - in short CEA (Despommier, 2011). CEA is a technology-based approach towards food production, that includes indoor agriculture such as single-level greenhouse productions and multi-level vertical farms.

Though CEA in urban settings is still in its early technological and scientific stages, great advancements in greenhouse technology resulted in a sharp vision for sustainable year-round crop productions. Whether artificial lighting is used as the sole source of lighting in so-called plant factories or is used to supplement the solar radiation that is transmitted through the glass windows of greenhouse enclosures, today's precise controllability of all influential cultivation conditions permits the setup of optimal plant growth environments. The careful management of temperatures, vapor pressure deficits, carbon dioxide (CO₂) concentrations and air movement, along with fine-tuned fertilizations (including total and individual nutrient concentrations and pH levels) as well as tailored light qualities and intensities from LEDs, customized lighting cycles and directions can facilitate high yields of nutritious fruits and vegetables on demand (Kozai, 2019; Benke & Tomkins, 2018).

The constraints of seasonality and the risks of extreme weather conditions resulting in crop failures can be reduced or even eliminated because of the semi-closed or closed nature of these CEA systems. Also, pest- and disease-related risks from pathogens, parasites, heavy metals or pesticides could be eradicated or at least strictly monitored and controlled in these (semi-) closed environment food production systems and would improve food availability and safety (Kozai, 2019; Benke & Tomkins, 2018).

Further, CEAs are highly resource efficient when soilless hydroponic or aeroponic cultivation systems are employed and when water and fertilizer inputs are reused and/or recycled (Kozai, 2019).

A central idea is to multiply the arable land area per footprint of land by either constructing multi-rack mechanized systems within greenhouses or by building a number of cultivation levels in high-rise buildings - food productivity scales up with each tier (Kozai, 2019; Benke & Tomkins, 2018; Despommier, 2011).

CEAs near the consumers (inside of large cities or near regional towns) would significantly reduce food spoilage of fresh produce that occurs during transportation and storage. The reduced food mileage concomitant with urban CEA implementations would substantially reduce fossil fuel consumptions and CO₂ emissions associated with transportation. At the same time, it is argued that the considerable CO₂ emissions related to the energy-demanding CEA can be lowered if renewable energy sources and storage batteries are utilized (Kozai, 2019; Benke & Tomkins, 2018; Despommier, 2011).

Today – a little over ten years after Despommier published the visionary concept of CEAs for the rapidly growing urban populations (Despommier, 2011) - multiple CEAs have been established in various cities around the globe and prove their feasibility (Benke & Tomkins, 2018).

Beyond the mentioned capabilities and opportunities, implementations and extensions of urban CEAs could further aid in reducing environmental pollutions from fertilizer run-offs, help in restoring

ecosystems and support economies due to the many and diverse job opportunities accompanied with the endeavor to construct, maintain and improve CEAs (Kozai, 2019; Benke & Tomkins, 2018; Despommier, 2011).

In short, urban CEA has the tremendous potential to aid substantially in achieving the Sustainable Development Goals (Figure 1) agreed upon by the United Nations member states in the near future (Kozai, 2019).



Figure 1 – Sustainable Development Goals (SDGs). In 2015, over 190 nations around the world committed to 17 SDGs, which are a collective call to action to end poverty, protect the planet and ensure peaceful and prosperous lives for all people (Adopted from UN, 2022).

1.1.3 Challenges of urban controlled-environment agriculture

Nevertheless, several impediments including high production costs, the currently low number of cultivable crop types and the lack of knowledge about optimal crop productions under highly controlled conditions must be overcome. Due to very expensive real estate in urban areas start-up costs are very high. The initial investments to construct high-tech CEAs intensify the required venture capital or government incentives. Once CEAs are “up and running”, labor and electricity consumption substantially affect running costs at present. So far, the food that is grown by modern CEAs is limited to a few high-priced specialty crops such as leafy green vegetables, lettuce, tomatoes, strawberries, bell peppers and cucumbers. Hence, the range

of crop types has to be extended. Low-value staple foods are economically unachievable at the moment, but with a persistently changing climate, scarce arable land and diminishing resources such as water and fertilizer this may change. Extensive research is required to optimize yields and plant responses to all controlled variables such as wavelengths and intensity of LEDs, temperature, humidity and CO₂ levels (Kozai, 2019; Benke & Tomkins, 2018).

1.2 LEDs and conventional lighting in horticulture

For decades, artificial lights including fluorescent lamps (FL) and high-intensity discharge (HID) luminaires (e.g., high-pressure sodium (HPS) and metal halide (MH) lamps) have successfully been used as either supplemental lighting to enhance greenhouse productions (van Ieperen & Trouwborst, 2008; Zheng et al., 2019) or as sole-source lighting to realize first food productions in Japanese plant factories (Goto, 2012). Main reasons for the widespread establishment of FLs and HID luminaires as assimilation light sources were their sufficient delivery of light intensity and their economical affordability (Xu, 2019; Zheng et al., 2019; Nelson & Bugbee, 2014). Currently, HPS luminaires are still the most commonly used light source in greenhouses around the globe (Katzin et al., 2020; Stober et al., 2017; Singh et al., 2015a), however, unique features and rapid technological improvements of LED lighting systems resulted in noticeable transitions from HPS to LED light applications in greenhouse industries (Kusuma et al. 2020) and have widely replaced FLs in vertical farming applications (Zheng et al., 2019; Benke & Tomkins, 2018, Goto, 2012).

For horticultural purposes, one of the most outstanding characteristics of LED lighting systems is their flexibility in spectral output (Massa et al., 2008; Morrow, 2008) (Figure 2). The controllability of spectral composition and light intensity differentiates LEDs from any other assimilation light source on the market (Xu, 2019).

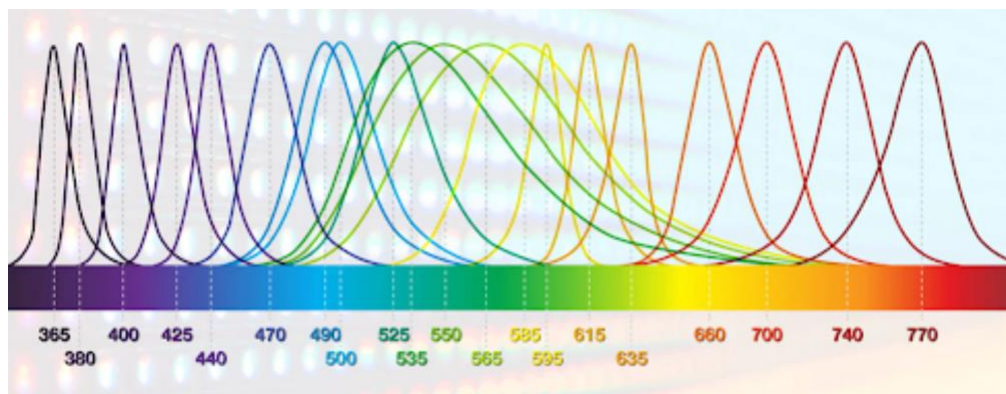


Figure 2 – Overview of the diverse light-emitting diodes and their peak wavelengths (nm). New LED wavelengths are continually developed. No claim of completeness. (Adopted from Arrow, 2022).

In addition, no other artificial light source has the ability to emit such high luminous fluxes ($\geq 2000 \mu\text{mol m}^{-2} \text{s}^{-1}$) as LED systems (Eichhorn Bilodeau et al., 2019; Singh et al., 2015a; Nelson & Bugbee, 2014).

Another exceptional advantage of most LEDs over traditionally applied lighting systems is their high electrical conversion efficiency. Monochromatic blue, red and far-red diodes (with peak wavelengths (λ) at 450, 660 and 730 nm, respectively) are currently 93, 81 and 77 % efficient in converting the electrical power input into optical power outputs. The conversion efficiency of broad-spectrum LEDs ranges currently between 69 and 76 % (Kusuma et al. 2020). It should be noted however, that LEDs emitting in the ultraviolet (UV) range of the spectrum (below 400 nm) and LEDs emitting monochromatic green (G, with a peak λ at 530 nm) are much less efficient in converting the power input: UV-C and UV-B are currently only 3 % efficient (Nichia, 2019a), UV-A LEDs are only 50-65% efficient to date (Nichia, 2019b), and green LEDs have a low conversion rate of 42 % today (Kusuma et al. 2020).

Though the range of the photosynthetically active radiation (PAR, 400-700 nm) is currently under debate (Zhen & Bugbee, 2020/2020a; please also see sections 1.3.1.4 and 1.4.2.2 for more details), the lamps' photosynthetic photon efficacies (PPE) have been established in an attempt to compare assimilation lights. PPE represents the converting rate from electrical input to PAR, is expressed in moles of photons of PAR emitted per energy input and is measured in micromoles per joule ($\mu\text{mol J}^{-1}$) (Nelson & Bugbee, 2014). While the PPE of FLs range between 0.74-0.95 $\mu\text{mol J}^{-1}$ (Wu et al., 2020), a PPE of 1.46 $\mu\text{mol J}^{-1}$ has been published for MHs (Nelson & Bugbee, 2014), and the efficacy of HPS lamps ranges between 1.7-1.85 $\mu\text{mol J}^{-1}$ (Katzin et al., 2021; Nelson & Bugbee, 2014). LEDs exceed these efficacies as they currently provide efficacies between 1.9 and 4.7 $\mu\text{mol J}^{-1}$ (Kusuma et al. 2020). However, these LED efficacies depend on their spectral range: While blue and red LEDs are currently able to emit 3.5 and 4.5 $\mu\text{mol J}^{-1}$, respectively, broadband white LEDs release between 2.6 and 2.9 $\mu\text{mol J}^{-1}$ and green LEDs currently emit only 1.9 $\mu\text{mol J}^{-1}$. With an efficacy of 4.7 $\mu\text{mol J}^{-1}$, far-red LEDs currently produce the most photons per energy input (Kusuma et al. 2020), however, as far-red light (700-800 nm) is currently not considered as PAR (400-700 nm) (Zhen & Bugbee, 2020), special attention must be given to the definition of PAR when comparing different assimilation light efficacies.

The overall high electrical conversion efficiencies as well as the high efficacies within the PAR range of LEDs translate into meaningful and direct energy-savings in greenhouse productions (Singh et al., 2015a; Nelson & Bugbee, 2014, Katzin et al. 2021). While common HPS lightings carry high financial and hence, environmental costs (due to high energy inputs and thus, carbon footprints), utilizing the more efficient LEDs will save around 40 % on electricity input for greenhouse lightings, as recently simulated by Katzin et al. (2021) across several greenhouse designs, control settings and various climates around the world.

While HPS lamps generate considerable amounts of radiative heat (≥ 200 °C) (Singh et al., 2015a), the low radiant heat production of LEDs enables their placement close to and even inside plant canopies (e.g., Joshi et al., 2019; Gómez et al., 2013) and facilitates the multi-tiered vertical farms (e.g., Kozai, 2019).

However, the very little heat emissions of LEDs and the accompanied increases in the greenhouse heating demand with uncertain financial consequences resulted in hesitant transitions from HPS to LED lighting systems in greenhouse industries thus far.

Greenhouse lighting and heating usually originate from different energy sources. While fossil-fueled power plants, photovoltaic cells, wind turbines, combined heat and power (CHP) generators are often the energy sources for lighting, heating is regularly supplied by boilers fueled with natural gas or other fuels, geothermal heat, heat pumps, heat buffers or CHP generators (Stanghellini et al., 2019). Thus, besides the local climate which is the prominent factor determining the energy saving potential (Katzin et al., 2021), the available energy resources affect the specific financial (and environmental) costs. Though heating considerably lowers the savings due to LED lighting alone, the studies by Katzin et al. (2021), Ouzounis et al. (2018) and Dieleman et al. (2016) show that total energy savings (lighting + heating) achieved by transitioning from HPS to LED still range between 7 and 27 %. Interestingly, significant reductions in watering, ventilation and CO₂ input were accompanied by LED lighting as well. In contrast, HPS lamps resulted in higher ventilation rates (for dehumidification and/or removal of excess heat), thus, intensified CO₂ demands and even increased the heating demand during winter when compared to greenhouses supplemented with LEDs (Katzin et al. 2021; Singh et al., 2015a).

In spite of the many advantages associated with LEDs, the lighting system still has its drawbacks. First and foremost, high acquisition costs (ranging from 1000-3000 \$ per kilowatt (kW)) significantly exceed the price of HPS fixtures (ranging from 200-350 \$ per kW) and hence, delay their establishment in the greenhouse industry as well (Kusuma et al., 2020; Singh et al., 2015a).

In addition, though it is often argued that light-emitting diodes have prolonged life spans over conventional assimilation light sources (e.g., HPS lifespan: 6000-40,000 h; FL lifespan: 9000-24,000 h; LED lifespan 25,000-100,000 h (Wu et al., 2020; Xu, 2019), a consumer survey revealed that the actual LED system lifespans only ranged from 1460 hours to 27,375 hours, because the lifetime of luminaire sub-components (comprising of optics, thermal designs, drive electronics, etc.) are currently not included in the providers' lifespan estimations (Casamayor et al., 2015).

Finally, while light intensities and qualities emitted by HPS and FL fixtures are distributed uniformly, LEDs distribute their light heterogeneously. The light intensities dramatically decline from the center to the edges of the LED systems (Figure 3A) and, if LEDs emitting mixed monochromatic

wavelengths are used, heterogeneous wavelength ratios occur at the plant canopy because of the linear diode arrangements (Figure 3B) (Wu et al. 2020).

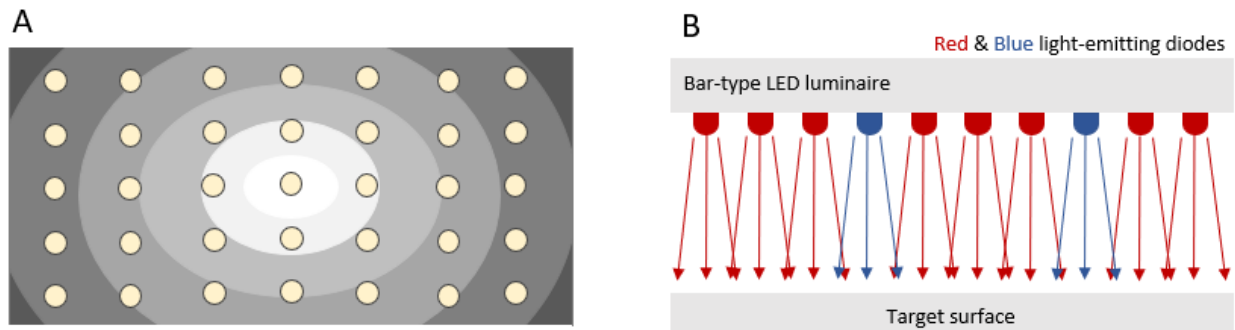


Figure 3 – Schematic depiction of the heterogeneous light intensity and wavelength distributions of common LED luminaires. (A) LED light intensities decline towards the sides, **(B)** Wavelength ratios at the target surface differ along bar-type LED luminaires.

Despite these drawbacks, LED lighting technology is expected to substitute traditional assimilation light sources in the near future (Shelford & Both, 2021, Bantis et al., 2018).

1.3 The significance of light

From the formation of organic molecules with chemical energy produced during the essential light reactions of photosynthesis, the plants' orientation in space and time through phototropism and photoperiodism, to the plants' various forms and structures via photomorphogenesis – light affects virtually all aspects of plant growth and development as it functions both as a source of energy and as an environmental indicator (Hart, 1988). Due to their ability to perceive electromagnetic radiation, plant pigments and photoreceptors play particularly important roles in the wide range of interactions between plants and light.

1.3.1 The role of plant pigments for photosynthesis

During the light reactions of photosynthesis, the lights' energy and water are used to generate chemical energy in the form of adenosine triphosphate (ATP) and nicotinamide adenine dinucleotide phosphate (NADPH), and oxygen is released as a by-product. The energy-rich molecules ATP and NADPH then drive the light-independent second part of photosynthesis – the Calvin Cycle, during which carbon dioxide is fixed from the atmosphere to form the building blocks of life. But it is only due to the light-harvesting pigments that these essential light reactions are possible (Nabors, 2007).

Although several light-harvesting pigments exist, most terrestrial plants use chlorophyll *a* (chl *a*), chlorophyll *b* (chl *b*) and beta-carotene (β -carotene) to harvest the lights' energy (Kume et al., 2018; Britton et al., 2008; Frank & Brudvig, 2004). Chl *a* represents the most abundant and chl *b* the second most abundant pigment in plant leaves (Kume et al., 2018; Esteban, 2014). With an average concentration of 10 mmol mol^{-1} of total chlorophyll *a+b* (Esteban, 2014), β -carotenes play only a subordinate role as light absorbers. Besides, the essential main function of carotenoids, to which β -carotenes belong, is to mitigate photodamages under excessive light conditions by quenching chlorophyll triplets and scavenging oxygen radicals (Maoka, 2020; Hashimoto, 2016; Frank & Brudvig, 2004).

1.3.1.1 The photosystems

While chl *a* is directly involved in the light reactions and has an unmatched essential role as an electron donor (Bjoern et al., 2009), chl *b* and β -carotene are only indirectly involved in the light reactions, which is why they are classified as auxiliary or antenna pigments. In addition to the assimilation of light, the main function of these auxiliary pigments is the transmission of excitation energy to chl *a*-molecules (Nabor, 2007). Thereby, chl *b* transfers energy from chlorophyll to chlorophyll with an efficiency of 100 %, whereas photosynthetic carotenoids transfer the excitation energy only with an efficiency of 35-90 % (Hogewoning, 2012).

Chl *a*, chl *b* and β -carotene (together with appendant protein molecules) form multiple pigment clusters in the thylakoid membranes of the chloroplasts. Each cluster consists of approximately 200-300 pigment molecules. The light reaction in each cluster is triggered by a chl *a*-molecule, which absorbs the energy of a photon and then releases an electron that is then quickly absorbed by a molecule called the primary electron acceptor. Together, the chl *a*-molecule and the primary electron acceptor are termed reaction center. The reaction center and the auxiliary pigments in every cluster work together as one light-harvesting unit – the photosystem. However, there are two types of photosystems. While photosystem I (PSI) is comprised of more chl *a* than chl *b*, the ratio of both chls is nearly balanced in photosystem II (PSII). PSII and PSI are connected through a series of electron transmitters and work linearly (Nabor, 2007).

1.3.1.2 The light reaction during photosynthesis

When the light energy reaches chl *a* in the reaction center (either directly or through energy transfer by the auxiliary pigments), an electron in the chl *a*-molecule gets excited and is transferred to the primary electron acceptor. Each released electron becomes quickly replaced by an electron from H₂O, after an enzyme breaks down an H₂O-molecule into two electrons, two protons and an oxygen atom. During the

photobiological water splitting, oxygen is formed. However, two H₂O-molecules have to be split in order to form one O₂-molecule.

Each released electron from the chl *a*-molecule passes the primary electron acceptor and loses energy as it passes through a series of electron transmitters (redox carriers, namely plastoquinone, cytochrome complex and plastocyanin), which form an electron transport chain. The movement from one redox carrier to the next occurs via a series of oxidation-reduction reactions (redox reactions). The energy released during the described electron flow indirectly powers the synthesis of ATP. Each electron that passes through the electron transport chain neutralizes the positively charged chl *a*-molecule in the reaction center of PSI. Thereby, the chl *a*-molecule is positively charged because it already transferred an electron to its primary electron acceptor after the absorption of a photon.

Finally, each released electron moves through one more electron transport chain comprised of ferredoxin and NADP⁺ reductase. The latter electron carrier in this chain is an enzyme that converts NADP⁺ into NADPH. Overall, two electrons have to pass the light reaction chain to synthesize NADPH successfully (Nabor, 2007).

1.3.1.3 Spectral light absorption of photosynthetic plant pigments

Each pigment type maximally absorbs light in different wavelength regions (Figure 4). While chls primarily absorb photons in the violet, blue and red regions of the visible light spectrum, carotenoids mainly absorb light in the blue and green light regions (Eichhorn Bilodeau et al., 2019; Hashimoto, 2016; Singh et al., 2015a).

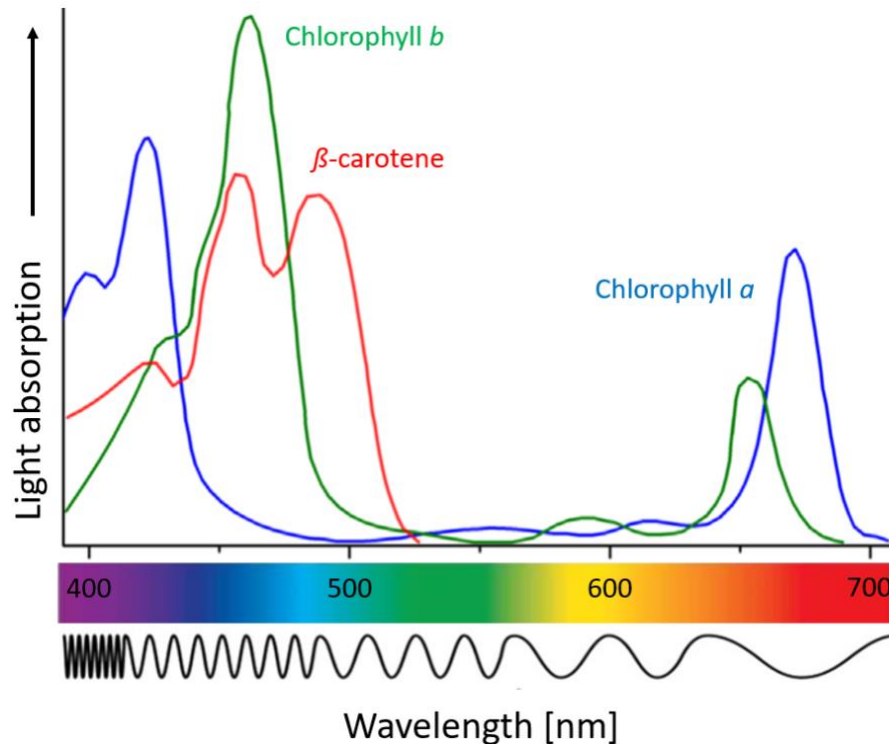


Figure 4 – Absorption spectra of chlorophyll *a*, *b* and β -carotene within the visible light spectrum. Note that the pigments' light absorptions are greatly influenced by solvents used during extraction procedures and can therefore differ by approximately 35 nm (e.g., Jaramillo et al., 2011). Hence, the pigments' light absorption curves depicted in this figure are only general approximations. (Adopted from Singh et al. (2015a) and Eichhorn Bilodeau et al. (2019)).

The main absorption peaks of chl *a* are proposed to be between 430-438 nm and between 662-664 nm, whereas the main absorption peaks of chl *b* are suggested to be between 457-468 nm and between 646-651 nm (Kume et al., 2018). Hence, the peak wavelengths of the absorption spectra of chl *a* and *b* differ by approximately 20 nm and function complementary to each other. With maximal absorbances found between 400-550 nm, β -carotenes expand the wavelength range over which light can support photosynthesis further into the green spectrum (Maoka, 2020; Eichhorn Bilodeau et al., 2019; Hashimoto, 2016; Tan & Soderstrom, 1988).

1.3.1.4 Photosynthetically active radiation (PAR)

Until today, the light action spectrum of photosynthesis is largely based on results published by McCree (1972a), who defined the range of wavelengths from approximately 400 to 700 nm as the photosynthetically active radiation (PAR). PAR is commonly quantified using the number of photons in the 400-700 nm range received by an area in a defined time frame and generally expressed in $\mu\text{mol m}^{-2} \text{s}^{-1}$. Using monochromatic light conditions, McCree's assay covered the spectral range from 350

to 750 nm in 25 nm waveband increments, and the photosynthetic activity of leaf fragments from 22 crop plant species was measured based on their CO₂ uptake rate. His measurements showed that different wavelengths result in different quantum yields for CO₂ fixations. McCree detected two broad peak maxima within the red and blue region of the visible light spectrum centered at 620 and 440 nm, with a shoulder at 670 ± 10 nm (Figure 5, McCree curve). The highest quantum yields were observed in the red light region between 600 and 640 nm. He pointed out that the relative photosynthetic activity at the blue peak (440 nm) was 70 % of the photosynthetic activity detected at the red peak (620 nm) and concluded that blue and green light (400-570 nm) were thus considerably less efficient in driving photosynthesis than red light. Therewith, McCree was the first to describe a plants' PAR curve by defining the light action spectrum and the wavelengths that are used most efficiently for glucose biosynthesis and storage of free chemical energy (McCree, 1972a & 1972b). His results were further reinforced by Inada (1976), who essentially applied the same methods to determine the action and quantum yield spectra of the photosynthetic CO₂ uptake and the absorptance spectra for 33 higher plant species (Figure 5, Inada curve) and observed a broad peak from 600 to 680 nm and lower peak at approximately 435 nm. The fairly close correlation with the spectral absorptions of the plants' chlorophylls (see previous section 1.3.1.3) would substantially direct early to present LED studies using narrow waveband LEDs - as detailed in section 1.4.1.

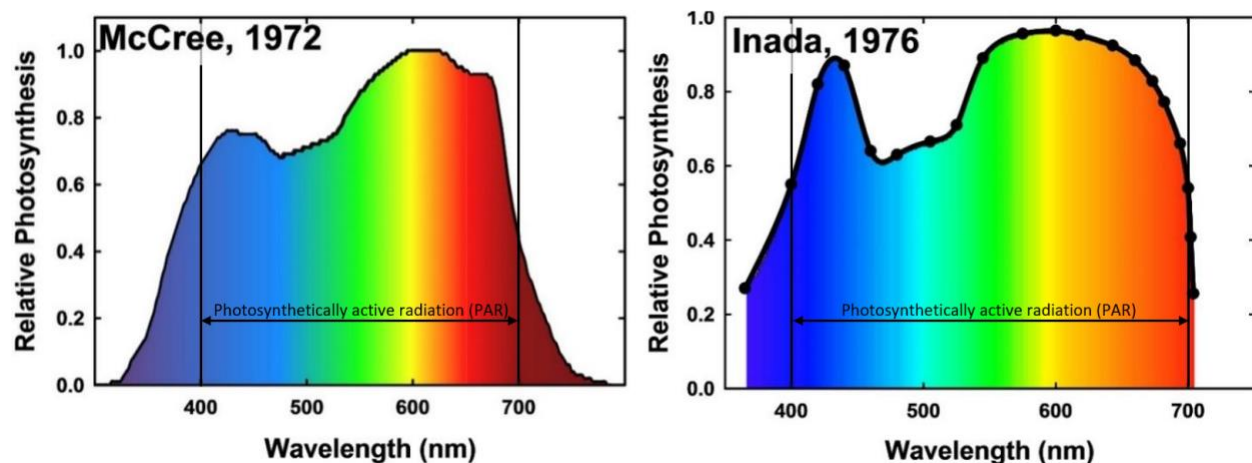


Figure 5 – Action spectra of photosynthesis from two different studies (McCree, 1972a & Inada, 1976). The curves reflect the quantum yield of photosynthesis per absorbed photon of a specific wavelength. Each black dot represents the wavelength at which measurements were taken. (Adopted from Bugbee, 2016)

However, as clearly evident in the flanking regions of both the McCree and Inada curve, light below 400 nm and above 700 nm induces photosynthetic activity as well (Figure 5). In example, radish and pigweed showed equally high quantum yields between 375 and 500 nm (McCree, 1972a) and all tested

herbaceous plants showed nonnegligible high quantum yields between 350 and 435 nm (Inada, 1976), which comes to no surprise considering that chl *b* is known to absorb photons well below 400 nm (as indicated in Figure 4).

In addition, recent results from Zhen & Bugbee (2020a) suggest that far-red (FR) photons between 701 and 750 nm should be included in the definition of PAR because the researchers showed (for 14 assorted crop species) that the addition of FR photons (701-750 nm) to a PAR spectrum (400-700 nm) enhances the photosynthetic activity of the canopies in the same way as the addition of equally many PAR photons increase the canopies' photosynthesis.

Due to these discoveries, a broadening of the photosynthetic action spectrum can be expected in the near future. The roles of an ultraviolet as well as far-red light-sensing plant photoreceptors (see following sections) in the development of stomata (which control the rate of gas exchange and transpiration) will probably encourage the redefining of the photosynthetically active radiation spectrum as well.

In the meantime, the term 'photobiologically active radiation' (PBAR) is frequently used to describe the whole range of light that is known to be perceived by plants (e.g., Kusuma et al., 2022). PBAR spans from 280 to 800 nm and hence, comprises the PAR spectrum and the adjoining spectral regions that are sensed by plant photoreceptors.

1.3.2 Photoreceptors

Plants employ a suite of structurally distinct photoreceptors to sense, monitor and respond to the quantity, quality and duration of light in their surrounding environment. After wavelength-dependent light absorptions, various (partially unidentified) photoreceptors (namely phytochromes, cryptochromes, phototropins and ultraviolet resistance locus 8 (UVR8)) undergo physical or chemical changes which initiate diverse and complex signal transduction cascades within the plant. These signaling pathways direct a plethora of intracellular processes, result in profound changes in gene transcriptions and ultimately affect a range of plant responses including its form, function and content at the cellular and whole-organism level (Jing & Lin, 2020; Zheng et al., 2019; Folta & Carvalho, 2015).¹

¹ The following sections focus on the differing light absorption spectra of photoreceptors and their resultant plant responses. For more details on the photoreceptors' structures, localizations and the complex signal transduction mechanisms, please refer to the following prevailing review articles: Łabuz et al., 2022; Jing & Lin, 2020; Legris et al., 2019; Jenkins, 2014.

1.3.2.1 Spectral light absorption of photoreceptors

The various photoreceptors enable plants to track and respond to a wide spectrum of the solar radiation that reaches the Earth's surface. Each photoreceptor is activated by discrete wavelengths ranging from the ultraviolet B to the far-red light spectrum and differs in their sensitivity to light (Figure 6). Phytochromes are mainly red/far-red light photoreceptors (600-800 nm) (Wang et al., 2021). Two interconvertible phytochrome forms undergo photo-transformational changes upon exposure to either red or far-red light. While the red light-absorbing form (P_r) transforms rapidly into a far-red light absorbing form (P_{fr}) once a red photon has been absorbed, P_{fr} quickly converts back to P_r upon far-red light exposure (Cordeiro et al., 2022, Eichhorn Bilodeau et al., 2019). To a lesser extent, phytochromes also absorb ultraviolet A and blue light (Folta & Carvalho, 2015; Xie et al., 2007). Cryptochromes primarily absorb ultraviolet A and blue light (320-500 nm) (Jones, 2018) but can also absorb green/yellow light (500-530 nm, Bouly et al. (2007) and respond in fluence rate-dependent manners (starting at as low as $2 \mu\text{mol m}^{-2} \text{s}^{-1}$ (Pedmale et al., 2016; Folta & Carvalho, 2015). Phototropins are also ultraviolet A and blue light-absorbing photoreceptors and absorb wavelengths between 320 and 550 nm (Łabuz et al., 2022) but initiate their responses even under dim pulses of light (Folta & Carvalho, 2015). From all known photoreceptors today, UV resistance locus 8 (UVR8) is the only photoreceptor that absorbs ultraviolet B radiation (290-320 nm) (Jenkins, 2014), but has recently been shown to perceive UV-A radiation as well (Rai et al., 2019). Furthermore, the existence of at least one green-sensing photoreceptor is plausible as discrete plant and leaf adaptations appeared independently of known photoreceptors as shown in phytochrome and cryptochrome knockout mutants (Smith et al., 2017).

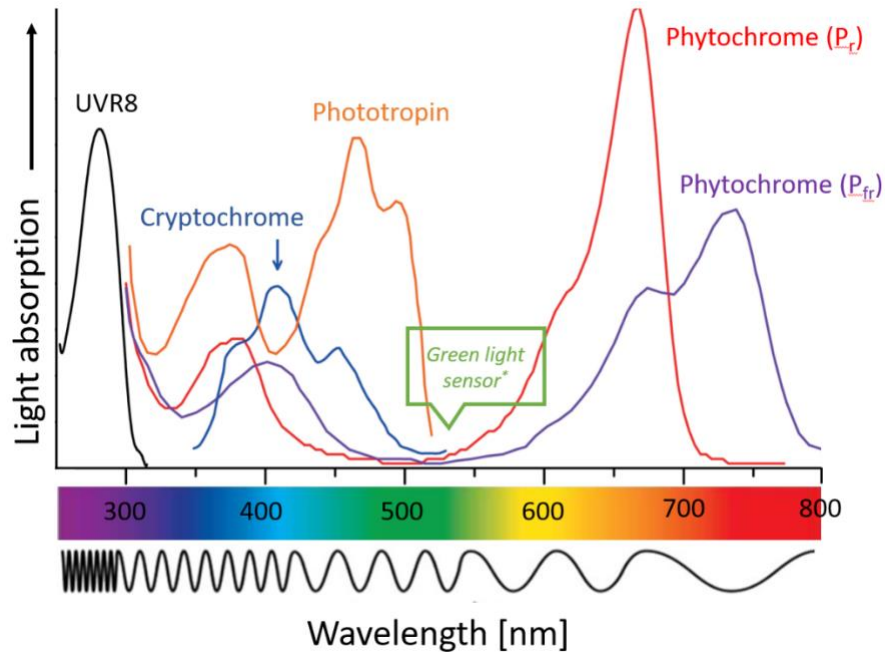


Figure 6 – Absorption spectra of photoreceptors. The photoreceptors’ light absorption curves depicted in this figure are only general approximations. *: Observations suggest the existence of a so far unidentified green light-sensing photoreceptor (e.g., Smith et al., 2017), UVR8: Ultraviolet resistance locus 8, P_r: red light-absorbing phytochrome form, P_{fr}: far-red light absorbing phytochrome form. (Adopted from Folta & Carvalho (2015) and Eichhorn Bilodeau et al. (2019))

1.3.2.2 Plant responses mediated by photoreceptors

Though the full extents of the photoreceptors’ physiological and morphological roles are not yet clear, more than two decades of extensive biochemical and genetic research efforts have discovered many plant adjustments which are brought about by photoreceptors. While some plant responses may be triggered by only one photoreceptor, the majority of physiological and morphological responses result from complex interactions of activated light-sensory pathways coordinated by multiple photoreceptors (e.g., Wang et al., 2022; Jing & Lin, 2020; Wang et al., 2017; Folta & Carvalho, 2015; Li & Yang, 2007; Casal, 2000). The following subsections report on the various responses triggered by these known photoreceptors and include evidence that supports the existence of a thus far unidentified green-sensing photoreceptor.

1.3.2.2.1 Phytochromes

As of today, the phytochrome family represents by far the most studied light-perceiving photoreceptor class and are known to control spectacular processes of the entire plant life cycle ranging from seed germination to the timing of reproductive development. Insights into phytochrome-functioning has

tremendously advanced via studies with *Arabidopsis thaliana* L. mutants deficient in all individual phytochromes, and novel regulatory roles and mechanisms are continuously being revealed. An overview of the various phytochrome-mediated processes is given in Table 1.

Table 1 – Processes involving phytochrome actions.¹

Seedling establishment	Germination De-etiolation Gravitropic orientation
Plant stature	Shade avoidance Leaf, shoot and root architecture Stomatal development
Reproduction	Transition to flowering
Photoperiod	Entrainment of the circadian clock

¹ All processes retrieved from the following review articles: Cordeiro et al. (2022), Wang et al. (2022), Jing & Lin (2020), Legris et al. (2019), Viczián et al. (2017), Fraser et al. (2016); Folta & Carvalho, 2015; Franklin & Quail, 2010.

Phytochromes regulate the germination of photoblastic seeds based on the quality of light. While red (R) light promotes the germination of seeds, far-red (FR) illumination after R light exposure, as well as light enriched in FR wavelengths (e.g., low R:FR ratios) can prevent these light-dependent seed germinations (Wang et al., 2022; Franklin & Quail, 2010; Lee et al., 2012; Borthwick et al., 1952). All phytochrome-mediated germination responses are facilitated even under very low fluence rates of $\leq 20 \mu\text{mol m}^{-2} \text{s}^{-1}$ (Lee et al., 2012; Shen et al., 2005).

In addition, phytochromes control the transition from skoto- to photomorphogenic seedling development (Folta & Carvalho, 2015; Franklin & Quail, 2010). While seedlings' skotomorphogenesis is characterized by etiolation (seedlings comprised of pale yellowish cotyledons and weak, elongated hypocotyls under dark conditions), seedlings' photomorphogenesis is exemplified by de-etiolation (informally known as "greening") which include i.e., inhibited hypocotyl lengths, cotyledon expansions and the synthesis of chlorophyll. Upon low red light exposures or (white) light with high R:FR ratios, phytochromes induce de-etiolations by suppressing transcription factors responsible for etiolated growth (Legris et al., 2019; Franklin & Quail, 2010). Besides promoting the seedlings' gravitropic hypocotyl and root orientations (Kim et al., 2016; Franklin & Quail, 2010; Shen et al., 2005), phytochromes are involved in the biosynthesis of chlorophylls upon R light exposure (Shen et al., 2005, Huq et al., 2004, Kim et al., 2003). In addition, phytochromes play crucial roles in inhibiting hypocotyl elongation (Oh et al., 2020; Jing & Lin, 2020; Trupkin et al., 2014; Shen et al., 2005, Kim et al., 2003) and inducing cotyledon opening and

expansion in a R intensity-dependent manner (Franklin & Quail, 2010). However, this described hypocotyl growth inhibition can be reversed and cotyledon expansion can be reduced by low R:FR ratios after de-etiolation (Legris et al., 2019; Procko et al., 2014, Trupkin et al., 2014).

Moreover, phytochromes substantially control plants' shade avoidance phenotypes (Legris et al., 2019; Franklin & Quail, 2010). Plants have evolved to perceive low R:FR ratios as shade (Franklin & Whitelam, 2007).² The specific R:FR ratios - perceived by particular plant tissues across various developmental stages - directly modify phytochrome action. When phytochromes sense a reduced R:FR ratio, a large set of far-reaching developmental responses are directly initiated (Legris et al., 2019). Shade conditions perceived by phytochromes induce substantial elongations of shoots and petioles (leaf stem) (Pantazopoulou et al., 2017, Cerdán & Chory, 2003) and increase apical dominance (meaning the suppression of lateral bud growth). The phytochromes' low R:FR perception further results in increased leaf areas and promotes leaf hyponasty (upward bending) (Pantazopoulou et al., 2017). In addition, new leaves develop less stomata when older leaves sense low R:FR ratios (Casson & Hetherington, 2014), and fewer lateral roots emerge when shoots perceive the described shade conditions (van Gelderen et al., 2018). Also, the photoreceptor triggers early flowering under prolonged exposure to low R:FR ratios (Cao et al., 2018; Valverde et al., 2014; Franklin & Quail, 2010; Jang et al., 2008; Cerdan & Chory, 2003). In contrast, all aforementioned shade avoidance responses are suppressed by phytochromes under high R:FR conditions. In addition, cryptochrome and UVR8 photoreceptors substantially regulate shade responses (e.g., hypocotyl elongations) under green, blue, UV-A and UV-B light conditions, which are described in sections 1.3.2.2.2 and 1.3.2.2.3 and represent a prime example of the plants' complex light signaling mechanisms.

Hence, phytochrome-mediated photoblastic seed germination, seedling establishment, shade avoidance and flowering are generally subject to R/FR reversibilities. However, continues FR radiation of high intensity ($\geq 100 \mu\text{mol m}^{-2} \text{s}^{-1}$) have been shown to inhibit the (typically R light-mediated) hypocotyl growth (Franklin & Quail, 2010).

Though phytochromes are not necessary for the entrainment of the circadian clock, phytochromes are known to participate (along with other photoreceptors) in timekeeping mechanisms as they aid in the perception of day-length and fine-tuning the circadian clock (Sanchez, 2020; Valverde et al., 2014; Cerdan & Chory, 2003; Millar et al., 1995).

² In addition, reductions of ultraviolet-A and blue light as well as green-enriched light conditions are also perceived as shade signals by plants. For details the reader is referred to Smith et al. (2017), Pedmale et al. (2016) and Casal (2012).

For the sake of completeness, it shall be noted that phytochromes are also known to respond to external temperature cues and internal hormone signals (Cordeiro et al., 2022; Jing & Lin, 2020; Franklin & Quail, 2010).

As partly mentioned above, phytochromes interact with other photoreceptors (cryptochromes, phototropins, UVR8). The next sections include these known antagonistic and synergistic plant responses.

1.3.2.2.2 Cryptochromes

Cryptochromes represent another class of extensively studied photoreceptors (Wang et al., 2017), which modulate gene expressions via transcriptional and post-translational regulations primarily upon blue light exposure (Li & Yang, 2007). Table 2 summarizes numerous cryptochrome-mediated processes.

Table 2 – Processes involving cryptochrome actions.¹

Seedling establishment	De-etiolation Primary root growth
Pigmentation	Chloroplast development Flavonoid and lycopene biosynthesis
Plant stature	Phototropism Shade avoidance Inhibit hypocotyl and internode lengths
Physiology	Stomatal opening ²
Reproduction	Transition to flowering
Photoperiod	Entrainment of the circadian clock

¹ All processes retrieved from the following review articles: Wang et al. (2022); Jing & Lin (2020); Sanchez, 2020; Fraser et al. (2016); Folta & Carvalho, 2015; Li & Yang et al. (2007).

² Involvement in this physiological process is mentioned in section 1.3.2.2.3, as cryptochromes act together with phototropins in the regulation of stomatal openings.

First and foremost, cryptochromes are known to promote the synthesis of chlorophylls (Giliberto et al., 2005) and the accumulation of multiple nutritious secondary metabolites under blue light conditions. More precisely, cryptochromes promote the accumulation of flavonoids (including anthocyanins) and lycopenes which impart a range of bright colors to fruits and vegetables and act as strong health-promoting antioxidants (Samanta et al., 2011; Lila, 2004; Kaur & Kapoor, 2001). Cryptochromes stimulate these pigment productions upon blue light exposures (Li & Yang, 2007; Giliberto et al., 2005; Ahmad et al., 1995). In addition, cryptochromes promote short hypocotyl and internode lengths under UV-A, B and partly G light conditions (Giliberto et al., 2005, Ahmad et al., 2002; Ahmad et al., 1995, Lin et al., 1995), and fundamentally control primary root growth of seedlings under blue light conditions (Canamero et al., 2006). Though the physiological significance is not clear, cryptochromes have

also been shown to induce blue-light dependent random hypocotyl-bendings in *Arabidopsis* seedlings (Ohgishi et al., 2004).

Besides these distinct physiological responses upon blue light exposure, which are thus far believed to be triggered by cryptochromes only (Wang et al., 2022; Casal & Mazzella, 1998), it has been shown that cryptochromes physically and functionally interact with phytochromes (Mas et al., 2000; Ahmad et al., 1998). As they partially share signaling pathways, cryptochromes and phytochromes co-regulate many diverse plant responses including de-etiolation, photomorphogenic growth, floral initiation, and the entrainment of the circadian clock (Wang et al., 2022; Franklin & Quail, 2010; Li & Yang, 2007).

Although cryptochromes were found to be the major photoreceptors responsible for chloroplast developments under blue light conditions, it was shown that a cooperative action with phytochrome is required for the response (Usami et al., 2004). Complementary, it was shown that cryptochromes enhance phytochrome-mediated chlorophyll productions under red light and that they are required for the phytochrome-mediated cotyledon expansions under blue light (Neff & Chory, 1998). In correspondence, conditional synergisms between crypto- and phytochromes were observed under suboptimal light conditions with regard to cotyledon expansion and hypocotyl inhibition by Casal & Mazzella (1998). However, under adequate prolonged dichromatic (blue and red) light conditions, both photoreceptors were observed to act independently during *Arabidopsis* seedling de-etiolation. Thus, although the conditional complex mechanisms of coaction are mostly unknown, cooperative interactions of cryptochromes with phytochromes during de-etiolation have been demonstrated.

While low R:FR conditions drive phytochrome-mediated shade avoidance responses (as described in section 1.3.2.2.1), low blue light conditions result in cryptochrome-mediated shade avoidance responses (Pedmale et al., 2016). Thus, both photoreceptors drive shade responses under different light conditions (Fraser et al., 2016). Though cryptochromes have been shown to promote hypocotyl elongations under low blue light conditions via direct interaction with phytochrome-interacting transcription factors (alike phytochromes), the shade avoidance responses appear to operate, at least in part, through separate mechanisms (Pedmale et al., 2016).

Cryptochromes and phytochromes regulate floral initiation antagonistically. While phytochromes inhibit the transition to flowering under red light (Mockler et al., 1999, Guo et al., 1998), cryptochromes promote flowering under blue light conditions (Giliberto et al., 2005) and the latter appears to require the presence of phytochromes (Franklin & Quail, 2010; Mockler et al., 1999).

Cryptochromes promote short circadian rhythms (under both high and low intensities of blue light) and are required for the phytochrome-mediated signaling to the circadian clock under both red and

blue light conditions, as they act as signal transduction components in the phytochrome-signaling to the clock (Devlin & Kay, 2000). Thus, crypto- and phytochromes both have roles in perceiving and regulating the photoperiodic length (Sanchez, 2020; Franklin & Quail, 2010; Millar et al., 1995).

In similarity to the FR reversibility of phytochrome-mediated responses upon red light exposure (as described in section 1.3.2.2.1), a number of cryptochrome-mediated responses upon blue light exposure become reversed upon green light exposure and depend on the G:B ratio.

For example, green light causes reversal of blue light-mediated stomatal opening in diverse plant species (Talbot et al., 2002; Eisinger et al., 2003; Frechilla et al., 2000). The reversal response increases with increasing G:B ratio in all tested plant species (Talbot et al., 2002, Frechilla et al., 2000). Also, blue light-induced induction of flowering mediated by cryptochrome is reduced under green light exposure in *Arabidopsis*, and time to flower induction increases with increasing G:B ratio (Banerjee et al., 2007). Likewise, green light reverses blue-induced, cryptochrome-mediated anthocyanin accumulations in *Arabidopsis* and lettuce - an effect that increases with increasing G light proportions (Zhang & Folta, 2012). In addition, cryptochrome-mediated hypocotyl growth inhibitions upon blue light exposures become strongly reduced when long wavelengths of green light (≥ 518 nm (Bouly et al., 2007); ≥ 550 nm (Ahmad et al., 2002) are added, and result in significantly elongated hypocotyls (Lin et al., 1995). Thereby, the cryptochrome-mediated hypocotyl length decreases with increasing B:G ratios, and the ratio impact is higher under higher irradiances (Sellaro et al., 2010).

Whether these cryptochrome-mediated responses are reversed under green light conditions due to conformational changes of the photoreceptor itself (Meng & Runkle, 2019; Sellaro et al., 2010; Bouly et al., 2007; Banerjee et al., 2007), by a thus far unknown green-sensing photoreceptor (section 1.3.2.2.5; Zhang et al., 2011; Folta, 2004) and/or by the carotenoid zeaxanthin (Talbot et al., 2002, Frechilla et al., 2000) remains to be explored.

Finally, it was shown by Ma et al. (2016) that the cryptochrome-mediated hypocotyl inhibitions become enhanced by high temperatures (28 °C). Thus, cryptochrome action (alike phytochrome action) is influenced by environmental temperature conditions.

1.3.2.2.3 Phototropins

Phototropins are plant-specific photoreceptors that perceive changes in the intensity and direction of blue light and regulate responses which mostly serve to improve the plants' photosynthetic efficiency (Christie et al., 2014; Folta & Carvalho, 2015). Table 3 indicates general processes affected by phototropins.

Table 3 – Processes involving phototropin actions.¹

Seedling establishment	De-etiolation
Plant stature	Phototropism Shade avoidance
Physiology	Stomatal opening Chloroplast movement

¹ All processes retrieved from the following review articles: Łabuz et al. 2022; Zheng et al. (2019); Fraser et al. (2016); Folta & Carvalho, 2015; Christie et al. (2014); Franklin & Quail (2010); Li & Yang (2007); Casal (2000).

Using *Arabidopsis* mutants, Ogishi et al. (2004) showed that phototropins induce the expansion of cotyledons in de-etiolating seedlings at high blue fluence rates ($470 \pm 30 \text{ nm}$, $100 \mu\text{mol m}^{-2} \text{ s}^{-1}$) independently of blue light-sensing cryptochromes. Hence, cotyledon expansions are controlled by phytochromes and phototropins in light environments containing R, FR and B light.

Over a broad range of blue light intensities ($0.01\text{-}100 \mu\text{mol m}^{-2} \text{ s}^{-1}$), phototropins control the phototropic bending of leaves, hypocotyls, stems and roots towards the direction of light (Fraser et al., 2016; Inoue et al., 2008; Sakai et al., 2001; Casal, 2000). Nevertheless, phytochromes and cryptochromes have been shown to co-regulate phototropin-induced phototropism. E.g., *Arabidopsis thaliana* seedlings show enhanced hypocotyl curvatures towards blue light (450 nm) when exposed to red light (669 nm) prior to the blue light irradiation (Janoudi et al., 1997a), which soon after was shown to be regulated by phytochromes (Janoudi et al., 1997b). Via *Arabidopsis* mutants lacking cryptochromes, it was shown by Ahmad et al. (1998) that the phototropic curvature is reduced, indicating that the phototropin-driven phototropic curvature response is also modulated by cryptochromes. Soon after, Whippo et al. (2003) differentiated the involvement of cryptochromes in this response: while high blue fluence rates ($100 \mu\text{mol m}^{-2} \text{ s}^{-1}$) reduce the phototropic curvature through the coaction of phototropins and cryptochromes, both photoreceptors function together to enhance phototropism under low blue fluence rates ($< 0.1 \mu\text{mol m}^{-2} \text{ s}^{-1}$).

In addition, chloroplast movements are fundamentally controlled by phototropins (Wada, 2013, Sakai et al., 2001). While the phototropins' perception of low blue light intensities ($0.01\text{-}20 \mu\text{mol m}^{-2} \text{ s}^{-1}$) results in the accumulation of chloroplasts perpendicular to the direction of the light source to optimize photosynthetic efficiency, moderate blue light intensities ($20\text{-}40 \mu\text{mol m}^{-2} \text{ s}^{-1}$) induce an avoidance response by relocating the chloroplasts close to the cell walls parallel to the direction of the light source (Łabuz et al., 2022, Kagawa et al., 2001, Jarillo et al., 2001). High blue light intensities ($80\text{-}120 \mu\text{mol m}^{-2} \text{ s}^{-1}$), however, prompt a biphasic response in which a short partial chloroplast avoidance

precedes their accumulation (Łabuz et al., 2015; Luesse et al., 2010, Jarillo et al., 2001). Despite phototropins' essential role in these chloroplast relocation movements, phytochromes have been shown to reduce the high light avoidance response of phototropins but do not affect the chloroplast accumulation response (Luesse et al., 2010).

CO₂ uptake for photosynthesis and water evaporation for transpiration are tightly regulated by stomatal pores located in the epidermis of leaves. Their opening is regulated by a pair of surrounding guard cells which (among other stimuli) are regulated by phototropins in a blue light-dependent manner, meaning that the stomatal opening increases as the intensity of blue light increases (Kinoshita et al., 2001). However, it was shown that cryptochrome function additively with phototropins facilitating blue light-induced stomatal openings (Mao et al., 2005).

The significance of phytochromes in perceiving and signaling unfavorable shade conditions and in inducing multiple shade-avoiding strategies under increased far red light conditions has been described in section 1.3.2.2.1. Under very low blue (0.1 and 1 $\mu\text{mol m}^{-2} \text{s}^{-1}$) and low white light conditions (25 $\mu\text{mol m}^{-2} \text{s}^{-1}$) however, it is the phototropins that induce significant growth enhancements (threefold fresh weight increases) by optimizing chloroplast accumulations, stomatal openings and leaf flattening (Takemiya et al., 2005).

Just as described for some phyto- and cryptochrome actions, phototropin-mediated chloroplast movements upon blue light exposure are also affected by temperature. Under low and high light intensities, low temperatures enhance and prolong chloroplast avoidances, respectively (Łabuz et al., 2015).

1.3.2.2.4 UV resistance locus 8 (UVR8)

Although ultraviolet radiation represents a risk to plant integrity in large quantities (Hollósy, 2002), small doses of UV-A and UV-B induce important plant benefits, some of which are distinctly mediated by the UVR8 photoreceptor via transcriptional regulations (Rai et al., 2019; Neugart & Schreiner, 2018; Jenkins, 2014). Processes in which UVR8 is active are provided in Table 4.

Most importantly, UVR8 has been shown to induce the biosynthesis and accumulation of flavonoids upon UV-B exposure by inducing the genetic expression of chalcone synthase (CHS), which represents the first enzyme of the flavonoid biosynthetic pathway (Neugart & Schreiner, 2018; Jenkins, 2014, Morales et al., 2013; Li et al., 1993). Besides being highly beneficial to human health (Ballard and Maróstica, 2019), the UV-absorbing flavonoids prevent or at least reduce damages to the photosynthetic apparatus by shielding against ultraviolet radiation (Rai et al., 2019; Neugart & Schreiner, 2018; Hollósy,

Table 4 – Processes involving UV resistance locus 8 (UVR8) actions.¹

Pigmentation	Flavonoid biosynthesis
Plant stature	Suppression of elongation and expansion growth Inhibition of shade avoidance
Physiology	Stomata development Sinapate biosynthesis
Resistance	Tolerance to ultraviolet radiation Pest resistance
Photoperiod	Entrainment of the circadian clock

¹ All UV-B photoreceptor processes retrieved from the following review articles: Jing & Lin (2020); Eichhorn Bilodeau et al. (2019); Neugart & Schreiner (2018); Fraser et al. (2016); Jenkins (2014); Tilbrook et al., 2013; Casal (2000).

2002; Tevini et al., 1991). Similarly, UVR8 controls the expression of the sinapate biosynthetic pathway upon UV-B exposure (Demkura & Ballaré, 2012), which (as a precursor of lignin) is involved in cell wall strengthening. As some flavonoids and sinapates have been shown to deter insects from feeding and oviposition (Simmonds, 2001) and to reduce mold infections of *Bortrytis cinerea* (Demkura and Ballaré, 2012), UV-B-exposed UVR8 photoreceptors indirectly support plant resistances against insects and pathogens (Neugart & Schreiner, 2018).

Fuglevand et al. (1996) and Wade et al. (2002) demonstrated synergistic enhancements of CHS expressions when *Arabidopsis* was simultaneously irradiated with UV-B and blue or UV-B and UV-A. To the contrary, Rai et al. (2019) recently found that UVR8-mediated accumulations of flavonoids were antagonistically regulated by cryptochromes. And while phytochromes have been proposed to regulate the UV-B inductive pathway antagonistically as well (Jenkins et al., 2001), they have been shown to be required for a cryptochrome-mediated induction of CHS (Wade et al., 2002). Thus, clarifications are certainly necessary to unravel these complex photoreceptor interactions underlying the accumulation of flavonoids.

UVR8 alters plant morphology and tremendously reduces plant growth upon UV-B exposure. Generally, with increasing UV-B intensity, the length and area of leaves decrease while their thickness increases, and elongations of hypocotyls, plant stems and internodes as well as petioles become significantly suppressed by UVR8 activation (Jing & Lin, 2020; Neugart & Schreiner, 2018; Fraser et al., 2016; Jenkins, 2014). Evidently, many of these UVR8-mediated phenotypic effects oppose the effects induced by shade and thus, it comes to no surprise that UVR8 can directly antagonize shade avoidance responses (Fraser et al., 2016; Hayes et al., 2014). Nevertheless, UVR8 has also been shown to be required for the progression of epidermal cell differentiations, compensatory increases in epidermal cell sizes and

to promote the development of stomata under UV-B exposure (Wargent et al., 2009). Thus, UVR8 photoreceptors play significant roles in regulating morphological aspects required for survival upon UV-B exposure.

Lastly, UVR8 is necessary for the entrainment of the circadian clock under UV-B light as the photoreceptor has been shown to induce the transcription of several rhythmically expressed clock genes under UV-B light conditions (Sanchez et al., 2020; Fehér et al., 2011).

1.3.2.2.5 Putative green light-sensing photoreceptor

As previously mentioned (e.g., Figure 6), evidence exists that supports the existence of a thus far unidentified green-sensing photoreceptor (Smith et al., 2017; Folta & Maruhnich, 2007). In example, Zhang et al. (2011) detected elongated petioles and leaf hyponasty in *Arabidopsis* when G (525 nm) was added to backgrounds of RB (630/470 nm). The same green-light induced morphogenic effects were observed in cryptochrome (and phytochrome) mutant backgrounds, indicating that an unknown light sensor is participating in the acclimation to green-enriched light environments (Zhang et al., 2011). Similarly, Folta (2004) discovered elongated hypocotyls in *Arabidopsis* seedlings grown under RGB (630/525/470 nm) in comparison to seedlings grown under RB (630/470) alone. As the response persisted in mutants lacking cryptochrome- and phototropin-photoreceptors, his results are also indicative of a yet undetermined G light-sensor that promotes early stem elongations.³

All of these observed shade avoidance symptoms in G enriched light environments (typically observed in phytochrome-mediated FR light environments; section 1.3.2.2.1) appear to increase with both increasing G/B ratio (Sellaro et al., 2010) and increasing green light intensity (Zhang et al., 2011; Folta, 2004).

1.4 Impact of LED lighting on plant development

The majority of LED-based research has focused on the production of biomass and concentrated on the efficient use of specific photons for photosynthesis. Therefore, red and blue photons have received special attention and will therefore be addressed in the following section.

³ Nevertheless, keep in mind that hypocotyl length is also strongly controlled by cryptochrome-signaling (as described in section 1.3.2.2.2). Hence, hypocotyl growth is under complex light environmental control.

1.4.1 From red to red/blue LED lighting strategies

With the groundbreaking development of red LEDs with peak wavelengths near 660 nm (Barta et al., 1992) - thus, in close proximity to wavelengths at which maximal photosynthetic quantum yields (Figure 5) and chlorophyll assimilation (Figure 4) are found - first plant experiments were conducted and proved that e.g. *Arabidopsis*, lettuce (*Lactuca sativa*) and wheat (*Triticum aestivum* L.) could grow and complete their entire life cycle under red LEDs as the sole source of irradiation (Goins et al., 1997 & 1998; Hoenecke et al., 1992).

However, it was quickly noted that the addition of blue light improves plant stature and flowering. In example, Hoenecke et al. (1992) showed that undesirable hypocotyl extensions and cotyledon elongations of lettuce seedlings, induced by monochromatic red LEDs (660 ± 30 nm), could be prevented when the red LED illumination was supplemented with at least $15 \mu\text{mol m}^{-2} \text{s}^{-1}$ of blue light (400-500 nm) from blue, fluorescent lamps (FLs). Brown et al. (1995) also demonstrated that red LEDs supplemented with blue light (350-550 nm) from blue FLs improve the dry matter partitioning of peppers (*Capsicum annum* L.) in comparison to red LED illumination alone. The number of pepper leaves significantly increased, and their stem length drastically decreased under these red-and-blue light conditions. Also using blue FLs, Goins et al. 1997 observed larger wheat plants with greater seed yields when the red LEDs were supplemented with blue light in comparison to the monochromatic red light condition, and Yorio et al. (2001) found that dry weight accumulations of radish (*Raphanus sativus* L.), lettuce and spinach (*Spinacia oleracea* L.) significantly increased under dichromatic light conditions supplemented with blue FLs than under monochromatic red LEDs.

With the Nobel prize-winning discovery of high-brightness blue LEDs (Tsao et al., 2015) with a peak λ at 450 ± 35 nm (Nakamura et al., 1994) – thus, centering the maximal light absorption of chl *a* and *b* (Figure 4) and corresponding to the spectral region of the second highest quantum yield action during photosynthesis (Figure 5), the number of studies exploring different ratios and intensities of dichromatic red-and-blue LED arrays for various crop types exploded and continues to remain a focal point of photobiological research efforts.

Overall, additions of narrow B LEDs to narrow R LEDs are said - over-and-over-again - to improve leaf expansions, stomata openings, chlorophyll contents, photosynthetic efficiency and phytochemical contents (such as phenolics, carotenoids and volatiles), to inhibit excessive stem extensions and to reduce plant heights in various model organisms, horticultural and ornamental crops (as reviewed by Eichhorn-Bilodeau et al. (2019), Bantis et al. (2018), Hernández & Kubota (2016), Ouzounis et al. (2015) and Darko et al. (2014).

Understandably, not only the first commercial horticultural LED fixtures contained red and blue diodes (with peak λ at 660 and 450 nm, respectively), but they are still predominantly applied today (with 5-30 % of B) in growth chambers, greenhouses, vertical farms and plant factories (although nearly 100 different LED peak wavelengths (mostly within the photobiologically active radiation range) are currently available) (Kusuma et al., 2022 & 2020; Wu et al., 2020).

And as can be seen in Table 5, which summarizes the latest research findings involving differing red+blue LED combinations published since 2017, the applied light intensities (Hikosaka et al., 2021; Pennisi et al., 2020), particular R/B ratios (Hikosaka et al., 2021; Pennisi et al., 2019; Naznin et al., 2019; Hosseini et al., 2018; Lobiuc et al., 2017) as well as the specific narrow peak wavelengths (Rihan et al., 2020) can significantly affect appearance, yield and concentrations of functional and aromatic compounds in selected horticultural crops. In general, plant development and physiological functions under a particular R/B ratio accelerate and improve with increasing light intensity until the dose-dependent response peaks, plateaus and eventually becomes detrimental to the plant. In example, greatest sweet basil yields, and highest stomatal conductance were observed under a photosynthetic photon flux density (PPFD) of $250 \mu\text{mol m}^{-2} \text{s}^{-1}$ by Pennisi et al. (2020), who tested five light intensities ranging from 100 to $300 \mu\text{mol m}^{-2} \text{s}^{-1}$. Based on the review papers mentioned in the paragraph above, one may expect that e.g., phenolic compounds would increase with increasing B over R photons, however that is not the case. In example, in sweet basil cultivars, highest anthocyanin concentrations were found under low, equal and high R/B ratios (Table 5). Similarly, greatest antioxidant activities of purple sweet basil were recently detected under all three differing R/B ratios (Table 5). And lastly, no significant differences in phenolic concentrations were found in neither green nor red oakleaf lettuces under differing R/B ratios by Spalholz et al. 2020 (Table 5). To be highlighted are the recent results by Rihan et al. (2020), who showed that a shift of the narrow B wavelength from 450 nm (commonly applied) to 435 nm [in combination with R (663 nm) and nearly identical R/B ratios] significantly improves e.g., biomass and essential oil yields as well as the appearance of sweet basil (Table 5), as 435 nm represents the maximum light absorbance peak of its photosynthetic pigments (which was measured before assembling the R/B LED array).

Table 5 – Effects of different red/blue LED ratios, intensities and peak wavelengths on selected horticultural crops published in recent years.¹

Plant species	Effect ²	R/B ³ ratio	Peak λ^4	Light intensity ⁵	Photo- period	Reference
<i>Ocimum basilicum</i>	Linalool and eugenol were increased under PFD 150; DW _{Leaf} , LM _{Area} , P _{Height} and malformed leaves increased under PFD 300. β -carotene was increased under R ₁ B; DW _{Leaf} , LM _{Area} , LA, P _{Height} and malformed leaves were increased under R ₄ B ₁ .	1:4, 1:1, 4:1	665 / 466	150, 225, 300	16 h d ⁻¹	Hikosaka et al. 2021
<i>Ocimum basilicum</i>	g _s highest under PFD 200-300. FW _{Total} , EUE and LUE are the highest under PFD 250. WUE greatest under PFD 250 and 300.	3:1	669 / 465	100, 150, 200, 250, 300	16 h d ⁻¹	Pennisi et al. 2020
<i>Ocimum basilicum</i>	FW _{Total} , P _{Height} , Stem _{Diam} , L _{No} , LA, g _s , Pn, EO yield and LUE were reduced under RB 1:1, while increased under RB 1:1.4.	1:1, 1:1.5; 1:1.4	663 / 450 663 / 435	300	16 h d ⁻¹	Rihan et al. 2020
<i>Lactuca sativa</i> 'Green Oakleaf' & 'Red Oakleaf'	In 'Green Oakleaf', FW _{Total} , DW _{Total} , LA, L _{No} , L _{Stem} , TPC indifferent between treatments. In 'Red Oakleaf', DW _{Total} reduced under RB 1:4; FW _{Total} , LA, L _{No} , L _{Stem} , TAC indifferent between treatments.	1:4, 1:1, 1:4	659 / 452	200	18 h d ⁻¹	Spalholz et al. 2020
<i>Ocimum basilicum</i>	Chl reduced under R ₁ B ₂ and R ₂ B ₁ , increased under R ₃ B ₁ . While WUE reduced under R ₁ B ₂ , increased under R ₃ B ₁ . FW _{Total} reduced under R ₁ B ₁ , increased under R ₃ B ₁ . F _v /F _m , g _s , α -bergamotene and NUE increased under R ₁ B ₂ . TFC reduced under R ₁ B ₂ , increased under R ₃ B ₁ . Linalool reduced under R ₁ B ₂ , increased under R ₂ B ₁ . EUE, AOC and mineral concentrations increased under R ₃ B ₁ . α -bergamotene reduced under R ₄ B ₁ .	1:2, 1:1, 2:1, 3:1, 4:1	669 / 465	215	16 h d ⁻¹	Pennisi et al. 2019
<i>Lactuca sativa</i>	Chl <i>b</i> reduced under R _{4.9} B ₁ , increased under R ₁₀ B ₁ . Chl <i>a</i> and chl increased under R ₁₀ B ₁ . AOC increased under R _{4.9} B ₁ , reduced under R ₁₉ B ₁ . Car decreased under R ₁₉ B ₁ .	4.9:1, 10:1, 19:1	661 / 449	200	16 h d ⁻¹	Naznin et al. 2019

<i>Spinacia oleracea</i>	Chl <i>a</i> decreased under R _{4.9} B ₁ . AOC increased under R _{4.9} B ₁ , decreased under R ₁₉ B ₁ . Chl <i>b</i> and chl increased under R ₁₀ B ₁ . Car decreased under R ₁₉ B ₁ .	4.9:1, 10:1, 19:1	661 / 449	200	16 h d ⁻¹	Naznin et al. 2019
<i>Brassica oleracea</i> var. <i>sabellica</i>	FW _{Total} , chl <i>a</i> , chl <i>b</i> and chl decreased, while car and AOC increased under R _{4.9} B ₁ . Chl <i>a</i> , chl <i>b</i> and chl increased, while AOC decreased under R ₁₉ B ₁ .	4.9:1, 10:1, 19:1	661 / 449	200	16 h d ⁻¹	Naznin et al. 2019
<i>Ocimum basilicum</i>	Chl <i>a</i> and chl decreased under R _{4.9} B ₁ , increased under R ₁₀ B ₁ . Car increased under R _{4.9} B ₁ , decreased under R ₁₉ B ₁ . Chl <i>b</i> increased under R ₁₀ B ₁ . AOC increased and decreased under R _{4.9} B ₁ and R ₁₉ B ₁ respectively.	4.9:1, 10:1, 19:1	661 / 449	200	16 h d ⁻¹	Naznin et al. 2019
<i>Capsicum annuum</i>	P _{Height} , FW _{Total} decreased under R _{4.9} B ₁ , increased under R ₁₉ B ₁ . Chl <i>a</i> , chl decreased under R _{4.9} B ₁ , increased under R ₁₀ B ₁ . Car, AOC increased under R ₁₀ B ₁ , decreased under R ₁₉ B ₁ . Chl <i>b</i> increased under R ₁₀ B ₁ . DW _{Total} decreased, but L _{No} , flower initiation and Fruit _{No} increased under R ₁₉ B ₁ .	4.9:1, 10:1, 19:1	661 / 449	200	16 h d ⁻¹	Naznin et al. 2019
<i>Ocimum basilicum</i> Green 'Mobarake'	TAC and methyl chavicol increased under R ₁ B ₁ . AOC, TPC, α-pinene and 1,8-cineole increased under R _{2.3} B ₁ .	1:1, 2.3:1	660 / 450	250	16 h d ⁻¹	Hosseini et al. 2018
<i>Ocimum basilicum</i> Purple 'Ardestan'	While methyl chavicol increased under R ₁ B ₁ , AOC, TPC, TAC, limonene, α-pinene, fenchone and neral increased under R _{2.3} B ₁ .	1:1, 2.3:1	660 / 450	250	16 h d ⁻¹	Hosseini et al. 2018
<i>Ocimum basilicum</i> 'Sweet Genovese'	Cotyledone size, chl <i>a</i> , car and TFC indifferent between treatments. FW _{Total} and TPC reduced under R ₁ B ₂ . DW _{Total} and TPC increased, and TAC decreased under R ₂ B ₁ .	1:2, 1:1, 2:1	660 / 450	120	12 h d ⁻¹	Lobiuc et al. 2017

	Chl <i>a</i> , car and TFC indifferent between treatments.					
<i>Ocimum basilicum</i> 'Red Rubin'	Caffeic and rosmarinic acid increased under R ₁ B ₂ , reduced under R ₂ B ₁ . TAC increased and AOC decreased under R ₂ B ₁ .	1:2, 1:1, 2:1	660 / 450	120	12 h d ⁻¹	Lobiuc et al. 2017

¹ The reader may also be referred to Hernández & Kubota, 2016, Kang et al., 2016 and Son & Oh, 2015 cited in Table 7; Zhang et al., 2022, Jin et al., 2021, Ji et al., 2019 & 2020, Zou et al., 2019, Fanwoua et al., 2019, Meng & Runkle, 2019a, Kalaitzoglou et al., 2019, Meng et al., 2019, Kim et al., 2018, Craver et al., 2018, Park & Runkle, 2017 & 2018 and Zhen & van Iersel, 2017 cited in Table 8; Ke et al., 2022, Rihan et al., 2022, Zhang et al., 2018 and Han et al., 2017 cited in Table 9; Araújo et al. (2021), Hsie et al. (2019), Lazzarini et al. (2018) cited in Table 10.

² Descriptions of abbreviations are listed in alphabetical order: AOC = antioxidant capacity, car = carotenoid, chl *a* = chlorophyll *a*, chl *b* = chlorophyll *b*, chl = total chlorophyll content, DW_{Leaf} = leaf dry weight, DW_{Total} = total dry weight, EO yield = essential oil yield, EUE = energy use efficiency, Fruit_{No} = number of fruits, F_v/F_m = maximum quantum efficiency of photosystem II, FW_{Total} = total fresh weight, g_s = stomatal conductance (mmol CO₂ m⁻² s⁻¹), LA = leaf area, LM_{Area} = leaf mass per area, L_{No} = number of leaves, L_{Stem} = stem length, LUE = light use efficiency, NUE = nutrient use efficiency, P_{Height} = plant height, *Pn* = photosynthetic rate (μg cm⁻² s⁻¹), Stem_{Diam} = stem diameter, TAC = total anthocyanin content, TFC = total flavonoid content, TPC = total phenolic content, WUE = water use efficiency.

³ R/B: red and blue light.

⁴ Peak wavelength (λ) given in nanometers [nm].

⁵ Light intensity is expressed as photosynthetic photon flux density (PPFD) given in micromole per square meter and second (μmol m⁻² s⁻¹).

1.4.2 Influence of ultraviolet, green and far-red wavelengths on plant development

With the advancements in LED lighting technology, LED-based research started to focus on LED lighting composed of photons from the ultraviolet (280-400 nm), the green (500-600 nm) and/or the far-red (700-800 nm) range of the light spectrum sensed by plants, and found that illumination at these spectral ranges can improve important horticultural objectives such as plant yields, appearances and flowering times, phytochemical contents and their dietary value as well as the plants' resistances to herbivores and pathogens. The following three sections will therefore give an overview of the many morphological, physiological and phytochemical effects mediated by supplemental UV, G and FR wavelengths.

1.4.2.1 Plant responses to ultraviolet radiation (λ 280-400 nm)

Ultraviolet (UV) radiation (100-400 nm) is generally subdivided into UV-C (100-280 nm), UV-B (280-315 nm) and UV-A (315-400 nm) radiation (Lee et al., 2021). The sun's highly energetic UV-C emissions are completely, and the sun's UV-B emissions are mostly absorbed by the earth's stratospheric ozone shield. As a result, the comparatively small fraction of terrestrial UV light from 280 to 400 nm, representing around 5 % of the terrestrial solar radiation, consists of only around 1.5 % of UV-B and 98-99 % of UV-A radiation (Lee et al., 2021; Chen et al., 2019; Neugart & Schreiner, 2018). Hence, UV-B represents a minor and UV-A the mayor type of UV radiation available to plants on Earth. Therefore, only plant responses to UV-A and -B will be addressed in further detail.

While excessive UV radiation is known to be detrimental as it can lead to photoinhibitions and the generation of reactive oxygen species (ROS), limited plant growths and/or damages of the plants' DNA, proteins and lipids (e.g. Choudhury et al., 2017; Hideg et al., 2013), multiple reviews have highlighted some beneficial effects of low, ecologically-relevant UV-A and UV-B levels on plant growth, photosynthesis, morphology and secondary metabolism (Vázquez-Hernández et al., 2019; Bantis et al., 2018; Neugart & Schreiner, 2018; Verdaguer et al., 2017; Huché-Thélier et al., 2016; Jenkins, 2014).

However, experimental design limitations, especially the use of different cut-off filters and UV-A lamps whose spectral outputs exceed into the UV-B (< 315 nm) and B (> 400 nm) range, have obstructed UV-A studies independent of its flanking regions and resulted in inconsistent reports in the past (Chen et al., 2019; Neugart & Schreiner, 2018). Due to technological LED advancements in recent years, the exploration of UV-A effects on plants is currently gaining momentum (Table 6), and notable possibilities are emerging for the horticultural sector.

UV-B irradiations usually reduce the height of plants by suppressing stem and internode elongations and reduce the expansion of leaves – effects that have been observed in all investigated

horticultural and agricultural crops (Lee et al., 2021a; Qian et al., 2020; Neugart & Schreiner, 2018; Jenkins, 2014) and are to be attributed to UVR8 photoreceptor signaling (as described in section 1.3.2.2.4). Consequently, biomass productions are commonly reduced under UV-B wavelengths (Neugart & Schreiner, 2018).

The effects of UV-A on plant height and leaf expansion require a more differentiated view, however. While UV-A resulted in reduced stem and internode elongations in the majority of case studies (Yang et al., 2022; Qian et al., 2020; Neugart & Schreiner, 2018) and can be attributed to cryptochrome signaling (as described in section 1.3.2.2.2), additions of UV-A with $\lambda_s \geq 369$ nm to differing spectral backgrounds have increased the heights of kale and bok choy baby leaves (Li et al., 2020a), of kale (Gao et al., 2022) and of tomato seedlings (Kang et al., 2018). It is reasonable to believe that these observed elongations are associated with increased plant assimilations because long wavelengths of UV-A are known to be photosynthetically active (as established in sections 1.3.1.3 and 1.3.14). In addition, differing impacts of UV-A on leaf expansions have been reported. Lettuce leaf areas increased under different intensities (10, 20 and 30 $\mu\text{mol m}^{-2} \text{s}^{-1}$) and durations (10 $\mu\text{mol m}^{-2} \text{s}^{-1}$ for 5, 10 and 15 days prior harvest) of supplemental UV-A (365 nm) compared to a control lighting without UV-A (Chen et al. 2019). Interestingly, leaf areas of mustard microgreens increased with increasing wavelengths (366, 390 and 402 nm) when exposed to 10 h d^{-1} but increased only under 402 nm (= blue wavelength) when exposed to 16 h d^{-1} . In contrast, leaf expansions of cucumber seedlings remained indifferent after UV-A supplementation under greenhouse conditions (Yan et al. 2022, specific UV-A peak wavelengths not provided, however). The surface area of kale and red leaf lettuce leaves also remained unchanged after UV-A supplementation as published by Gao et al. (2022) and Samouliene et al. (2020). When supplied just prior to harvest under controlled conditions, leaf expansions of kale and ice plants also remained indifferent after supplementations with different (363, 375, 385 and 395 nm) narrow UV-A-emitting LEDs compared to control treatments without additional UV-A (Choi et al. 2022; Lee et al. 2021). These findings taken together indicate that leaf areas can increase if species-dependent intensity and/or duration thresholds are not exceeded. These findings also indicating a wavelength-specificity: It appears, leaf expansions commonly increase with increasing UV-A wavelengths towards the blue range of light, which is most likely under the influence of multiple photoreceptors (e.g., UV-A-sensing phytochromes, cryptochromes and phototropins) known to control the expansion of leaves in blue backgrounds (as described in sections 1.4.1 and 1.4.2.2). In addition, as the specific leaf mass (mg cm^{-2}) increased in kale exposed to continuous supplemental UV-A (24 h exposure with 370 nm and 385 nm, respectively) for five days prior to harvest (Lee et al. 2019), it is also reasonable to assume that plants acclimate to damagingly

high intensities of UV-A by increasing the thickness of its leaves, which is a well-known acclimation response of UV-B exposed plants (Neugart & Schreiner, 2018).

As observed by Yan et al. (2022) and Samuoliene et al. (2020) in cucumber seedlings and red leaf lettuces, UV-A-induced suppressions of stem elongations and/or inhibited leaf expansions result in reduced biomasses. However, in the vast majority of recent research, increased biomass accumulations upon UV-A exposures have been found and appear to correlate well with increased photosynthetic activities and/or structural plant acclimations observed in these studies: In example, with increasing UV-A wavelengths, Choi et al. (2022) detected increasing photosynthetic rates (Pn , $\mu\text{mol CO}_2 \text{ m}^{-2} \text{ s}^{-1}$) as well as increasing shoot dry weights in kale. Similarly, shoot and root dry weights of kale increased under UV-A exposures of differing duration (6 and 12 h d^{-1}) (Gao et al., 2022) as well as under differing wavelengths (370 and 380 nm) (Lee et al., 2019), and were associated with improved maximum quantum efficiencies (F_v/F_m) and improved quantum yield efficiencies (Φ_{PSII}) of PS II in both independent studies. Also in ice plants, UV-A-induced biomass increases were concomitant with increased Pns (Lee et al., 2021). Further, though internode lengths decreased in UV-A exposed cucumber seedlings, increased stem weights, stem sturdiness, leaf and root weights were observed by Qian et al. (2020). Also, the studies by Li et al. (2020a) and Chen et al. (2019) indirectly support an increase in photosynthetic activities because the number of kale and bok choy baby leaves and lettuce leaves were found to be increased due to supplemental UV-A radiation. That contents of chlorophyll and/or carotenoid pigments do more often than not increase under low UV-A supplementations (Yan et al., 2022; Gao et al. 2022; Lee et al., 2021; Samuoliene et al., 2020; Li et al., 2020a; Mao et al., 2020) further substantiates the ability of plants to enhance their photosynthetic assimilations under UV-A supplemented conditions. In contrast, UV-B exposures are generally associated with low photosynthetic pigment contents and assimilations (Li et al., 2020; Neugart & Schreiner, 2018).

Aside from the effects of low UV doses on plant morphology, photosynthesis and growth described above, UV radiations are known to upregulate the biosynthesis of phenylpropanoids and glucosinolates.

Phenylpropanoids represent essential components of cell walls, provide protection from excessive and UV irradiations, defend against herbivores and pathogens and mediate plant-pollinator interactions as floral pigments and scent compounds (Deng & Lu, 2017). They derive from the shikimate pathway, that is used by plants (as well as by bacteria, archaea, fungi and algae) to synthesize vitamin B₉ and three aromatic amino acids (namely tyrosine, tryptophan and phenylalanine) (Maeda & Dudareva, 2012). While the intake of tyrosine is non-essential, tryptophan and phenylalanine represent indispensable amino acids for humans as we cannot synthesize them in adequate quantities (Maeda & Dudareva, 2012; Hyun et al., 2011).

Within three enzymatic steps, phenylalanine becomes transformed into 4-coumaroyl-coenzyme-A, the central intermediate in the biosynthesis of myriads of phenylpropanoids, including flavonoids and hydroxycinnamic acids among many others (Deng & Lu, 2017).

But before UV effects on some of these investigated phenylpropanoids are described in more detail in this chapter, it is important to note that Li et al. (2020) and Qian et al. (2019) observed increased gene expressions of the phenylpropanoid pathway in purple tea and cucumber seedlings exposed to supplemental UV-A and UV-A/B radiations – a phenomenon well-known for plants exposed to UV-B radiations (Neugart & Schreiner, 2018). In addition, gene expression levels and/or enzymatic activities of phenylalanine ammonia lyase (PAL) - the enzyme that catalyzes the conversion of phenylalanine to cinnamic acid (Deng & Lu, 2017) - were found to be increased under supplemental UV-A in kale, and under supplemental UV-A and UV-B in cucumber seedlings (Choi et al., 2022; Qian et al., 2019). Also, the genetic expression of cinnamate 4-hydroxylase – the enzyme that transforms cinnamic acid into coumaric acid (Deng & Lu, 2017) – was found to be increased in these cucumber seedlings under both supplemental UV treatments (Qian et al., 2019).

Flavonoids, an important class of phenylpropanoids, have diverse roles in plant physiology and human health: Besides the various pigmentations they provide to flowers, fruits, seeds and leaves to attract pollinators and seed dispersers, flavonoids protect plants against abiotic and biotic stresses such as threatening radiations, low temperatures, pathogen infections and herbivorous attacks. Upon these exposures, the biosynthesis of flavonoids becomes induced to attenuate possible DNA, lipid and protein degradations (Neugart & Schreiner, 2018; Deng & Lu, 2017).

While UV-B irradiations are already well-known to enhance flavonoid accumulations in plants (Neugart & Schreiner, 2018), similar effects of UV-A irradiations were published recently as well. Total flavonoid contents (TFC) increased in kale when exposed to 30 W m^{-2} of different narrow UV-A wavebands for seven days prior to harvest (Choi et al., 2022) and when exposed to 20 and $30 \mu\text{mol m}^{-2} \text{ s}^{-1}$ of 365 nm for 13 days prior to harvest (Chen et al., 2019). In addition, though TFC remained statistically indifferent in kale when exposed to $40 \mu\text{mol m}^{-2} \text{ s}^{-1}$ for different daily UV-A durations (6 and 12 h d^{-1} with 380 nm), an increasing trend in TFC was still observable (Gao et al., 2022), indicating that the accumulation of flavonoids upon UV-A is wavelength- and intensity-dependent. In contrast, TFC was found to decrease in purple tea upon four hours of daily exposures with 600 mW m^{-2} of UV-A and/or UV-B (Li et al., 2020) and underlines species-dependent responses to UV.

Similarly, contents of specific biologically active flavonoids with tremendous health benefits for humans have been repeatedly found to increase under UV-A radiation: Anthocyanins – strong antioxidants

with anti-inflammatory and neuroprotective effects, potentials against cancer, obesity and diabetes and with cardiovascular benefits (Li et al., 2015) – increased in the leaves of tea, red and green bok choy as well as in red and green lettuces upon different UV-A exposures (Li et al., 2020; Mao et al., 2020; Chen et al., 2019; Samuoliene et al., 2020). In a greenhouse experiment however, total anthocyanin contents (TAC) remained indifferent in kale and bok choy baby leaves compared to their control treatments when irradiated with 40 W m^{-2} of UV-A (380 nm) for twelve hours daily. Instead, TACs increased only under narrow B wavelengths in this study (Li et al., 2020a). Contents of the flavonoid luteolin – a strong anticancer agent (Imran et al., 2019) – were increased in red leaf lettuce and remained indifferent in green leaf lettuce under UV-A exposures but were found to be decreased under UV-A/B and UV-B exposures in both lettuce cultivars (Lee et al., 2021a), suggesting UV wavelengths- and species-dependency. The same study found analogous effects for apigenin – a flavonoid effective against various types of cancer, diabetes, arthritis, memory loss, depression and sleeplessness (Salehi et al., 2019; Ali et al., 2017). Another important flavonoid is quercetin - due to its cardioprotective effects (Dmello et al., 2023) - which was found in increased concentrations upon supplemental UV-A radiation in red leaf lettuce and kale baby leaves (Lee et al., 2021a; Li et al., 2020). However, an UV-A exposure did not change the content of quercetin in bok choy baby leaves in the study by Li et al. (2020a). Finally, also contents of kaempferol – a flavonoid with beneficial effects against asthma, cancer, diabetes, obesity and cardiovascular diseases (Imran et al., 2018) – can be improved by UV-A in kale and kale baby leaves (Lee et al., 2019; Li et al., 2020a) and by UV-A/B and UV-B in tomatoes (Lee et al., 2021a), though kaempferol contents remained indifferent in bok choy baby leaves and tomatoes upon UV-A exposure (Lee et al., 2021a; Li et al., 2020a). These findings clearly show that the accumulation of various health-promoting flavonoids can be enhanced under UV-A and/or UV-B. Though, wavelength, intensity and duration as well as the species and cultivar clearly influence the outcome, genetic studies conducted by Li et al. (2020), Qian et al. (2019) and Choi et al. (2022) verify the fact that UVs increase the biosynthesis of flavonoids because the genetic expression and/or enzyme activity levels of chalcone synthase (the first committed enzyme in flavonoid biosynthesis), flavonoid 3-hydroxylase and anthocyanidin synthase were found to be significantly enhanced under various supplemental UV treatments.

Another important class of phenylpropanoids, whose contents are also influenced by UV radiation are hydroxycinnamic acids. These phenolic acids are intermediates in the biosynthesis of lignin, which represents the structural material of plant tissues and confers the rigidity of cell walls (Humphrey & Chapple, 2002)). As reviewed by Coman & Vodnar (2019), these hydroxycinnamic acids were also shown to be beneficial to human health: Caffeic acid (CA), the main representative of hydroxycinnamic acids (and

phenolic acids in general), has shown antioxidant, anti-inflammatory, anti-cancer and anti-HIV activities (Touaibia et al., 2011). Its contents were elevated upon UV-A exposure in kale (Lee et al., 2019). In lettuce however, UV-A did not alter CA content. Instead, only exposures of supplemental UV-B and UV-A/B increased the lettuces' CA contents (Lee et al., 2021a). In the same study, contents of chlorogenic acid (a derivative of caffeic acid with antioxidant, antibacterial, anti-viral, anti-inflammatory, fever-reducing, anti-obesity, hepato-, cardio- and neuro-protective properties (Naveed et al., 2018)) also remained indifferent upon UV-A exposure, but decreased upon UV-B and UV-A/B. Further, both contents of chicoric acid (another derivative of caffeic acid with antioxidant, anti-inflammatory, anti-viral, anti-aging, neuroprotective and immune-stimulating properties (Yang et al., 2022)) and of ferulic acid (also a derivative of caffeic acid with antioxidant, anti-inflammatory, anti-fibrosis, anti-apoptosis and anti-platelet effects (Li et al., 2021)) were increased after supplemental UV-A was employed on tomatoes (Lee et al., 2021a) and kale (Lee et al., 2019), respectively. That total phenolic contents (TPC) and antioxidant capacities (AOC) (which strongly correlate with one another (Noreen et al., 2017)) were both found to be heightened upon UV radiations in the vast majority of recent studies further confirms the potential of UV light to improve these health-supporting phytochemicals.

Finally, previous investigations on multiple cabbage species (including bok choy, broccoli, brussel sprouts and kale) concluded that different UV-A wavelengths, intensities and durations could promote the biosynthesis and accumulation of glucosinolates (Gao et al., 2022, Mao et al., 2020, Li et al., 2020 & 2020a). Glucosinolates impart the characteristic pungent taste and flavor to these cruciferous vegetables and function as plant defenses against a variety of pests and diseases (Liu et al., 2021).

Though all described UV effects are clearly wavelength-, intensity and duration-dependent and can differ between species and even cultivars, the implementation of UV lighting has the potential to benefit not only the horticultural industry but also human health by improving plant stature and their nutritional qualities.

When applied as a mild abiotic stress, UV radiation can be used effectively to produce shorter, more compact and sturdy plants – a phenotype preferred not only during cultivation in space-limited multi-leveled plant factories and during subsequent transport, but also by the consumers. Additionally, the repeatedly observed UV-induced enrichments of many secondary metabolites could substantially contribute to improve the visual appearance of plants (e.g., by increasing anthocyanin and other flavonoid pigment concentrations), enhance the aroma and taste of fruits, vegetables and herbs (e.g., by increasing glucosinolate and aromatic phenylpropanoid contents), better the nutritional quality (e.g., by increasing phenolic acid, vitamin and nutrient contents).

In addition, though UV wavebands are currently still excluded from what is considered photosynthetically active radiation (as described in section 1.3.1.4), supplemental UV-A wavelengths (especially when nearing the blue spectrum) have repetitively shown to accelerate plant development. Thus, UV-A could help in shortening production cycles.

However, because UV-emitting LEDs are currently more expensive and less cost-effective than LEDs that emit longer wavelengths (as described in section 1.2) and given the fact that excessive levels of UV radiation cause damages to plants, short-term supplemental UV radiations just prior to harvest are recommended, and minimal radiation requirements ought to be investigated.

Table 6 – Morphological, physiological and phytochemical effects mediated by ultraviolet wavelengths (λ 280-400 nm).⁴

Plant species	Effect ¹	Light spectrum	Peak λ^2	Light intensity and duration ³	Reference
<i>Lilium candidum</i> bulblets	Under RB+UV-A, L_{Length} , $Root_{No}$, ratio of bulbscales regenerating roots and car decreased in comparison to RB, $bulblets_{No}$, $bulblets$ diameter, $Root_{Length}$, chl and $Sugar_{Sol}$ contents tended to decrease, however, number and ratio of bulbscales regenerating bulblets with leaves and $phenol_{Sol}$ content remained indifferent between multichromatic treatments.	R_{670} , B_{430} , R_{7B3} , RG_{528B} , RB_{Y600} , RB+UV-A, $RBFR_{730}$, $W_{400-750}$, FL	400	40; 20 of UV-A	Palka et al. 2023
<i>Cucumis sativus</i> seedlings 'Tianjiao No. 5'	In a greenhouse experiment, all supplemental LED light treatments reduced $Hypo_{Length}$, P_{Height} and SLA, and increased L_{Length} and substomatal CO_2 contents compared to solar light alone (control). All supplemental LED treatments but UV-A increased SQI, $Stem_{Diam}$, L_{Width} , LA, mesophyll conductance, FW_{Shoot} , DW_{Shoot} , FW_{Root} , DW_{Root} , R_{Length} , RSA, R_{Volume} , $R_{Activity}$ in comparison to control. Of all supplemental treatments, UV-A increased chl content, Pn and g_s , Tr, $Stem_{Firmness}$, cellulose content and decreased stomatal limitation value the least. Of all supplemental treatments, cytokinin content and LUE were greatest under UV-A.	Sun \pm W; UV-A; W+B; W+UV-A; W+B+UV-A	na	Sun (128) + LED (180); 15 of UV-A	Yan et al. 2022
<i>Brassica oleracea</i> var. <i>acephala</i>	395 and 405 nm improved most of the assessed growth characteristics and photosynthetic rates compared to control. DW_{Shoot} , Pn increased with increasing UV-A wavelength. Only 405 nm increased LA in comparison to control. 375-405 nm increased DW_{Root} in comparison to control. $Leaf_{No}$ remained indifferent between treatments. F_v/F_m started to decrease after 1 day of UV exposure; after 5 days, ROS increased with decreasing UV-A wavelengths; TPC, TFC and AOC were	R_{655} + $W_{456/558}$ + B_{456} \pm UV-A	363, 375, 385, 395, 405	150 \pm UV-A ⁴ (for 7 d PTH)	Choi et al. 2022

⁴ The reader may also be referred to the following review articles: Landi et al. (2020), Bantis et al. (2018), Neugart & Schreiner (2018), Verdaguer et al. (2017), Huché-Thélier et al. (2016) and Jenkins (2014), to the studies by Semenova et al. (2022) cited in Table 10.

	<p>increased after 7 days under all UV-A treatments compared to the control treatment.</p> <p>PAL and CHS gene expression and PAL enzyme activity increased under supplemental UV-A treatments in comparison to the control treatment, however, remained indifferent between UV-A treatments.</p>				
<i>Brassica alboglabra</i> 'Lvobao'	<p>Additions of UV-A equally increased FW_{Shoot}, DW_{Shoot}, DW_{Root}, SLW, $Sugar_{Sol}$, F_v/F_m, Φ_{PSII}, UVR8 gene expression, transcription factor genes and genes related to the GL biosynthesis pathway and GL accumulation.</p> <p>Compared to control, 12 h UV-A exposure increased P_{Height} and chl contents, and decreased time to flowering and car contents more than 6 h UV-A treatment.</p> <p>Only 6 h UV-A treatment decreased nitrate contents.</p> <p>Only 12 h UV-A treatment increased $Stem_{Diam}$.</p> <p>Leaf_{No}, LA, NPQ, qP, qL, ETR, Protein_{Sol}, TPC, TFC, AscAC, AOC and content of mineral elements remained indifferent between treatments.</p>	<p>W₃₅₀₋₇₅₀ with elevated R₆₅₅ and to a lesser extent B₄₅₀ ± UV-A</p>	380	250 ± 40 of UV-A (for 0, 6, 12 h d ⁻¹)	Gao et al. 2022
<i>Mesembryanth e-mum crystallinum</i>	<p>375-395 nm increased DW_{Shoot}, tended to increase FW_{Shoot}, LA and chl in comparison to control.</p> <p>While only 385 and 395 nm increased P_n during the day, all UV-A treatments increased P_n during the night.</p> <p>All UV-A treatments enhanced TPC, AOC, PAL activity and contents of pinitol, myo-inositol and sucrose, decreased F_v/F_m compared to control.</p>	<p>W₄₀₀₋₇₀₀ with elevated R₆₆₀ and to a lesser extent B₄₄₅ ± UV-A</p>	365, 375, 385, 395	200 ± UV-A ⁴ (for 7 d PTH)	Lee et al. 2021
<i>Lactuca sativa</i> 'New Red Fire' & green 'Two Star'	<p>In a greenhouse experiment, FW_{Shoot}, DW_{Shoot}, chl, car remained indifferent between treatments in both cultivars.</p> <p>In green leaf lettuce, all UV treatments increased protein concentrations, UV-B increased FW_{Root}, however, DW_{Root}, LA and AOC remained indifferent between all treatments; UV-B and UV-A/B increased caffeic acid contents, but decreased chlorogenic acid, luteolin and apigenin contents.</p> <p>In red leaf lettuce, all UV treatments inhibited FW_{Root}, DW_{Root}, UV-A treatment increased TPC (incl. luteolin, quercetin, apigenin), AOC tended to increase; UV-B and UV-A/B treatments decreased LA, luteolin, apigenin; UV-A/B increased chl <i>b</i> contents.</p>	<p>Sun ± UV-A; UV-B; UV-A/B</p>	340, 313	Sun (719) + UVs ⁴ : UV-A 24 h d ⁻¹ for 5 d PTH; UV-B 2 h d ⁻¹ for 4 d PTH; UV-AB 2 h d ⁻¹ for 2 d, then 4 h d ⁻¹ for 2 d PTH)	Lee et al. 2021a

<i>Solanum lycopersicum</i> 'BHN-589'	<p>In a greenhouse experiment, UV-B (6 and 9 h exposure) and UV-A/B (3 and 9 h exposure) increased TPC in tomato fruits, however, TPC remained indifferent under UV-A; chlorogenic acid increased under UV-A and UV-A/B (3 h exposure); caffeic acid increased under UV-A/B (3 h exposure), however, decreased under 9 h exposure; chicoric acid increased under UV-A, UV-B (6 h exposure) and UV-A/B (3 and 9 h exposure); luteolin decreased under UV-B (3 h) but increased under UV-A/B (3h); apigenin increased under UV-A, UV-A/B (3 and 6 h); kaempferol increased under UV-B (9 h), UV-A/B (3, 6 and 9 h) in ripe tomato fruits.</p> <p>UV-A increased lutein and β-carotene, while UV-A/B increased lycopene in ripe tomatoes.</p> <p>Protein and nutrient contents, AOC remained indifferent between all treatments.</p>	Sun + UV-A; UV-B; UV-A/B	340, 313	Sun (719) + UVs ⁴ : UV-A 24 h d ⁻¹ for 6 d PTH; UV-B 1.5 h d ⁻¹ for 2, 4 and 6 d PTH (3, 6, 9 h); UV-AB 1.5 h d ⁻¹ for 2 d for 2, 4 and 6 d PTH (3, 6, 9 h)	Lee et al. 2021a
<i>Lactuca sativa</i> 'Maiko'	<p>While 387 nm increased car, TAC and Φ_{PSII}, 367 and 402 nm decreased TAC.</p> <p>While 402 nm tended to increase DW_{Leaf}, 367 and 387 nm tended to decrease DW_{Leaf}.</p> <p>While 402 nm increased LA, 367 nm decreased, and 387 nm tended to decrease LA in comparison to RB alone.</p> <p>Pn, gS and LUE increased under 367 and 402 nm and tended to increase under 387 nm compared to RB.</p> <p>While Tr increased under 367 nm, Tr remained indifferent between other treatments.</p> <p>367 nm decreased F_v/F_m.</p> <p>NPQ remained indifferent between treatments.</p> <p>While 402 nm increased and 367 and 387 nm decreased sucrose contents compared to RB, fructose and glucose contents increased and raffinose decreased under all UV treatments compared to RB.</p>	R ₆₆₅ B ₄₄₇ ± UVs	367, 387, 402	250 ± UVs ⁴	Samuoliene et al. 2020
<i>Cucumis sativus</i> 'Hi Jack' seedlings	<p>Internode_{Length} decreased under both UV treatments, however, decreased more under UV-B.</p> <p>Internode_{Diam} decreased under UV-B but remained indifferent between UV-A and control.</p>	Sun + HPS ± UV-A or UV-B	340, na	Sun + 150-200 (HPS) ± UVs ⁴ (for 4 h d ⁻¹)	Qian et al. 2020

	<p>Stem weight per unit Stem_{Length} and sturdiness increased under UV-A and decreased under UV-B compared to control.</p> <p>UV-A increased SLM, DW_{Leaf}, DW_{Root}, however, DW_{Stem} remained indifferent compared to control.</p> <p>UV-B decreased SLM, DW_{Shoot}, DW_{Stem}, DW_{Root} and delayed fruiting compared to control.</p> <p>F_v/F_m, FW_{Fruit} remained indifferent between treatments.</p>				
<i>Camellia sinensis</i> 'Ziyan'	<p>All UV treatments increased TAC, enzyme activities of CHS, F3H and ANS, and decreased TFC, enzyme activities of LAR and ANR, car and chl compared to W in dark purple tea leaves; however, DFR activity remained indifferent between treatments.</p> <p>UV-A increased TAC the most.</p> <p>While UV-A and UV-A/B treatments upregulated structural and regulatory genes in the anthocyanin pathway differently, UV-B decreased most structural genes involved in the phenylpropanoid and flavonoid pathways compared to control.</p>	<p>W_{na} ±</p> <p>UV-A;</p> <p>UV-B;</p> <p>UV-A/B</p>	<p>311;</p> <p>365</p>	<p>200 ± UVs⁴</p> <p>(for 4 h d⁻¹)</p>	<p>Li et al.</p> <p>2020</p>
<i>Brassica alboglabra</i> 'Bailey' baby leaves	<p>In a greenhouse, additions of all λs increased FW_{Leaf}, DW_{Leaf}, P_{Height}, Leaf_{Width} and Leaf_{No} compared to control treatment; Leaf_{Length} was increased by supplemental 380, 430 and 564 nm, however not by 400 nm; Smallest differences were observed between 400 nm and control.</p> <p>Chl, car, kaempfer, AOC and ProteinSol were increased by all supplemental λs; TAC increased by 430 and 465 nm only; AscAC and TPC increased under supplemental B only (λs ≥ 400); quercetin and Sugar_{Sol} increased only under 380 and 400 nm; vitamin E remained indifferent between all treatments.</p> <p>B λs (≥ 400) increased total GLs more than UV-A (380 nm) compared to control.</p> <p>All λs decreased K, Ca, Mg, Zn and Fe contents (g kg⁻¹ DW); all supplemental λs but 430 nm increased P content; S contents remained indifferent between all treatments.</p>	<p>SUN ±</p> <p>B; UV-A</p>	<p>380,</p> <p>400,</p> <p>430,</p> <p>465</p>	<p>400-1000 ±</p> <p>B; UV-A⁴ (for</p> <p>12 h d⁻¹ for</p> <p>10 d)</p>	<p>Li et al.</p> <p>2020a</p>
<i>Brassica campestris</i> 'Makino' baby leaves	<p>In a greenhouse, additions of all λs increased FW_{Leaf}, DW_{Leaf}, Leaf_{Length} and Leaf_{No} compared to control treatment; P_{Height}, TAC, kaempfer and quercetin contents were increased by supplemental B only (λ ≥ 400 nm); Leaf_{Width} was increased by supplemental 380, 430 and 465 nm.</p>	<p>SUN ±</p> <p>B; UV-A</p>	<p>380,</p> <p>400,</p> <p>430,</p> <p>465</p>	<p>400-1000 ±</p> <p>B; UV-A⁴ (for</p> <p>12 h d⁻¹ for</p> <p>10 d)</p>	<p>Li et al.</p> <p>2020a</p>

	<p>Chl, car, AOC, TPC and ProteinSol were increased by all supplemental λs; vitamin E and Sugar_{Sol} increased only under 430 nm; AscAC was increased by supplemental 380, 430 and 564 nm.</p> <p>While supplemental 400 nm increased total GLs, 430 and 465 nm decreased total GLs; no difference in GLs between UV-A (380 nm) and control.</p> <p>All λs decreased K, Ca, Mg, Zn and Fe contents; all supplemental λs but 430 nm increased P; S remained indifferent between all treatments.</p>				
<i>Brassica rapa</i> (Red and green bok choy)	<p>In a greenhouse, supplemental B and UV-A increased FW_{Total}, FW_{Shoot}, FW_{Root}, DW_{Total}, DW_{Shoot}, DW_{Root} and Protein_{Sol} contents in both cultivars. TAC and AOC increased, and nitrate contents decreased with decreasing λs in both cultivars.</p> <p>In red bok choy, chl increased under 380-430 nm; car increased under 400-460 nm; TFC increased and Sugar_{Sol} decreased under all supplemental λs; GLs increased under 380, 400 and 460 nm but decreased under 430 nm.</p> <p>In green bok choy, chl increased under 400-460 nm; car decreased under 460 nm; Sugar_{Sol} content increased only under 430 nm but decreased under all other supplemental λs; TFC increased only under 400 and 430 nm; GLs increased under 380 nm but decreased under all other treatments.</p> <p>In both cultivars, TPC increased only under 400 and 430 nm.</p> <p>In general, amino acid and AscAC decreased and/or remained unaffected by supplemental λs.</p>	Sun \pm B; UV-A	380, 400, 430, 460	400-1000 \pm 100 of B or UV-A (12 h d ⁻¹ for 10 d PTH)	Mao et al. 2020
<i>Lactuca sativa</i> 'Klee'	<p>Compared to control, FW_{Shoot}, DW_{Shoot}, LA, Leaf_{No}, SOD and CAT activity, Sugar_{Sol}, Protein_{Sol}, TAC, AscAC increased under all UV-A intensities, however, SLA, S:R ratio, Pn, g_s, chl, car remained indifferent between treatments.</p> <p>20 and 30 $\mu\text{mol m}^{-2} \text{s}^{-1}$ increased TFC.</p> <p>30 $\mu\text{mol m}^{-2} \text{s}^{-1}$ increased TPC, MDA and decreased F_v/F_m.</p> <p>O₂⁻ generation rate increased with increasing UV-A intensity.</p>	R ₆₆₅ B ₄₅₅ FR ₇₄₅ with elevated R \pm UV-A	365	237 \pm 10, 20, 30 (for 13 d PTH)	Chen et al. 2019
<i>Lactuca sativa</i> 'Klee'	<p>Compared to control, FW_{Shoot}, DW_{Shoot}, LA, Leaf_{No}, TAC, AscAC and Sugar_{Sol} contents increased under all UV-A durations, however, TFC remained indifferent.</p> <p>Only 10 d UV-A treatment increased TPC.</p>	R ₆₆₅ B ₄₅₅ FR ₇₄₅ with elevated R \pm UV-A	365	237 \pm 10 (for 5, 10 or 15 d PTH)	Chen et al. 2019

Cucumis sativus 'Hi Jack'	<p>In a greenhouse, UV-A and UV-B upregulated the expression of genes in the phenylpropanoid and flavonoid biosynthesis pathway by upregulating PAL, C4H and CHS genes.</p> <p>CHS was highly upregulated under both UV treatments in the leaves.</p> <p>Under UV-A, PALs were upregulated mainly in roots, while PAL was upregulated in leaves, stems and roots under UV-B.</p> <p>Only under UV-B, C4H was upregulated in all organs.</p>	Sun + HPS ± UV-B; UV-A	na; 340	Sun + HPS (150-200) ± UVs ⁴ (for 4 h d ⁻¹ for 10 d PTH)	Qian et al. 2019
<i>Brassica oleracea</i> var. <i>acephala</i>	<p>FW_{Shoot}, DW_{Shoot}, FW_{Root}, DW_{Root}, LA and caffeic acid content increased more under 385 nm than 370 nm compared to control, however, ferulic acid, H₂O₂ and O₂⁻ contents remained indifferent between all treatments. SLA and kaempferol content increased under both UV-A treatments equally compared to control.</p> <p>TPC and AOC increased with decreasing UV-A λ and increasing duration compared to control.</p> <p>F_v/F_m increased and Pn tended to increase with increasing UV-A λ compared to control.</p> <p>While both UV-A treatments tended to increase transcription levels of PAL, CHS and F3H, PAL activity was partially increased only under supplemental 385 nm.</p>	FL ± UV-As	370; 385	136 ± UV-A ⁴ (24 h d ⁻¹ for 5 d PTH)	Lee et al. 2019
<i>Brassica juncea</i> 'Red Lion'	<p>Chl, FW_{Shoot} and DW_{Shoot} remained indifferent between all treatments in mustard microgreens.</p> <p>After 10 h UV-A exposures, LA and TPC increased with increasing UV-A λ; while AOC increased, TAC and AscAC decreased under all UV-A treatments; α-T decreased under 366 nm, increased under 402 nm but remained indifferent under 390 nm compared to control; lutein, zeaxanthin and nitrate contents increased under 366 and 390 nm but decreased under 402 nm compared to control; car increased under 366 nm but decreased under 390 and 402 nm compared to control; S increased and P, Mg, Na, Mn, Fe, Zn, Cu, B decreased under all UV-A treatments; K and Ca decreased only under 366 and 402 nm.</p> <p>After 16 h UV-A exposures, lutein and zeaxanthin contents increased under all UV-A treatments; LA, AscAC and α-T increased only under 402 nm; TPC increased under 390 and 402 nm; nitrate content increased only under 366 and 390 nm; AOC decreased under 366 and 390 nm</p>	R _{638/665} + B ₄₄₇ + FR ₇₃₁ ± UV-As	366; 390; 402	300 ± 12.4 of UV-A ⁴ (for 10 or 16 h d ⁻¹)	Brazaityté et al. 2019

compared to control; car increased under 390 nm, decreased under 366 nm; TAC remained indifferent between all treatments; P, S, Mn increased only under 390 and 402 nm; B increased only under 390 nm; K increased only under 366 and 390 nm; Mg and Na increased under 402 nm but decreased under 366 and 390 nm; Fe decreased under all UV-A treatments; Zn increased under 390 and 402 nm but decreased under 366 nm; Cu increased under 402 nm, decreased under 366 nm but remained indifferent between 390 nm and control; Ca remained indifferent between treatments.

<i>Solanum lycopersicum</i>	All UV-A treatments increased Stem _{Length} compared to control. With increasing duration of supplemental UV-A, DW _{Total} , LA, Pn, Φ _{PSII} , g _S increased.	R ₆₅₀ B ₄₅₀	220 ± UV-A ⁴	Kang et al. 2018
'Beijing Cherry Tomato' seedlings	While 16 h UV-A exposure increased ETR and TPU, 8 and 16 h UV-A exposure increased SD _{Abaxial} compared to control. P _{max} , α, R _d , V _{c,max} , chl, F _v /F _m , LMA, SD _{Adaxial} remained indifferent between treatments.	(9:1) ± UV-A	(for 4, 8 or 16 h d ⁻¹)	

¹ Descriptions of abbreviations are listed in alphabetical order: α = leaf photosynthetic efficiency (μmol μmol⁻¹ photons), α-T = alpha-tocopherol, ANS = anthocyanidin synthase, ANR = anthocyanidin reductase, AOC = antioxidant capacity, AscAC = ascorbic acid content (*vitamin C*), B = blue light (400-500 nm), B = boron, bulblets_{No} = number of bulblets, C4H = cinnamic acid 4-hydroxylase, Ca = calcium, car = carotenoid content (mg m⁻²), CAT = catalase, chl = chlorophyll content (mg m⁻²), CHS = chalcone synthase, Cu = copper, DFR = dihydroflavonol 4-reductase, DW_{Leaf} = leaf dry weight, DW_{Root} = root dry weight, DW_{Shoot} = shoot dry weight, DW_{Stem} = stem dry weight, DW_{Total} = total dry weight, ETR = electron transport rate, F3H = flavonoid 3-hydroxylase, Fe = iron, FL = fluorescent lamp, FR = far red (700-800 nm), F_v/F_m = maximum quantum efficiency of photosystem II, FW_{Fruit} = fruit fresh weight, FW_{Leaf} = leaf fresh weight, FW_{Shoot} = shoot fresh weight, G = green light (500-600 nm), GL = glucosinolate, g_s = stomatal conductance (mol CO₂ m⁻² s⁻¹), Hypo_{Length} = hypocotyl length, Internode_{Diam} = internode diameter, K = potassium, LA = leaf area (cm²), λ = wavelength (*Lambda*), LAR = leucoanthocyanidin reductase, L_{Length} = leaf length, LMA = leaf mass area (g m⁻²), LUE = light use efficiency (plant dry weight per unit of incident light (g mol⁻¹), L_{Width} = leaf width, MDA = malondialdehyde content, Mg = magnesium, Mn = manganese, *na* = not available, Na = sodium, NPQ = non-photochemical quenching, P = phosphorus, PAL = phenylalanine ammonia lyase, P_{Height} = plant height, Phenol_{Sol} = soluble phenolics, Φ_{PSII} = quantum yield efficiency of photosystem II, P_{max} = maximal photosynthetic rate (μmol CO₂ m⁻² s⁻¹), Pn = photosynthetic rate (μmol CO₂ m⁻² s⁻¹), Protein_{Sol} = soluble protein (mg g FW⁻¹), PTH = prior to harvest, qL = fraction of open PSII centers, qP = photochemical quenching, R = red light (600-700 nm), R_{Activity} = root activity (g h⁻¹), RB = red and blue light, R_d = dark respiration rate (μmol m⁻² s⁻¹), RGB = red, green and blue light, R_{Length} = root length, ROS = reactive oxygen species, RSA = root surface area (cm²), R_{Volume} = root volume (cm³), S = sulfur, SD_{Abaxial} = abaxial stomatal density (number mm⁻²), SD_{Adaxial} = adaxial stomatal density (number mm⁻²), SLA = specific leaf area (cm² mg⁻¹), SLW = specific leaf weight (mg cm⁻²), SOD = superoxide dismutase, SQI = seedling quality index, S:R = Shoot-to-root ratio (w/w), Stem_{Diam} = stem diameter, Sugar_{Sol} = soluble sugar, TAC = total anthocyanin content, TFC = total flavonoid content, TPC = total phenolic content, TPU = triose phosphate utilization rate, Tr = transpiration rate (mol H₂O m⁻² s⁻¹), V_{c,max} = maximum carboxylation rate of Rubisco, W = broadband white light within PAR (photosynthetically active radiation; 400-700 nm), Y = yellow light (600 nm), Zn = zinc.

² Peak wavelength (λ) of applied ultraviolet (and blue) light.

³ Light intensity is given in micromole per square meter and second ($\mu\text{mol m}^{-2} \text{s}^{-1}$). UV light durations are given in hours per day (h d^{-1}) and/or in days (d) if variant to other applied light sources.

⁴ Choi et al. (2022), Lee et al. (2021) and Lee et al. (2019) applied 30 W m^{-2} of UV-A; Lee et al. (2021a) applied 8.11 W m^{-2} of UV-A, 1.97 W m^{-2} of UV-B and $5.08+1.55 \text{ W m}^{-2}$ of UV-A/B; Samuoliene et al. (2020) applied 2.2 mW cm^{-2} of UV-A; Qian et al. (2020) applied 3.6 W m^{-2} of UV-A and 83.4 mW m^{-2} of UV-B; Li et al. (2020) applied $600 \mu\text{W cm}^{-2}$ of UV; Li et al. (2020a) applied 40 W m^{-2} of supplemental UV-A; Qian et al. (2019) applied 3.6 W m^{-2} of UV-A or 83.4 mW m^{-2} of UV-B; Brazaitytė et al. (2019) applied 4.0 W m^{-2} of 366 nm, 3.8 W m^{-2} of 390 nm and 3.7 W m^{-2} of 402 nm, Kang et al. (2019) applied 2.29 W m^{-2} of UV-A. (*For comparison, 1 to 3 $\text{kW m}^{-2} \text{d}^{-1}$ are considered ambient levels of UV radiation (Neugart & Schreiner, 2018).*)

1.4.2.2 Plant responses to green light (λ 500-600 nm)

Due to the general dip found in plant leaves' light absorbances and due to the chlorophylls' generally minimal light absorbances both occurring around 550 nm in the green region of PAR, green light (500-600 nm) has often been dismissed as inefficient and unnecessary for plant growth (Figure 4; McCree, 1972a). This perception resulted in green light being rarely considered as a useful additive to the commonly applied dichromatic R and B light backgrounds in horticultural environments. However, it is a misconception that plants do not make efficient and effective use of the green regions of the PAR spectrum.

In fact, G light strongly drives leaf photosynthesis (McCree, 1972a; Sun et al., 1998; Terashima et al., 2009; Hogewoning et al., 2012). Not only McCree himself - who defined PAR (as previously described in section 1.3.1.4) - measured high CO₂ fixation rates in cantaloupe (*Cucumis melo* L.), corn (*Zea mays* L.), oat (*Avena sativa* L.) and sugar beet (*Beta vulgaris* L.) leaves in the green (500-600 nm) light region, which all exceeded the quantum yields measured in the blue (400-500 nm) region of the PAR spectrum (McCree, 1972a). Also, Sun et al. (1998) and Hogewoning et al. (2012) observed higher CO₂ fixation rates under G light in spinach (*Spinacia oleracea* L.), cabbage (*Brassica oleracea* L.) and cucumber (*Cucumis sativus* L.) leaves, respectively, than under B [411±54 nm; 400-500 nm] light conditions. In addition, Hogewoning et al. (2012) showed that the quantum yield losses in the B range of the light are due to absorptions by carotenoids and non-photosynthetic pigments. Instead, the greatest maximal CO₂ fixation rates were caused by broad white (400-700 nm), red (648 nm) and green (544 nm) light (Sun et al., 1998) on a whole leaf basis in spinach. Similar observations were made by Hogewoning et al. (2012), who detected maximal CO₂ fixation rates under red (600-700 nm), followed by green (500-600 nm) wavelengths in cucumber leaves. And Terashima et al. (2009) found that G (550 nm) light increased the fixation rate of CO₂ in sunflower (*Helianthus annuus* L.) leaves even more efficiently than red (680 nm) light in moderate to strong white light.

The reason for these efficient quantum yields for CO₂ fixations detected in these diverse plant species is the ability of green light to penetrate much deeper into leaves as well as into whole plant canopies as red and blue photons (Bian et al., 2018; Smith et al., 2017; Hogewoning et al., 2012; Sun et al., 1998). While B light is rapidly absorbed by multiple pigments in the top layers of leaf cells, and R light is strongly absorbed by chlorophylls in the top leaf layers, G light can reach the bottom layers of plant leaves (Figure 7).

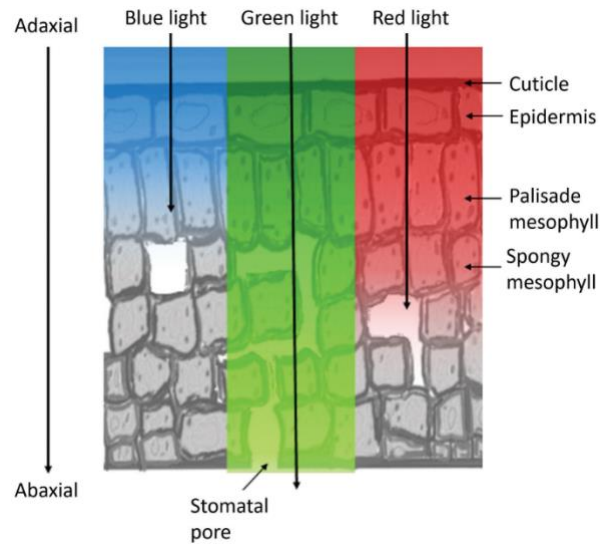


Figure 7 – Representation of monochromatic blue, green and red light penetrating through the vertical profile of a leaf illuminated from above the adaxial surface. (Retrieved from Smith et al., 2017)

It has been argued that due to

- (1) the chlorophylls' weaker absorption in the G (known as the '*green window*'),
- (2) the scattering of G light within leaves (known as the '*detour effect*'), and
- (3) the plants' partial reflections of G light (10-50 %)⁵,

G photons are deeply transmitted into leaves and shaded parts of canopies. Consequently, chlorophylls located in the lower layers of leaves and canopies are able to absorb these G photons, which ultimately enhance the plants' photosynthetic capacities by increasing net photosynthetic rates (Bian et al., 2018; Smith et al., 2017). Thus, the ability of G photons to efficiently drive leaf photosynthesis (especially in deeper sections of leaves and lower plant canopies where B and R wavelengths are severely depleted) should no longer remain neglected in horticultural applications.

In addition to these detected contributions on carbon assimilation, the literature is punctuated with cases in which monochromatic and broadband green wavebands clearly modulate plant development. Table 6 (attached at the end of this section) summarizes studies in which effects of G wavelengths were investigated. Many of the findings are described and addressed below.

Plants grown under conditions enriched in G light often exhibit shade characteristics. As shown by Folta (2004), within minutes of monochromatic G (534±20 nm) illuminations, the hypocotyls of

⁵ The partial reflections of green wavelengths are the reason for the green appearance of plants (Smith et al., 2017).

Arabidopsis seedlings rapidly elongated. The same study also showed that seedlings grown under a dim background of RB with added G (525±16 nm) were taller than seedlings grown under RB alone, indicating that G light can antagonize the inhibition of hypocotyl growth observed under RB illuminations. Soon after, Bouly et al. (2007) also showed that monochromatic G (563±10 nm) light elongates the hypocotyl of *Arabidopsis* seedlings. Additionally, the study demonstrated that the applied G photons reverse B light-induced inhibitions of hypocotyl elongations. Sellaro et al. (2010) then revealed that the hypocotyl lengths of *Arabidopsis* seedlings increase linearly with decreasing B:G ratios (437:547 nm) over a broad range of fluence rates. A year later, Zhang et al. (2011) reinforced the understanding that shade symptoms are induced in a G light-dependent manner: With increasing additions of G (525 nm; 10 and 40 $\mu\text{mol m}^{-2} \text{s}^{-1}$) to a constant background of RB (90 $\mu\text{mol m}^{-2} \text{s}^{-1}$), increased stem and petiole elongations and upward-orientated leaves were observed in *Arabidopsis*. It shall be noted here that the studies by Folta (2004), Bouly et al. (2007) and Zhang et al. (2011) are all examples of shade acclimation responses despite increased PAR irradiations as G was added. Nonetheless, Zhang et al. (2011) also obtained the described shade avoidance phenotypes when PAR intensity was kept the same by reducing the fluence rate of R to add G.

Since then, further studies detected green-induced symptoms of shade avoidance in various plant species: In example, Snowden et al. (2016), who investigated the development of a variety of food crops under increasing percentages of G (500-600 nm) in diverse artificial lighting backgrounds (including narrow to broad G wavebands with differing G peak wavelengths), observed expanding leaf areas in wheat (*Triticum aestivum* L.), cucumber (*Cucumis sativa* L.) and lettuce (*Lactuca sativa*), lengthening stems in tomato (*Solanum lycopersicum*), soybean (*Glycine max*), pepper (*Capsicum annum*) and lettuce, as well as elongating petioles in soybean and radish (*Raphanus sativus*) with increasing percentages of G. A similar trend was observed by Kaiser et al. (2019) in a greenhouse setting as leaf areas and plant heights of the investigated tomatoes tended to increase with increasing percentages of G in RB backgrounds. Park & Runkle (2018a), who investigated the development of ornamentals under RB, RGB and multiple W LED light treatments also found that begonia (*Begonia x semperflorens*), geranium (*Pelargonium x hortorum*), snapdragon (*Antirrhinum majus*) and especially petunia (*Petunia x hybrida*) grew taller under all G-containing light treatments in comparison to the RB treatment lacking G wavebands. Also, Meng et al. (2019) confirmed that increasing substitutions of B with G (526 nm) in a constant R background trigger shade avoidance responses in lettuce and kale. Finally, also Schenkels et al. (2019) found that the height of basil as well as the length and width of its leaves increase when 15 $\mu\text{mol m}^{-2} \text{s}^{-1}$ of narrow G (505 nm) are added to a white LED background and when these G photons partially replace R and B photons (to

equalize PAR intensity). However, Zhang et al. (2022) did not observe stem elongations in tomato (*Solanum lycopersicum*) plants when partially replacing an RB background with 20 % of G (525 nm) and keeping total PAR and R:B ratios constant. Interestingly, only in the presence of FR (known to induce stem elongations via phytochrome action (section 1.3.2.2.1) reducing the R:FR ratio, the partial replacement of RB with G resulted in significantly elongated stems which were even more elongated than under RB+FR alone.

To shield themselves from damaging conditions of excessive lighting, numerous plants are known to produce non-photosynthetic anthocyanins which then accumulate in their leaves (Ma et al., 2021). These colorful pigments with great antioxidant capacities (as previously mentioned in section 1.3.2.2.2) have often been found to be down-regulated in G-enriched light environments: Bouly et al. (2007) found a decreased content of anthocyanins in *Arabidopsis* under dichromatic BG light with a ratio of 1:1 compared to the contents found under monochromatic B, again, suggesting that G light is able to reverse B light-induced cryptochrome-mediated responses such as anthocyanin productions (section 1.3.2.2.2). Zhang & Folta (2012) also found that increasing additions of G (525 nm) to a constant background of RB decreased anthocyanin accumulations in *Arabidopsis*. Similarly, anthocyanin concentrations were found to decrease in lettuce when B was increasingly substituted with G (526 nm) in a constant R background (Meng et al., 2019). However, no differences in anthocyanin contents were observed by Mizuno et al. (2011) who compared phytochemical contents in red and green leaf cabbages exposed to monochromatic R, B, G (525 nm) and BG (500 nm) light. As the study was conducted under a low light intensity of $50 \mu\text{mol m}^{-2} \text{s}^{-1}$ and elongated petioles were observed under monochromatic B (which normally mediates growth inhibitions instead of elongations) in both cultivars, it appears that the study was conducted under insufficient lighting conditions that make the production of anthocyanins unfavorable to begin with. Also, Li & Kubota (2009) did not observe differences in anthocyanin contents in baby leaf lettuces when monochromatic G (526 nm) partially replaced a background of white light emitted from cool white, fluorescent lamps. However, in this experimental setup, the replacement of broad W with narrow G was concomitant with significant reductions in both R and B photon fluxes (from 76 to 42 and from 71 to $49 \mu\text{mol m}^{-2} \text{s}^{-1}$, respectively), which again represents a condition unfavorable for anthocyanin productions, and the W background lighting already consisted of 52 % G (500-600 nm) which may repressed anthocyanin productions under all treatments. Another contrasting result was published by Johkan et al. (2012): Intense monochromatic G light ($\geq 400 \mu\text{mol m}^{-2} \text{s}^{-1}$) with 510 nm promoted the content of anthocyanins in red leaf lettuces (Johkan et al., 2012) – a finding which can probably be attributed to residual absorptions of short G wavelengths by cryptochrome and thus, activations of cryptochromes, which are known to trigger the accumulation of anthocyanins.

At first, the influence of G light on photosynthetic pigment contents appears perplexing, as research results span from detrimental and non-influential to beneficial: High monochromatic G (520 nm) and especially monochromatic Y (590 nm) illuminations ($320 \mu\text{mol m}^{-2} \text{s}^{-1}$) have been shown to result in the development of abnormal leaf tissue cells and dysplastic chloroplasts in cherry tomato leaves (Xiaoying et al., 2011). In addition, increasing fractions of G in RGB backgrounds as well as increasing substitutions of B with G in a constant R background have been correlated with decreasing chlorophyll contents in cucumber and lettuces (Snowden et al., 2016; Kang et al., 2016; Meng et al. 2019). However, no differences in total chlorophyll and/or carotenoid contents were observed in cucumber seedlings (Hernández & Kubota, 2016), tomatoes (Kaiser et al., 2019) and a variety of lettuces (Son & Oh, 2015; Lin et al., 2013; Li & Kubota, 2009; Kim et al., 2004) exposed to RB, RGB and/or FL light conditions with differing percentages of G light. Also, no changes in carotenoid contents were found in red and green leaf cabbages exposed to monochromatic B, BG (500 nm) and G (525 nm) light conditions. In contrast, chlorophyll and carotenoid contents of lettuces were found to be increased under W+G (522 nm) compared to lettuces exposed to W+Y (596 nm) (Chen et al., 2016). In accordance, Dougher and Bugbee (2001) found that increasing proportions of long G wavelengths between 580-600 nm suppressed the formation of chlorophyll in lettuce (as evaluated via SPAD meter which measures the leaf's green coloration).

These variable results may indicate that the broad definition of G light - spanning from 500 nm all the way across to 600 nm is misleading. The results rather suggest that additions of short G wavelengths - which are absorbable by photosynthetic pigments - can improve chlorophyll and/or carotenoid contents (possibly via residual cryptochrome actions known to induce chlorophyll synthesis and/or zeaxanthin actions), and that additions of long G wavelengths - unfavorable for photosynthesis - restrain their production (possibly via inactivation of cryptochromes and/or zeaxanthin signaling) until more favorable light conditions for photosynthesis have been reached (following G-induced elongation growths). After conducting a comprehensive meta-analysis on plant responses to the spectral range between 500 and 600 nm, also Battle et al. (2020) recently suggested a subdivision between short (G) and long (Y) wavelengths, as the shorter wavelengths were found to complement while longer wavelengths were found to antagonize many B-induced responses.

Contrasting are also the findings of G-mediated flower responses: In example, while G light (563 nm) reduced B light-induced flowering in *Arabidopsis* (Banerjee et al., 2007), flowering accelerated in *Arabidopsis*, petunia, chrysanthemum and marigold under increasing intensities of monochromatic G light (521 nm) and W light with high percentages and intensities of G light (558 nm) (Meng & Runkle, 2019; Park & Runkle, 2018a). Evidently, more research is needed to clarify the impact of G light on flowering.

Considering that G light has been shown to strongly drive carbon fixation rates and was shown to induce elongation and expansion growths, one might expect noticeable yield increases, however, opposing results were published: While the addition of and/or replacement with G in W, RB and/or R backgrounds resulted in increased biomass productions in basil (505 nm, Schenkels et al., 2019), tomato (531 nm, Kaiser et al., 2019), kale (526 nm, Meng et al., 2019) and diverse red and green leaf lettuce cultivars (526 nm, Meng et al., 2019; 518 nm, Son & Oh, 2015; 535 nm, Kim et al., 2004; broadband G 500-600 nm, Lin et al., 2013), indifferent yields were found in a variety of ornamentals (Park & Runkle, 2018a) and food crops (Zhang et al., 2022; Snowden et al., 2016; Hernández and Kubota, 2016; Li & Kubota, 2009) with G peak wavelengths ranging from 525-580 nm. In contrast, reduced lettuce yields were correlated with increasing proportions of 580-600 nm by Dougher & Bugbee (2001), which agrees with results from Kim et al. (2004) who also detected decreased lettuce yields under W light with high percentages of Y with 580 nm. And again, these research findings combined suggest a wavelength dependency: With increasing “green” peak wavelengths from 500 to 600 nm, crop yields appear to decrease. In accordance with this view are the findings by Chen et al. (2016): Though additions of R and B to a background of W were found to increase the yield of lettuce more than the addition of G (522 nm), respectively, the same study showed that the addition of G (522 nm) increased biomass more than the addition of Y (596 nm).

Finally, it has long been known that wavelengths of 490-580 nm reverse the B light-induced opening of stomata. (Frechilla et al., 2000, Talbott et al., 2002). First, Frechilla et al. (2000) showed that a short pulse of G light was able to stop B light-mediated stomatal opening in *Vicia faba* epidermal peels and that the last light quality applied (G or B) dictates the physiological response of the stomata. It was also shown that the B-induced stomatal opening was most effectively reversed by 540 nm, while weakest reversals were detected at 490 and 580 nm, respectively (Frechilla et al. 2000). The same research group found out that the degree of G-induced stomatal closure was directly proportional to the change in the B:G ratio, with full reversal when G was twice that of B light (Talbott et al., 2002). As this G reversal effect was found in a diverse suite of plant species (Talbott et al., 2002), it might be a universal effect in the kingdom of plants.

Clearly, G wavebands are precisely sensed and monitored by plants and play crucial roles in regulating plant growth and development throughout the life cycle of plants. Various discrete responses - spanning from contributing to carbon gains, altering elongation and expansion growths, adjusting phytochemical contents, controlling stomatal closures to changing the time of flowering - have been attributed to G wavebands.

These G light effects often oppose those directed by R and B wavebands. The best example for this generalization may be the detection of shade avoidance symptoms under increasing G light ratios in a constant background of R and B despite an overall increase in light intensity (Zhang et al., 2011).

It appears, G wavelengths are harnessed as a signal to strategically adjust plant form, composition and physiology to optimize light capture and photosynthetic efficiency when light quantities and/or qualities are unfavorable. The fact that many responses have been found to be triggered by very low G light intensities (commonly found under conditions of shade) is consistent with this idea.

Though contradicting results exist, G light could be strategically used - especially in R and B saturated light environments - to increase contents of photosynthetic pigments, to improve the rates of carbon fixation and photosynthesis and to minimize water losses by controlling stomatal apertures. Consequently, adequate additions of G light could significantly contribute to improve crop yields and water use efficiencies in controlled-environment agriculture industries.

However, great research efforts are necessary to understand the specific G wavelengths, intensities and ratios that are required to fine-tune these crops responses beneficially.

In conclusion, a great scientific framework exists that supports the inclusion of green light in horticultural production systems.

Table 7 – Morphological, physiological and phytochemical plant effects mediated by green wavelengths (λ 500-600 nm).⁶

Plant species	Effect ¹	Light spectrum	B/G ² ratio	Peak λ ³	Light intensity ⁴	Reference
<i>Solanum lycopersicum</i> 'MoneyMaker'	Partial (20 %) replacement of RB with G did not change P_{Height} , DW_{Total} , S:R ratio. Partial replacement of RB with G in the presence of FR enhanced P_{Height} more than RB with FR alone; however, DW_{Total} , S:R ratio and LA remained indifferent.	R ₆₆₇ B ₄₄₇ , RBG, RBF _{R730} , RBGFR [R:B 3:1]	1:1	525	150	Zhang et al. 2022
<i>Solanum lycopersicum</i> 'Komeett'	FW_{Total} increased linearly with increasing % G; FW_{Leaf} , FW_{Shoot} , LA, P_{Height} , Internode _{No} , chl <i>a</i> tended to increase linearly with increasing % G. Top leaf canopy: Φ_{CO_2} , g_s , L_{Th} unaffected. Middle leaf canopy: chl <i>a:b</i> ratio, car increased with increasing % of G; Φ_{CO_2} , g_s , L_{Th} unaffected. Chl <i>b</i> higher in leaves of middle canopy than in leaves of top canopy.	R ₆₆₇ B ₄₄₈ + Sun RG _{Low} B + Sun RG _{High} B + Sun [high R:B]		531	171	Kaiser et al. 2019
<i>Ocimum basilicum</i> 'Marian'	Addition of 15 $\mu\text{mol m}^{-2} \text{s}^{-1}$ of G 505 nm to W_{Low} increased FW_{Total} , FW_{Leaf} , FW_{Stem} , DW_{Total} , DW_{Leaf} , DW_{Stem} , Stem _{Length} , Stem _{No} , L _{Length} , L _{Width} , L _{No} , LM compared to W_{Low} ; LA indifferent. Partially replacing RB intensity in W_{High} with G ($W+G_{\text{High}}$) increased FW_{Total} , FW_{Leaf} , FW_{Stem} , DW_{Total} , DW_{Stem} , Stem _{Length} , L _{Length} , L _{Width} compared to W_{High} ; DW_{Leaf} , LA, L _{No} indifferent. Chl contents and ratio of L _{Length} :L _{Width} indifferent between all treatments.	W_{Low} W_{High} $W+G_{\text{High}}$ [$W_{400-700}$ with elevated R _{633/664}]		505	108 _{Low} 123 _{High}	Schenkels et al. 2019
<i>Lactuca sativa</i> 'Rex' & 'Rouxai', <i>Brassica oleracea</i> var. <i>sabellica</i> 'Siberian'	Substituting G for B triggers shade avoidance responses. Substitution increased L _{Length} , LA, FW_{Shoot} in both crops and Pet _{Length} in kale, however, decreased chl (more than FR substituting B), TAC and Assimilation _{Net} in both crops. (Parameters were more strongly or equally affected by FR substituting B than G substituting B (Table 7).)	Elevated R ₆₆₄ \pm B ₄₄₉ ; G; FR ₇₃₃	\searrow with \nearrow G	526	180 incl. 0, 20, 40, 60 of G	Meng et al. 2019

⁶ The reader may also be referred to the following review articles: Landi et al. (2020), Smith et al. (2017), Wang & Folta (2013) and Folta & Maruhnich (2007) and to the studies by Liu et al. (2017) cited in Table 9, Araújo et al. (2021), Andrade et al. (2017), Carvalho et al. (2016), Noguchi & Amaki (2016), Alvarenga et al. (2015) cited in Table 10.

LDP: <i>Petunia</i> , <i>Ageratum</i> , <i>Antirrhinum</i> , <i>Arabidopsis</i> SDP: <i>Chrysanthemum</i> , <i>Tagetes</i>	Flowering accelerated, L_{No} tended to decrease in LDPs with increasing G intensity. P_{Height} of LDPs significantly reduced under G treatments than under R+W+FR. Flowering delayed, L_{No} and P_{Height} tended to increase in SDPs with increasing G intensity.	9 h Sun + 7 h daylight extension with G or with $R_{669}+W_{400-700}+FR_{743}$	521	0 2 13 25	Meng & Runkle 2019
<i>Begonia</i> , <i>Pelargonium</i> , <i>Petunia</i> , <i>Antirrhinum</i>	LA, FW_{Total} , DW_{Total} indifferent between treatments in all species. In Snapdragon, P_{Height} reduced under RB. In <i>Petunia</i> , P_{Height} increased, and flowering accelerated under W with high % and intensity of G with 558 nm.	Multiple $W_{400-700}$, $R_{660}B_{447}$ (5.7:1), RGB (1:2:2)	W: 558 RGB: 531	160	Park & Runkle 2018a
<i>Solanum lycopersicum</i> 'Early girl', <i>Cucumis sativa</i> 'Sweet Scice', <i>Capsicum annum</i> 'California Wonder', <i>Raphanus sativus</i> 'Cherry Belle', <i>Glycine max</i> 'Hoyt', <i>Lactuca sativa</i> 'Waldmann's Green', <i>Triticum aestivum</i> 'USU-Apogee'	DW_{Total} indifferent with increasing % of G in all species but radish; at high intensity, increasing % of G decreased DW_{Total} in radish. LA indifferent with increasing % of G in all species but wheat, cucumber, lettuce; at high intensity, increasing % of G increased LA in wheat, cucumber; at low intensity, increasing % of G decreased LA in lettuce. $Assimilation_{Net}$ indifferent with increasing % of G in all species but soybean and cucumber; at low intensity, increasing % of G decreased $Assimilation_{Net}$ in soybean and cucumber. $Stem_{Length}$ indifferent with increasing % of G in all species but tomato, soybean, pepper and lettuce; at high intensity, increasing % of G increased $Stem_{Length}$ in tomato, at low intensity, increasing % of G increased $Stem_{Length}$ in soybean, pepper, lettuce. Pet_{Length} increased with increasing % of G in soybean under low intensity and in radish under high intensity, indifferent in other species and treatments. Chl content indifferent with increasing % of G in tomato, radish, soybean, wheat; at high intensity, chl content decreased in cucumber; at low intensity, chl content decreased in cucumber, pepper and lettuce.	Multiple $W_{400-800}$, G, $R_{650}B_{450}$, RGB	G in Ws 580/550; 525; G in RGB 530	200 500	Snowden et al. 2016

<i>Cucumis sativus</i> seedlings	Partial replacement of RB by 28 % G had no effect on growth (FW_{Total} , DW_{Total} , L_{No} , LM_{Area} , chl concentration), morphology (P_{Height} , LA), Pn and g_s in comparison to RB treatments.	R_{660} , B_{473} , RBs RGB	0.7	532	100	Hernández & Kubota 2016
Lettuce	W+G (522 nm): decreased nitrate content, increased $Sugar_{Sol}$ content compared to all other treatments. W+Y (596 nm): lettuce appeared sparse and twisted. Chl, car, AscAC, $Sugar_{Sol}$ contents, FW_{Root} , DW_{Total} , DW_{Root} increased under W+G in comparison to W+Y; P_{Height} , FW_{Total} , $Stem_{Diam}$, L_{No} indifferent.	$W_{400-900} \pm$ B_{450} ; G_{522} ; Y_{596} ; R_{660} ; FR_{850}	0.7	522 596	135	Chen et al. 2016
Lettuce	Addition of 10 % G ($15 \mu mol m^{-2} s^{-1}$) decreased Pn ; highest under $R_{80}B_{20}$. Chl content highest in RGB treatment with B:G ratio of 3:1; however, decreased in RGB treatments with B:G ratio of 1:1 and 2:1. G had no distinct effect on L_{Length} , L_{Width} , S:R ratio.	R_{625} , RB_{465} [9:1, 4:1, 7:3], RGBs [with elevated R]	1:1 2:1 3:1	525	150	Kang et al. 2016
Red and green leaf lettuce	Partial substitution of B with G in the presence of a fixed proportion of R enhanced FW_{Shoot} and LA; decreased L_{Thick} in both cultivars. Density of epidermal cells and stomata showed an increasing tendency as B was replaced by G in both cultivars. TPC and AOC tended to decrease as B was replaced by G in both cultivars. Chl contents tended to decrease in red leaf lettuce; however, tended to increase in green leaf lettuce.	$R_{655}B_{456}$ [9:1, 4:1, 7:3], RG [9:1] RGB [8:1:1, 7:1:2]	0:1 1:1 2:1	518	173	Son & Oh 2015
Lettuce	Under RGB, FW_{Root} , FW_{Shoot} and DW_{Total} , $Sugar_{Sol}$ content higher, LA greater, nitrate content and S:R ratio lower than under RB. Crispness, sweetness, shape optimized under RGB compared to RB. Chl, car and $protein_{Sol}$ contents indifferent.	$R_{660}B_{454}$, RGB [both with elevated R]		500-600	210	Lin et al. 2013
Red leaf lettuce	With increasing intensity of G, DW_{Shoot} and DW_{Root} tended to increase, Pet_{Width} and Pn increased; LA remained indifferent between G intensity treatments; FW_{Total} , L_{Length} , L_{Width} and Pet_{Length} showed no distinct intensity trend; intensity $\geq 400 \mu mol m^{-2} s^{-1}$ of 510 nm promoted TAC.	G		510 524 530	100 200 300	Johkan et al. 2012

	With increasing G λ , Pn tended to decrease, Pet_{Length} tended to increase; LA remained indifferent between G λ treatments; FW_{Total} , L_{Length} , L_{Width} and Pet_{Width} showed no distinct G λ trend.					
Red and green leaf cabbage	FW_{Total} , L_{No} and car indifferent between treatments and cultivars. In green leaf cabbage, chl contents tended to increase under B and BG; Pet_{Length} increased under B; Pet_{Length} and $Stem_{Length}$ decreased under R; LA and TAC remained indifferent. In red leaf cabbage, LA tended to increase in both G-containing treatments, TAC increased under R; $Stem_{Length}$ and chl remained indifferent.	B_{470} , BG_{500} , G_{525} , R_{660}		500 525	50	Mizuno et al. 2011
Arabidopsis	Addition of increasing amounts of G light to a constant RB background caused shading symptoms, including petiole elongation, upward orientation of leaves and decreased TAC.	$R_{630}B_{470}$ [5:4], $RG_{525}B$ [5:4:1, 5:4:4]	4:1 1:1	525	100-130; increased with increasing G	Zhang et al. 2011 ⁵
Cherry tomato	Pn , $Stomata_{No}$, L_{Thick} increased under RGB; decreased under G and Y. Chl abnormal under Y; palisade and spongy tissue cells in leaves abnormal under G and Y.	R_{640} , B_{450} , G_{520} , Y_{590} , RB [1:1], RGB [3:1:3]	3:1	520 590	320	Xiaoying et al. 2011
Baby leaf lettuce	TAC, xanthophyll, β -carotene, chl, TPC, AscAC, FW_{Total} , DW_{Total} , L_{No} , $Stem_{Length}$, L_{Length} , L_{Width} indifferent compared to FL.	FL + UV-A; B; G; R; FR		526	300	Li & Kubota 2009
Arabidopsis	$Hypo_{Length}$ increased under G and BG (with G 563 nm) compared to monochromatic B. TAC decreased under BG (with G 582 nm) compared to monochromatic B.	G, BG	1:1	563 \pm 10 582 \pm 10	10 20	Bouly 2007
Arabidopsis	G reduced B-induced early flowering.	G, BG	1:1	563	2	Banerjee et al. 2007
Lettuce	LA, FW_{Total} and DW_{Total} enhanced under RB supplemented with 24 % G in comparison to RB; Pn and chl contents indifferent. LA, FW_{Total} , DW_{Total} , Pn and chl contents indifferent under FL with 51 % G in comparison to RB.	RB, RB+GFL, GFL, FL		535 535 580	150	Kim et al. 2004

	LA, FW _{Total} , DW _{Total} and <i>Pn</i> reduced under GFL with 86 % G in comparison to RB; chl content indifferent.					
Arabidopsis	Monochromatic G rapidly stimulates hypocotyl elongation under continues and under a short single pulse. Supplemental G antagonizes B and R light inhibition of hypocotyl elongation.	G, RGB		534±20 525±16	≥ 0.1 ≥ 1	Folta 2004
Faba bean, Arabidopsis	G light reduced B-induced stomatal opening.	UV-B, UV- A, B, G		550	500	Eisinger et al. 2003
Faba bean, Asiatic dayflow er, Peas, Arabidopsis, Tabacco, Onion, Barley	Simultaneous exposure to equal intensity of B and G resulted in 50 % reversal of normal B-induced stomatal opening. Complete reversal occurred when G intensity doubled B intensity.	B, G, BG	1:1 1:2 2:1	540	5 10 15	Talbott et al. 2002
Lettuce	Increasing proportions of 580-600 nm reduced DW _{Total} , suppressed chl or chloroplast formations.	HPS, MH		580-600	200 500	Dougher & Bugbee 2001
Faba bean	G immediately reversed B-induced stomatal opening. B immediately reversed G-induced stomatal closure only when B preceded G light pulse. Continuous monochromatic G stimulated a slight stomatal opening. G reversal on stomatal opening depends on intensity; complete reversal occurred when G intensity doubled B intensity.	Xenon arc lamp + B Plexiglas and/or G broad- band filters		505-560	5, 10, 20	Frechilla et al. 2000

¹ Descriptions of abbreviations are listed in alphabetical order: AOC = antioxidant capacity, AscAC = ascorbic acid content (*vitamin C*), Assimilation_{Net} = net assimilation = dry mass per unit leaf area (g m⁻²), B = blue light (400-500 nm), B:G = blue-to-green ratio, car = carotenoid content (mg m⁻²), chl = chlorophyll content (mg m⁻²), DW_{Root} = root dry weight, DW_{Shoot} = shoot dry weight, DW_{Stem} = stem dry weight, DW_{Total} = total dry weight, FL = fluorescent lamp, FR = far red light (700-800 nm), FW_{Leaf} = leaf fresh weight, FW_{Root} = root fresh weight, FW_{Shoot} = shoot fresh weight, FW_{Stem} = stem fresh weight, FW_{Total} = total fresh weight, G = green light (500-600 nm; 520-522 nm), g_s = stomatal conductance (mmol CO₂ m⁻² s⁻¹), HPS = high pressure sodium lamp, Hypo_{Length} = hypocotyl length, Internode_{No} = number of internodes, LA = leaf area, λ = wavelength (*Lambda*), LDP = long-day plants (petunia, ageratum, snapdragon, arabidopsis), L_{Length} = length of leaves, LM_{Area} = leaf mass per area, L_{No} = number of leaves, L_{Thick} = leaf thickness, L_{Width} = width of leaves, MH = metal halide lamp, Pet_{Length} = petiole length, Pet_{Width} = petiole width, P_{Height} = plant height, Φ_{CO₂} = photosynthetic quantum yield (μmol CO₂ μmol photon⁻¹), *Pn* = photosynthetic rate (μmol CO₂ m⁻² s⁻¹), Protein_{Sol} = soluble protein (mg g FW⁻¹), R = red light (600-700 nm), RB = red and blue light, RGB = red, green and blue light, SDP = short-day plants (chrysanthemum, marigold), S:R = shoot-to-root ratio (w/w), Stem_{Diam} = stem diameter, Stem_{No} = number of stems, Stomata_{No} = number of stomata, Sugar_{Sol} = soluble sugar, TAC =

total anthocyanin content, TPC = total phenolic content, UV-A = ultraviolet A radiation (320-400 nm), UV-B = ultraviolet B radiation (280-320 nm), W = broadband white light within PAR (photosynthetically active radiation; 400-700 nm), Y = yellow light (590-596 nm).

² Blue-to-green ratio.

³ Peak wavelength (λ) of applied green light.

⁴ Light intensity applied in micromole per square meter and second [$\mu\text{mol m}^{-2} \text{s}^{-1}$].

⁵ Specifications on detected anthocyanin accumulations during the experiments described in Zhang et al. (2011) were later published in Zhang & Folta (2012).

1.4.2.3 Plant responses to far-red light (λ 700-800 nm)

Overall FR radiation is often considered to be primarily reflected and transmitted by leaves (Kasperbauer, 1987) and to have negligible impact on photosynthesis because of its poor absorption by photosynthetic pigments (Figure 4), leaves and the steep decline in quantum yields found when exposed to monochromatic wavelengths ≥ 680 nm (Figure 5; McCree, 1972a; Hogewoning et al., 2012). The minimal photosynthetic contribution of narrow monochromatic FR wavelengths shown by McCree (1972a) resulted (wrongfully as the reader may see) in the exclusion of FR in the classic definition of photosynthetic active radiation (PAR) (McCree, 1972b).

However, short wavelengths of FR radiation are a strong informational signal for plants. FR light has long been known to induce substantial (phytochrome-mediated) morphological and physiological responses (e.g., Viczián et al., 2017; Ruberti et al. 2012; Franklin, 2008), and has recently been shown to remarkably improve photochemical efficiency and photosynthesis when combined with shorter wavelengths (Zhen & Bugbee, 2020/2020a; Zhen et al., 2018; Zhen and van Iersel, 2017; Park & Runkle, 2017).

Plants experience spatial and temporal variations in R:FR ratios and they have evolved to recognize these R:FR variations e.g., to sense the seasons, detect the time of day and identify neighboring vegetation (Smith et al., 2000). In natural environments, R:FR ratios decrease significantly from the top to the middle and bottom of plant canopies, since red photons become strongly absorbed (as previously described in section 1.4.2.1), while FR photons are mostly reflected or transmitted by leaves (Smith et al., 2017). These low R:FR ratios on the bottom of canopies usually coincide with reduced PAR and deliver a message to plants that they are probably under conditions of shade, which then triggers a plethora of shade avoidance responses (Ruberti et al., 2012) in pursuit to improve light capture, outperform competition and ensure survival.

Please be reminded that R:FR ratios are detected by the plants' phytochrome photoreceptors (section 1.3.2.2.1). Present R:FR ratios dynamically affect the equilibrium of the two interconvertible phytochrome forms (active P_{fr} and inactive P_r). Based on the equilibrium of these phytochrome photostationary states - meaning the ratio of phytochrome in the active to the total phytochrome in the active and inactive state ($P_{fr}/(P_{fr}+P_r)$), shade avoidance responses remain either inhibited or become induced, respectively (Sager et al., 1988).

Upon low R:FR perceptions, shade-avoiding plants typically provoke (phytochrome-mediated) rapid changes in gene expressions that result in responses such as apical dominance via hypocotyl, internode and stem elongations and suppressed branching, petiole extensions, leaf expansions and

hyponasties, and/or accelerated flowering in an attempt to escape unfavorable conditions of shade (Ballaré & Pierik, 2017; Frankhauser & Batschauer, 2016; Leduc et al., 2014; Casal, 2012; Ruberti et al., 2012; Franklin, 2008, Table 7) and represent delightful examples of plants' phenotypic malleability.

However, the specific shade avoidance responses induced by low R:FR ratios are species- and even cultivar-dependent. The best example of this dependency may be the research conducted by Botto & Smith (2002), who analyzed the elongation of hypocotyls and the acceleration of flowering (as two major shade avoidance responses typically observed under FR-enriched conditions) of over 100 accessions of the model plant *Arabidopsis* and found that both shade responses varied tremendously between accessions. Though all hypocotyls elongated upon FR exposure, the extent of hypocotyl elongations varied widely among accessions, and while the majority of *Arabidopsis* accessions accelerated their time to flowering, several accessions responded recalcitrant to the FR signal. In addition, no correlation between both traits was found.

Elongation results under artificial LED lighting - both under greenhouse conditions including natural sunlight and under highly controlled conditions with LEDs as the sole-source lighting - highly align with the findings from Botto & Smith (2002): Spanning from microgreens and leafy greens to ornamentals and fruit-bearing crops, increasing FR additions to PAR, increasing FR substitutions with PAR and FR light as an end-of-day treatment, all reliably induce increasing elongation growths in all horticultural crops that were recently investigated (Table 7).

Currently, LED-based research addressing photobiological responses to FR often calculate the R:FR ratio (regardless of other artificial wavelengths included in their studies) to indicate the phytochrome photostationary states of the investigated plants, because the equilibrium between the two phytochrome forms was found to strongly correlate with R:FR ratios (Franklin, 2008). Recently it was suggested by Kusuma & Bugbee (2021) however, that the percentage of FR (700 to 750 nm) to the overall photons (from 400 to 750 nm) better predict plants' stem elongation rates (possibly because it accounts for phytochrome-cryptochrome coactions in this extension response).

Also, in alignment with Botto & Smith (2002), LED-based research findings show that the flowering response to R:FR ratios can differ between species and cultivars (Table 7). While flowering time was found to be unaffected by different fractions of FR light in sweet pepper (*Capsicum annuum* L. cv. Frazier), bell pepper cultivars (*Capsicum annuum* L. cv. Maureno, Gina and Eurix) and the ornamental potting plants geranium (*Pelargonium x hortorum*) and coleus (*Solenostemon scutellariodes*) (Chen et al., 2022; Park & Runkle, 2018b), flowering was found to be accelerated in tomatoes (*Solanum lycopersicum* cv. Moneymaker (as shown in two independent studies) and *S. lycopersicum* cv. Komeett), grafted tomatoes

(*S. lycopersicum* x *S. habrochaites*), ornamental coreopsis (*Coreopsis grandiflora*), pansy (*Viola x wittrockina*) and petunia (*Petunia x hybrida* (as shown in two independent studies)) (Ji et al., 2020, Ji et al., 2019; Kalaitzoglou et al., 2019; Kim et al., 2019; Craver et al., 2018; Park & Runkle, 2018b).

Indeed, accelerated flowering induced via low R:FR ratios could result in quicker fruit formations and seed productions. However, photobiological study designs analyzing plant development beyond the flowering stage are currently scarce. Nevertheless, noteworthy are the insights recently published on peppers and tomatoes.

While the time of flowering was indifferent between sweet peppers (*Capsicum annuum* L. cv. Frazier) exposed to differing fractions of FR, all FR treatments induced undesirable flower and fruit abortions, which ultimately resulted in significantly reduced sweet pepper yields compared to the sweet pepper yields observed under the control treatment lacking FR (Chen et al., 2022). While Lanoue et al. (2022) also found no effect in the time to flowering between bell peppers exposed to broadband white light and bell peppers exposed to prolonged end-of-day FR lighting in three different bell pepper cultivars, the number and biomass of the peppers remained unaffected by the differing light treatments (contrasting the findings of Chen et al., 2022).

In comparison to peppers, very different flower and fruit responses due to FR-enrichments were found in multiple independent tomato studies covering a range of tomato cultivars (Table 7). Throughout all tomato cultivars, additions of FR to a background of RB and W (with or without natural sunlight) or as an end-of-day treatment resulted in accelerated flower formations and fruit ripening, which subsequently lead to greater individual and total tomato fruit yields. All responses were found to intensify with increasing fractions of FR (Ji et al., 2020; Fanwoua et al., 2019; Ji et al., 2019; Kalaitzoglou et al., 2019; Zhang et al., 2019; Kim et al., 2019). In addition, the number of tomato fruits (Kalaitzoglou et al., 2019) and fruit sugar concentrations (Ji et al., 2020; Fanwoua et al., 2019) were shown to increase with increasing FR fractions, and the expression of genes associated with sugar transportation and metabolism were found to be upregulated (Ji et al., 2020). However, fruit sugar contents were found to decrease with increasing FR fractions in the study by Zhang et al. (2019).

Though enlargements of leaves are commonly observed in most shade-avoiding plant species exposed to FR-enriched light conditions (Demotes-Mainard et al., 2016) and are often presumed to increase the capacity to capture light (e.g., Zou et al., 2019; Meng & Runkle, 2019b; Li & Kubota, 2009), the specific leaf expansion responses vary between species and cultivars (Table 7).

While tomato leaf areas were found to increase with increasing additions of FR by Zhang et al. (2022), Zhang et al. (2019) and Kalaitzoglou et al. (2019), no significant effect on leaf area was found by Ji

et al. (2019) who cultivated the same cultivar as Zhang et al. (2022). The differences between the two studies are that Zhang et al. (2022) investigated a greater range of FR additions (34, 40 and 100 μmol of FR) under highly controlled conditions, while Ji et al. (2019) added only 30 and 50 $\mu\text{mol m}^{-2} \text{s}^{-1}$ of FR under greenhouse conditions. Thus, dose-dependent differences may have been masked by the solar light in the latter study. An (unusual) decrease in tomato leaf areas was observed by Kim et al. (2019). However, FR was not added but partially substituted R radiation and had a narrow peak wavelength of 770 nm (which was recently shown to be part of the ineffective range of FR radiation (Zhen & Bugbee, 2020a).

In addition, while three bell pepper cultivars responded with leaf expansions when FR was applied at the end of the day for 8 hours (Lanoue et al., 2022), leaf sizes remained indifferent in sweet peppers when FR was added during the day (Chen et al., 2022). Thus, it appears that peppers can respond with leaf expansions, however, only very low R:FR ratios may enable the response.

Significant leaf expansions due to FR additions and/or substitutions have also been found in a variety of ornamentals including coreopsis, pansy, petunia, coleus and snapdragon (Craver et al., 2018; Park & Runkle, 2018b). Contrasting appear the leaf expansion results published by Park & Runkle (2017) and Park & Runkle (2018b) for geranium, as increasing and indifferent leaf sizes to increasing R:FR ratios were found. However, as increased leaf areas were detected under the greater range of R:FR ratios tested (Park & Runkle, 2017), geranium's leaf size can clearly be altered by manipulating the ratio of R:FR.

Finally, all recently investigated lettuce cultivars ((Liu & van Iersel, 2022, Legendre & van Iersel, 2021; Jin et al., 2021, Zou et al., 2019; Meng & Runkle, 2019a; Meng et al., 2019)), kale (Meng et al., 2019) and basil seedlings (Meng & Runkle, 2019a) have been shown to respond with leaf expansions when R:FR ratios decrease.

In addition to these morphological leaf responses, low R:FR ratios have frequently been shown to reduce the concentrations of anthocyanin (Liu & van Iersel, 2022; Meng & Runkle, 2019a; Meng et al., 2019), carotenoid (Zou et al., 2019; Kalaitzoglou et al., 2019) and chlorophyll pigments (Liu & van Iersel, 2022; Lanoue et al., 2022; Zou et al., 2019; Meng & Runkle, 2019a; Kalaitzoglou et al., 2019; Meng et al., 2019; Kim et al., 2019; Park & Runkle, 2017; Li & Kubota, 2009) in the leaves of horticulturally relevant crops including lettuces, kale, bell peppers, tomatoes and petunia (Table 7), which appears to contradict the theory that leaves expand to increase the interception of light under conditions of shade. However, the pigment decline may be a trade-off strategy in order to allocate more resources into elongations and/or expansions until more favorable photosynthetic conditions are reached.

And indeed, different allocation strategies have been reported in response to FR (Table 7). In example, peppers significantly increase their biomass partitioning strongly towards stems (Chen et al.,

2022; Lanoue et al., 2022). Tomato plants on the other hand, increase their biomass partitioning predominantly towards fruits (Ji et al., 2020; Ji et al., 2019; Kalaitzoglou et al., 2019; Kim et al., 2019), to a lesser extent toward stems (Ji et al., 2019) and reduce partitioning towards the leaves (Ji et al., 2019; Kim et al., 2019). Hence, in response to FR signals, plants employ different allocation strategies by dividing up their assimilates towards different organs of the plant.

In the vast majority of case studies, the described morphological shade avoidance responses upon FR additions (elongation and expansion responses above all, but also the accelerated flowering with subsequently hastened ripening of fruits) are accompanied with substantial yield increases in all horticultural crops investigated lately (Table 7).

These positive FR effects on the yields of so many horticultural crops clearly suggest that FR radiation is able to effectively drive plant photosynthesis when combined with PAR wavelengths.

And indeed, photosynthetic enhancement effects of FR wavelengths when combined with shorter wavelengths have been observed in the past. First described as the Emerson enhancement effect in 1957, Emerson et al. noted that the photosynthetic rate was greater when the freshwater green alga *Auxenochlorella pyrenoidosa* (formerly known as *Chlorella pyrenoidosa*) was simultaneously illuminated with wavelengths ≥ 685 nm and shorter wavelengths than the sum of the photosynthetic rates measured under both light conditions separately (Emerson et al., 1957). Later, Pettai et al. (2005) found that FR photons support oxygen evolution in sunflower (*Helianthus annuus* L.) and bean (*Phaseolus vulgaris* L.) leaves up to 780 nm. Between 700-780 nm, the quantum yields were found to peak at 745 nm, representing approximately 20 % of the maximum quantum yields measured at 650 nm. Then, Hogewoning et al. (2012) proved that wavelengths between 700 and 730 nm enhance the CO₂ quantum yield in cucumber (*Cucumis sativus* L.) leaves when a broadband light extends into the near infrared spectrum. While Emerson and others ascribed the enhancement of quantum yields of long wavelength light to the presence of short wavelength light, the reverse effect – the enhancement of quantum yields of short wavelength light by far-red light was investigated by Zhen & van Iersel (2017):

As previously described in sections 1.3.1.1 and 1.3.1.2, the light-dependent reaction of photosynthesis begins with the excitation of PSII followed by the excitation of PSI. While PSII prefers wavelengths shorter than 680 nm for excitation, PSI favors slightly longer wavelengths (700 nm) (Evans, 1987; Nabor, 2017; Hogewoning et al., 2012). To achieve high linear electron transport rates from PSII to PSI, both photosystems should work at matching rates. However, light between 400-570 nm and 620-690 nm tend to over-excite PSII compared to PSI (Zhen et al., 2018), which induces non-photochemical quenching (NPQ (the dissipation of excessive excitation energy)) and restricts optimal quantum yields

(especially under artificial light conditions that are solely composed of B (400-500 nm) and R (600-700 nm) radiation). Hence, it is of great consequence that Zhen & van Iersel (2017) recently showed that a simultaneous exposure to FR (735 nm) and RB or broadband W light can balance the excitation energy between the two photosystems by preferentially exciting PSI. The scientists found that the addition of FR immediately increased the quantum yield of PSII (Φ_{PSII}), which increased even further the longer the lettuce leaves were exposed to the added FR radiation. Additionally, photosynthetic rates increased and NPQ decreased with increasing FR photon flux densities ranging from 0 to 90 $\mu\text{mol m}^{-2} \text{s}^{-1}$ added to the constant background of RB and W (PPFD 200 $\mu\text{mol m}^{-2} \text{s}^{-1}$), respectively (Table 7). Soon after, Zhen et al. (2018) demonstrated that FR light enhances the photochemical efficiency in a wavelength-dependent manner (Table 7). That increasing wavelengths from 678 to 703 nm continuously increased Φ_{PSII} in the studied lettuce leaves, indicates that the longer wavelengths within this region are increasingly used more efficiently by PSI than by PSII. However, quantum yields between 703 and 721 nm were found to be similar, tended to decrease from 721 to 731 nm (presumably due to reduced light absorbance and low photon energy), while adding FR with 752 nm had no effect on Φ_{PSII} anymore.

While FR was added in the abovementioned studies conducted by Shuyang Zhen and partners, 50 $\mu\text{mol m}^{-2} \text{s}^{-1}$ of FR (730 nm) were either included or excluded in a total photon flux intensity of 350 $\mu\text{mol m}^{-2} \text{s}^{-1}$ to investigate photosynthetic responses of lettuces (Zhen & Bugbee, 2020). Though FR substitutions did not affect canopy quantum yields and carbon use efficiency, the FR substitutions did in fact increase canopy photon capture, daily carbon gains and biomass through increased leaf expansions (Table 7). In the same year, the research team demonstrated that FR photons increase canopy photosynthesis of 14 different horticultural crops as effectively as PAR photons when combined with photons of shorter wavelengths (400-700 nm) (Zhen & Bugbee, 2020a). In all species (including C3 and C4 species), adding up to 40 % of FR in a PAR background (RB or W) affected the canopy quantum yields and the carbon use efficiencies in the same way as adding the same amount of traditionally defined PAR photons. In addition, crop yields generally increased with FR substitutions during long-term plant cultivation. All effects decreased with increasing FR wavelength (711, 732, 735, 746 nm) however (Table 7). Their findings indicate that FR photons with 700 to 750 nm are equally efficient in driving photosynthesis in plants when acting synergistically with 400-700 nm photons.

Though Liu & van Iersel (2022), Jin et al. (2021), Ji et al. (2019), Kalaitzoglou et al. (2019), Park & Runkle (2018b) detected indifferent Φ_{PSII} and/or photosynthetic rates (P_n ; $\mu\text{mol CO}_2 \text{m}^{-2} \text{s}^{-1}$) with increasing additions of FR (730, 735, 740 nm) on single leaf bases in lettuce and tomato cultivars and ornamental plants, and Zou et al. (2019) in fact detected a lower P_n in lettuce, increased light interceptions

through either leaf expansions and/or shoot elongations resulted in increased biomasses in the majority of these studies.

The data of all these studies combined provide compelling evidence that the current definition of photosynthetically active radiation should be extended by FR photons from 700 to 750 nm.

Whether FR increases light interception by altering plant architecture (e.g., Kalaitzoglou et al. 2019) and/or by balancing the photosynthetic machinery (Zhen and van Iersel 2017), the potential benefits of including FR in horticultural applications are tremendous.

From larger leafy greens and higher fruit yields for human consumption (via leaf expansions and through increased assimilate partitioning towards fruits, respectively) to reduced fruit stacking and simpler grafting (via stem and internode elongations (e.g. Lanoue et al., 2022; Chia & Kubota, 2010) to greater production turnovers of ornamentals and fruit-bearing crops (by accelerating time to flowering) and overall production yield increases (through increased light interceptions): the FR-induced morphological, phytochemical and photosynthetic adaptations can effectively improve horticultural production processes and boost produce yields.

Since FR photons are more efficiently generated by LEDs than W light qualities (Kusuma et al., 2020, section 1.2), CEA growers could partially exchange their light environments with FR LEDs to induce the desired shade avoidance responses and to improve their light use efficiencies. Hence, production costs could be lowered, and profitability improved.

Since end-of-day FR treatments (in the absence of (other) photosynthetically active photons) can easily provide lower phytochrome photostationary states than when the same amount of FR is applied in combination with PAR during the day, short FR-EOD treatments may be able to invoke the desired shade avoidance responses energetically more efficiently than long daytime FR applications (e.g., Zhang et al., 2019; Kalaitzoglou et al., 2019).

However, some shade avoidance responses induced by FR may not always be beneficial (Demotes-Mainard et al., 2016). In example, long stems in flowering pot plants or long stems at the expense of the growth of other plant organs can be highly undesirable. To ensure quality and productivity, optimal FR applications for each crop of interest need to be investigated with the specific production goals in mind.

Table 8 – Morphological, physiological and phytochemical plant effects mediated by far-red wavelengths (λ 700-800 nm).⁷

Plant species	Effect ¹	Light spectrum	Peak λ ²	Light intensity ³	Reference
Sweet pepper	All FR treatments reduced fruit set, induced flower and fruit abortions, and reduced FW_{Fruit} and DW_{Fruit} . FR resulted in increased $Stem_{\text{Length}}$, F_{Stem} and more upright branches. Only FR during the daytime increased DW_{Total} and DW_{Leaf} . LA indifferent between all treatments.	RW; RW+FR; RW+FR-EOD	700-800	130 incl. 0, 50 or 100 of FR; 30 (FR-EOD)	Chen et al. 2022
Tomato	FR increased P_{Height} , DW_{Total} and LA compared to RB. S:R ratio remained indifferent to RB.	RB; RGB; RB+FR; RGB+FR	740	150 + 34, 40 or 100 of FR	Zhang et al. 2022
Lettuce cultivars	Though light interceptions increased with increasing FR, Φ_{PSII} and Pn remained indifferent. At 7 DAT, P_{Height} was found to be increased with increasing FR in all three cultivars. At 16 DAT, chl content index was found to be decreased with increasing FR in all three cultivars; TAC was found to be decreased with increasing FR in red leaf lettuce cv. 'Cherokee'. At 20 DAT, L_{Length} was found to be increased with increasing FR in all three cultivars, DW_{Shoot} was found to be increased with increasing FR in cv. 'Little Gem' and 'Cherokee'. At 21 DAT, LA was found to be increased with increasing FR in cv. 'Little Gem' and 'Cherokee'. At 35 DAT, LA was found to be increased with increasing FR in cv. 'Green Saladbowl', $Stem_{\text{Length}}$ was found to be increased with increasing FR in cv. 'Green Saladbowl' and 'Cherokee', DW_{Shoot} was found to be increased with increasing FR in cv. 'Cherokee' and 'Little Gem'.	W+FR	730	204 + 5-76 of FR	Liu & van Iersel 2022
Bell pepper cultivars	FR-EOD increased $Internode_{\text{Length}}$, P_{Height} , LA, SLA, decreased L_{No} and chl contents, however, did not affect $Fruit_{\text{No}}$, FW_{Fruit} .	W; W+B-EOD;	734	DLIs remained constant	Lanoue et al. 2022

⁷ The reader may also be referred to the following review articles: Landi et al. (2020), Viczián et al. (2017), Demotes-Mainard et al. (2016), Frankhauser & Batschauer (2016), Pierik & de Wit (2014), Ruberti et al. (2012) and Franklin (2008) and the study by Carvalho et al. (2016) cited in Table 10.

	With increasing R:FR ratio, F_{Leaf} decreased, F_{tem} and Internode _{Length} increased.	W+B&FR-EOD; W+FR-EOD			
Lettuce	With increasing FR under a constant background of W , L_{Length} , L_{Width} , LA, canopy size and DW_{Total} increased linearly. Increasing FR was more effective than increasing PAR at increasing incident light and biomass.	W+FR	735; 733	207 + 4-28 of FR; 111-245 + 5-33 of FR	Legendre & van Iersel 2021
Lettuce	FR increased FW_{Leaf} , DW_{Leaf} , DW_{Total} , LA, RUE, LUE, LUE _{int} , however, SLA and P_n remained indifferent. Effects were plant density-dependent with FR effects stronger at low plant density compared to moderate and high plant densities.	RB; RB+FR	740	219 ± 52 of FR	Jin et al. 2021
Lettuce	FR increased canopy photon capture ⁵ , daily carbon gain ⁶ and biomass in both treatments. Canopy quantum yields ⁷ and CUE ⁸ indifferent between treatments. Photosynthesis increased linearly with increasing photon capture and enhanced in FR-treated lettuces through increased LA.	RB; W	730	350 incl. ± 50 of FR	Zhen & Bugbee 2020
14 horticultural crops species ⁴	Adding FR (up to 40 %) in a background of PAR increased canopy photosynthesis equal to adding PAR in all species. Effect decreases with increasing FR wavelength.	FR + SUN; RB; W	711; 732; 735; 746	525; 400 + 40-140 of FR; 510 + 50 of FR	Zhen & Bugbee 2020a
Tomato	FR increased individual and total DW_{Fruit} , fruit sugar (fructose & glucose) concentration, accelerated fruit ripening time, upregulated expression of genes associated with sugar transportation and metabolism, however, $Fruit_{\text{No}}$, DW_{Total} , $Seed_{\text{No}}$, flowering time, sucrose concentration remained indifferent.	RB; RB+FR	735	150 ± 50 of FR	Ji et al. 2020
Lettuce	RB+FR increased FW_{Total} , DW_{Total} , LA, SLA, canopy size, chl a:b ratio, $Sugar_{\text{Sol}}$ content, $PNUE_{\text{max}}$, P_{max}/chl , RUE more than RB+FR-EOD compared to RB. S:R ratio increased under FR-EOD, however, S:R ratio remained indifferent between RB and RB+FR. Nitrate content, NPQ increased and P_{max} decreased under RB+FR, however, remained indifferent between RB and RB+FR-EOD.	RB; RB+FR; RB+FR-EOD	740	200; + 50 of FR; + 50 of FR-EOD	Zou et al. 2019

	<p>RB+FR decreased chl, car and N content, Pn, g_s more than RB+FR-EOD compared to RB.</p> <p>Φ_{PSII}, qP, R_d, α, F_v/F_m indifferent between treatments.</p>				
Tomato cultivars	<p>RB+FR increased $Sugar_{Sol}$ (glucose, fructose, sucrose) in tomato fruits and decreased fruit water content compared to RB, however, malic acid contents remained indifferent.</p> <p>First, FW_{Fruit} was higher under RB, at fruit maturity higher under RB+FR.</p> <p>First, starch and citric acid content were higher under RB+FR, at fruit maturity higher under RB.</p> <p>Dilution by soluble and storage compounds indifferent in mature tomato fruits under RB and RB+FR.</p> <p>RB+RB increased FW_{Fruit} in both cultivars compared to HPS+RB, increased citric acid content in one cultivar, however, metabolism of other fruit biochemical compounds (glucose, fructose, sucrose, starch and malic acid) remained indifferent in both cultivars under both treatments.</p>	SUN + HPS+RB; RB+RB; RB; RB+FR	739	125 + 106; 106 + 110; 200; 200 + 40 of FR	Fanwoua et al. 2019
Seedlings of lettuce cultivars and basil	<p>FR increased L_{Length}, FW_{Shoot}, DW_{Shoot} of all crops (more pronounced under high than low B:R ratio).</p> <p>FR increased DW_{Root} in basil and one lettuce cultivar.</p> <p>$Hypo_{Length}$ and L_{No} remained indifferent in all treatments.</p> <p>FR decreased chl content in lettuce, but not in basil.</p> <p>TAC increased with increasing B:R ratio but decreased under FR in red leaf lettuce.</p>	R; B; RBs \pm FR	732	R_{180} ; B_{180} ; $B_{30}R_{150}$; $B_{90}R_{90}$ \pm 30 of FR	Meng & Runkle 2019a
Lettuce cultivars	<p>Increasing FR increased FW_{Shoot}, DW_{Shoot}, L_{Length}, $Hypo_{Length}$, however, reduced chl content (more under high than low PPFD) under both light intensity treatments.</p> <p>Increasing FR increased L_{Width} and L_{No} only in one cultivar.</p> <p>DW_{Shoot}, chl and TAC increased with PPFD.</p>	RB; RB+FR	732	$B_{90}R_{90}$; $B_{180}R_{180}$; \pm 30 or 75 of FR.	Meng & Runkle 2019a
Tomato	<p>FR increased individual and total DW_{Fruit}, F_{Fruit}, F_{Stem}, flower appearance rate and L_{No} (more pronounced with increasing FR), however, decreased F_{Leaves}.</p> <p>DW_{Total}, LA, Pn, F_{Root} remained indifferent.</p> <p>FR reduced resistance against <i>Botrytis cinerea</i>.</p>	Sun + RB; W; \pm FR	735	150 \pm 30 or 50 of FR	Ji et al. 2019

Tomato	<p>With increasing FR, LA, DW_{Total}, $Fruit_{No}$, individual and total FW_{Fruit}, petiole angle increased, flowering and fruit ripening accelerated, however, leaf absorbance, chl <i>a</i>, chl <i>b</i>, chl <i>a:b</i> ratio, <i>car</i>, g_s decreased. F_{Root} and P_n remained indifferent between all treatments. FR-EOD resulted in similar results observed under RB+FR treatments, however, P_{Height} was increased, flowering was delayed, individual and total FW_{Fruit} was reduced.</p>	Sun + RB; RB+FR; RB+FR- EOD	730	150 + 0, 54, 119 or 154 of FR; 17 of FR-EOD	Kalaitzoglou et al. 2019
Lettuce and Kale	<p>Substituting FR for B triggers shade avoidance responses. Substitution increased L_{Length}, LA, FW_{Shoot} in both crops and Pet_{Length} in kale, however, decreased chl (less than G substituting B), TAC and $Assimilation_{Net}$ in both crops. <i>(Most parameters were more strongly or equally affected by FR substituting B than G substituting B (Table 6).)</i></p>	R + B, G, FR	733	180 incl. 0, 20, 40, 60 of FR	Meng et al. 2019
Tomato	<p>All overhead FR treatments increased $Internode_{Length}$, $Stem_{Length}$, LA, $L_{Length}:L_{Width}$ ratio, FW_{Total}, DW_{Total}, FW_{Fruit}, DW_{Fruit} compared to RB alone. With increasing FR, $Sugar_{Sol}$ (glucose, fructose) content decreased in ripe tomato fruits. FR-EOD increased LA more than the long FR treatment during the day. DW_{Leaf}, DW_{Stem} were increased under 12h FR and 1.5h FR-OED treatments, however, not under 0.5 h FR-EOD treatment compared to RB-ICL alone. Dry matter partitioning remained indifferent between all treatments.</p>	Sun+RB- ICL + FR (12 h); + FRs-EOD	735	144 + 43 of FR or of FRs-EOD	Zhang et al. 2019
Tomato	<p>FR increased FW_{Fruit}, DW_{Fruit}, DW_{Leaf}, L_{Thick}, F_{Fruit}, F:S ratio and accelerated flowering and fruiting, decreased LA, chl content, F_{Leaves}, F_{Stem}, L_{WC}. $Stem_{Length}$, L_{No}, S:R ratio, FW_{Root}, P_n, g_s, remained indifferent between all treatments. $Fruit_{No}$, FW_{Fruit} increased under LED and HPS treatments compared to control; F_{Fruit}, F:L ratio increased under LEDs compared to control. While LEDs increased FW_{Total}, individual and total FW_{Fruit} and DW_{Fruit} DW_{Total}, DW_{Leaf}, L_{Thick}, F_{Fruit}, F:S ratio compared to HPS, HPS increased $Node_{No}$ compared to LEDs.</p>	Sun + HPS; LED-ICL: RB; R; R+FRs	770	230	Kim et al. 2019

Lettuce	FR light preferentially excited PSI; RB excites PSII. Φ_{PSII} increased with increasing FR wavelengths from 678 to 703 nm; similar Φ_{PSII} between 703 and 721 nm; Φ_{PSII} tended to decrease from 721 to 731 nm. Adding 752 nm did not affect Φ_{PSII} .	SUN; RB+FR	678- 752	202	Zhen et al. 2018
Coreopsis, Pansy and Petunia	FR increased/tended to increase $Stem_{Length}$, stem caliper, DW_{Shoot} , LA, time to flower in all three ornamentals (more than G). FR did not affect sturdiness. FR increased DW_{Root} and quality index only in coreopsis, decreased $Node_{No}$ only in petunia, decreased select macro- and micronutrients in coreopsis and pansy. <i>Stem caliper, DW_{Root}, DW_{Shoot}, sturdiness, quality index of seedlings generally increased and $Stem_{Length}$, macro- and micronutrient concentrations generally decreased with increasing intensity, regardless of light quality.</i> <i>$Node_{No}$ remained indifferent between different light intensities.</i> <i>LA decreased in petunia, remained indifferent in coreopsis and increased in pansy with increasing intensity.</i> <i>Time to flower decreased in coreopsis and pansy, however, remained indifferent in petunia with increasing light intensity.</i>	RB; RB+FR; RB+G	740	105, 210, 315 incl. 7 % of FR or 18 % of G	Craver et al. 2018
Geranium, Petunia and Coleus	With decreasing R:FR ratio, $Stem_{Length}$ increased in all species; LA, DW_{Shoot} increased in two ornamentals. L_{No} , DW_{Leaf} , S:R ratio, $Assimilation_{Net}$, Pn remained indifferent between light quality treatments in all species. FR promoted flowering, especially under low light intensity, and decreased chl concentration only in petunia. Under low light intensity, DW_{Root} decreased with decreasing R:FR ratio only in geranium. With increasing intensity, $Assimilation_{Net}$ and Pn increased.	RB \pm FR with 1:0, 2:1 and 1:1 R:FR ratio	731	B ₃₂ + 96 or 288 of R+FR (R ₆₄ ; R ₆₄ FR ₃₂ ; R ₆₄ FR ₆₄ ; R ₂₅₆ FR ₁₂₈ ; R ₂₅₆ FR ₂₅₆)	Park & Runkle 2018b
Geranium, Petunia, Snapdragon, and Impatiens	With increasing additions of FR, $Assimilation_{Net}$ increased linearly in geranium, snapdragon and impatiens, however, remained indifferent in petunia. With decreasing R:FR ratio, P_{Height} increased linearly in all species; LA increased linearly in geranium and snapdragon, chl content decreased	RB \pm FR with 1:0, 3:1, 1:1, 8:1, 4:1	731	B ₃₂ + R+FR (R ₁₂₈ ; R ₁₂₈ FR ₁₆ ; R ₁₂₈ FR ₃₂ ; R ₁₂₈ FR ₆₄ ;	Park & Runkle 2017

	linearly in geranium, petunia and snapdragon, however, LA remained indifferent in petunia and impatiens, chl content remained indifferent in impatiens, DW _{Shoot} remained indifferent in geranium and snapdragon. Inclusion of FR accelerated flowering in snapdragon, however, remained indifferent in geranium, petunia and impatiens.	and 2:1 of R:FR ratio			R ₉₆ FR ₃₂ ; R ₆₄ FR ₆₄)
Lettuce	FR addition immediately increased Φ_{PSII} which increased further with increasing duration of FR radiation. Φ_{PSII} and Pn increased and NPQ decreased with increasing amounts of FR (ranging from 0-90 $\mu\text{mol m}^{-2} \text{s}^{-1}$) under a constant background of RB or W with PPFD of 200 $\mu\text{mol m}^{-2} \text{s}^{-1}$. However, Φ_{PSII} decreased and NPQ increased with increasing PPFDs.	RB; W + FRs	735	0-800	Zhen & van Iersel 2017

¹ Descriptions of abbreviations are listed in alphabetical order: α = leaf photosynthetic efficiency ($\mu\text{mol } \mu\text{mol}^{-1} \text{ photons}$), $\text{Assimilation}_{\text{Net}}$ = net assimilation = dry mass per unit leaf area (g m^{-2}), B = blue light (400-500 nm), car = carotenoid content (mg m^{-2}), chl = chlorophyll content (mg m^{-2}), cv = cultivar, DAT = days after transplant, DLI = daily light integral ($\text{mol m}^{-2} \text{d}^{-1}$), DW_{Fruit} = fruit dry weight, DW_{Leaf} = leaf dry weight, DW_{Root} = root dry weight, DW_{Shoot} = shoot dry weight, DW_{Stem} = stem dry weight, DW_{Total} = total dry weight, EOD = end-of-day light treatment (Chen et al., 2022: 30 minutes; Lanoue et al., 2022: 8 hours; Kalaitzoglou et al, 2019: 15 minutes; Zou et al., 2019: 60 minutes; Zhang et al., 2019: 90, 30 minutes), F_{Fruit} = dry mass partitioning to fruits, F:L = fruit-to-leaf ratio (w/w), F_{Leaves} = dry mass partitioning to leaves, FR = Far red (700-800 nm), F_{Root} = dry mass partitioning to roots, Fruit_{No} = number of fruits, F:S = fruit-to-stem ratio (w/w), F_{Stem} = dry mass partitioning to stems, F_v/F_m = maximum quantum efficiency of photosystem II, FW_{Fruit} = fruit fresh weight, FW_{Leaf} = leaf fresh weight, FW_{Shoot} = shoot fresh weight, G = green light (500-600 nm), g_s = stomatal conductance ($\text{mol CO}_2 \text{m}^{-2} \text{s}^{-1}$), Hypo_{Length} = hypocotyl length, ICL = intra-canopy lighting, LA = leaf area (cm^2), λ = wavelength (*Lambda*), L_{Length} = leaf length, L_{No} = number of leaves, L_{Thick} = leaf thickness, LUE = light use efficiency (plant dry weight per unit of incident PAR (400-700 nm), g mol^{-1}), LUE_{int} = intercepted light use efficiency (plant dry weight per unit of intercepted PAR (400-700 nm), g mol^{-1}), L_{WC} = leaf water content, L_{Width} = leaf width, N = nitrogen, Node_{No} = number of nodes, NPQ = non-photochemical quenching, Pet_{Length} = petiole length, P_{Height} = plant height, Φ_{PSII} = quantum yield efficiency of PSII, P_{max} = maximal photosynthetic rate ($\mu\text{mol CO}_2 \text{m}^{-2} \text{s}^{-1}$), P_{max}/chl = chlorophyll use efficiency of maximum leaf photosynthesis, Pn = photosynthetic rate ($\mu\text{mol CO}_2 \text{m}^{-2} \text{s}^{-1}$), P_{NUe}_{max} = nitrogen use efficiency of maximum leaf photosynthesis, PPFD = photosynthetic photon flux density ($\mu\text{mol m}^{-2} \text{s}^{-1}$), PSI & PSII = photosystem I & photosystem II, PSS = phytochrome photostationary state (the ratio of phytochrome in the active state (Pfr) to the total phytochrome in the active and inactive state (Pfr+Pr) (Sager et al., 1988; section 1.3.2.2.1), qP = photochemical quenching, R = red light (600-700 nm), RB = red and blue light, R_d = dark respiration rate ($\mu\text{mol m}^{-2} \text{s}^{-1}$), R:FR = red-to-far-red ratio, RGB = red, green and blue light, RUE = radiation use efficiency (plant dry weight per unit of incident radiation, g mol^{-1}), Seed_{No} = number of seeds, SLA = specific leaf area ($\text{m}^2 \text{kg}^{-1}$), S:R = Shoot-to-root ratio (w/w), Sugar_{sol} = soluble sugar, TAC = total anthocyanin content, W = broadband white light within PAR (photosynthetically active radiation; 400-700 nm).

² Peak wavelength (λ) of applied far-red light.

³ Light intensity applied in micromole per square meter and second ($\mu\text{mol m}^{-2} \text{s}^{-1}$).

⁴ Three lettuce cultivars, basil, spinach, kale, soybean, tomato, potato, cucumber, sunflower, bean, wheat, rice, corn and sorghum.

⁵ Canopy photon capture = absorbed mole per mole of incident photons.

⁶ Daily carbon gain (g d^{-1}) = net photosynthesis minus respiration rate at night.

⁷ Canopy quantum yields = CO₂ fixed in gross photosynthesis per mole of absorbed photons integrated over 400 to 750 nm.

⁸ CUE = Carbon use efficiency = daily carbon gain per gross photosynthesis.

1.5 Towards broad-bandwidth LED light spectra to improve plant development

Since the beginning of their time, plants on earth have adapted to the natural sunlight spectrum in its entirety. Plants identify daily, seasonal as well as local changes in the Sun's spectral composition with their complex photoreceptor networks and respond with numerous adaptation mechanisms in order to ultimately secure the survival of their species (Fiorucci & Frankhauser, 2017).

As you read in the last sections, various plant reactions can be ascribed to fairly specific wavelength regions. However, probably due to imbalanced activations of the plants' photosystems (Zhen & van Iersel, 2017) and photoreceptors, the use of only narrow LED wavebands has often resulted in abnormal plant developments (Massa et al., 2008) and likely limits the exploitation of the plants' full genetic potential.

The many beneficial light effects inducible by narrow LEDs as explored in the last two decades (and addressed in the previous section) in combination with LED technology advances has encouraged investigations of broad LED light spectra on plants by widening R and B wavebands and by incorporating UV, G and/or FR LED wavelengths. Notable LED studies that investigated plant growth and development under such broad LED light spectra thus far are summarized in Table 9 and will be the topic of this section.

Generally speaking, broadband LED spectra (which emit light within the photobiologically active range have predominantly resulted in better and/or indifferent plant performances in comparison to narrow monochromatic and dichromatic LED systems and other traditional lighting sources such as fluorescent and high-pressure sodium lamps.

In a unique study by Han et al. (2017), responses of lettuce were investigated under a broad W LED spectrum that closely resembled its photosynthetic absorption spectrum. In comparison to monochromatic R and B wavelengths, all responses (including number, size and weight of leaves and their photosynthetic rate) were enhanced under the tailored W light spectrum. Though root length compared to a monochromatic R treatment as well as soluble sugar and phenolic contents compared to a monochromatic B treatment were found to be reduced under a broad W light spectrum (370-755 nm), best *in vitro* micropropagations of lily bulblets were found under the W light treatment (Palka et al., 2023). Similarly, though flavonol indices of green and purple basil, lambs' lettuce and garden rocket were highest under supplemental monochromatic B light, and leaves of purple basil and garden rocket were longer under supplemental monochromatic R light compared to a W spectrum (400-700 nm), respectively, all four species developed best under the supplemental W light treatment in terms of plant heights, leafy yields, chlorophyll contents and the overall number of developed leaves in this greenhouse experiment (Matysiak & Kowalski, 2019). And last but definitely not least, an exceptional study by Sankhuan et al.

(2022) investigated the leaf biomass of the medicinal plant *Artemisia annua*, its contents of bioactive compounds including artemisinin, artemisinic acid and terpenoids under a broad W spectrum (400-700 nm with little R) as well as under monochromatic R and B lighting in a plant factory. Though the highest content of artemisinic acid was found under the monochromatic B light treatment, all other investigated traits were highest under the W light treatment and resulted in the greatest anti-malarial activity against the drug-resistant parasite *Plasmodium falciparum*. In contrast to the abovementioned studies, a broad W light treatment (400-800 nm) was outperformed by monochromatic R and B illuminations: Fresh and dry yields of lettuce and soluble sugar contents were highest under monochromatic R, soluble protein, vitamin C and flavonoid contents were highest under monochromatic B, and undesirable nitrate and ammonium contents (due to food safety concerns (e.g. Pérez-Urrestarazu et al., 2019)) were lowest under monochromatic R and B, respectively (Zhang et al., 2018). However, the W spectrum applied in this study was characterized by unusually high fractions of G and Y wavelength, which most likely explain the reduced assimilation rates.

As previously explained in section 1.4.1, combinations of R and B are widely established in many horticultural applications due to their high photosynthetic efficiencies and the desirable plant performances they cause. Therefore, RB treatments are often used as control treatments in comparative photobiological research studies that aim at investigating influences of these new broad-bandwidth LED light spectra on plant performances:

As mentioned above, the best *in vitro* micropropagation of lily bulblets was found under W and that included a comparison to an RB treatment with a ratio of 7:3, which resulted in the development of less leaves per lily bulblet compared to W (Palka et al., 2023). Though the photosynthetic rate and radiation use efficiency were both found to be higher under an RB treatment (ratio 9:1), leaf developments, morphologies and yields remained indifferent between a broad W (400-800 nm) and two narrow RB treatments (9:1 and 3:1) after 9 to 10 days of light exposure in tomato plants (Ke et al., 2022). The same study observed increased chlorophyll contents under W compared to both RB treatments. However, whether these findings would hold true after longer exposure times remains questionable. More informative is the study from Ji et al. (2019) on tomato plants and fruits. In similarity to Ke et al. (2022), the research team found no differences between broad W (400-700/780 nm) and RB spectra (regardless of in- or exclusion of FR) in terms of dry mass partitions towards tomato fruits, stems and roots, photosynthetic parameters nor in terms of *Botrytis cinerea* infection levels. However, tomato fruit yields were increased under W+FR compared to RB+FR, and leaf partitioning was decreased under W compared to RB. Noteworthy are the findings from Zhen & van Iersel (2017), who – regardless of the applied light

intensity or FR treatments - persistently detected higher quantum yield efficiencies of PSII and higher photosynthetic rates as well as continually lower non-photochemical quenching in lettuce under a broad W spectrum compared to a narrow RB spectrum. Likewise, Leonardo et al. (2019) consistently measured improved photosynthetic activities under two different W LED spectra (400-700 nm with or without elevated R) compared to an RB treatment with elevated R in chrysanthemum. Park & Runkle (2018a) detected very comparable growth attributes in begonia, geranium and snapdragon seedlings under four W light treatments with increasing fractions of R and an RB light treatment with elevated R. Petunia seedlings stood out in their study due to the decreasing number of flower buds and the decreasing hypocotyl length with increasing R fractions in the W light treatments, which showed that the sensitivity to spectral light changes does vary between species. Importantly though, the photosynthetic photon efficacy was best under RB compared to all broad W light treatments. And again, though leaf areas of lemon balm were greater under an RB treatment (1.6:1 ratio; B peak λ 435 nm) compared to a broad W spectrum (370-780 nm), and though maximum quantum efficiency of PSII were greater under all RB treatments (which differed either in their RB ratio or peak wavelength of B (435/450 nm)), height, biomass and essential oil content of lemon balm were greatest under W compared to all other RB treatments, and the number of nodes as well as chlorophyll contents remained indifferent between W and all RB treatments (Rihan et al., 2022). Also, Yan et al. (2020) who compared the growth and development of two lettuce cultivars under two different broad W light spectra (410-750 nm with and without elevated fractions of R) with an RB treatment, determined that the broad W light treatments were best for the cultivation of green lettuce because chlorophyll, nitrate and vitamin C contents, photosynthetic rates, leaf and root yields as well as light and energy use efficiencies were either improved or indifferent compared to the RB treatment. Similarly, purple lettuce grew best under the broad W light treatment with elevated R fractions, though root mass was lower than under RB with elevated R fractions. In contrast, the W treatment with low R fractions was not suitable for the cultivation of purple lettuce as photosynthetic rates and yields alongside light and energy use efficiencies were significantly reduced compared to RB. Furthermore, the cultivation of red bok choy and red lettuce can benefit from broadband lighting: Mickens et al. (2019) compared a variety of W LED spectra (400-800 nm) with an artificial sunlight research module (ASRM; 350-800 nm) and an RB treatment (ratio 3:1). In comparison to RB, they observed either greater or equal leaf lengths, leaf yields and elemental nutrient contents under W and ASRM at harvest. However, the expansion and number of leaves, their anthocyanin contents as well as the bok choy's shoot diameter were greater under RB, which may have resulted from the exceptionally high photosynthetic fluence rate of R under RB compared to all other treatments on one side, and the low B:G ratios under ASRM and W

treatments on the other. In the year before, the same research team compared a similar variety of W LED spectra (400-800 nm) with an RB treatment (ratio 1.5:1). And again, in comparison to RB, broad white treatments exceeded or resulted in indifferent leaf numbers, lettuce yields, chlorophyll and mineral contents compared to RB with the exception of lutein which was found to be enhanced most under RB. The above-mentioned study by Han et al. (2017) - which applied a broad W LED spectrum that closely resembled the photosynthetic absorption spectrum of lettuce - found that the tailored spectrum was able to increase the lettuce's leaf area and yield more than two differing RB treatments, increase the number of lettuce leaves equally to both RB treatments and increase the rate of photosynthesis alike the RB treatment with elevated R.

However, two comparative studies found narrow RB combinations to be superior to broadband W spectra: An RB treatment with an increased proportion of B resulted in better photosynthetic activities and resulted in bigger leaves, higher biomasses and essential oil yields in sweet and bush basil compared to W (400-780 nm). However, the applied W treatment consisted of very low proportions of R and very high proportions of G and Y. Also, in the aforementioned lettuce study by Zhang et al. (2018), a broad W light treatment (400-800 nm) was outperformed by RB treatments (ratios 9:1 and 4:1) in terms of biomass accumulation and nutritional contents, but again, the applied W spectrum was characterized by unreasonably high proportions of G and Y.

Besides the fact that white lighting conditions tremendously improve visual quality assessments as well as the growers' light environment (e.g., Ke et al., 2022; Yan et al., 2019; Park & Runkle, 2018), the reviewed data clearly suggests that broad-bandwidth LED lightings with emissions within the photobiologically active range are able to improve plant performances. The majority of recent findings agree with Tegashima et al. (2009), Hogewoning et al. (2012) and Zhen & van Iersel (2017), who all demonstrated increased quantum yields under widened light spectra. Nevertheless, the specific wavelength compositions of the tested W light spectra varied tremendously in the abovementioned studies. The diverse spectral compositions of what is loosely defined as "white light" strongly impacted the outcomes and must receive special attention.

In a basil study, conducted by Kivimäenpää et al. (2022), proportions of UV-A, B and G linearly decreased while proportions of R and FR linearly increased in three different broad W light spectra. Though many parameters remained unaffected by the differing W LED light spectra, leaf expansions were greatest under the spectrum with elevated UV-A, B and G fractions, and photosynthetic pigment contents were highest under the intermediate spectrum. In addition, under the spectrum with elevated R and FR fractions, contents of major phenolic acids, lengths of internodes and dry yields of basil were increased,

and the concentrations and emission rates of major terpenoids and the phenylpropanoid eugenol were decreased. Yan et al. (2022), found the most compact cucumber seedlings with superior mechanical properties for transport when a W spectrum consisted of low proportions of UV-A and elevated proportions of B. While green lettuce responded insensitive to two different W LED spectra which mainly differed in their proportions of G and R, purple lettuce showed improved leaf and root yields under the W spectrum with lower G/higher R proportions (Yan et al., 2020). Similarly, an improved development of purple lettuce was found under a W spectrum (400-700 nm) with an elevated RB ratio of 2.7. Only the purple anthocyanin content was improved by a reduced RB ratio of 0.9. The formerly mentioned studies by Mickens et al. - who compared multiple W light spectra with elevated fractions of different specific narrow wavebands - revealed that R supplementations (635 nm) increase the number of leaves and anthocyanin contents, that B supplementations (460 nm) increase most mineral contents and that FR (745 nm) supplementations elongate shoots, increase its diameter and the specific leaf area, however, reduce chlorophyll concentrations in red bok choy (Mickens et al., 2019). While W supplemented with G (520 nm) resulted in the highest yield and shoot diameter in 14-day old red lettuce seedlings, W supplemented with R (635 nm) resulted in the highest yield in 28-day old red lettuces. Further, W supplemented with B (460 nm) resulted in the smallest leaves, lowest lettuce heights and dry matter yields but the highest mineral contents and purple pigmentations in red lettuce (Mickens et al., 2018). As one of the first to study the influence of narrow LED wavebands added to a background light consisting of a broad W LED light spectrum, Chen et al. (2016) found the greatest photosynthetic pigment contents and lettuce yields under W with supplemental R (660 nm) and B (450 nm) respectively, greatest leaf number under W with supplemental R and lowest nitrate contents under W with supplemental B and G (522 nm). The latter also improved the soluble sugar contents. To the contrary, W supplemented with Y (596 nm) negatively affected root and shoot yields, photosynthetic pigment contents as well as vitamin C contents. Also, W supplemented with FR (850 nm) negatively affected lettuce in terms of root and shoot yields, photosynthetic pigment contents, nitrate contents and stem diameter, however enabled the highest vitamin C contents. However, with a peak wavelength at 850 nm, this far-red wavelength clearly surpassed the photobiologically active range of the FR-sensing phytochrome system (e.g., Zhen & Bugbee, 2020). Further, though root dry weights of lettuce were increased under a W spectrum (400-800 nm) lacking G emissions between 480 and 560 nm, photosynthetic pigment contents and parameters as well as yields were enhanced under a broad spectrum including these G wavelengths (Liu et al., 2017). Similarly, photosynthetic assimilation rates, the number and size of lettuce leaves as well as overall lettuce yields

were found to be greater under a broad W spectrum (400-800 nm) with a high RB ratio compared to a broad W spectrum with a low RB ratio as evaluated by Han et al. (2017).

Taken together, the research findings indicate that high fractions of R and B as well as their ratios to one another remain of great importance in broad-bandwidth LED lighting strategies. In example, elevated fractions of R noticeably often resulted in high photosynthetic rates, superior yields, and markedly often resulted in improved leaf numbers and sizes, and elevated fractions of B significantly improved the concentrations of essential minerals and secondary metabolites (including nitrates, phenolics, anthocyanins, terpenoids, phenylpropanoids and vitamin C).

Nevertheless, many beneficial effects of UV-A, G and FR came through as well. In example, UV-A improved plant rigidity and compactness, G enabled improved photosynthetic pigment contents and yields, and FR permitted leaf expansions, shoot elongations and higher yields as. Only additions of Y light between approximately 590-600 nm appear to be of negligible or even of negative influence for efficient plant development as pigment contents and yields were found to be significantly reduced. Thus, the published research findings under broad white LED light spectra are in fairly good agreement with the published data under narrow light spectra, although crop age, species and cultivar dependencies obviously exist. Also, special emphasis must be given to the energy use efficiencies (EUE) of broad LED light spectra which can be reduced under W compared to RB (Park & Runkle, 2018a). However, EUE can be improved significantly by increasing fractions of R (Yan et al. 2020; Yan et al. 2019; Park & Runkle, 2018a).

Finally, we will briefly address to which extend W light emitted from LEDs has been superior to traditionally applied light sources based on recent publications. Besides rooting parameters, the W LED spectrum was mostly better than or indifferent to the classically applied fluorescent lamps for the micropropagation of lily bulblets (Palka et al., 2023). Though the maximal photosynthetic rate was measured to be higher, and the stomatal conductance was temporarily found to be increased under high-pressure sodium (HPS) lamps compared to broad W LED lamps in two different *Ocimum* species, all morphological traits and yields, including essential oil yields, remained indifferent between the two light sources (Aldarkazali et al., 2019). However, the low R content within the applied LED spectrum allows the assumption that there is room for spectral upgrades which would exceed the non-adjustable plant developments under HPS. Also, although Leonardos et al. (2019) detected a few differences in some measured photosynthetic characteristics, a W LED spectrum with high content of R was as effective for chrysanthemums' carbon gain as the HPS and only a W LED spectrum with low R content reduced carbon effectiveness.

Table 9 – Morphological, physiological and phytochemical plant effects mediated by broad white LED light spectra (λ 350-800 nm).⁸

Plant species	Effect ¹	Light spectrum	Spectral range ²	Light intensity ³	Reference
Lily bulblets	W translated into the highest efficiency of lily bulblet formation and greatest number of bulbs with developed leaves compared to all other treatments. Ratio of bulbscales generating bulblets, bulblet _{No} , L _{Length} , Root _{No} , chl b were indifferent between W and the respective light treatments with the best outcome. However, under W, bulblet _{Diam} , chl a, total chl and car were reduced compared to RGB; ratio of bulbscales regenerating roots was reduced compared to FL; Root _{tLength} was reduced compared to FL, R and RGB; Phenol _{sol} was reduced compared to B, RBFR and RGB; Sugar _{sol} was reduced compared to B.	R; B; R _{7B3} ; RGB; RBY; RB+UV-A; RBFR, W, FL	370-755	40	Palka et al. 2023
Basil	P _{Height} , Pet _{Length} , FW _{total} , P _n , g _s , chl b, chl a:b ratio, TAC, leaf anatomical traits, SD _{Abaxial} , SD _{Adaxial} , TD _{Abaxial} , TD _{Adaxial} remained indifferent between all treatments. Internode _{Length} was increased under C. L _{Width} , L _{Length} , was highest under A, lowest under B. DW _{Total} was highest under C, lowest under B. Chl a and car were highest under B, lowest under C. Major phenolic acid contents were highest under C, lowest under A. Concentrations and emission rates of major terpenoids and the phenylpropanoid eugenol were indifferent between A and B, but lower under C.	Ws ⁴	380-800	300	Kivimäenpää et al. 2022
Cucumber seedlings	In a greenhouse experiment, the combination of W, B and UV-A resulted in the most compact growth, superior mechanical properties and most preferable growth performances compared to all other treatments.	Sun ± W; UV-A; WB;	na	Sun + 180	Yan et al. 2022

⁸ The reader may also be referred to the review article by Landi et al. (2020) and the following studies: Choi et al. (2022), Gao et al. (2022), Lee et al. (2021), Li et al. (2020) and Qian et al. (2019) cited in Table 6; Schenkels et al. (2019), Meng & Runkle (2019) and Snowden et al. (2016) cited in Table 7; Chen et al. (2022), Liu & van Iersel (2022), Lanoue et al. (2022), Legendre & van Iersel (2021), Zhen & Bugbee (2020; 2020a) and Ji et al. (2019) cited in Table 8; Ahmadi et al. (2021), Araújo et al. (2021), Chaves et al. (2020), Hsieh et al. (2019), Lazzarini et al. (2018), Andrade et al. (2017), Noguchi & Amaki (2016), Batista et al. (2016) in Table 10.

		W+UV-A; WB+UV- A			
<i>Artemisia annua</i>	FW _{Leaf} , artemisinin, terpenoids and anti-malarial activity were highest under W compared to monochromatic R and B. Artemisinic acid was highest under B, followed by W and lowest under R. W and B exhibited 4 times greater antimalarial activity than GH-grown plants.	W; B; R	400-700	200 ± 10	Sankhuan et al. 2022
Tomato	Stem _{Length} , Leaf _{No} , light transmittance in the B and R range, chl a:b ratio remained indifferent between treatments after 9/10 days of treatment. FW _{Total} , LA, light reflectance, Pn increased with increasing light intensity. SLA, RUE, pLUE, light transmittance in the G range, chl a, chl b, total chl decreased with increasing light intensity.	W	400-800	300, 500, 700	Ke et al. 2022
Tomato	Leaf _{No} , FW _{total} , LA, light reflectance in the B and R range remained indifferent between treatments after 9/10 days of treatment. Light reflectance in the G range were reduced, and chl a, chl b and total chl were increased under W. Pn was highest under R ₉ B ₁ , lowest under R ₃ B ₁ and intermediate under W. Stem _{Length} , DW _{Total} , pLUE were reduced under R ₃ B ₁ . RUE was increased and SLA was decreased under R ₉ B ₁ .	W; R ₃ B ₁ ; R ₉ B ₁	400-800	300	Ke et al. 2022
Lemon balm	FW _{Total} , DW _{Total} , P _{Height} , and Internode _{Length} were highest under W. LA under W was smaller than under R-rich RB, equal to B-rich RB with 435 nm and B-rich RGB with 450 nm, but higher than under B-rich RB with 450 nm. F _v /F _m and NDVI were equally reduced under W and B-rich RGB treatments. EO contents were highest under W and B-rich RGB with 450 nm, but lowest under B-rich RB with 435 nm. Number of nodes and chl contents remained indifferent between treatments.	W; RBs RGB	380-780	125 ± 10	Rihan et al. 2022
Cucumber seedlings	In a greenhouse experiment, chl, Stem _{Diam} , Stem _{Firm} increased, SLA decreased with increasing supplemental light duration. Pn, L _{Length} , L _{Width} , FW _{Shoot} , FW _{Root} , DW _{Shoot} , DW _{Root} , SQI increased from 0 to 10 h d ⁻¹ , but then decreased.	Sun ± Ws	400-750	6 h of 287; 8 h of 208; 10 of 167; 12 h of 139	Yan et al. 2021

	<p>Tr, substomatal CO₂ concentration and g_s increased from 0 to 8 h d⁻¹, but then decreased.</p> <p>RSA, R_{Volume} and R_{Activity} increased with increasing light duration from 0 to 8 h d⁻¹, but remained indifferent between 8, 10 and 12 h d⁻¹ of supplemental light.</p> <p>SOD and CAT activities were reduced under supplemental light treatments compared to sunlight treatment without supplemental lighting.</p> <p>LUE was reduced under the 12 h d⁻¹ light duration, but was indifferent between 6, 8 and 10 h d⁻¹.</p>					to provide equal DLI of 6 mol m ⁻² d ⁻¹
Green and purple lettuces	<p>In green lettuce, broad W light treatments resulted in best and/or indifferent outcomes with the respective narrow light treatments with the best outcome in terms of chl a, chl b, total chl, Pn, FW_{Leaf}, FW_{Root}, DW_{Leaf}, DW_{Root}, LUE and EUE; Nitrate content was reduced under WR. Vitamin C content was highest under W and increased under WR compared to RGB and RBFR.</p> <p>In purple lettuce, broad W light treatments generally resulted in best and/or indifferent outcomes with the respective narrow light treatments with the best outcome in terms of chl a, chl b, total chl, Pn, nitrate, vitamin C, TAC, FW_{Leaf}, DW_{Root}, LUE and EUE. Under W however, Pn was reduced compared to RB; FW_{Leaf}, DW_{Leaf}, DW_{Root}, LUE were reduced compared to all other treatments; EUE was reduced compared to WR, RB and RBUV-A. Under WR, FW_{Root} was reduced compared to W, RB, RBUV-A, and RBFR; DW_{Root} was reduced compared to RBFR; DW_{Leaf} was reduced compared to RB and RB-UV-A.</p>	W; WR; RB; RGB; RBUV-A; RBFR	410-750	200		Yan et al. 2020
Sweet and bush basil	<p>For both cultivars, from HPS to W to RB P_{max} increased; F_v/F_m was increased under RB, P_{Height} remained indifferent between light treatments.</p> <p>In sweet basil, while g_s was indifferent between treatments 40 DAS, g_s was increased from HPS to W to RB after 54 DAS; LA, FW_{total} and EO content were increased under RB; LEDs improved relative abundance of linalool, eugenol, <i>trans</i>-cinnamate; RB increased 1,8-cineole compared to W and HPS; abundance of methyl chavicol and DW_{Total} remained indifferent between treatments.</p> <p>In bush basil, g_s was increased from HPS to W to RB at 40 and 54 DAS; LA remained indifferent between light treatments; while FW_{total} was increased</p>	HPS; W ₃₈₀₋₇₈₀ with elevated B; R _{632B452} with elevated B	400-780	470		Aldarkazali et al. 2019

	under W 40 DAS, FW_{total} was increased under RB 54 DAS; while DW_{total} was indifferent 40 DAS, DW_{total} was increased under RB 54 DAS.				
Green and purple basil, lamb's lettuce, garden rocket	For all species, W resulted in best outcome or was indifferent to the respective monochromatic light treatment with the best outcome in terms of FW_{Shoot} , P_{Height} , L_{No} , chl. While indifferent L_{Length} were observed between supplemental treatments, L_{Length} of purple basil and garden rocket were reduced compared to R. While W was more effective than R in increasing flavonol index in lamb's lettuce and garden rocket, B was most effective in increasing flavonol index in all species compared to all other light treatments.	Sun ± W; R; B	400-700	Sun + 130	Matysiak & Kowalski, 2019
Tomato	When no FR was added, DW_{Fruit} , F_{Fruit} , F_{Stem} , F_{Roots} , Pn , Φ_{PSII} , ETR and lesion area after <i>Botrytis cinerea</i> infection remained indifferent between W and RB; F_{Leaf} was increased under RB compared to W. When FR was added, F_{Leaf} , F_{Stem} , F_{Roots} , Pn , Φ_{PSII} , ETR and lesion area after <i>Botrytis cinerea</i> infection remained indifferent between W and RB; DW_{Fruit} was increased under W compared to RB;	Sun + R _{16B1} ; RBFR; W; WFR	400-780	150 ± 30 of FR	Ji et al. 2019
Purple lettuce	In general, L_{No} , vitamin C content remained indifferent, Pn decreased, and L_{Length} increased with increasing R:B ratio under all light intensities. Best FW_{Leaf} , FW_{Root} , DW_{Leaf} , DW_{Root} were found under W with R:B 2.7. The best PC, LUE and EUE were found under W with R:B 2.7 and 3.6. Lowest nitrate contents were found under W with R:B 1.8 and 2.7. Highest TAC were found under W with R:B 0.9. In general, Pn , L_{No} , FW_{Leaf} , PC increased, and L_{Length} , nitrate content, TAC, vitamin C content, LUE, EUE decreased with increasing light intensity.	Ws with differing R:B ratios (0.9; 1.8; 2.7; 3.6)	400-700	100, 150, 200, 250, 300	Yan et al. 2019
Red bok choy	14 DAS, $Shoot_{Length}$ was greatest under ASRM and WFR, FW_{Shoot} was greatest under RB, followed by ASRM and WFR; chl reduced under ASRM and WFR; TAC greatest under RB. 21 DAS, $Shoot_{Length}$ was greatest under ASRM, followed by WFR and RB; chl reduced under ASRM, WG-R and WFR; TAC greatest under RB, followed by WR. 28 DAS, LA and TAC greatest under RB; SLA greatest under ASRM, followed by RB and WFR; L_{No} greatest under RB, followed by ASRM, WR and WG-R; FW_{Shoot} and DW_{Shoot} greatest under RB and ASRM; $Shoot_{Length}$ greatest under ASRM, followed by WFR; $Shoot_{Diam}$ greatest under RB, followed by	W; WR; WG-R ⁵ ; WFR; R _{3B1} ; ASRM	400-800	180	Mickens et al. 2019

	ASRM and WFR; Ca, K greatest under W and RB, followed by WR; Mg indifferent between treatments; P greatest under W, followed by RB and WG-R, S greatest under W and WR, followed by RB; chl reduced under WFR;				
Chrysanthemum	All narrow and broad light treatments drove photosynthesis. RB and WR were as effective for carbon gain as HPS, however, WUE was decreased under RB and WR compared to HPS. During long-day photoperiod, P_{max} greatest under HPS, followed by Y and W; Φ_{PSII} greatest under W and HPS, followed by RB and Y; lowest LCP found under Y and WR; Pn greatest under HPS, W and Y; g_s greatest under B and RB; C_i greatest under B, followed by RB; WUE greatest under W, R and HPS, Tr and R_d remained indifferent between treatments. During short-day photoperiod, P_{max} greatest under WR and lowest under B; Φ_{PSII} greatest under Y and HPS, followed by W; Pn greatest under HPS and W; g_s , C_i and Tr greatest under B; WUE greatest under W, WR and R; LCP and R_d remained indifferent between treatments.	HPS; W; WR; R; B; RB; Y; G	400-700	0-120	Leonardos et al. 2019
Seedlings of begonia, geranium, petunia and snapdragon	PPE was best under RB. $DW_{Efficacy}$ increased under $WR_{66\%}$, $WR_{80\%}$ and RB in begonia, geranium and petunia, but remained indifferent between all treatments in snapdragon. LA , FW_{Total} , DW_{Total} remained indifferent between all treatments in all species. P_{Height} remained indifferent between treatments in begonia and geranium but was reduced under RB and RGB in snapdragon. In petunia, $Stem_{Length}$ and flower bud formation decreased with increasing R fraction in W light treatments and was shortest/lowest under RB and RGB.	Ws with increasing fractions of R (26; 44; 66; 80 %); RGB; $R_{5.7B_1}$	400-800	160	Park & Runkle 2018a
Lettuce	FW_{Shoot} was greatest under R and reduced most under G, followed by Y, then W. DW_{Shoot} was greatest under R and R_4B_1 and reduced most under G, followed by Y, then W. $Sugar_{Sol}$ was highest under R, followed by R_9B_1 , then R_4B_1 and reduced most under Y, G and B_{419} . $Protein_{Sol}$ and vitamin C were highest under B_{437} and R_4B_1 and reduced most under Y, followed by G, W and R.	W; B_{419} nm; B_{437} nm; R; G; Y; R_9B_1 ; R_4B_1	400-800	200	Zhang et al. 2018

	<p>TPC was highest under W and B₄₁₉, lowest under G and R_{4B1}. TFC was highest under B₄₃₇, lowest under Y. Nitrate and ammonium contents were lowest under B₄₃₇, R and R_{4B1}, highest under G, followed by B₄₁₉, then W. NR_{Activity} was highest under R_{4B1}, followed by R_{9B1} and lowest under G, followed by Y, then W. NiR_{Activity} was highest under R_{4B1} and lowest under G, followed by R and Y.</p>				
Red lettuce	<p>14 DAS, WG resulted in greatest, while RB and WB resulted in lowest FW_{Total} and Shoot_{Diam}. 21 DAS, WG, WR and RGBFR resulted in greatest FW_{Total}; WG, WFR and RGBFR resulted in greatest Shoot_{Diam}; RB and WB resulted in lowest FW_{Total} and Shoot_{Diam}. 28 DAS, LA was greatest under RGBFR and WFR, lowest under RB, WB and W; SLA was highest under RGBFR, lowest under WFR; L_{No} was highest under RGBFR and WFR, indifferent between all other treatments; FW_{Total} was greatest under RGBFR and WR, lowest under RB and W; DW_{Total} was greatest under RGBFR, lowest under RB and WB; P_{Height} was greatest under WFR, lowest under RB and WB; Shoot_{Diam} was greatest under RGBFR, WFR and WG, lowest under RB; Chl was reduced under WFR and RGBFR and indifferent between all other treatments; Highest mineral contents (Ca, K, Mg, P) were found under WB, lowest under RGBFR; Lutein was highest under RB, lowest under RGBFR; pigmentation was highest under WB and RB.</p>	<p>W; R_{1.5B1}; WB; WG; WR; WFR; RGBFR</p>	400-800	180	Mickens et al. 2018
Lettuce	<p>DW_{Root}, I_c were increased under W lacking G. DW_{Shoot}, SLA, chl, car, chl:car, absorptance, P_n, g_s, Ci, Tr, F, I_{sat}, P_{max}, Φ_{PSII}, R_d, ETR, V_{c,max}, TPU were increased under W. Chl a:b ratio and photorespiration remained indifferent between treatments.</p>	<p>W; W minus G (480- 560 nm)</p>	360-710	100	Liu et al. 2017
Lettuce	<p>L_{No} is the greatest under RYB, W (high R:B), RB (high R:B) and R, however, lowest under B, RB (low R:B), W (low R:B). LA is the greatest under RYB, lowest under RB (low R:B), B and W (low R:B). FW_{Total} highest under RYB, followed by R and RB (high R:B), lowest under RB (low R:B), followed by B and W (low R:B).</p>	<p>R; B; RBs (high or low R:B); RYB⁶; Ws (high or</p>	400-800	150	Han et al. 2017

	<i>Pn</i> highest under RYB and RB (high R:B), lowest under B, W (low R:B), followed by RB (low R:B).	low R:B ratio)			
Lettuce	Regardless of FR treatment and light intensity, Φ_{PSII} , <i>Pn</i> were consistently greater, and NPQ was consistently lower under W than under RB.	RB; W \pm FR	400-800	0-800	Zhen & van Iersel 2017
Lettuce	<p>P_{Height} was reduced under WB.</p> <p>FW_{Shoot} was increased under WR and WB, reduced under WFR.</p> <p>FW_{Root} was increased under W, WR and WB, reduced under WFR and WY.</p> <p>DW_{Shoot} was increased under WR and WB, reduced under WFR and WY.</p> <p>DW_{Root} was increased under W, followed by WB, reduced under WFR and WY.</p> <p>$Stem_{Diam}$ was increased under WR, reduced under WFR.</p> <p>L_{No} was increased under WR, reduced under WFR.</p> <p>S:R ratio was highest under WFR and WR, lowest under W.</p> <p>Chl a, chl b, chl and car were highest under WR and WB, followed by W, lowest under WFR and/or WY, followed by WG.</p> <p>The lowest nitrate content was found under WG and WB, highest under WY, followed by WFR.</p> <p>AscAC was highest under WFR, followed by WR and WG, lowest under W and WY.</p> <p>Sugar_{sol} was highest under WG, followed by WFR and WR, lowest under W and WB.</p>	W; WB; WG; WY; WR; WFR	400-900	135	Chen et al. 2016

¹ Descriptions of abbreviations are listed in alphabetical order: AscAC = ascorbic acid content (*vitamin C*), ASRM = artificial sunlight research module, B = blue light (400-500 nm), $bulb_{Diam}$ = diameter of bulblet, $bulb_{No}$ = number of bulblets, Ca = calcium, car = carotenoid content, CAT = catalase, chl = chlorophyll content, C_i = intracellular CO₂ concentration, DAS = days after sowing, DW_{Fruit} = fruit dry weight, DW_{Leaf} = leaf dry weight, DW_{Root} = root dry weight, DW_{Shoot} = shoot dry weight, DW_{Total} = total dry weight, EO = essential oil, ETR = electron transport rate, EUE = energy use efficiency, F = vapor pressure deficit (kPa), F_{Fruit} = dry weight partitioning to fruit, FL = fluorescent lamp, F_{Leaf} = dry weight partitioning to leaf, FR = far red (700-800 nm), F_{Root} = dry weight partitioning to root, F_{Stem} = dry weight partitioning to stem, F_m/F_m = maximum quantum efficiency of photosystem II, FW_{Leaf} = leaf fresh weight, FW_{Root} = root fresh weight, FW_{Shoot} = shoot fresh weight, FW_{Total} = total fresh weight, G = green light (500-600 nm), g_s = stomatal conductance (mol CO₂ m⁻² s⁻¹), I_c = compensation irradiance (μmol m⁻² s⁻¹), I_{sat} = saturation irradiance (μmol m⁻² s⁻¹), K = potassium, LA = leaf area (cm²), λ = wavelength (*Lambda*), LCP = light compensation point, L_{Length} = leaf length, L_{No} = number of leaves, LUE = light use efficiency (plant dry weight per unit of incident light (g mol⁻¹), L_{width} = leaf width, Mg = magnesium, *na* = not available, NDVI = normalized difference vegetation index, NiR = nitrite reductase, NPQ = non-photochemical quenching, NR = nitrate reductase, P = phosphorus, PC = power consumption, P_{Height} = plant height, $Phenol_{sol}$ = soluble phenolics, Pet_{Length} = petiole length, Φ_{PSII} = quantum yield efficiency of photosystem II, pLUE = photosynthetic light use efficiency (mm CO₂ mol⁻¹), P_{max} = maximal photosynthetic rate (μmol CO₂ m⁻² s⁻¹), *Pn* = photosynthetic rate (μmol CO₂ m⁻² s⁻¹), PPE = photosynthetic photon efficacy (μmol J⁻¹), $Protein_{sol}$ = soluble protein (mg g FW⁻¹), R = red light (600-700 nm), $R_{Activity}$ = root activity (g h⁻¹), RB = red and blue light, R_d = dark respiration rate (μmol m⁻² s⁻¹),

RGB = red, green and blue light, RSA = root surface area (cm^2), RUE = radiation use efficiency (g mol^{-1}), R_{Volume} = root volume (cm^3), SD_{Abaxial} = abaxial stomatal density (number mm^{-2}), SD_{Adaxial} = adaxial stomatal density (number mm^{-2}), $\text{Shoot}_{\text{Diam}}$ = shoot diameter, SLA = specific leaf area ($\text{cm}^2 \text{mg}^{-1}$), SOD = superoxide dismutase, SQI = seedling quality index, S:R = Shoot-to-root ratio (w/w), $\text{Stem}_{\text{Diam}}$ = stem diameter, $\text{Stem}_{\text{Firm}}$ = stem firmness, $\text{Sugar}_{\text{Sol}}$ = soluble sugar, TAC = total anthocyanin content, TD_{Abaxial} = abaxial trichome density (number mm^{-2}), TD_{Adaxial} = adaxial trichome density (number mm^{-2}), TFC = total flavonoid content, TPC = total phenolic content, TPU = triose phosphate utilization rate ($\mu\text{mol m}^{-2} \text{s}^{-1}$), Tr = transpiration rate ($\text{mol H}_2\text{O m}^{-2} \text{s}^{-1}$), UV-A = ultraviolet light (350-400 nm), $V_{c,\text{max}}$ = maximum carboxylation rate of Rubisco, W = broadband white light usually within PAR (photosynthetically active radiation; 400-700 nm \pm flanking regions including ultraviolet (UV) A and/or FR), WUE = water use efficiency ($\mu\text{mol CO}_2 \text{mmol}^{-1} \text{H}_2\text{O}$), Y = yellow light (560-640 nm).

² Broad waveband range of the applied white light.

³ Light intensity is given in micromole per square meter and second ($\mu\text{mol m}^{-2} \text{s}^{-1}$).

⁴ Proportions of UV-A, B and G linearly decreased, and proportions of R and FR linearly increased from A to C, respectively.

⁵ White with additional monochromatic green LED light treatment was switched to white with additional monochromatic red LED light after 21 days.

⁶ RYB represents a broad white LED spectrum which closely resembles the photosynthetic absorption spectrum of the lettuce investigated in this study.

1.6 Essential oils under LED lighting

Aromatic plants synthesis, accumulate and secrete essential oils (EOs) in specialized cell structures such as (but not limited to) floral fragrance glands (osmophores) or peltate glandular hairs (trichomes), which significantly contribute to the plants' survival strategies: Fragrant EO compounds attract not only insect pollinators, seed dispersers and natural enemies of herbivores, but are also a fascinating means of communication between plants. In addition, EOs defend plants against bacterial and fungal pathogens, protect them from extreme temperatures and contribute to the conservation of moisture (Bunse et al., 2022; Rehman et al., 2016).

For centuries, humans have appreciated these aroma-yielding plants as well as their extracted volatile oils for their medicinal, culinary and fragrant properties. Following oral and dermal administrations and inhalations, EOs are not only used to treat a plethora of illnesses and injuries, but they are also indispensable ingredients of hygiene and dental formulations. And as flavorings and part of perfumes, adhesives and pesticides, EOs represent crucial components in diverse food, chemical and agricultural industries (Bunse et al., 2022; Rehman et al., 2016).

EOs mainly consist of terpenoids, phenylpropanoids as well as aromatic aldehydes, alcohols and ketones. These organic substances originate from different primary metabolic precursors and are generated through various biosynthetic pathways⁹. Thanks to the diverse molecular structures and multitude of functional groups of the countless EO constituents, EOs can interact with a variety of (protein) molecules (including peptides, enzymes, receptors, transcription factors and DNA). The ability of these lipophilic EO compounds to cross biomembranes and cellular compartments as well as their capacity to interact with these diverse molecules via attachments and/or incorporations are the fundamental reason for their efficient absorption by living organisms and for their wide range of chemical, physiological and thus, pharmacological and therapeutic effects, which we however are only beginning to fathom (Bunse et al., 2022).

In the forefront of EO regulations is the development of the aromatic plants themselves as the biogenesis and accumulation of EOs are endogenous processes. In other words, the production of EOs is part of the plants' genetic constitution. Hence, EO yields and their compositions depend on the individual plant species (the genotype), the specific developmental stage of the aromatic plant and its organs. In example, close correlations between leaf ontogenesis and oil synthesis and accumulation have been revealed in some aromatic plants of the *Lamiaceae* family which are of industrial relevance: Only the

⁹ Detailed descriptions of the diverse biosynthetic pathways of essential oil constituents are not an objective of this introduction. The reader may be referred to Rehman et al. (2015), Vogt (2010) and Sangwan et al. (2001).

youngest leaves of marjoram (*Origanum majorana* L.) possess high terpene-yielding capacities (Croteau, 1977). Similarly, most rapid terpene accumulations were observed in the oil glands of immature leaves of sage (*Salvia officinalis* L.) during their period of maximal expansion (Croteau et al., 1981), and in the glandular trichomes of peppermint (*Mentha x piperita* L.), terpene synthesis was found to be restricted to leaves 12 to 20 days of age (McConkey et al., 2000). In addition, though individual leaves show a progressive decline in oil yield with increasing dry matter and age of leaves, the concentration of menthol (as the most desired terpene in mints) increases towards leaf maturity after which it starts to decline again (Duriyaprapan & Britten, 1982). As a result of these highly regulated and intrinsically coordinated EO productions, the quantity and quality of desired EOs for human use substantially depend on the time of harvest.

Besides being exerted in a developmental-specific manner, the physiological regulation of EOs is highly susceptible to environmental factors. As well reviewed and summarized by Bunse et al. (2022), Rehmann et al. (2016) and Sangwan et al. (2001), EO contents and compositions are not only influenced by geographic distributions and seasonal variations in climate (including temperature, humidity and precipitation conditions), but become modulated through agricultural management practices (including soil conditions, salt levels and fertilizer applications) and can be altered upon pest infestations.

Additionally, the lights' intensity and quality are known to affect EO yields and compositions, and a few examples may be mentioned hereafter. One might expect that EO yields increase with increasing sunlight intensities simply due to accelerated plant developments, however, that is not always the case. In example, though highest EO yields were found under full sunlight conditions in thyme (*Thymus vulgaris* L.), highest EO yields were found in sage when exposed to only 45 % of full sunlight (Li et al., 1996). Further, while not significant in one chemotype of spearmint (*Mentha spicata* L.), an enhanced UV-B supplementation substantially increased EO production in the leaves of another spearmint chemotype as investigated in a pot experiment under field conditions (Karousou et al., 1998). Also, peppermint leaves exposed to UV-B showed elevated EO productions, but menthol concentrations were considerably decreased and other constituents such as menthone, menthofuran and methyl acetate were increased. Hence, the chemical composition of the oil was substantially affected by the quality of light (Maffei & Scannerini, 2000).

Even though EOs are crucial ingredients for multiple industries, and environmental conditions can significantly hamper production goals, research focusing on essential oil contents and especially essential oil compositions in medicinal and aromatic plants (MAPs) under differing LED light spectra and intensities

are fairly unexplored¹⁰. Concomitantly, our knowledge and understanding about how LED lights can be used to manipulate and improve essential oil contents and compositions in an effective and reproducible manner is still characterized by many gaps. The following section including Table 10 summarizes and reviews relevant information in this regard.

Awareness of fundamental species- and cultivar-dependent LED responses to different LED light qualities found in the last decade is of great importance as these findings indicate that there may not be one light scenario that fits all.

Representing two species from the genus *Salvia* (commonly known as sage) within the Lamiaceae family, Ghaffari et al. (2019) investigated EO contents and compositions of *Perovskia abrotanoides* and *P. atriplicifolia* under different LED lights as well as under GH conditions as a control treatment. Interestingly, under monochromatic R, the major (and strongly aromatic) compound camphor remained either undetected or was found at its lowest concentration (4.8 %). The highest relative concentration of camphor (and its precursor borneol) was observed under GH conditions (22.8 and 10 %) in *P. abrotanoides*, while in *P. atriplicifolia* under an unspecified white (W_?) LED light treatment (29.5 and 13.5 %). In contrast, borneol acetate accumulated under the W_? light treatment in *P. abrotanoides*, while under GH conditions in *P. atriplicifolia*. And while the main monoterpenes α -pinene, δ -3-carene (piney and sweet earthy in fragrance, respectively) as well as the main sesquiterpenes *trans*-caryophyllene and α -humulene (both giving of earthy, spicy and herbal scents) were enhanced under identical light treatments, both *Perovskia* species responded differently in terms of the monoterpene 1,8-cineole (also known as eucalyptol) and the monoterpene camphene: While 1,8-cineole accumulated most under GH and B light conditions (15.9 and 14.4 %) in *P. abrotanoides*, this mint-like smelling and spicy, cooling tasting compound accumulated most under GH, W_? and R light conditions (21.3, 27.1 and 31 %) in *P. atriplicifolia*. And while camphene was only recovered under GH conditions in *P. abrotanoides*, camphene (with its pungent, damp, earthy, herbal aroma) was found under R, B, GH and RB light conditions in decreasing proportions, and remained undetected under the W_? light treatment. In addition, both species differed in their overall EO yields as affected by the light qualities: While EO yields of *P. abrotanoides* decreased substantially from W_? (2.66 %), B (1.7 %), R (1.2 %), GH (0.7 %) to RB (0.4 %), EO yields of *P. atriplicifolia* lessened from B (1.9 %) to R (1.7 %), RB (1.6 %), W_? and GH (1.5 %) in a less drastic manner.

Earlier, one of the researchers from the above mentioned study (and colleagues) compared EO contents of three mint species (genus *Mentha* in the Lamiaceae family) under the identical LED light

¹⁰ Currently, no comprehensive scientific literature reviews about LED lighting affecting essential oil contents and compositions exist.

treatments applied in the study above, and also observed divergent EO accumulation patterns. While EO yields decreased from R, RB to B and were lowest under the W₂ light treatment in *Mentha piperita*, EO yields decreased from B, R to RB and were lowest under the W₂ light treatment in *Mentha spicata* and decreased from B, R, to W₂ and were lowest under B in *Mentha longifolia* after a cultivation period of 60 days. Importantly, EO yields were found to be significantly reduced in all three *Mentha* species when grown under field conditions for the same duration (Sabzalian et al. 2014).

Also belonging to the Lamiaceae family, the same research group investigated four species from the genus *Thymus* (commonly known as thyme) under the same light conditions applied in both aforementioned studies. In contrast to Ghaffari et al. (2019) and Sabzalian et al. (2014), EO contents were found to decrease from R to RB, to W₂, B and followed by GH conditions regardless of thyme species (*Thymus carmanicus*, *T. kotschyanus*, *T. migricus*, *T. vulgaris*). Also, limonene (a monoterpene with orange-like fragrance) was found to be substantially increased and decreased under R and GH conditions independent of the species. However, in accord with findings from Ghaffari et al. (2019), the observed compositional changes of main constituents (including the monoterpenes α - and γ -terpinene (often described with a floral, fresh and woody aroma), *p*-cymene (with a mild pleasant aroma), and the monoterpenoids thymol and carvacrol (derivatives of *p*-cymene) did not appear to follow a common theme in response to the different light treatments (Tohidi et al. 2019).

Batista et al. (2016) studied three different chemotypes¹¹ of *Lippia alba* L. (Verbenaceae) under *in vitro* conditions exposed to FL, W and RB lighting. Though these chemotypes belong to the same species, the research team found that EO compositions were more influenced by the chemotype than by the differing light qualities after 40 days of propagation. In addition, rhizomes of *Melissa officinalis* L. (Lamiaceae), which were collected from two different geographic locations of Iran, were exposed to either greenhouse (GH) or different LED light conditions. Even though these lemon balm ecotypes¹² belong to the same species and the main aromatic compound (lemon-scented) citronellal and other monoterpenes were found in their highest concentrations under monochromatic R and dichromatic RB light conditions in both ecotypes, these monoterpenes were also elevated under W in the ecotype from Ilam, while elevated under B and GH conditions in the ecotype from Isfahan. Also, while sesquiterpene contents were found to be highest under B in Ilams' lemon balm, they were highest under W and GH conditions in Isfahans' lemon balm (Ahmadi et al. 2021).

¹¹ A chemotype describes a morphologically indistinguishable variety within a plant species whose secondary metabolite composition is chemically distinct.

¹² An ecotype describes a genetically distinct geographic variety within a plant species, which is genotypically adapted to its environment.

Also, Hosseini et al. (2018) compared two ecotypes of *Ocimum basilicum* L. (Lamiaceae) from Iranian Ardestan and Mobarakeh. While the main phenylpropanoid methyl chavicol (also known as estragole with a licorice odor) was found in highest relative abundance under a monochromatic B (89.8 %), followed by a monochromatic R light treatment (85.5 %) in the green basil ecotype, the compound was found in highest relative abundance under a W (71.9 %), followed by the monochromatic R light treatment (67.7 %) in the purple basil ecotype. Limonene, as the second most abundant constituent, was elevated under W (3.7 %) and lowest under R (1 %) in the green ecotype, while significantly increased under R (7.5 %) and lowest under B and W (2.7 % respectively) in the purple ecotype.

Taken together, all of the studies above show not only that different species but also differing cultivars, chemotypes and even ecotypes within the same species respond differently to varying light qualities. In many cases, the responses even appear to oppose each other. Thus, understanding that the endogenous control of these diverse aromatic plants on their essential oil contents and compositions is substantial and can be greater than effects induced by LED light scenarios (tested thus far) is paramount.

The next section reviews differences in EO yields as affected by different light qualities¹³. In only three of eleven studies, EO yields of the investigated MAPs were stated to be indifferent between LED light treatments. Semenova et al. (2022) states indifferent EO contents per fresh weight (FW) in 'Red Ruby' basil plants upon exposure to FL with or without UV-A, UV-AB or UV-C radiation. However, it remains unclear if the given EO contents relate to equal fresh weights (e.g., EO yield per gram of FW) or to total fresh weights (e.g., EO yield per total FW). Since, after 60 days of cultivation, significantly greater leaf fresh weights were observed under FL+UV-A (15.9 g) and FL+UV-AB (9.3 g) compared to FL (6.7 g) and FL+UV-C (5.6 g), it may be reasonable to assume that the overall EO yields could be significantly greater under basil exposed to supplemental UV-A and UV-AB. Along the same lines, Ahmadi et al. (2021) stated indifferent EO contents per gram of shoot dry weight in the two aforementioned *M. officinalis* ecotypes. But again, the greater overall shoot yields as well as the substantially higher leaf counts under monochromatic R (660 nm) and dichromatic RB (660 and 460; 7:3 ratio) as compared to the unspecified W, B and GH light conditions described in this study suggest that EO yields can be improved via high R light proportions. Finally, Ascrizzi et al. (2018) stated equal EO contents per equal weights in parsley (*Petroselinum crispum*, Lamiaceae) after a four-month exposure to FL with or without four hours of monochromatic R (660 nm) at the end of the day (EOD). As the study does not include information on biomass yields, EO yields based on overall biomass cannot be estimated. However, since R efficiently drives photosynthesis and the EOD-treatment increased

¹³ To my knowledge, the influence of different LED light intensities on essential oil yields has not been investigated yet.

the daily light exposure for a duration of four month, biomass yield and concomitantly, EO yields per total biomass were probably considerably higher than under the FL treatment without additional EOD-R exposure.

In contrast, significant changes in EO yields were detected in the majority of the LED studies. While the studies by Tohidi et al. (2019) and Sabzalian et al. (2014) found monochromatic R (650-665 nm) to enable higher EO yields than monochromatic B (460-475 nm) in four thyme and two mint species, the studies by Sankhuan et al. (2022), Ghaffari et al. (2019) and Sabzalian et al. (2014) discovered monochromatic B (445-475 nm) to facilitate greater EO yields than monochromatic R (650-665 nm) in medicinal *Artemisia annua* (Asteraceae), two sage species and spearmint. Similarly, greater EO yields were recovered in *O. basilicum* when the proportions of B (435; 450 nm) were greater than the proportion of R (663 nm) by Rihan et al. (2020).

While Aldarkazali et al. (2019), Ghaffari et al. (2019), Tohidi et al. (2019) and Sabzalian et al. (2014) detected greater EO contents under monochromatic R, B and dichromatic RB treatments compared to a $W_{400-780}$ light treatment with high fractions of G and unspecified W light treatments in a variety of species belonging to the Lamiaceae family, broad W LED light spectra and combinations of RGB ($B \geq 450$ nm) improved EO yields more than mono- and dichromatic LED lightings (Sankhuan et al. (2022), Rihan et al. (2022), Ghaffari et al. (2019).

Though only three of these nine referenced studies proclaim information on leaf-morphological yields, increased EO yields correlated with increased (leaf) fresh weights, greater leaf numbers and leaf areas (Sankhuan et al., 2022; Rihan et al., 2019, Aldarkazali et al., 2019). Consequently, it appears that EO yields can be indirectly improved by supplying light qualities that improve the biomass partitioning towards those plant organs which contain the EO glands. As to which light qualities enable high EO yields the most, the reviewed literature currently points towards dichromatic RB and broad W light spectra that contain elevated proportions of B and R.

Also, UV-A radiation seems to be a promising light quality to increase EO yields as shown by Semenova et al. (2022) mentioned earlier. However, the employed UV treatments were added to an FL exposure which did not only change the light quality but also increased the incident light intensity over the experimental period of 60 days. As established in section 1.4.2.1, long UV-A wavelengths can significantly contribute to photosynthetic activity. Hence, whether and to which extent UV-A supplementations (instead of additions) truly cause greater EO biosyntheses in MAPs remains to be explored.

In addition, that R light was found to increase EO compound diversity more than B light in four of five studies (Sankhuan et al., 2021; Araújo et al., 2021; Lazzarini et al., 2018; Andrade et al., 2017) suggests that R light might be one of the more effective wavebands in stimulating EO biosynthesis. In example, via proteomic sensing a total of 335 proteins associated with terpenoid pathways were detected under monochromatic R (660 nm), whereas under B (445 nm) only 260 differential terpenoid proteins were detected (Sankhuan et al., 2021). In contrast, Alvarenga et al. (2015) detected one EO compound more under monochromatic B than under monochromatic R, but since the main peak of their applied R light treatment was at 630 nm (instead of at 660 nm which is commonly applied and closer to the chlorophylls' maximal absorption (section 1.3.1.3), their contrasting finding could be the result of this peak shift towards the yellow range of the light spectrum. That monochromatic Y light results in low numbers of EO compounds (as shown by Araújo et al. (2021) and Andrade et al. (2017)) further substantiates the prior statement.

As evident throughout all LED studies summarized in Table 10, EO compositions can be altered by differing light intensities and light qualities, and these changes can be substantial even within hours and days of exposure. In example, only eight hours of monochromatic LED exposures – especially R₆₆₈, followed by FR₇₅₅ – increased the emission of multiple aromatic volatiles (including aldehydes, benzenoids and phenylpropanoids) in excised petunia flowers (Colquhoun et al., 2013). The same research team found that these eight hours of monochromatic light exposure (including B₄₅₅) partly reduced some main volatile emissions in harvested strawberries and blueberries. Though negligible during postharvest, only three days of monochromatic R and B exposure prior to harvest was sufficient to promote the accumulation of diverse aromatic compound classes (including terpenes, benzenoids and phenylpropanoids (Figure 8)) and to raise the expression levels of enzymes that catalyze their biosynthesis in tea (*Camellia sinensis*) leaves (Fu et al., 2015).

How severe these changes in EO compositions can be, may be exemplified by Ghaffari et al. (2019) and Nguyen & Saleh (2019). Camphor – typically the most abundant aroma compound found in *Perovskia* species – remained below the detectable threshold in *P. abrotanoides* and was significantly reduced in *P. atriplicifolia* (4.8 %) after two month of monochromatic R light exposure, while concentrations of 22.8 and 29.5 % were found under broad light spectra (Ghaffari et al., 2019). Similarly, emissions of carvone and limonene – the major aromatic compounds of spearmint – remained entirely undetected after three weeks of monochromatic B light exposure, while their emissions released after three weeks of monochromatic R and G light exposures resembled the emissions released under GH conditions (carvone under R, G and GH conditions: 79.2, 75.3 and 81.9 %, respectively; limonene under R, G and GH conditions: 17.7, 18.1 and

16.5 %, respectively). Instead, high emissions of carvone oxide (65.2 %) and 1,8-cineole (22.0 %) appeared exclusively under the B light treatment (Nguyen & Saleh, 2019). The studies by Ahmadi et al. (2021), Tohidi et al. (2019) and Ascrizzi et al. (2018) represent additional examples of major aroma compounds existing under one treatment while non-detectable under another (Table 10).

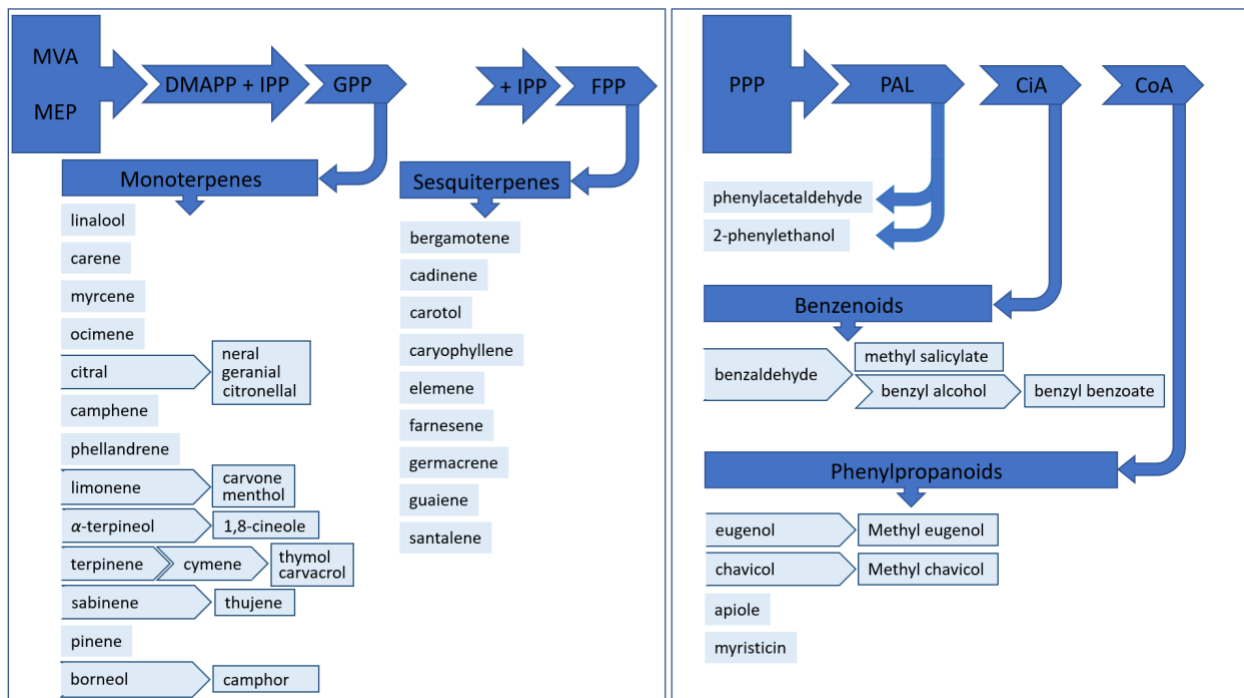


Figure 8 – Biosynthesis of major volatile aromatic compounds in plants¹⁴. Descriptions of abbreviations (from left to right): MVA = mevalonate pathway, MEP = methyl-erythritol-phosphate pathway, DMAPP = dimethylallyl pyrophosphate, IPP = isopentenyl pyrophosphate, GPP = geranyl pyrophosphate, FPP = farnesyl pyrophosphate, PPP = phenylpropanoid pathway, PAL = phenylalanine, CiA = cinnamic acid, CoA = coumaric acid.

As stated above, the list of studies which describe compositional changes in EOs upon LED light exposure is growing (Table 10), but their underlying causes and the mechanisms involved are widely unknown and general statements are hardly possible at this time. In example, though varying chemical compositions were identified in the leaves of *Aeollanthus suaveolens* (an African mint species belonging to the Lamiaceae family) under *in vitro* growth conditions with five different light intensities ($20\text{-}139 \mu\text{mol m}^{-2} \text{s}^{-1}$) emitted from a broad white LED treatment, no clear relationships between major compound concentrations and increasing PFDs could be derived from the results (Araújo et al., 2021). Also, the concentrations of the main aroma ingredients identified in an investigated sweet basil cultivar by

¹⁴ Included in this simplified depiction are major volatiles detected in the LED studies as summarized in Table 10.

Hikosaka et al. (2021) – the monoterpenoid linalool and the phenylpropanoid eugenol - which are both known for their pleasant but distinct scents, did not follow a linear relationship when exposed to neither increasing PFDs nor increasing RB ratios.

Currently, it appears as if monochromatic R and B light exposures result in the most profound compositional changes, however, both light treatments represent the most investigated spectral light regions thus far (Table 10). That RB treatments with elevated proportions of R often show noticeable and strong impacts on EO compositions as well, could indicate that red light regions may have the greatest effect on modifying EO compositions. But this interpretation must be considered cautiously because monochromatic B was found to be most impactful on EO compositions in the studies by Noguchi & Amaki (2016), Lazzarini et al. (2018), Hsie et al. (2019) and Nguyen & Saleh (2019). Further, quite often, broad white LED spectra resulted in the strongest compositional changes when compared to mono- and dichromatic LED light treatments. Unfortunately, however, in the vast majority of these cases, the specific spectral compositions were not or not adequately described and hence, are not conducive for narrowing down particularly influential wavelengths. And after all, relative concentrations of volatile aromatic terpenoids and phenylpropanoids were found to be altered by the entire spectrum of photobiologically active radiation emitted by and investigated under LEDs thus far: Substantial changes in EO compositions were observed under additional UV-A and UV-AB irradiations (e.g., Semenova et al., 2022), under all monochromatic LED treatments (including B, G and Y (Araújo et al., 2021), R and FR wavelengths (e.g., Colquhoun et al., 2013)), dichromatic RB (Ahmadi et al., 2021; Aldarkazali et al., 2019) and trichromatic LED treatments (e.g. Rihan et al., 2022) and under varying broad white LED treatments.

How challenging it is to associate specific LED colors with specific EO compound accumulations may be exemplified by the phenylpropanoid eugenol. Since volatile phenylpropanoids are biosynthesized via the phenylpropanoid pathway (alike e.g., flavonoids and phenolic acids) which has been shown to be upregulated by UV and B light regions (as described in section 1.4.2.1), one might expect to find elevated eugenol concentrations within these ranges. In accordance with this reasoning, eugenol as the main aroma compound in basil was found in higher concentrations when exposed to broad white LED light spectra with elevated UV-A and blue wavebands compared to a broad white LED light spectra with elevated R and FR wavebands (Kivimäenpää et al., 2022). Yet, in a cultivar of *Melissa officinalis*, eugenol concentration was greater under monochromatic R than monochromatic B (Ahmadi et al., 2021). (The results of Colquhoun et al. (2013) and Carvalho et al. (2016) are additional examples of volatile phenylpropanoid emissions being elevated under R and/or FR wavelength bands in petunia flowers and basil leaves compared to B light regions.)

Even though we are currently far from applying LEDs as effective and targeting tools to purposefully tailor EO yields and compositions of medicinal and aromatic plants, their profound impact on EOs is indisputable and various areas of application are envisioned: First and foremost, under CEA conditions the application of species-matched LED light scenarios could enable consistently high EO quantities with desired EO qualities. On the basis of human sensory evaluations, LEDs may be used to improve the smell and taste of a variety of herbs, fruits and vegetables towards aromatic blends preferred by consumers. The flower and perfume industry may benefit from new fragrances arising from EO alterations via LED light settings. In the near future, LEDs may be applied for a short period of time during preharvest (Fu et al., 2015) or as postharvest treatments during transport and/or retail storage (Colquhoun et al., 2013). Also, LED light strategies are anticipated to improve medicinal properties (Sankhuan et al., 2022), expected to lower health-concerning compounds of EO blends (Semenova et al., 2022) and will likely be employed to produce high amounts of specific compounds which are needed by diverse industries (Dedino et al., 2022). For the moment however, much prospective research and comprehensive meta-analyses based on the pool of existing findings lie ahead to identify the underlying causes and mechanisms that lead to these highly diverse EO alterations.

Table 10 – Essential oil contents and compositions of aromatic and medicinal plants as affected by LED lighting (λ 100-800 nm).¹⁵

Plant species	Effect ¹	Light spectrum	Light intensity ²	Reference
<i>Acmella oleracea</i>	45 DAS, <i>in vitro</i> cultivation induced the synthesis of more EO compounds than pot cultivation after continues light exposure treatments (24 h d ⁻¹). Regardless of cultivation method, <i>trans</i> -caryophyllene and 2-tridecanone increased upon R exposure. α -cadinol and 4-epi-cubedol increased upon W light exposure.	W $\lambda_{380-780}$, R $\lambda_{610-640}$	60	Dedino et al. 2022
<i>Ocimum basilicum</i> 'Red Ruby'	60 DAS, total EO contents (0.15-0.22 % per FW) remained indifferent between all treatments. Proportion of linalool increased under UV-AB and (to a lesser extent) under UV-A; UV-C reduced proportions of linalool, sabinene and fenchone, induced eugenol methyl ether, and increased proportions of α -guaiene, β -cubebene and α -bulnesene. [60 DAS, UV-A and (to a lesser extent) UV-AB increased FW_{Leaf} , P_{Height} , DW/FW ratio, LA, chl a, compared to control without UV; FW_{Stem} increased under UV-A; LA reduced under UV-C; TAC increased under UV-C and (to a lesser extent) under UV-A, however remained indifferent under UV-AB; chl b, car increased under all UV treatments compared to control.]	FL \pm UV-A; UV-AB; UV-C	120 \pm 10 (3.9 of UV-A; 0.2 of UV-AB and UV-C, respectively)	Semenova et al. 2022
<i>Artemisia annua</i>	3 month old plants were exposed to light treatments for 7 days. A total of 289, 260 and 335 terpenoid proteins were detected in the leaves after W, B and R exposures, respectively. R induced the highest number of differential terpenoid proteins (53) followed by B (31), then W (20). R resulted in high proportions of sesquiterpene and tetraterpene (car) synthases. W and B resulted in higher proportions of functional proteins related to MVA and MEP pathways and high proportions of sesquiterpene synthases. Among the LED spectra, R was most effective for regulating terpenoid proteins.	W (main peaks at λ_{445} and λ_{544}), R λ_{660} , B λ_{445}	200 \pm 10	Sankhuan et al. 2021

¹⁵ The reader may also be referred to the studies by Hikosaka et al. (2021), Rihan et al. (2020), Pennisi et al. (2019) and Hosseini et al. (2018) cited in Table 5; Kivimäenpää et al. (2022), Sankhuan et al. (2022), Rihan et al. (2022), Aldarkazali et al. (2019) cited in Table 9.

<i>Melissa officinalis</i> 'Ilam' & 'Isfahan'	<p>EO contents remained indifferent between all treatments (0.27-0.32 %). Citronellal and other monoterpenes were highest under R and RB in both genotypes; linalool highest under RB, lowest under GH conditions in both genotypes.</p> <p>In 'Ilam', monoterpenes were also elevated under W, while in 'Isfahan' elevated also under B and GH conditions; while sesquiterpene contents were highest under B in 'Ilam', they were highest under W and GH conditions in 'Isfahan'.</p> <p>In 'Ilam', α-pinene highest under GH conditions and R; myrcene highest under W and GH conditions, lowest under RB and R; γ-3-carene highest under GH conditions, followed by B, lowest under R; limonene highest under W, lowest under R; 1,8-cineole highest under R, lowest under RB and GH conditions; γ-terpinene highest under W and R, lowest under B; <i>cis</i>-sabinene highest under W and R; β-thujone highest under GH conditions; thymol highest under B, lowest under RB; carvacrol highest under B; lowest under W and RB; β-caryophyllene highest under B, lowest under RB; eugenol is increased under W, however, <i>nd</i> under R.</p> <p>In 'Isfahan', α-pinene highest under GH conditions and B, lowest under W and R; myrcene highest under B, lowest under RB and GH conditions; γ-3-carene highest under W, lowest under RB; limonene highest under B; lowest under RB; 1,8-cineole highest under W and B, lowest under RB; γ-terpinene highest under RB and GH, lowest under W; <i>cis</i>-sabinene reduced under W and B; β-thujone highest under B; thymol highest under W, lowest under RB; carvacrol highest under W and R, lowest under RB; β-caryophyllene highest under GH conditions, lowest under W and B; eugenol highest under GH conditions and R, lowest under RB and B.</p> <p>[In both cultivars, LED treatments generally increased FW_{Shoot}, DW_{Shoot}, L_{No} and AOC compared to GH treatment; in 'Ilam', FW_{Shoot} increased most under RB; in 'Isfahan', FW_{Shoot} increased most under RB and R, followed by W; In 'Ilam', DW_{Shoot} increased most under RB, followed by R and W; in 'Isfahan', DW_{Shoot} increased most under RB, followed by R, then W and GH; in 'Ilam', L_{No} decreased significantly from RB, R, GH, W to B; in 'Isfahan', L_{No} increased most under RB, followed by R, then B and W.]</p>	GH, R λ_{660} , B λ_{460} , RB $_{7:3}$, W $\lambda_{380-760}$	300	Ahmadi et al. 2021
--	---	---	-----	--------------------

<i>Aeollanthus suaveolens</i>	<p>After 40 days under <i>in vitro</i> conditions, number of VOC compounds differed between treatments: 24, 25 and 26 VOCs detected under PFD 57, 78 and 102; 28 VOCs under PFD 20 and 139; relative contents of major VOCs differed between treatments: linalool (31.8 %) highest under PFD 102; linalool acetate (19.4 %) highest under PFD 20; <i>cis</i>-β-farnesene (36 %) and α-sanatalene (6 %) highest under PFD 139; massoia lactone (6.7 %) highest under PFD 78.</p> <p>[After 40 days under <i>in vitro</i> conditions, S_{No}, L_{Root}, DW_{Leaf}, DW_{Shoot}, generally increased, while <i>chl</i> and <i>car</i> generally decreased with increasing PFD; L_{Shoot}, R_{No}, DW_{Root} greatest under PFD 78, followed by PFD 102 and 139; DW_{Total} highest under PFD 139, followed by PFD 78 and 102; LA highest under PFD 139 and 78, lowest under PFD 20; SLA lowest under PFD 139, followed by PFD 78 and 102.]</p>	W $\lambda_{300-800}$ with elevated B λ_{450}	20, 57, 78, 102, 139	Araújo et al. 2021
<i>Aeollanthus suaveolens</i>	<p>After 40 days under <i>in vitro</i> conditions, number of VOC compounds differed between treatments: 20 VOC detected under FL; 21 under G and Y; 24 under $R_1B_{2.5}$, B and R; 25 under R_1B_1 and $R_{2.5}B_1$, 27 VOC under W; relative contents of major VOCs differed between treatments: linalool (33.3 %) highest under W; linalool acetate (18.2 %), α-sanatalene (7.1 %) and <i>cis</i>-β-farnesene (39.7 %) highest under FL, massoia lactone (9.6 and 9.5 %) highest under G and Y respectively.</p> <p>[After 40 days under <i>in vitro</i> conditions, L_{Shoot}, highest under G, followed by Y and R; L_{No} reduced under Y, R, B, $RB_{2.5:1}$; R_{No} highest under FL and W, significantly reduced under R, followed by Y; L_{Root} highest under G and B, significantly reduced under R; DW_{Leaf} decreased from W, to FL, to G and RBs, then Y, R and B; DW_{Shoot} reduced under R, Y, B and $RB_{2.5:1}$; DW_{Root} decreased from FL to W, to G and $RB_{1:1}$, to $RB_{1:2.5}$ and B, followed by $RB_{2.5:1}$ and Y, then R; DW_{Total} decreased from FL and W, to $RB_{1:1}$ and G, to $RB_{1:2.5}$, followed by $RB_{2.5:1}$, B, Y and R; <i>chl a</i> highest under Y and G, lowest under B and $RB_{1:2.5}$; <i>chl b</i> highest under W, followed by G, Y and FL, lowest under B and $RB_{2.5:1}$; total <i>chl</i> decreased from Y, to G and W, to FL, R, $RB_{1:1}$, to B, followed by $RB_{2.5:1}$ and $RB_{1:2.5}$; <i>car</i> decreased from Y, to G, then $RB_{1:1}$, to R and FL, followed by $RB_{2.5:1}$, then W, B and $RB_{1:2.5}$.]</p>	W $\lambda_{300-800}$ with elevated B λ_{450} , G λ_{510} , Y λ_{595} , B λ_{450} , R λ_{660} , $RB_{2.5:1}$; 1:2.5; 1:1, FL	42	Araújo et al. 2021
<i>Lippia filifolia</i>	After 45 days under <i>in vitro</i> conditions, only little differences in mayor terpenoid VOC compositions were observed: limonene (6.3 and 4.7 %),	W $\lambda_{400-700}$ with elevated B,	36	Chaves et al. 2020

	<p>thujene (17.1 and 17.3 %) and caryophyllene (6.4 and 6.1 %) highest under B and RB respectively; while 1,8-cineole (57.1 and 56.4 %) and γ-terpinene (6.1 and 6.3 %) was highest under W and R, and α-pinene was highest under W and B (12.6 and 12.7 %).</p> <p>[After 45 days under <i>in vitro</i> conditions, P_{Height} greatest under R and W, lowest under RB; S_{No} highest under RB; NS_{No} highest under RB, lowest under R and W; FW_{Total} highest under RB; chl a highest under W, lowest under B and RB; chl b highest under W, lowest under B; total chl highest under W, lowest under B; car highest under W, lowest under B and RB; Sugar_{Sol} concentration highest under RB and B, lowest under W; sucrose concentration highest under RB, lowest under W; reducing sugar concentration highest under RB and R; MDA highest under RB and W, lowest under B.]</p>	B λ_{450} , R λ_{653} , RB $\lambda_{448/664}$ with elevated R		
<i>Lippia rotundifolia</i>	<p>After 45 days under <i>in vitro</i> conditions, mayor VOC compounds differed between light qualities: myrcenone (33.3 %) reduced under B, myrcene (23.5 and 21.6 %) highest under R and B respectively, limonene (13.0 %) highest under B, <i>cis</i>-ocimene (12.0-15.5 %), α-terpineol (0.6-0.8 %) remained indifferent between treatments, linalool (1.7 %) highest under R.</p> <p>[After 45 days under <i>in vitro</i> conditions, $Shoot_{Length}$ greatest under R, lowest under B and $R_1B_{2.5}$; L_{No} highest under $R_{2.5}B_1$, lowest under R, $R_1B_{2.5}$ and R_1B_1; DW_{Shoot} highest under R, $R_{2.5}B_1$ and W, lowest under $R_1B_{2.5}$ and B; DW_{Leaf} highest under R_1B_1, lowest under R and B; DW_{Root} and DW_{Total} reduced under B and $R_1B_{2.5}$; chl a reduced most under R_1B_1, followed by W; chl b highest under W, lowest under R_1B_1 and R; total chl reduced under R and R_1B_1; car highest under B and R, followed by $R_{2.5}B_1$.]</p>	W $\lambda_{400-800}$ with elevated RB, R λ_{660} , B λ_{450} , RB $_{2.5:1}$; 1:2.5; 1:1	42	Hsie et al. 2019
<i>Perovskia abrotanoides</i> & <i>P. atriplicifolia</i>	<p>In both cultivars, proportion of major compound camphor was lowest or <i>nd</i> under R; α-pinene was significantly enhanced under GH conditions (7.2 and 8.5 % respectively); δ-3-carene elevated under B (11.4 and 6.6 % respectively) and R (8.1 and 8.6 % respectively); <i>trans</i>-caryophyllene highest under W (10.2 and 8.1 % respectively), lowest under GH conditions (4.9 and 3.9 % respectively); similarly, α-humulene highest under W (9.1 and 7.7 % respectively), lowest under GH conditions (3.9 and 3.3 % respectively).</p>	W $\lambda_{380-780}$, R $\lambda_{650-665}$, B $\lambda_{460-475}$, RB $_{7:3}$, GH	300	Ghaffari et al. 2019

	<p>In <i>P. abrotanoides</i>, EO yield decreased from W (2.66 %), B (1.7 %), R (1.2 %), GH (0.7 %) to RB (0.4 %); camphor highest under GH conditions (22.8 %); borneol highest under GH conditions (10.0 %), lowest under R (4.6 %); borneol acetate highest under W (7.2 %), lowest under R (3.4 %); 1,8-cineole highest under GH and B (15.9 and 14.4 % respectively) and lowest under W (4.2 %), camphene (3.2 %) only present under GH conditions;</p> <p>In <i>P. atriplicifolia</i>, EO yield decreased from B (1.9 %), R (1.7), RB (1.6 %) to W and GH (1.5 % respectively); camphor highest under W (29.5 %); 1,8-cineole highest under R, W and GH conditions (31.0, 27.1 and 21.3 % respectively); borneol highest under W (13.5 %), lowest under RB (5.1 %); borneol acetate highest under GH conditions (11.1 %), lowest under W (3.7 %); camphene <i>nd</i> under W, but decreasing from R, B, GH to RB (4.0, 3.4, 2.7 and 2.3 % respectively).</p>			
<p><i>Thymus carmanicus</i>, <i>T. kotschyanus</i>, <i>T. migricus</i>, <i>T. vulgaris</i></p>	<p>In all cultivars, EO yields decreased from R, RB, W, B to GH conditions. In all species, limonene was substantially increased under R and significantly decreased under GH conditions.</p> <p>In <i>T. vulgaris</i> and <i>T. kotschyanus</i>, α-terpinene were highest under R (4.1 and 18 % respectively), lowest under GH conditions (1.9 and 0.2 % respectively). However, substantial differences between species were observed in terms of EO yields and compositions as well as all other components.</p> <p>In <i>T. carmanicus</i>, thymol highest under B (52.4 %), lowest under R (18.5 %); carvacrol highest under RB and R (10.3 and 8.3 % respectively), lowest under GH conditions (2.4 %); <i>p</i>-cymene highest under GH conditions (30.1 %), low under all other treatments (0.1-2.7 %); γ-terpinene highest under W (8.4 %), <i>nd</i> under B; α-terpinene highest under W (10.7 %), lowest under B (1.5 %); limonene highest under R (21.3 %), lowest under GH conditions (1.3 %); linalool highest under W (15.3 %), lowest under RB (0.4 %).</p> <p>In <i>T. kotschyanus</i>, thymol highest under W and B (42-44 %), lowest under RB; carvacrol highest under B and GH conditions (2.4 % respectively), <i>nd</i> under R and W; <i>p</i>-cymene highest under B (5.7 %), <i>nd</i> under R and W; γ-terpinene highest under R and W (12.5 and 11.7 % respectively), lowest</p>	<p>R $\lambda_{650-665}$, B $\lambda_{460-475}$, RB_{7:3}, W $\lambda_{380-760}$, GH</p>	<p>300</p>	<p>Tohidi et al. 2019</p>

	<p>under GH conditions (0.5 %); limonene highest under R and RB (20.0 and 17 %), lowest under GH conditions (0.2 %); linalool highest under GH conditions (21.6 %), lowest under B (1.9 %).</p> <p>In <i>T. migricus</i>, thymol highest under R, RB and GH (46-48 %), lowest under W (19.6 %); carvacrol increased under GH conditions (3.9 %); <i>p</i>-cymene highest under R (3.7 %), lowest under B and GH conditions (1.0 % respectively); γ-terpinene highest under R (12.5 %), <i>nd</i> under GH conditions; α-terpinene highest under R (4.6 %), lowest under B (1.0 %); limonene highest under W (31.7 %), lowest under GH conditions (0.3 %); linalool highest under W (19 %), lowest under GH conditions (1.6 %).</p> <p>In <i>T. vulgaris</i>, thymol was highest under W (65.5 %), lowest under GH conditions (39.5 %); carvacrol highest under W (5.5 %), lowest under R (2.9 %); <i>p</i>-cymene reduced under W (8.3 %); γ-terpinene highest under GH conditions and R (11.0 and 10.5 % respectively), lowest under W (2.8 %); limonene highest under R (2.2 %), lowest under W and GH conditions (0.9 % respectively); linalool highest under GH conditions (2.9 %), lowest under B and W (0.8 and 0.9 % respectively).</p>			
<i>Mentha spicata</i>	<p>Mature spearmint plants were exposed to light treatments for three weeks.</p> <p>Under R and G, released VOCs were similar to GH conditions (limonene: 17.7, 18.1 and 16.5 % respectively; carvone: 79.2, 75.3 and 81.9 % respectively), however both main VOCs (limonene and carvone) were <i>nd</i> under B, instead, carvone oxide (65.2 %), 1,8-cineole (22.0 %) and ocimene (7.8 %) appeared (while <i>nd</i> under all other treatments).</p> <p>α-pinene, β-pinene, camphor, β-bourbonene, caryophyllene released in higher concentrations under B (4.6, 5.2, 1.3, 1.4, 2.3 % respectively); sabinene released in lower concentrations under R (0.1 %); β-bourbonene released in lower concentrations under GH conditions (0.1 %); γ-terpinolene remained indifferent between treatments.</p>	GH, R λ_{623} , B λ_{453} , G λ_{514}	<i>na</i>	Nguyen & Saleh 2019
<i>Petroselinum crispum</i>	<p>After four month, EO yields (0.05 % per g FW) remained indifferent between all treatments.</p> <p>R supplementation only significantly increased β-phellandrene (26 %) and decreased carotol (0.9 %) and apiole (10.9 %) compared to FL (17.2, 7.4 and 15.5 % respectively).</p>	FL \pm R λ_{660} ; 12 h of FL, then 4 h of R as EOD	60	Ascrizzi et al. 2018

	<p>EOD-R caused a decrease in β-phellandrene (2.4 %), appearance of <i>cis</i>-β-ocimene (2.4 %), methyl carvacrol (2.7 %), bicyclogermacrene (4.8 %), α-farnesene (14.8 %), δ-cadinene (3.9 %), 7-epi-α-eudesmol (7.4 %); an increase in <i>trans</i>-β-ocimene (4.2 %), β-caryophyllene (1.9 %), <i>trans</i>-β-farnesene (3.3 %), germacrene D (13.2 %). While <i>nd</i> under EOD-R, terpinolene (7.1, 5.3 %), <i>p</i>-cymene (2.5, 1.8 %), 1,3,8-<i>p</i>-menthatriene (17.7, 18.3 %), phenylpropanoids myristicin (19.4, 23.7 %) and apiole (15.5, 10.9 %) are high in relative abundance under FL and FL+R.</p>			
<p><i>Lippia gracilis</i></p>	<p>After 30 days under <i>in vitro</i> conditions and differing light qualities, <i>p</i>-cymene highest under $R_1B_{2.5}$ (32.4 %), lowest under R and B (24.5, 24.9 % respectively); carvacrol highest under B (48.1 %), lowest under RBs (41.1-41.6 %); α-pinene, limonene, umbellulone, thymol methyl ether remained <i>nd</i> under B, while indifferent between other light qualities (0.3-0.4, 0.4-0.5, 0.3-0.5, 0.3-0.5 % respectively); myrcene (1.7 %), α-terpinene (1.3 %), terpinene-4-ol (0.3 %) reduced under B; γ-terpinene highest under R (7.4 %), lowest under B (3.7 %); <i>cis</i>-sabinene hydrate remained <i>nd</i> under B and W, while indifferent between other light qualities (0.2-0.3 %); <i>trans</i>-caryophyllene highest under B (11.7 %); α-humulene was only detected under R (0.3 %). Highest number of VOC compounds detected under R (16), lowest under B (10).</p> <p>[After 30 days under differing light qualities using apical segments for micropropagation, L_{Shoot} increased from $R_1B_{2.5}$, to $R_{2.5}B_1$, to B and W, to R; DW_{Leaf} increased from B and $R_{2.5}B_1$, to $R_1B_{2.5}$, to W, followed by R; DW_{Root} increased from RBs to W, followed by R, then B; chl a highest under B, lowest under R and W; chl b highest under B, followed by B and $R_1B_{2.5}$, then $R_{2.5}B_1$, lowest under W; total chl highest under B, then $R_1B_{2.5}$, followed by $R_{2.5}B_1$ and R, lowest under W; car lowest under W, followed by $R_1B_{2.5}$ and R. Using nodal segments under differing light qualities for micropropagation, L_{Shoot} was increased under R; DW_{Leaf} was increased under B; DW_{Root} was reduced under B and $R_{2.5}B_1$; chl a lowest under R, followed by $R_1B_{2.5}$; chl b highest under $R_{2.5}B_1$ and W, lowest under $R_1B_{2.5}$ and R; total chl highest</p>	<p>W λ_{na}, R λ_{na}, B λ_{na}, $R_{2.5}B_1$, $R_1B_{2.5}$</p>	<p>42</p>	<p>Lazzarini et al. 2018</p>

	<p>under $R_{2.5}B_1$ and W, then B, lowest under $R_1B_{2.5}$; car highest under W, lowest under R.</p> <p>Regardless of segments used, L_{Root} increased under W and R, decreased under B; DW_{Shoot} highest under B, followed by R; DW_{Total} lowest under $R_{2.5}B_1$, followed by $R_1B_{2.5}$ and W; NS_{No}, L_{No} remained indifferent between light qualities.]</p>			
<i>Hyptis suaveolens</i>	<p>After 30 days under differing light qualities using nodal segments for micropropagation, relative abundance of sabinene was highest under R_4B_{10} (12.9 %), Y (13.0 %) and B (12.6 %), while reduced under R_1B_1 (5.8 %), $R_{10}B_4$ (7.4 %), R (7.5 %) and FL (8.1 %); β-pinene was highest under R (17.4 %), $R_{10}B_4$ (14.2 %) and R_1B_1 (12.9 %), lowest under B (7.1 %) and R_4B_{10} (8.3 %); <i>trans</i>-caryophyllene decreased from FL (22.5 %), R_1B_1, W, B, R_4B_{10}, G, $R_{10}B_4$, R, Y (17.4 %); germacrene D highest under Y (19.7 %), R_4B_{10} (17.2 %), lowest under R (13.0 %) and $R_{10}B_4$ (13.5 %); bicyclogermacrene highest under R_1B_1, lowest under $R_{10}B_4$ (9.6 %); β-phellandrene remained fairly indifferent between treatments (5.5-6.9 %).</p> <p>In addition, FL inhibited 10 VOCs (camphene, δ-3-carene, α-terpinene, <i>cis</i>-sabinene hydrate, borneol, α-terpineol, β-cubebene, epi-bicycle sesquiphellandrene, <i>cis</i>-muurola-3,5-diene, <i>trans</i>-cadina-1,4-diene) compared to LED treatments; R inhibited <i>cis</i>-sabinene hydrate and caryophyllene oxide, $R_{10}B_4$ inhibited <i>cis</i>-sabinene hydrate and β-cubebene. Number of VOC compounds decreased from R and $R_{10}B_4$ (38), G and R_4B_{10} (37), B (36), W (35), R_7B_7 (33), Y (31) to FL (30).</p> <p>[After 30 days under differing light qualities using nodal segments for micropropagation, NS_{No} highest under $R_{10}B_4$, followed by B, R_4B_{10}, W and R; L_{Shoot} highest under G, followed by R and Y, then FL, W and $R_{10}B_4$; L_{No} highest under W and $R_{10}B_4$, followed by R_4B_{10}, B, R, then R_7B_7 and FL; DW_{Leaf} highest under W, followed by RBs, lowest under G and Y; DW_{Shoot} highest under $R_{10}B_4$, R_4B_{10} and W, followed by R and G; DW_{Root} highest under R_4B_{10}, $R_{10}B_4$, followed by W, R, then R_7B_7; DW_{Total} highest under $R_{10}B_4$, followed by W and R_4B_{10}, then R_7B_7 and R.]</p>	[λ_{na} R, B, Y, G, R_4B_{10} , $R_{10}B_4$, R_1B_1 , W, FL	47	Andrade et al. 2017
<i>Ocimum basilicum</i>	In the GH and the LED chambers respectively, evaluated parameters differed between seasons and between temporal replications.	R λ_{na} , B λ_{450} , R_1B_1 , G λ_{520} ,	100 (R, B, RB, G, Y); 150	Carvalho et al. 2016

	<p>VOC emissions changed over time (weekly measurements between 2- and 6-week old basil) and changed differently under differing light qualities; highest diversity of VOCs was found during week 4 (carboxylic acid esters, fatty acid esters, fatty alcohols and aldehydes, mono- and sesquiterpenoids, phenylpropanoids); only mono- and sesquiterpenoids and phenylpropanoids remained relatively high in intensity after week 4. Adding a third λ to RB increased emissions of several mono- and sesquiterpenes and phenylpropanoids by at least 1.5-fold in comparison to RB and GH conditions; R, B and RB enhanced emissions compared to GH conditions; while RYB and RGB increased monoterpenoid emissions, RBFR increased phenylpropanoid emissions.</p> <p>[<i>LA and FW_{Total} were maximized when RB was supplemented with G, Y or FR.</i>]</p>	Y λ_{600} , FR λ_{735} , GH	(RGB, RYB, RBFR)	
<i>Plectranthus amboinicus</i>	<p>Propagated cuttings were exposed to light conditions for 70 days. VOC emission analyses were only conducted on the youngest leaves. Generally, R increased monoterpene emissions (short RTs); B increased sesquiterpene emissions (long RTs), G increased emissions of compounds with intermediate RTs. Compared to W+RGB, B resulted in the greatest VOC emission changes, followed by R. While W+RGB and B released more α-terpinene, linalool and β-farnesene than other treatments, B additionally increased release of germacrene D and elemene compared to all other treatments. While G and R released more α-pinene, β-pinene, G additionally increased release of limonene compared to all other treatments, and R increased release of fenchyl acetate and bornyl acetate.</p> <p>[<i>P_{Height} increased under R and G; Lateral S_{No} increased under G and R, reduced under B; L_{Thick} and FW_{Leaf} increased under B and R.</i>]</p>	B λ_{470} , G λ_{525} , R λ_{660} , W+RGB (3:1:1:1)	100	Noguchi & Amaki 2016 ³
Three chemotypes of <i>Lippia alba</i>	<p>After 40 days of <i>in vitro</i> propagation, differences in EO composition were more influenced by chemotype than by the light qualities.</p> <p>[<i>After 40 days of in vitro propagation, chl and car increased under RB; P_{Height} remained indifferent between chemotypes and light treatments. While RB increased FW_{Total} in BGEN-01 and BGEN-02, RB decreased FW_{Total} in BGEN-42.</i>]</p>	FL, W $\lambda_{400-750}$ with elevated B and low R, R ₄₅₀ B ₆₆₀ with elevated R	41	Batista et al. 2016

	<i>DW_{Total} differed strongly between chemotypes and light qualities: While RB resulted in greatest DW_{Total} in BGEN-01, RB and W resulted greatest DW_{Total} in BGEN-02 and FL resulted in greatest DW_{Total} in BGEN-42.]</i>			
<i>Camellia sinensis</i>	At preharvest, R and B promoted accumulation of volatile fatty acid derivatives VFADs, volatile phenylpropanoids and benzenoids VPBs and volatile terpenes VTs within three days of exposure compared to darkness. In addition, R and B upregulated expression levels of 9/13-lipoxygenases LOX involved in VFAD formations, phenylalanine ammonialyase PAL involved in VPB formation and terpene synthase TS involved in VT formation. R and B had less influence on harvested leaves.	Dark, B λ_{470} , R λ_{660}	75	Fu et al. 2015
<i>Achillea millefolium</i>	After 45 days of <i>in vitro</i> cultivation of rhizomes, with decreasing broadness of the spectrum number of VOCs generally decreased (FL (29), RGB and G (28), B (27), R (26)). Sabinene was increased under R (30.8 %), decreased under FL (9.6 %); borneol was increased under FL (15.7 %), decreased under R (6.0 %), β -caryophyllene was slightly decreased under RGB and FL; 1,8-cineole was slightly decreased under G (5.3 %), β -cubebene was increased under RGB (21.6 %) and G (18.5 %), decreased under FL (9.3 %). [After 45 days of <i>in vitro</i> cultivation of rhizomes, DW_{Shoot} , DW_{Total} highest under B, lowest under G; DW_{Root} increased under B; L_{Shoot} increased under B and G; L_{Root} increased under B and FL, decreased under G; R_{No} decreased from B, to FL, to RGB and R, lowest under G; survival rate was decreased under W and G; rooting rate was increased under B but decreased under G; chl a and total chl increased under G, decreased under RGB and R; chl b increased under G; car increased under G and FL.]	B λ_{455} , R λ_{630} , G λ_{515} , RGB, FL	25	Alvarenga et al. 2015
<i>Mentha piperita</i> , <i>M. spicata</i> , <i>M. longifolia</i> ,	After 60 days of cultivation, EO contents of <i>M. piperita</i> were highest under R (7 %), followed by RB (5.1 %), then B (3.1 %), W (2.34 %), lowest under FCs (1.4 %). EO contents of <i>M. spicata</i> were highest under B (5.0 %), followed by R (4.3 %), then RB and W (2.6 % respectively), lowest under FCs (0.7 %). EO contents of <i>M. longifolia</i> were highest under RB (4.9 %) and R (4.3 %), followed by W (3.5 %), FC (3.3 %) and B (3.2 %).	R $\lambda_{650-665}$, B $\lambda_{460-475}$, R ₇ B ₃ , W $\lambda_{380-760}$, FC	500	Sabzalian et al. 2014

	[After 60 days of cultivation compared to field conditions, P_n was increased under RB and mostly decreased under B, followed by W and R; P_{Height} and FW_{Total} were decreased, water and EO contents were increased under all LED treatments.]			
<i>Petunia x hybrida</i> 'Mitchell Diploid', <i>Fragaria x ananassa</i> 'Strawberry Festival', <i>Vaccinium corymbosum</i> 'Scintilla', <i>Solanum lycopersicum</i> 'M82'	In excised petunia flowers exposed to 8 hours of treatment and compared to dark treatment, phenylacetaldehyde emissions increased under R and FR, followed by FL, then B; benzyl alcohol emissions increased under R and FR; 2-phenylethanol emissions increased under R, followed by FR; benzaldehyde emissions increased most under R, followed by FR and FL, then B; benzyl benzoate emissions increased under R, FR and B, followed by FL; isoeugenol emissions increased under FL and R; methyl benzoate emissions increased under R, FL and FR, followed by B; eugenol emissions increased under FL; methyl salicylate emissions increased under FL, B and R. In strawberries exposed to 8 hours of treatment and compared to dark treatment, ethyl caproate emissions increased under FL but decreased under B, FR and R, hexyl butyrate decreased under B, <i>cis</i> -3-hexen-1-ol and methyl butyrate emissions remained indifferent. In blueberries exposed to 8 hours of treatment, hexanal increased under FR, emissions of <i>trans</i> -2-hexenal and 1-hexanol remained indifferent, <i>trans</i> -2-hexen-1-ol emissions decreased under FR. In tomato fruits exposed to 10 days of treatment, <i>cis</i> -3-hexenal emissions increased under FR but decreased under R, 3-methyl-1-butanol and 2-methyl butanal emissions decreased under all LED treatments, <i>cis</i> -3-hexen-1-ol decreased under FL, B and R.	Dark, FL, B λ_{455} , R λ_{668} , FR λ_{755}	50	Colquhoun et al. 2013
<i>Ocimum basilicum</i>	After 70 days of light treatments, the first, third and fifth leaf was harvested for headspace GC analysis. Volatile emissions were higher under B (185.6 mg kg ⁻¹ FW), followed by W (76.0 mg kg ⁻¹ FW), indifferent between BG, G and R (50.4, 29.2 and 26,3 mg kg ⁻¹ FW). B changed VOC composition the most. Emissions of α -pinene, β -pinene and limonene remained indifferent between treatments; myrcene and linalool were increased under B (31.3 and 28.7 mg kg ⁻¹ FW) and reduced under G (1.8 and 0.5 mg kg ⁻¹ FW) and R	W λ_{na} , B λ_{470} , BG λ_{500} , G λ_{525} , R λ_{660}	50	Amaki et al. 2011

(1.9 and 1.0 mg kg⁻¹ FW); 1,8-cineole and γ -terpinene were increased under B.

¹ Descriptions of abbreviations are listed in alphabetical order: AOC = antioxidant capacity, B = blue light (400-500 nm), BG = blue/green light (500 nm), car = carotenoids, chl = chlorophyll, Dark = darkness, DAS = days after sowing, DW = dry weight, DW_{Leaf} = leaf dry weight, DW_{Root} = root dry weight, DW_{Shoot} = shoot dry weight, DW_{Total} = total dry weight, EO = essential oil, EOD = end-of-day light treatment, FC = field conditions, FL = fluorescent lamp, FR = far red light (700-800 nm), FW = fresh weight, FW_{Leaf} = leaf fresh weight, FW_{Shoot} = shoot fresh weight, FW_{Total} = total fresh weight, G = green light (500-600 nm), GC = gas chromatography, GH = green house, LA = leaf area, λ = wavelength (*Lambda*), λ_{na} = wavelengths not available, L_{No} = number of leaves, LOX = 9/13-lipoxygenase, L_{Root} = root length, L_{Shoot} = shoot length, L_{Thick} = leaf thickness, MDA = malondialdehyde, MVA = mevalonate pathway, MEP = methylerythritol 4-phosphate pathway, *na* = not available, *nd* = not detectable, NS_{No} = number of nodal segments, PAL = phenylalanine ammonia lyase, PFD = photon flux density ($\mu\text{mol m}^{-2} \text{s}^{-1}$), P_{Height} = plant height, *Pn* = photosynthetic rate, R = red light (600-700 nm), RB = red and blue light, RGB = red, green and blue light, R_{No} = number of roots, RTs = retention times, SLA = specific leaf area ($\text{cm}^2 \text{mg}^{-1}$), S_{No} = number of shoots, TAC = total anthocyanin content, TS = terpene synthase, UV-A = ultraviolet light (315-400 nm), UV-B = ultraviolet light (280-315 nm), UV-C = ultraviolet light (100-280 nm), VFAD = volatile fatty acid derivatives, VOC = volatile organic compound, VPB = volatile phenylpropanoids and benzenoids, VT = volatile terpenes, W = broadband white light usually within PAR (photosynthetically active radiation; 400-700 nm \pm flanking regions including ultraviolet (UV) A and/or FR), Y = yellow light (560-640 nm).

² Light intensity is given in micromole per square meter and second ($\mu\text{mol m}^{-2} \text{s}^{-1}$).

³ Unidentified compounds are excluded from this review.

2. LED4Plants

Within the framework of the European Innovation Partnership ‘Agricultural Productivity and Sustainability’ (EIP-AGRI) - an initiative intended to (1) warrant food safety and availability, (2) diversify production systems of food and non-food products, (3) strengthen their long-term supplies and (4) improve value chains of the primary sector - the Ministry of Agriculture, Environment and Climate Protection of the German State of Brandenburg and the European Union financed the research project ‘LED4Plants – efficient, specific crop production by LEDs’ via the European Agricultural Fund for Rural Development (EAFRD) between 2017 and 2020.

Project partners from research, technology and horticultural practices joined together to develop and test plant-appropriate LED-based lighting systems and an innovative vertical farming system for year-round productions of herbs and ornamentals in Berlin and Brandenburg. Further objectives of the project were to provide practical support for the horticultural sector by exploring strategies to improve the yield, quality and resistance of select horticultural plants and to shorten cultivation periods with these pilot technologies. The project further intended to investigate the feasibility and energy demands of these newly developed systems.



Figure 9 – Project partners and their tasks within LED4Plants.

A brief project overview in form of a short video was created by the German Networking Agency for Rural Areas (DVS) and can be accessed via the following link: <https://www.youtube.com/watch?v=Hu5TpMrRkBM>. Detailed information as well as the final report of the project are available at <https://eip-agri.brandenburg.de/eip-agri/de/projekte/led4plants-beendet/>. In

addition, a master thesis titled ‘Studies on greenhouse cultivation of turmeric (*Curcuma longa* L.) – Effects of supplemental LED lighting on yield and secondary metabolites’ arose from the LED4Plants project (Mehldau, 2020)¹⁶. Furthermore, project outcomes were presented at the Young Scientist Meeting and the International Plant Spectroscopy Conference in form of posters (Köppe et al., 2018; Köppe et al., 2019¹⁷) and at the 30. Bernburger Winter Seminar for Medicinal and Spice Plants in form of a presentation (Tabbert, 2020).

2.1 List of published peer-reviewed articles

Within the framework of the LED4Plants research project, the following three peer-reviewed articles¹⁸ have been published under CC BY licenses (<https://creativecommons.org/licenses/by/4.0/>) and represent the heart of this dissertation.

Tabbert, J.M., Schulz, H. & Krähmer, A. (2021)

Increased plant quality, greenhouse productivity and energy efficiency with broad-spectrum LED systems: A case study for thyme (*Thymus vulgaris* L.).

Plants. 10:960. <https://doi.org/10.3390/plants10050960>¹⁹

Tabbert, J.M., Schulz, H. & Krähmer, A. (2022a)

Investigation of LED light qualities for peppermint (*Mentha x piperita* L.) cultivation focusing on plant quality and consumer safety aspects.

Front. Food Sci. Technol. 2:852155. <https://doi.org/10.3389/frfst.2022.852155>²⁰

Tabbert, J.M., Riewe, D., Schulz, H. & Krähmer, A. (2022b)

Facing energy limitations – Approaches to increase basil (*Ocimum basilicum* L.) growth and quality by different increasing light intensities emitted by a broadband LED light spectrum (400-780 nm).

Front. Plant Sci.13:1055352. <https://doi.org/10.3389/fpls.2022.1055352>²¹

Each publication including supplemental information will be presented in the following three chapters.

¹⁶ The master thesis was supervised by Jenny Manuela Tabbert, author of this dissertation and reviewed by Hartwig Schulz, scientific supervisor of LED4Plants.

¹⁷ During the preparation of this dissertation, I married my husband James Alfred Tabbert III and changed my maiden name Köppe into Tabbert.

¹⁸ Copyright: © 2021 by the authors.

¹⁹ Licensee: MDPI, Basel, Switzerland. Disclaimer: MDPI stays neutral with regard to jurisdictional claims in published maps and institutional affiliations.

^{20,21} Licensee: Frontiers Media SA, Lausanne, Switzerland. Disclaimer: All claims expressed in this article are solely those of the authors and do not necessarily represent those of their affiliated organizations, or those of the publisher, the editors and the reviewers. Any product that may be evaluated in this article, or claim that may be made by its manufacturer, is not guaranteed or endorsed by the publisher.

Increased Plant Quality, Greenhouse Productivity and Energy Efficiency with Broad-Spectrum LED Systems: A Case Study for Thyme (*Thymus vulgaris* L.)

Abstract: A light-emitting diode (LED) system covering plant-receptive wavebands from ultraviolet to far-red radiation (360 to 760 nm, “white” light spectrum) was investigated for greenhouse productions of *Thymus vulgaris* L. Biomass yields and amounts of terpenoids were examined, and the lights’ productivity and electrical efficiency were determined. All results were compared to two conventionally used light fixture types (high-pressure sodium lamps (HPS) and fluorescent lights (FL)) under naturally low irradiation conditions during fall and winter in Berlin, Germany. Under LED, development of *Thymus vulgaris* L. was highly accelerated resulting in distinct fresh yield increases per square meter by 43% and 82.4% compared to HPS and FL, respectively. Dry yields per square meter also increased by 43.1% and 88.6% under LED compared to the HPS and FL lighting systems. While composition of terpenoids remained unaffected, their quantity per gram of leaf dry matter significantly increased under LED and HPS as compared to FL. Further, the power consumption calculations revealed energy savings of 31.3% and 20.1% for LED and FL, respectively, compared to HPS. In conclusion, the implementation of a broad-spectrum LED system has tremendous potential for increasing quantity and quality of *Thymus vulgaris* L. during naturally insufficient light conditions while significantly reducing energy consumption.

Keywords: light-emitting diode, daily light integral, volatile organic compounds, energy consumption, plant morphology, biomass efficacy

1. Introduction

Insufficient natural light intensities and short photoperiods drastically limit plant development during winter months in northern regions. Although most common horticultural crops depend on daily light integrals (DLIs) of 6 to 50 mol m⁻² d⁻¹ (Faust et al., 2018), outdoor solar DLIs often do not exceed 10 mol m⁻² d⁻¹ in higher latitudes during light-limited winter months (Korczynski et al., 2002) and are further reduced by up to 60 % inside greenhouses (Pramuk & Runkle, 2005; Kong et al., 2017; Matysiak & Kowalksi et al., 2019). Therefore, greenhouse industries and research facilities seasonally apply supplemental light sources to prolong cultivation periods and optimize plant growths. However, potentials for (year-round) horticultural productions remain under-utilized, as traditional light sources consume unfeasible amounts of energy (Nelson & Bugbee, 2014) and are not tailored to the plants’ photoreceptors (Eichhorn-Bilodeau et al., 2019). Hence, new technology, which significantly reduces electricity

consumption while improving crop value, is of great interest to greenhouse industry and research facilities (Darko et al., 2014).

Today, light-emitting diodes (LEDs) have the potential to replace traditional light sources such as high-pressure sodium lamps (HPS) (Martineau et al., 2012; Wojciechowska et al., 2015) and fluorescent lights (FL) (Park et al., 2012). They show important technical advantages such as high energy efficiency, small size, durability, long operating lifetime, low thermal emission, and adjustable spectral wavelength range (reviewed in Massa et al., 2008; Morrow, 2008; Bourget, 2008). Consequently, the utilization of LED technology as horticultural lighting increases (Mitchel et al., 2015).

However, the majority of LED radiation studies on plant development have only included narrow wavebands of red (R) and blue (B) light, as these wavelengths are maximally absorbed by the plant's light-capturing chlorophylls (McCree, 1972a). Initial LED plant-lighting research proved that plants could complete their life cycle with R light alone (Goins et al., 1998), but the plants' morphogenesis including compact growth and leaf expansion, as well as plants' flowering, were significantly improved when differing proportions of B light were included (Hoenecke et al., 1992; Ahmad et al., 2002; Folta & Spalding, 2001; Yorio et al., 2001; Hernández & Kubota, 2016). Additionally, specific B light proportions positively influence physiological plant responses such as stomatal opening, chlorophyll contents, and secondary metabolism (Darko et al., 2015; Hernández & Kubota, 2016).

Recently, studies have suggested further photosynthetic improvements by adding far-red (FR) wavelengths to R spectra, for example, increasing FR radiations promoted growth of seedlings by increasing leaf expansion and whole-plant net assimilation, decreased anthocyanins and carotenoids, and reduced antioxidant potentials (Park & Runkle, 2017; Stutte & Edney, 2009). As recent studies confirm, green (G) light can also contribute to plant development and growth (Schenkels et al., 2020; Smith et al., 2017; Johkan et al., 2012). Enhanced lettuce growth under RB illumination complemented with G light and improved cucumber growth under HPS supplemented with G light have been reported (Kim et al., 2004; Kong et al., 2015; Novičkovas et al., 2012). However, G light stimulates early stem elongation and stomatal closure, antagonizing the typical blue-light mediated growth inhibition and stomatal opening (Folta, 2004; Frechilla et al., 2000; Talbott et al., 2002).

Due to the multitude of photobiological studies conducted, it is now well established that wavelengths between ~ 360 and 760 nm influence plants' photosynthesis, physiology, morphogenesis, and phytochemical contents (Eichhorn-Bilodeau et al., 2019) and that specific spectral regions can be used to induce specific plant traits of interest. Nevertheless, negative side effects resulting from narrow waveband LED applications, such as unwanted photomorphogenic and physiological disorders, pest and disease

pressures, as well as difficult visual assessment of plant-status absent under (natural) broad light spectra, have to be further minimized (Goins et al., 1998; Gómez & Izzo, 2018).

In consequence, LED fixtures with broader spectral quality covering the range of the photosynthetically active radiation (PAR) between 400 and 700 nm (perceived as white light) sometimes including the flanking regions of UV (~360–400 nm) and FR (~600–760 nm) radiation are emerging recently (Ouzounis et al., 2015) and are becoming popular as sole-source lighting for horticulture (Cope & Bugbee, 2013; Burattini et al., 2017).

For example, Spalholz et al. (2020) compared the response of two lettuce cultivars to a sun-simulated spectrum and other commonly applied B:R spectra, providing a biologically active radiation between 300–800 nm of $200 \mu\text{mol m}^{-2} \text{s}^{-1}$. The study elucidated unique responses including greatest fresh-to-dry mass ratio, greater leaf area, excessive stem extension, and flower initiation under the sun-simulated spectrum despite a 36 % greater photosynthetic photon flux density (PPFD) in B:R treatments. Coinciding results were published by Gao and coworkers (2020), who tested the effects of white and different monochromatic (B, G, Y, R) LEDs on Welsh onions (Gao et al., 2020). In addition to increased plant yield, net photosynthetic rate and photosynthetic efficiency were significantly higher under white light than under those of the monochromatic light treatments. Matysiak and Kowalski (2019) observed greatest fresh weights under W and R light treatment for lamb's lettuce and garden rocket, whereas for two sweet basil cultivars, no differences in fresh weight were detected under all tested light treatments. However, supplementation with B resulted in more compact growth of green-leaved basil. For red bok choy, a white light including UV and FR was evaluated as ideal for best overall yield performance (Mickens et al., 2019), and the importance of white light on shoot and root fresh weights of lettuce was demonstrated (Lin et al., 2013).

Thus, it has been found that broad LED spectra, covering a wider plant-receptive spectral range rather than single narrow bands, and at best including flanking regions in the FR and UV, can lead to greater plant development. So far, however, such a broad LED spectrum has not been tested under insufficient light conditions in greenhouses. Therefore, our aim was to evaluate the advantages and disadvantages of broadband LED lighting during the winter season in northern central Europe (Berlin, Germany, 52.5 °N, 1.33 °E) in a practical case study and to compare the results with the common HPS and FL setups found in the greenhouse industry and research facilities today.

As a model plant, we chose moderately light-dependent *Thymus vulgaris* L., which belongs to the Lamiaceae family rich in other genera such as *Salvia* and *Organum* (Perrino et al., 2021) and which is widely used in European cuisine and folk medicine for its expectorant, antitussive, antibroncholic,

antispasmodic, antimicrobial, antioxidant, anti-inflammatory, anthelmintic, carminative, and diuretic properties. The major bio-active metabolite responsible for the therapeutic properties of aromatic *Thymus vulgaris* L. is the monoterpene thymol (Salehi et al., 2018).

The aim of this study was to conduct a greenhouse experiment during winter in order to assess the development, biomass, and health-promoting terpenoid yields of *Thymus* under a prototype broad-spectrum LED, as well as to obtain the prototypes' power consumption and efficacy. To further evaluate the practical applicability and potential for greenhouse businesses and research facilities, we aimed at comparing the broad-spectrum LED results with results assessed under HPS and FL fixtures under their common setup conditions.

2. Materials and methods

2.1 Experimental design

To investigate biomass yields and contents of volatile organic compounds (VOCs) of *Thymus vulgaris* L. grown under a broad-spectrum LED system, and to compare the lights' productivity as well as electrical efficiency with conventionally used lighting fixtures for the cultivation of thyme under naturally low irradiated greenhouse conditions during fall and winter in Berlin, Germany, a one-factorial experiment with a randomized block design with three different supplemental light sources and four spatially independent replications ($N = 384$; $n = 32$ thyme plants per replication) was conducted.

2.2 Lighting systems and illumination conditions

Three different supplemental light sources ((1) fan-cooled light-emitting diode (LED) (SUNtec Technology, FUTURELED®, Berlin, Germany, dimensioning 47.5 × 21.5 × 19.5 cm³), (2) high-pressure sodium (HPS) lamps (bulb: SON GreenPower CG T 400 W E40 1SL, PHILIPS, Hamburg, Germany; ballast: HST, SILL Leuchten®, Berlin, Germany, dimensioning 50 × 30 × 19 cm³), and (3) fluorescent lamps (FL) (VENEDIG, Pracht®, Berlin, Germany, dimensioning 50 × 50 × 16 cm³)) were horizontally mounted onto given steel frames 1.40 m above greenhouse benches, resulting in distances between the bottom of the LED, HPS, and FL light sources and the greenhouse benches of 1.14, 1.13, and 1.09 m, respectively. Based on weather recordings from WetterKontor (Kontor, 2018), plants were exposed to an average of 2.5 h of sunshine per day during the experiment. In addition to the natural sunlight, plants were subject to supplemental lighting from 6:00 a.m. to 8:00 p.m. for a photoperiod of 14 h per day during the greenhouse experiment. Plastic sheeting extending from above the light fixtures to below the greenhouse benches eliminated neighboring light pollution.

2.3 Irradiance profile measurements

Irradiance measurements of the light fixtures were taken prior to the experiment using a spectral PAR meter (PG200N, UPRtek, Aachen, Germany) at night. Light intensity, spectral composition, and irradiance profiles (light distribution patterns) were measured and recorded at bench level under experimental conditions. The software package of the spectrometer (uSpectrum PC laboratory software) automatically calculated all electromagnetic parameters including photon flux density (PFD in $\mu\text{mol m}^{-2} \text{s}^{-1}$) and spectral irradiance ($\text{W m}^{-2} \text{nm}^{-1}$) between 360 and 760 nm and photosynthetic photon flux density (PPFD in $\mu\text{mol m}^{-2} \text{s}^{-1}$) between 400 and 700 nm. During a sunny day, light transmission between 350 and 800 nm of the natural irradiance through the greenhouse glass was determined to be 28% ($\pm 5\%$) by comparing the output of the spectrometer inside the greenhouse with the output outside the greenhouse and resulted in a photon flux density of $\sim 434 \mu\text{mol m}^{-2} \text{s}^{-1}$ at bench level, which amounts to an approximate natural daily light integral of $3.9 \text{ mol m}^{-2} \text{d}^{-1}$ when combined with the weather recordings (Section 2.2). Light spectra and detailed spectral compositions of the supplemental lighting systems are depicted in Figure 10 and summarized in Table 11, respectively.

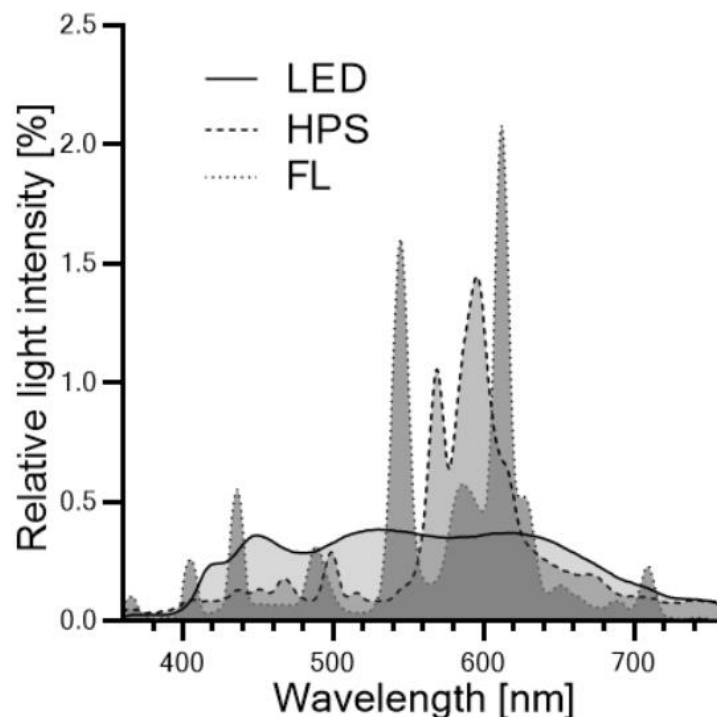


Figure 10 – Light spectra of the three artificial light sources used during the greenhouse experiment. Solid line: LED = light-emitting diode, dashed line: HPS = high-pressure sodium lamp, dotted line: FL = fluorescent light.

2.4 Plant material and growth conditions

Seeds of *Thymus vulgaris* L. (Rühlemann's Kräuter- und Duftpflanzen, Horstedt, Germany) were sown in 128-cell plug trays (\varnothing 4 cm) filled with potting substrate (Fruhstorfer Einheitserde Typ P, HAWITA, Vechta, Germany) on 9 October 2018 and placed under the differing lighting fixtures in a NS-orientated greenhouse located in Berlin, Germany (52.5° N, 13.3° E). After six weeks on 20 November 2018, 32 representative seedlings were transplanted into pots (\varnothing 9 cm) containing substrate with an elevated nutrient composition (Fruhstorfer Einheitserde Typ T, HAWITA, Vechta, Germany) and evenly placed (quadratic) within 1 m² under each light fixture. Each treatment was replicated four times, positioned in a randomized block design, and surrounded by 28 border plants to avoid boundary effects. Starting 27 December 2018, plants were fertilized weekly with 100 mL of a 0.2% (v/v) nutrient solution (Hakaphos® Blau, COMPO EXPERT®, Muenster, Germany) containing 15% N, 10% P₂O₅, 15% K₂O, 2% MgO, 0.01% B, 0.02% Cu, 0.075% Fe, 0.05% Mn, 0.001% Mo, and 0.015% Zn. However, due to the low biomass accumulation of the plants grown under the fluorescent lamp system, the plant fertilization was started two weeks later under the FL treatment. All thyme plants grew for a total period of 18 weeks until harvest on 12 February 2019. Climatic conditions including temperature and relative humidity of the greenhouse air were continuously monitored at canopy level via data loggers (EL-USB-2, Lascar, CONRAD, Hirschau, Germany). Average temperatures (°C \pm SD) under LED, HPS, and FL lighting were 20.4 \pm 1.4, 21.1 \pm 2.0, and 20.9 \pm 1.2, with a measuring accuracy of 1 °C. Average humidities (%rh \pm SD) under LED, HPS, and FL lighting were 47.2 \pm 7.0, 44.2 \pm 7.1, and 38.8 \pm 7.1 with a measuring accuracy of 2.25%rh. Both climatic conditions did not differ between treatments.

2.5 Harvest and crop management

To analyze the effect of the supplemental lighting systems on the yield, all 32 experimental thyme plants were harvested separately from each treatment condition and replication. Fresh matter (FM) of the above-ground plant parts was individually recorded at harvest on 12 February 2019. Total dry matter (DM) was measured after drying the samples in a circulated drying oven at 30 °C until stable mass was attained (\leq seven days). Leaf dry matter (L_{DM}) was determined for 16 plants selected from each treatment and replication, and the corresponding shot dry matter (S_{DM}) was calculated by subtracting the L_{DM} from DM. All dried leaf samples were vacuum-sealed (V.300®, Landig + Lava GmbH & Co KG, Bad Saulgau, Germany) and stored in the dark at 4 °C until further processing.

2.6 Energy measurements

The power draw of current (I) and voltage (U) as well as electrical characteristics including real power (P) and apparent power (S) from representative lamps of each lighting treatment were measured using a power meter (ENERGY MONITOR 3000, VOLT CRAFT®, Wernberg-Köblitz, Germany) in order to estimate energy consumptions and biomass efficacies of the light fixtures. To correct for the detected difference between P and S due to heat dissipation of the HPS system, the measured cos phi of 0.93 was incorporated into the HPS' power consumption calculations. According to the manufacturer's specifications, the HPS system allows a homogeneously illuminated area of 1.56 m² (1.2 × 1.3 m). Thus, the measured power consumptions were adjusted to the power consumption per square meter (W m⁻²) via rule of three. No adjustments were necessary for the LED and FL system.

2.7 Chemicals

Pure standard substances (α -pinene, α - and γ -terpinene, β -caryophyllene, borneol, carvacrol, limonene, linalool, myrcene, p-cymene, sabinene, thymol, and 6-methyl-5-penten-2-one) were purchased as analytical standards with a purity of at least 95% for GC reference analysis from Alfa Aesar (Kandel, Germany), Carl Roth (Karlsruhe, Germany), Merck KGaA (Darmstadt, Germany), and Fluka (Seelze, Germany). Isooctane (> 99%, HPLC grade) for solvent extraction of volatile organic compounds was obtained from Th. Geyer (Renningen, Germany).

2.8 Extraction of volatile organic compounds

The volatile organic compounds (VOCs) of 16 plants per treatment and replication ($n = 64$) were extracted according to the following procedure: 100 mg ($\pm 2\%$) of gently oven-dried and powdered (3 intervals of 10 s at 15,000 rpm via Tube Mill control, IKA®, Staufen, Germany) thyme leaves were transferred into 2 mL screw cap micro tubes (SARSTEDT AG & Co. KG, Nümbrecht, Germany) including two steel grinding balls ($\varnothing 2$ mm). The plant material was homogenized in 1.0 mL of isooctane (containing 1:40,000 (v/v) 6-methyl-5-penten-2-one as internal standard) for 10 min at 30 rps with a ball mill (MM400, Retsch®, Haan, Germany). After 10 min of ultra-sonication (Sonorex RK 106, BANDELIN electronic GmbH & Co. KG, Berlin, Germany) and 10 min of centrifugation at 13,000 rpm (Heraeus™ Labofuge™ 400 R, Thermo Scientific™, Osterode, Germany) at 22 °C respectively, the supernatants were transferred into GC-vials and stored at -70 °C until analysis.

2.9 GC-FID and GC-MS analysis

A total of 1 μL of the obtained extracts of volatiles was analyzed by GC-FID using an Agilent gas chromatograph 6890N fitted with an HP-5MS column (30 m \times 250 μm \times 0.5 μm) in splitless mode. Detector and injector temperatures were set to 250 $^{\circ}\text{C}$. The following oven temperature program was used: 50 $^{\circ}\text{C}$ for 2 min, heating from 50 to 320 $^{\circ}\text{C}$ at a rate of 5 K min^{-1} . The final temperature was held for 6 min. Hydrogen was used as carrier gas with a constant flow rate of 1.2 mL min^{-1} . GC-MS was performed using an Agilent mass spectrometer 5975B, on an HP-5MS column (see GC), operating at 70 eV ionization energy, using the same temperature program as above. Helium was used as carrier gas with a constant flow rate of 1.2 mL min^{-1} . Retention indices were calculated by using retention times of C6-C24-alkanes that were injected under the same chromatographic conditions.

2.10 Identification and quantification of volatile organic compounds

All main organic compounds of the volatile extracts were identified by comparing their mass spectra with those of internal reference libraries (Adams, NIST). Additionally, the identification of α -pinene, α - and γ -terpinene, β -caryophyllene, borneol, carvacrol, limonene, linalool, myrcene, *p*-cymene, sabinene, and thymol was confirmed by authentic reference standards by comparing their individual retention indices. Quantitative data of each main compound were obtained with serial dilutions of external standard solutions using at least six known concentrations (β -caryophyllene, *cis*-sabinene hydrate and linalool: 0.5, 1, 2, 5, 10, and 50 $\text{ng } \mu\text{L}^{-1}$; α -pinene, α -terpinene, borneol, limonene, myrcene, and sabinene: 1, 2, 5, 10, 50, and 100 $\text{ng } \mu\text{L}^{-1}$; *p*-cymene: 1, 2, 5, 10, 50, 100, 200, and 400 $\text{ng } \mu\text{L}^{-1}$; γ -terpinene: 1, 2, 5, 10, 50, 100, 200, 400, and 600 $\text{ng } \mu\text{L}^{-1}$; carvacrol: 1, 2, 5, 10, 50, 100, 200, 400, 600, and 1200 $\text{ng } \mu\text{L}^{-1}$; thymol: 5, 10, 50, 100, 200, 400, 600, 1200, and 1800 $\text{ng } \mu\text{L}^{-1}$), which covered concentration ranges detected for each compound in all samples.

2.11 Statistical analysis

Statistical analysis was performed using GraphPad Prism 8.4.2.679 (San Diego, MO, USA). Data of each spatial replication were tested for normality via Anderson-Darling, D'Agostino and Pearson, Shapiro-Wilk test, and Kolmogorov-Smirnov test. If normality test failed, outliers were identified via ROUT method ($Q = 10\%$) and removed to establish normality of all data sets. The means of each spatial replication ($n = 4$) were tested for normality with the Shapiro-Wilk test, and all data sets passed the normality test at $\alpha = 0.05$. Finally, all data sets were statistically analyzed using a Brown-Forsythe and Welch ANOVA test due to unequal variances between treatments. Multiple comparisons were conducted via Dunnett T3. Two-tailed

Pearson correlation between biomasses and DLIs was calculated after first computing means of 18 replicates per spatially independent light treatment and then analyzing those means ($n = 12$). Biomass efficacies ($\text{g or mg kWh}^{-1} \text{ m}^2$) were calculated based on electricity consumed within a square meter during the cultivation period.

3. Results and discussion

3.1 Biomass yield, partitioning, and morphology

The LED system resulted in distinct yield increases, biomass partitioning, and a differentiated morphological appearance of *Thymus vulgaris* L. in comparison to the HPS and FL systems (Figures 12 and 13).

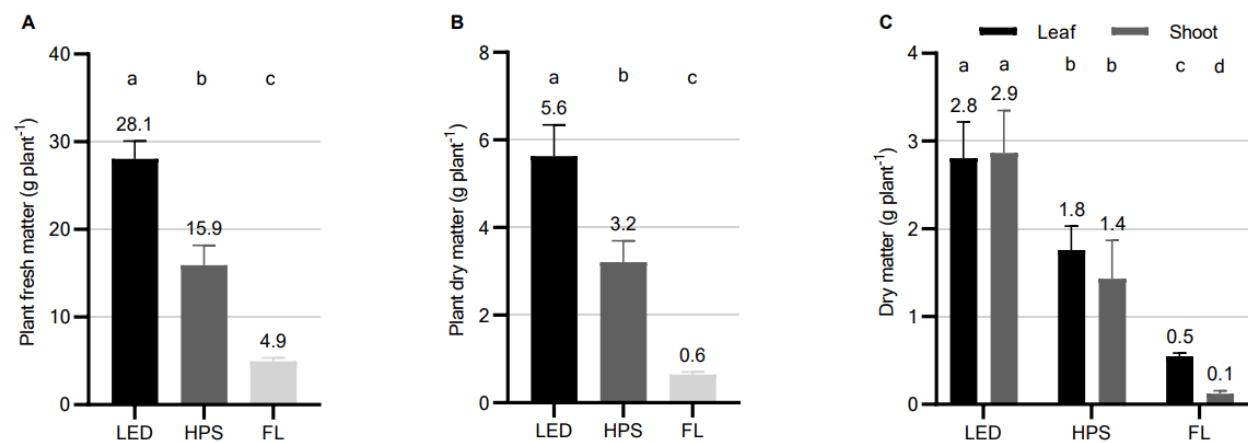


Figure 12 – Biomass yields and partitioning of *Thymus vulgaris* L. cultivated under different supplemental lighting systems during fall and winter in Berlin, Germany. LED = light-emitting diode, HPS = high-pressure sodium lamp, FL = fluorescent light. **(A)** Fresh matter yields in gram per plant¹, **(B)** Dry matter yields in gram per plant¹, **(C)** Leaf and shoot dry matter partitioning in gram per plant².

¹ Presented are mean plant yields of four independent spatial replications per light treatment ($n = 4$) \pm standard deviation (SD) of 32 harvested plants per spatial replication and light treatment ($N = 384$, $n = 128$ plants per supplemental light treatment, $n = 32$ plants per spatial replication). Significant differences ($p \leq 0.01$) were determined according to Dunnett's T3 multiple comparisons test after Brown-Forsythe and Welch ANOVA test ($p \leq 0.001$). Different letters indicate significant differences.

² Presented are mean dry leaf and shoot matter yields of four independent spatial replications per light treatment ($n = 4$) \pm SD (standard deviation) of 16 harvested plants per spatial replication and light treatment ($N = 192$, $n = 64$ plants per supplemental light treatment, $n = 16$ plants per spatial replication). Significant differences ($p \leq 0.05$) were determined according to Dunnett's T3 multiple comparisons test after Brown-Forsythe and Welch ANOVA test ($p \leq 0.001$). Different letters indicate significant differences.

While the LEDs produced a fresh biomass of averagely $28.1 \pm 2.0 \text{ g plant}^{-1}$, the HPS systems accounted for a fresh biomass of $15.9 \pm 2.3 \text{ g plant}^{-1}$ within the same cultivation period. The lowest fresh biomass of $4.9 \pm 0.4 \text{ g plant}^{-1}$ was produced under FL (Figure 12A). Accordingly, dry matter yields of *Thymus*

vulgaris L. were significantly enhanced by the LED system ($5.6 \pm 0.8 \text{ g plant}^{-1}$) in comparison to HPS ($3.2 \pm 0.5 \text{ g plant}^{-1}$) and FL ($0.6 \pm 0.1 \text{ g plant}^{-1}$), representing an increase of 1.75- and eight-fold, respectively (Figure 12B). Thereby, the weight proportion of dry leaves did not differ from the (mostly lignified) weight proportion of stems in thyme plants cultivated under the LED and HPS systems, respectively. Under FL, however, the majority of dry yield consisted of leaves (83.3%) and only 16.7% consisted of (unwooded) shoots (Figure 12C). With a Pearson correlation coefficient of $r = 0.97$ and $R^2 = 0.95$ ($p < 0.001$), dry mass yields under the differing supplemental lighting systems were highly related to the individual daily light integrals (DLI).

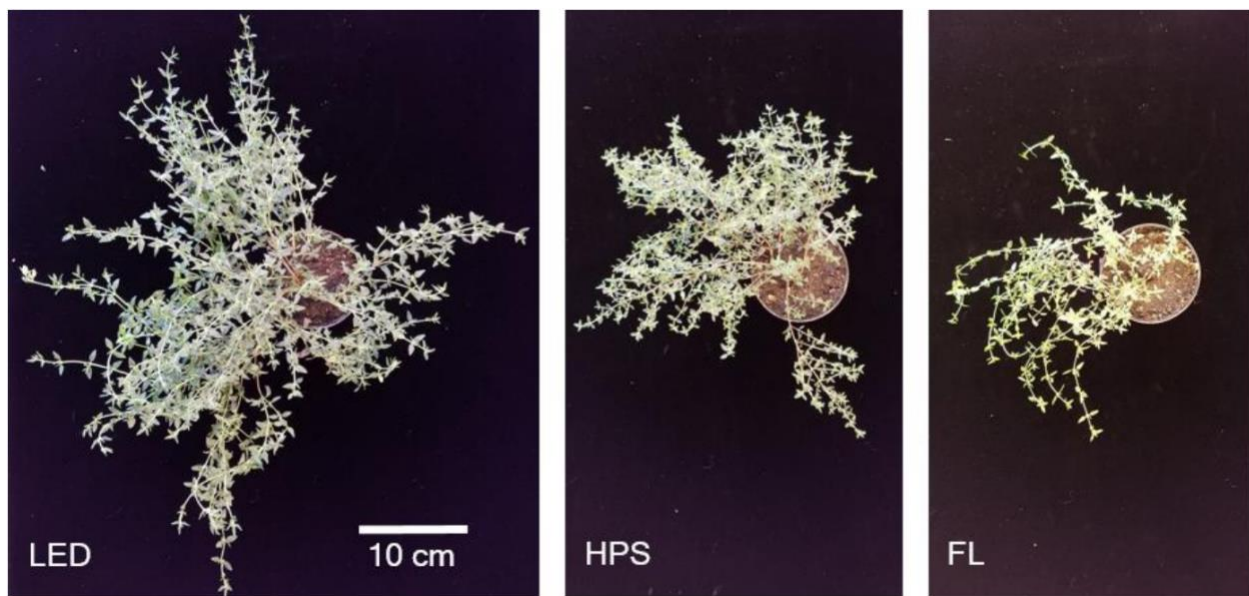


Figure 13 – Visual appearance of *Thymus vulgaris* L. at harvest cultivated under different supplemental lighting systems during fall and winter of Berlin, Germany. LED = light-emitting diode, HPS = high-pressure sodium lamp, FL = fluorescent light.

As indicated in Figure 13, the stem biomass of *Thymus vulgaris* L. was greatly increased under the LED system at the end of the experimental period and led to a profoundly different visual appearance in comparison to thyme plants grown under the other two supplemental lighting fixtures. Despite the lowest corresponding leaf-to-shoot ratio, which was 0.9 for LED, 1.3 for HPS, and 5 for FL, the leaf dry matter (L_{DM}) of thyme was significantly increased and highest under LED (Figure 12C).

The reason for the outstanding biomass accumulations and the concomitant rapid thyme development under the LED system is clearly found in the heightened DLI between 400 and 700 nm, as shown by the correlation coefficient of $r = 0.97$ ($R^2 = 0.95$). That increasing DLIs accelerate the development and growth of plants up to a certain point is well established (Craver et al., 2019; Faust, 2020). The

correlation of DLIs and plant growth is known to be linear between each species-specific light compensation point and light saturation point (Eichhorn-Bilodeau et al., 2019). Faust stated that optimal DLIs vary from 6 to 50 mol m⁻² d⁻¹ for various crops, and moderately light-dependent thyme requires a DLI of at least 18 mol m⁻² d⁻¹ (Faust, 2020). The natural average DLI in greenhouses during winter in northern latitudes however is often as low as 1 to 5 mol m⁻² d⁻¹ and reached approximately 3.9 mol m⁻² d⁻¹ during our greenhouse trial (Pramuk & Runkle, 2005; Kong et al., 2017; Matysiak & Kowalski, 2019). Hence, supplemental lighting is essential for winter greenhouse productions. Since FLs raised the total DLI (natural DLI 3.9 mol m⁻² d⁻¹ + supplemental DLI 3 mol m⁻² d⁻¹) only to approximately 7 mol m⁻² d⁻¹ during winter production, the FLs are neither suitable for the production of thyme nor presumably for the majority of greenhouse crops under the given cultivation conditions. HPS elevated the total DLI (natural DLI 3.9 mol m⁻² d⁻¹ + supplemental DLI 7 mol m⁻² d⁻¹) to an estimated level of 11 mol m⁻² d⁻¹. Therewith, the biomass accumulation of *Thymus vulgaris* L. increased significantly in comparison to FL; however, the DLI remains insufficient for an optimal thyme production during winter. With a total DLI of approximately 16 mol m⁻² d⁻¹ (natural DLI 3.9 mol m⁻² d⁻¹ + supplemental DLI 11 mol m⁻² d⁻¹) during the low light season, the tested LED system achieved the highest DLI and approached the recommended DLI of ≥ 18 mol m⁻² d⁻¹ the most (Table 11 under material and methods). Further, only the LED system would be able to achieve the recommended DLI of the moderately light-dependent thyme by simply extending the photoperiod from 14 to 16 h per day during winter.

3.2 Content and composition of volatile organic compounds (VOCs)

Applying GC-MS analysis, 12 monoterpenes and one sesquiterpene were identified in the leaf extracts of *Thymus vulgaris* L., representing ≥ 94 % of all detected volatile constituents. Major identified volatile organic compounds (VOCs) in the leaf extracts of *Thymus vulgaris* L. under the supplemental lighting systems were thymol, γ -terpinene, and *p*-cymene, respectively, which is consistent with the results of former research (Thompson et al., 2003; Rota et al., 2008). Thereby, the chemical makeup remained unaffected by the different lighting systems. The total content of VOCs per g of L_{DM} is highly enhanced by LED (2.7 %) and HPS (2.3 %) as compared to by FL (1.1 %). The difference in quantity of VOCs per g of L_{DM} between thyme plants cultivated under LED and HPS is not significant ($p = 0.088$). The LED considerably increased the amounts of all 13 evaluated terpenoids in the leaves of *Thymus vulgaris* L. in contrast to the FL system. The HPS system also enabled considerable increases in comparison to the FL system, even though the differences between the amounts of γ -terpinene and borneol are less profound, with $p = 0.099$ and $p = 0.075$, respectively. Differences between LED and HPS treatments were only detected for α -pinene,

while myrcene ($p = 0.077$) as well as limonene ($p = 0.057$) differed only in tendency. All results are summarized in Table 12.

Table 12 – Effect of three different supplemental lighting systems on the chemical composition of 13 main volatile substances of *Thymus vulgaris* L. cultivated in the greenhouse during fall and winter of Berlin, Germany.

Compound	Light-emitting diode (LED)			High-pressure sodium lamp (HPS)		Fluorescent light (FL)	
	RI ¹	% ²	µg 100 mg ⁻¹ L _{DM} ³	%	µg 100 mg ⁻¹ L _{DM}	%	µg 100 mg ⁻¹ L _{DM}
<i>Monoterpene hydrocarbons</i>							
α-pinene	938.0 ± 0.4	0.8 ± 0.1	14.03 ± 0.8 ^a	0.8 ± 0.1	11.41 ± 1.1 ^b	1.0 ± 0.1	7.22 ± 1.1 ^c
sabinene	977.8 ± 0.4	1.4 ± 0.4	34.21 ± 8.5 ^a	1.5 ± 0.6	33.57 ± 6.4 ^a	1.3 ± 0.5	13.95 ± 1.5 ^b
myrcene	991.8 ± 0.3	1.6 ± 0.2	35.16 ± 1.8^a	1.5 ± 0.2	28.50 ± 3.6^a	1.8 ± 0.2	17.19 ± 1.6 ^b
α-terpinene	1020.8 ± 0.3	1.9 ± 0.4	39.47 ± 4.3 ^a	2.1 ± 0.7	33.43 ± 3.2 ^a	2.2 ± 0.8	19.72 ± 2.1 ^b
p-cymene	1029.1 ± 0.5	8.5 ± 2.2	157.70 ± 27.4 ^a	8.3 ± 2.5	123.90 ± 8.0 ^a	6.9 ± 2.5	55.16 ± 4.7 ^b
limonene	1033.1 ± 0.3	0.6 ± 0.1	9.81 ± 0.7^a	0.6 ± 0.1	8.22 ± 0.8^a	0.6 ± 0.1	4.59 ± 0.5 ^b
γ-terpinene	1064.4 ± 0.8	15.2 ± 5.4	323.20 ± 56.7 ^a	16.0 ± 4.7	259.90 ± 49.0^{ab}	20.1 ± 6.3	179.50 ± 22.6^b
<i>Oxygenated monoterpenes</i>							
cis-sabinene hydrate	1071.7 ± 0.4	1.3 ± 0.1	28.41 ± 2.3 ^a	1.4 ± 0.2	25.38 ± 1.6 ^a	1.3 ± 0.3	12.31 ± 0.8 ^b
linalool	1100.9 ± 0.5	2.6 ± 0.7	61.92 ± 11.3 ^a	2.7 ± 0.8	52.22 ± 11.2 ^a	2.3 ± 0.9	21.25 ± 1.9 ^b
borneol	1173.6 ± 0.3	0.9 ± 0.4	44.44 ± 2.6 ^a	1.0 ± 0.6	46.50 ± 5.9^{ab}	1.5 ± 0.7	31.75 ± 3.7^b
thymol	1297.6 ± 1.8	54.6 ± 6.9	1134.00 ± 86.3 ^a	52.9 ± 6.4	917.10 ± 142.9 ^a	50.2 ± 7.9	429.90 ± 57.3 ^b
carvacrol	1304.6 ± 1.1	2.4 ± 0.4	60.82 ± 4.9 ^a	2.3 ± 0.5	48.82 ± 8.2 ^a	2.0 ± 0.6	21.42 ± 2.9 ^b
<i>Sesquiterpene hydrocarbons</i>							
β-caryophyllene	1436.6 ± 0.5	3.1 ± 1.3	47.69 ± 7.1 ^a	3.67 ± 1.1	49.50 ± 7.0 ^a	3.32 ± 1.1	21.91 ± 3.4 ^b
% of total extract ^[2]			94.93±1.50	94.68±2.22		94.53 ± 1.95	
Total volatiles [% g ⁻¹ L _{DM}] ^[4]			2.7±0.22^a	2.3±0.25^a		1.1 ± 0.10 ^b	

¹ Retention indices relative to C₆-C₂₄ n-alkanes on a HP-5MS column. Indices are presented as means ± SD with *n* = 192.

² Percentages were calculated from GC-FID TIC data after weight correction and presented as means ± SD with *n* = 64.

³ Amounts of major compounds were calculated based on density corrected calibration functions obtained from reference standards analyzed under the same GC-FID conditions as the samples. Presented are mean amounts of volatile compounds [µg 100 mg⁻¹ L_{DM} (= leaf dry matter)] of four independent spatial replications per light treatment (*n* = 4) ± SD of 16 collected dried leaf samples per spatial replication and light treatment (*N* = 192, *n* = 64 dry leaf samples per supplemental light treatment, *n* = 16 dry leaf samples per spatial replication). Significant differences (*p* ≤ 0.05) were determined according to Dunnett's T3 multiple comparisons test after Brown-Forsythe and Welch ANOVA test (*p* ≤ 0.02). Different letters within a row indicate significant differences at *p* ≤ 0.05 and bold amounts indicate significant differences at *p* ≤ 0.1.

⁴ Percentage of total volatiles were calculated based on the results of the internal standard (6-Methyl-5-penten-2-one) which was co-analyzed in each sample. Presented are mean percentages per g L_{DM} [% g⁻¹ L_{DM} (= leaf dry matter)] of four independent spatial replications per light treatment (*n* = 4) ± SD of 16 collected dried leaf samples per spatial replication and light treatment (*N* = 192, *n* = 64 dry leaf samples per supplemental light treatment, *n* = 16 dry leaf samples per

spatial replication). Significant differences ($p \leq 0.05$) were determined according to Dunnett's T3 multiple comparisons test after Brown-Forsythe and Welch ANOVA test ($p \leq 0.001$). Different letters within a row indicate significant differences at $p \leq 0.05$ and bold amounts indicate significant differences at $p \leq 0.1$.

Gouinguene and Turlings (2002) showed in their study that young corn plants (*Zea mays* L.) significantly increased their emissions of volatiles as light intensity increased up to 10,000 lumen (lm). However, beyond 10,000 lm volatile emissions in *Zea mays* L. did not enhance any further, suggesting a kind of saturation or limitation was reached. Spring et al. (1986) and Gleizes et al. (1980) also detected this proposed light quantity-dependency. Multiple studies also suggest that terpene synthesis involves phytochromes ((Spring et al., 1986; Gleizes et al., 1980; Yamaura et al., 1991; Tanaka et al., 1989), red and far-red light-sensing photoreceptors (reviewed by Franklin, 2008)), making the production of terpenes also dependent on light quality, specifically on the R/FR ratio (Kegge et al., 2013). For example, in thyme seedlings, red light strongly promoted the production of mono- and sesquiterpenes (thymol, γ -terpinene, *p*-cymene and carvacrol, β -caryophyllene) and the number of essential oil-containing trichomes per cotyledone, two stimulatory effects that proved to be completely reversible by a subsequent exposure to far-red irradiation (Yamaura et al., 1991; Tanaka et al., 1989). Later, a partial reduction of volatile emissions was detected in *Arabidopsis thaliana* (L.) Heynh exposed to a low R/FR ratio of 0.2 as compared to plants exposed to a high R/FR ratio of 2.2 when controlling for light intensity (Kegge et al., 2013). These findings could explain the comparatively low VOC contents detected in thyme leaves grown under FL, as both their light intensity (PFD 60 $\mu\text{mol m}^{-2} \text{s}^{-1}$, PFD-R 7.6 $\mu\text{mol m}^{-2} \text{s}^{-1}$) as well as their R/FR ratio (0.1) were significantly reduced as compared to LED and HPS under our experimental conditions. It would also suggest that the similar contents of VOCs per gram of thyme leaves found under LED and HPS are the result of their similar high R/FR ratios of 2.8 and 2.4, respectively. However, R/FR ratios dramatically decline under vegetational canopies. As described by Franklin (2008), a single leaf reduces a given R/FR ratio of 1.2 to 0.2 for the leaves growing underneath, and the ratio reduces further to 0.1 underneath a second leaf (Franklin, 2008). As leaf and shoot yields of *Thymus vulgaris* L. significantly increased under the LED system, it is reasonable to believe that the actual R/FR ratio underneath the more densely stands of thyme plants grown under the LED system was much lower than under the less dense canopy of thyme plants grown under HPS. This idea coincides with the result from Kegge et al. (2013), who detected a reduction of volatile emissions in plants grown in high density stands. Another explanation for the similar contents of VOCs per gram of thyme leaves found under LED and HPS may be found in the high B light proportion found under the broad LED light spectrum, as it was recently shown that essential oil contents of *Thymus vulgaris* L. decrease with increasing proportions of blue light (Tohidi et al., 2019). The associated suppressions of terpene synthesis under low R/FR ratios as well as under low R/B ratios may have been partially compensated by the LEDs' elevated light intensity (PFD 232 $\mu\text{mol m}^{-2} \text{s}^{-1}$, PFD-R 55.3 $\mu\text{mol m}^{-2} \text{s}^{-1}$) compared to the intensity of the HPS system (PFD 143 $\mu\text{mol m}^{-2} \text{s}^{-1}$, PFD-R 24.3 $\mu\text{mol m}^{-2} \text{s}^{-1}$) in our

study. Additionally, though air temperatures under the given experimental conditions did not differ between the supplemental lighting systems, it is known that leaf temperature increases under HPS lights as compared to other lighting systems (Poel & Runkle, 2017). As elevated temperatures evidently increase the emission of volatiles (Gouinguene & Turlings, 2002), a greater leaf temperature under HPS may have been present and contributed to the terpene synthesis in HPS-grown thyme plants. Further, as we did not adjust fertilization, though the LED system yielded much greater biomasses than FL and HPS, it is plausible that a reduced nutrient availability for LED-grown thyme plants limited their production of VOCs, as demonstrated by Gouinguene and Turlings (2002), who showed that fertilization rate positively effects volatile emissions.

Nevertheless, as the LED lights were able to increase the production of volatiles in thyme leaves significantly compared to the HPS lights, the LEDs' volatile productivity per square meter doubled in absolute terms (2.5 vs. 1.3 g m⁻²) with $p < 0.06$ (Table 13).

Table 13 – Fresh and dry plant productivity as well as content of volatile fraction of thyme (*Thymus vulgaris* L.) per m² under three supplemental lighting systems.

Light fixture	FM per square meter [g m ⁻²] ¹	DM per square meter [g m ⁻²] ¹	VC per square meter [mg m ⁻²] ²
LED	897.9 ± 64.65 ^a	180.2 ± 24.69 ^a	2472 ± 626.4^a
HPS	509.4 ± 72.88 ^b	102.6 ± 16.87 ^b	1273 ± 334.0^a
FL	158.0 ± 6.73 ^c	20.62 ± 2.06 ^c	199.1 ± 30.98 ^b

LED = light-emitting diode, HPS = high-pressure sodium lamp, FL = fluorescent light, FM = total fresh matter, DM = total dry matter, VC = total volatile content of total leaf dry matter.

¹ Presented data are means of cumulated fresh and dry matter productions of four independent spatial replications per light treatment ($n = 4$) ± SD of 32 harvested plants per spatial replication and light treatment ($N = 384$, $n = 128$ plants per supplemental light treatment, $n = 32$ plants per spatial replication). Significant differences ($p \leq 0.01$) were determined according to Dunnett's T3 multiple comparisons test after Brown-Forsythe and Welch ANOVA test ($p \leq 0.001$). Different letters indicate significant differences.

² Presented data are means of cumulated volatile productions in thyme leaves of four independent spatial replications per light treatment ($n = 4$) ± SD of 16 harvested plants per spatial replication and light treatment ($N = 192$, $n = 64$ dry leaf samples per supplemental light treatment, $n = 16$ dry leaf samples per spatial replication). Significant differences were determined according to Dunnett's T3 multiple comparisons test after Brown-Forsythe and Welch ANOVA test ($p \leq 0.002$). Different letters within the column indicate significant differences at $p \leq 0.02$ and bold amounts indicate a difference by trend at $p < 0.06$.

3.3 Productivity

The broad-spectrum LED system enabled a highly significant increase in leaf and stem production of fresh thyme per square meter, representing increases of 43.3 % and 82.4 % in comparison to the HPS and FL system, respectively. Additionally, the dry matter productions of HPS and FL were highly reduced by 43.1 % and 88.6 % in comparison to the LED system. Further, the LED system enabled an increase in production

of VOCs per square meter under the given greenhouse conditions in comparison to the conventionally used HPS system (at p -value of 0.051). Both systems (LED and HPS) considerably promoted the VOC production in comparison to the FL system. Table 13 summarizes the results. Despite the lower leaf-to-shoot ratio for LED lighting of 0.9 as compared to both HPS (1.3) and FL (5, see section 3.1), absolute L_{DM} and overall quantity of VOCs were highest for LED. Therefore, LED lighting offers an attractive alternative for thyme cultivation, both for essential oil production and delivery to fresh market.

3.4 Power consumption and biomass efficacy

The LEDs consumed the least electricity with 257.7 W m^{-2} , followed by the FLs with the use of 299.4 W m^{-2} , whereas the HPS lamp consumed the highest amount of electricity with 374.9 W m^{-2} . At the end of the cultivation period, the power consumptions per m^2 of LED and FL lighting system resulted in high energy savings of 31.3 % and 20.1 %, respectively, when compared to the consumption of the HPS system. While each LED system enabled $\pm 1.92 \text{ g}$ of fresh thyme per kWh and square meter, the HPS and FL enabled only $\pm 40 \%$ and $\pm 16 \%$ of these yields per kWh and square meter, respectively. Accordingly, the dry thyme production per kWh and square meter under LED ($\pm 396.3 \text{ mg}$) was significantly higher than the dry thyme production under HPS ($\pm 155.2 \text{ mg}$) and FL ($\pm 39.1 \text{ mg}$). Further, the production of VOCs per kWh and square meter was significantly elevated underneath the LEDs ($\pm 5.4 \text{ mg}$) as compared to HPS ($\pm 1.9 \text{ mg}$) and FL ($\pm 0.4 \text{ mg}$). Results and calculations are combined in Table 14.

Our power consumption results and thus the potential of LEDs for reducing energy costs coincide with numerous studies and reviews (Nelson & Bugbee, 2014; Martineau et al., 2012; Wallace & Both, 2016), stating energy reductions up to 70 % compared to traditional light sources while producing similar crop yields at equal light intensities, and confirm the current trend of LEDs' increasing photon efficiencies: While HPS and LED fixtures had nearly identical photon efficiencies until ~ 2015 (Nelson & Bugbee, 2014; Gómez & Izzo, 2018), the best evaluated LED fixture was 40 % more photon-efficient than HPS due to technological improvements of LEDs within the PAR region soon after (Gómez & Izzo, 2018; Wallace & Both, 2016). A current study by Hernandez et al. (2020) confirms the corresponding increase in biomass efficacy of LEDs, as their LED treatment led to a 2.4 to 3.1 times greater biomass efficacy than HPS, which matches our findings (Hernandez et al., 2020). Another study in which LED and FL treatments were compared, reported a biomass efficacy three to five times higher under LED than under FL lighting (Piovene et al., 2015). In contrast, the LED system used in this current study greatly exceeds their findings, as the LED enabled a biomass efficacy 6 to 10 times higher than the FL system (Table 14) under our experimental conditions. Further, in our study, plant growth may have been limited by nutrient availability, and an

adjustment of fertilization based on the differing thyme growth rates may further increase biomass efficacies under HPS and especially under the broad-spectrum LED system. Nevertheless, when using the broad-spectrum LED lighting system, the significantly more inhomogeneous light intensity distribution compared to HPS and FL lamps (as depicted in the material and method section in Figure 11) must be taken into account when light uniformity is necessary for the greenhouse application as it demands more LED light fixtures per area.

Table 14 – Power consumption of different supplemental lighting fixtures per square meter for the production of thyme (*Thymus vulgaris* L.) grown in a greenhouse during fall and winter of Berlin, Germany.

Light fixture	Power consumption per meter ² [W m ⁻²] ^[2]	Power consumption for thyme cultivation [kWh m ⁻²]	Power savings compared to HPS [%]	Fresh thyme production ¹ [g kWh ⁻¹ m ⁻²]	Dry thyme production ¹ [mg kWh ⁻¹ m ⁻²]	VOC production ² [mg kWh ⁻¹ m ⁻²]
LED	257.7	454.6	31.3	1.92 ± 0.15 ^a	396.3 ± 54.31 ^a	5.4 ± 1.4 ^a
HPS	374.9	661.3	<i>na</i>	0.77 ± 0.11 ^a	155.2 ± 25.5 ^a	1.9 ± 0.5 ^a
FL	299.4	528.1	20.1	0.30 ± 0.03 ^c	39.1 ± 3.9 ^c	0.4 ± 0.1 ^c

HPS = high-pressure sodium lamp, LED = light-emitting diode, FL = fluorescent light, *na* = not applicable.

¹ Presented are calculated average fresh and dry thyme productions per power consumption of each light fixture type within a square meter during the cultivation period (g or mg per kWh and m²) of four independent spatial replications per light treatment ($n = 4$) ± SD of 32 harvested plants per spatial replication and light treatment ($N = 384$, $n = 128$ plants per supplemental light treatment, $n = 32$ plants per spatial replication). Significant differences ($p \leq 0.01$) were determined according to Dunnett's T3 multiple comparisons test after Brown-Forsythe and Welch ANOVA test ($p \leq 0.001$). Different letters indicate significant differences.

² Presented are calculated average productions of volatile organic compounds (VOC) per power consumption of each light fixture type within a square meter during the cultivation period (mg per kWh and m²) of four independent spatial replications per light treatment ($n = 4$) ± SD of 16 harvested plants per spatial replication and light treatment ($N = 192$, $n = 64$ plants per supplemental light treatment, $n = 16$ plants per spatial replication). Significant differences ($p \leq 0.05$) were determined according to Dunnett's T3 multiple comparisons test after Brown-Forsythe and Welch ANOVA test ($p \leq 0.004$). Different letters indicate significant differences.

Nevertheless, at their edges, where the lowest light intensities occur, the LEDs achieve values of 16 W m⁻² nm⁻¹, which are sufficient for high-quality thyme production. Therefore, if homogenous plant development is not necessarily required, plants of marketable quality are also available with the LED setup used here without additional lamps.

4. Conclusion

With its outstanding biomass as well as terpenoid efficacy, the broad-spectrum LED system represents a strong competitor to the conventionally used HPS and FL lighting systems in greenhouses under naturally insufficient light conditions as investigated in this study. Marketable *Thymus vulgaris* L. can

be achieved faster and thus more often when replacing HPS and FL light sources with the tested LED system, ultimately resulting in greater revenues at simultaneously highly reduced production costs for greenhouse growers. The comparatively high initial capital costs of LEDs which have delayed their establishment in the past are decreasing (Wallace & Both, 2016). Based on our results, combined with the typically low maintenance and long operating lifetime (Morrow, 2008; Mitchel et al., 2015; Yeh & Chung, 2009; Barta et al., 1992), the initial investment into LEDs should quickly become a source of profit for greenhouse growers. Additionally, different adaptive control approaches making use of the dimmability of LEDs (Gómez & Izzo, 2015; Van Iersel & Gianino, 2017) can further decrease the power consumptions and help to achieve consistent growth rates at a daily and seasonal level as shown by Hernandez et al. (2020) and (Harbick et al. (2016)). Our results suggest that an implementation of a broad-spectrum LED system in greenhouses could provide the possibility to cultivate a greater variety of crops with greater DLI-requirements under naturally insufficient light levels as conventional lighting systems are capable of today. Further, the broad-spectrum LED system could extend greenhouse production seasons, which are currently constrained by low supplemental DLIs, and allow a year-round production of a wider variety of selected greenhouse crops than HPS and FL systems are able to at present. However, further trials with a variety of greenhouse crops need to be investigated to confirm the suggested applicability for a range of crops. Therefore, in prospective broad-spectrum LED studies, the crops' individual DLI requirements need to be incorporated and compared to commonly applied mono- and dichromatic LED light spectra at equal light intensities for advancing our knowledge on the impact of LED light spectra on morphological, physiological, and metabolic plant responses. In addition, more studies examining the impact of light qualities on terpenoid biosynthesis, content, and composition are needed to optimize the quality of aromatic plant species in the future.

Investigation of LED light qualities for peppermint (*Mentha x piperita L.*) cultivation focusing on plant quality and consumer safety aspects

Abstract: To understand how peppermint responds to different LED light qualities during the early vegetative phase, peppermints were illuminated with three different LED light conditions (RB = Red/Blue, RGB = Red/Green/Blue, SUN = artificial sunlight closely resembling the terrestrial sunlight spectrum between 380 and 780 nm) in an automated vertical cultivation system. RB resulted in compact growth, whereas both green-containing lighting conditions induced excessive stem and side branch elongations and significant leaf expansions. Although peppermint plants achieved marketable appearances regardless of lighting condition, essential oil (EO) compositions with highly elevated amounts of pulegone and menthofuran did not meet consumer safety requirements. Both artificial SUN and RB spectra showed lower concentrations of pulegone in the EO at 41 and 43%, respectively, than detected under RGB at more than 49%. Reasons for this undesirable EO composition are discussed as a result of the lighting conditions applied and the early harvest time, leading to an incomplete reduction of pulegone to menthone during biosynthesis. Based on these findings, aromatic peppermint cultivation under LEDs can be improved to meet regulatory requirements and highlights the need for analytical quality controls regarding consumer safety to evaluate the applicability of LED lighting for fresh herb productions.

Keywords: light-emitting diode, peppermint (*Mentha piperita L.*), essential oil, plant morphological characteristics, biomass

1. Introduction

As modern agriculture is challenged by its own negative environmental impacts and climate change, indoor vertical farms are increasingly seen as an alternative food production system as they could principally enable an increased supply of high-quality foods on a regional year-round scale (Orsini et al., 2020). Once optimal lighting strategies (as well as efficient water, nutrient and climate control systems) become available and comprehensively integrated, vertical farms are expected to become a viable and sustainable food production system for a wide range of crops (Kozai 2019).

In the last decade, light-emitting diodes (LEDs) proved to be highly versatile and energetically efficient lighting systems, and their technical as well as spectral advantages over traditional light sources for plant cultivation have been well described (Eichhorn-Bilodeau et al., 2019).

As red (R) and blue (B) wavebands are maximally absorbed by the plant's light-capturing chlorophylls (McCree 1972), most LED studies remain focused on different RB ratios to optimize plant

growth, morphology and physiological responses (e.g., Pennisi et al., 2019). However, addition of other wavelengths shows potential to improve plant traits of interest even further. For example, addition of far-red wavelengths (FR, > 700 nm) can increase net photosynthesis (Park and Runkle 2017; Kalaitzoglou et al., 2019), and ultraviolet radiation (UV, < 400 nm) can promote the accumulation of certain secondary metabolites (Behn et al., 2010; Rechner et al., 2017). Green (G) light (400–500 nm) was reported to increase chlorophyll contents (Saengtharapip et al., 2020) and carbon assimilations (Terashima et al., 2009), and the latter seems to be a consequence of the G lights' capability to penetrate deeper into the canopy than R and B wavelengths (Terashima et al., 2009). Thus, scientists hypothesized that addition of G light could potentially increase plant yields under artificial lighting systems (Sun et al., 1998; Folta 2004; Smith et al., 2017). So far however, this theoretical G light potential has only been shown for basil and tomato (Kaiser et al., 2019; Schenkels et al., 2020). In these two studies, partial replacements of R and B with G wavelengths resulted in increased biomasses, stem lengths and leaf areas.

In addition, recent LED studies using broad light spectra covering the whole range of radiation relevant for plant development (300–800 nm) suggest further improvements as greater plant yields and photosynthetic rates are found when compared to dichromatic spectra (Kozai, 2019).

Peppermint (*Mentha x piperita L.*), a medicinal and aromatic plant from the Lamiaceae family, does not only demonstrate a plethora of therapeutic activities, inducing antioxidant, antispasmodic, antiseptic, antibacterial, antiviral, anticarcinogenic, antitumorigenic, antiallergic, anti-inflammatory, antifungal, antimutagenic and antinauseant properties. It is also widely used as a tea infusion, culinary herb and spice, in confections, as an aromatic flavoring agent, as well as in the cosmetic, personal hygiene and perfumery industry for its fragrance properties (Malekmohammad et al., 2019).

Although peppermint represents one of the most important essential oil-bearing herbal plants worldwide (Mahendran and Rahman 2020), there is only limited knowledge about suitable supplemental lighting programs for its cultivation. Though based on experiments conducted with diverse lighting technologies, light intensities ranging from 113 to 1,200 $\mu\text{mol m}^{-2} \text{s}^{-1}$ have been suggested for different mint developmental stages (Behn et al., 2010; Sabzalian et al., 2014; Alvarenga et al., 2018), and photoperiods of 14–16 h have been reported to increase the essential oil (EO) content and quality of *Mentha x piperita L.* (Burbott and Loomis 1967; Clark and Menary 1980). Further, UV added to white background lighting (W) as well as monochromatic R light have been shown to increase EO contents in peppermint (Behn et al., 2010; Sabzalian et al., 2014). However, monochromatic B light as well as B light added to W decreased the EO content in *Mentha x piperita L.* (Maffei and Scannerini 1999; Sabzalian et al., 2014). Best results in terms of plant growth and EO content were achieved under RB when compared

to monochromatic R and B light supplied by LEDs (Sabzalian et al., 2014); however, the study does not include information on the composition and thus, quality of the EO, which is predominantly determined by the quantity and composition of its monoterpenoid constituents. Here, 30–55 % of menthol, 14–32 % of its precursor menthone and low levels of pulegone (< 4 %), menthofuran (1–9 %) and methyl acetate (2.8–10 %) are considered peppermint EOs of high quality (Schmiedel 2008).

Related to the above-mentioned peppermint cultivation conditions and plant developmental improvements, we conducted an LED-based lighting experiment in a vertical cultivation system applying three different light qualities at equal photon flux density. The aim of this study was to investigate whether a partial replacement of R and B with G light (RGB) or a broad white light spectrum including UV and FR (SUN) results in the recently suggested improvements in terms of biomass accumulation and morphological traits in *Mentha x piperita* L. when compared to the commonly applied dichromatic RB spectrum. Even though it is known that cultivation conditions strongly impact the quality of peppermint EO, no data is currently available on the influence of LED light spectra on its composition (Salehi et al., 2018). Therefore, we investigated the peppermints' EO composition with special emphasis on the harmful metabolites pulegone and menthofuran which are synthesized during early development in mint leaves grown under insufficient light intensities (Croteau et al., 2005; Rios-Esteva et al., 2008).

2. Materials and methods

2.1 Experimental design

To investigate morphology, biomass yields and EO composition of peppermint samples under three different spectral lighting conditions, a one-factorial experiment with a randomized block design and three spatially independent replications per light treatment ($N = 270$; $n = 30$ peppermint plants per replication) was conducted in three vertical three-leveled cultivation systems at the same time.

2.2 Plant material and growth conditions

Stock plants of *Mentha x piperita* var. *piperita* cv. *Multimentha* were cultivated at Julius Kühn-Institute (JKI), Institute for Breeding Research on Horticultural Crops (51.8° N, 11.1° E) under field conditions. At JKI, Institute for Ecological Chemistry, Plant Analysis and Stored Product Protection, stolon segments (5 cm) from one established stock plant (to ensure genetically identical plants) were cultivated in propagator trays filled with potting substrate (Fruhstorfer Einheitserde Type P, HAWITA, Vechta, Germany) in a greenhouse (~22 °C) under a natural average daily light integral (DLI) of 12.6 mol m² (based on weather recordings from WetterKontor (Kontor, 2021)) starting April 10th 2019. After sprouting, uniform nodal segments with

three equally developed leaf pairs were transferred to 128-cell plug trays (\varnothing 4 cm) filled with the same potting substrate, and covered with a plastic hood (light transmittance \geq 90 %, data not shown) to promote rooting on May 6th 2019 (26 days of cultivation (DOC)) in the greenhouse (\sim 22 °C) under natural light conditions. After 10 days, on May 16th 2019 (36 DOC), 270 representative plantlets were transplanted into pots (\varnothing 12 cm) containing 0.69 L of substrate with an elevated nutrient composition (Fruhstorfer Einheitserde Type T, HAWITA, Vechta, Germany) and evenly placed on each of nine cultivation shelves (lined with water-permeable drainage fleece to avoid clogging of the watering system) under the LED lighting fixtures, resulting in 30 plants per cultivation shelf. In the nine available cultivation shelves, three light treatments were set up three times (30 peppermint plants per cultivation shelf amounted to a total of 90 peppermint plants per light treatment), resulting in three independent experimental replications per light treatment (Figure 14).

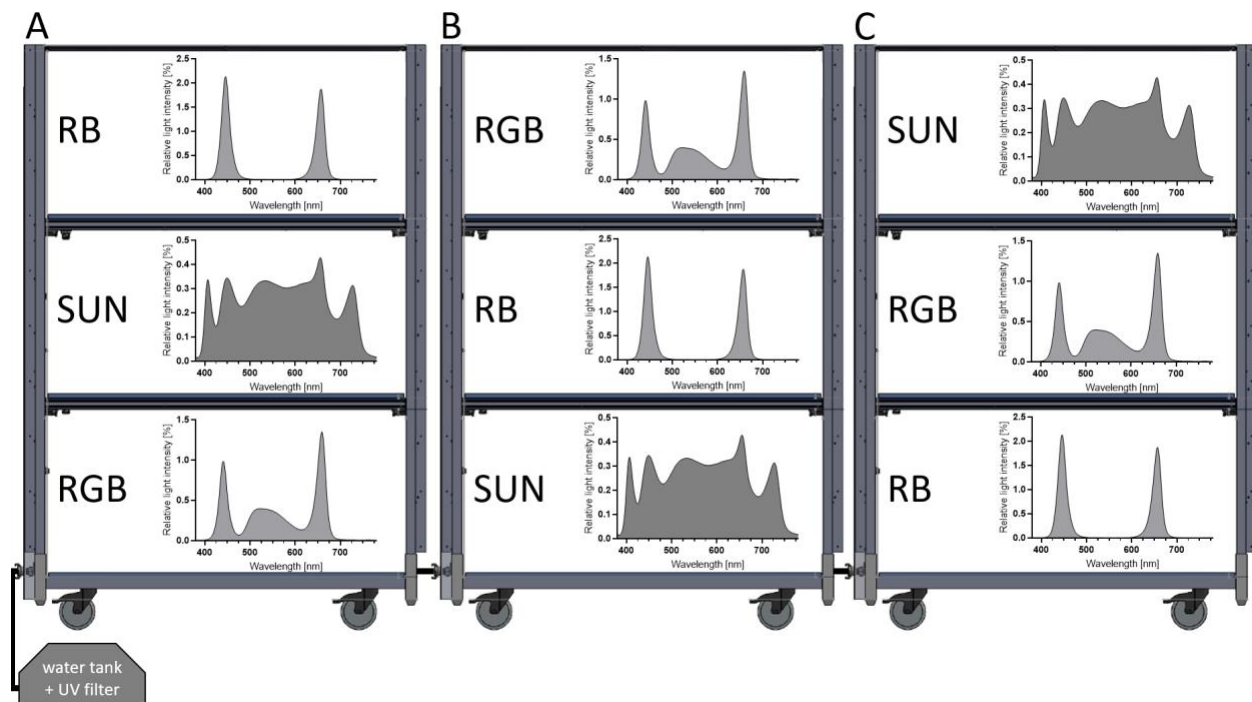


Figure 14 – Conceptual pictogram of the conducted LED light experiment. RB = Red/Blue LED light treatment, RGB = Red/Green/Blue LED light treatment, SUN = artificial sunlight treatment.¹

¹ Depicted are the three vertical cultivation systems (A-C) used during the experiments, which are connected to an automated water and nutrient supply system including a UV filter (bottom left). Each vertical cultivation system consists of three stacked cultivation layers. Each cultivation layer was fitted with a different light quality (RB, RGB, SUN) at equal light intensity (Please note the differently scaled y-axes in the depicted light spectra). 30 peppermint plants were grown in each cultivation layer resulting in 90 investigated plants per light quality during the LED light experiments.

To induce branching, the youngest (not fully developed) leaf pair of each peppermint was pinched on May 29th, 2019 (49 DOC). Daily, peppermints were automatically irrigated via submersion of plant pots from 9:00 to 9:15 a.m. Electrical conductivity (EC), oxygen content (O₂), pH and temperature (°C) of the water were analyzed with the multi-parameter measuring device WTW Multi3430 (Weilheim, Germany) twice a day on the first four consecutive days of the experiment ($n = 8$): EC = $553.5 \pm 28.4 \mu\text{S cm}^{-1}$, O₂ = $8.0 \pm 2.0 \text{ mg L}^{-1}$, pH = 7.6 ± 0.2 and °C = 22.2 ± 4.1 . After refilling the water tank on June 12th, 2019, the water was measured twice with the same device (EC = $735 \pm 3.55 \mu\text{S cm}^{-1}$, O₂ = $5.9 \pm 0.7 \text{ mg L}^{-1}$, pH = 7.5 ± 0.1 and °C = 25.6 ± 0.5). The same day, peppermints were fertilized with NPK (15-5-15) nutrient solution (Phytogrow) supplied by GND Solutions GmbH (Berlin, Germany) by diluting 75 g of fertilizer in the tank. As the fertilized water was reused daily by the automated watering system, the peppermints were fertilized daily until the end of the experiment (June 18th, 2019). Salinity measurements were conducted directly in moist pot substrates with an activity measuring instrument PNT 3000 (STEP Systems GmbH, Nuremberg, Germany) once before fertilization ($0.23 \pm 0.02 \text{ g L}^{-1}$) and four times (every other day) after fertilization (0.31 ± 0.02 , 0.30 ± 0.04 , 0.32 ± 0.03 , $0.35 \pm 0.03 \text{ g L}^{-1}$; measurements took place in two pots per light treatment and replication ($n = 18$) to assure optimal fertilization status. To eliminate aphids detected on May 27th, 2019, *Chrysoperla carnea* larvae ($n \sim 1,000$) and *Aphidius matricariae* ($n \sim 1,000$; recommended for 250 m²) supplied by Katzbiotech (Baruth, Germany) were applied on May 29th, 2019, and resulted in aphid elimination before June 11th 2019. Climatic conditions were continuously monitored at canopy level via data loggers (EL-USB-2, Lascar, CONRAD, Hirschau, Germany). Average temperatures (C° ± standard deviation) under RB, RGB and SUN were 25.6 ± 2.9 , 25.5 ± 2.8 and 25.5 ± 2.8 , with a measuring accuracy of ± 1 °C. Average humidities (%RH ± SD) under RB, RGB and SUN were 64.0 ± 7.0 , 67.1 ± 6.8 and 65.3 ± 6.9 with a measuring accuracy of 2.25 %RH. None of the climatic conditions differed between treatments. For control, genetically identical stolon segments of *Mentha x piperita* L. var. piperita cv. Multimentha were grown under field conditions.

2.3 Cultivation system

Each of the three LED cultivation systems was 1.85 m high and consisted of three shelves (124 × 55 × 60 cm). For automated ebb-and-flow-watering (and nutrient supply), the interconnected vertical LED cultivation systems were connected to a water tank with a capacity of 300 L. Before water entered back into the water tank for re-use, a UV-filter sterilized the back-flowing water after submersive irrigation was completed (Figure 14).

2.4 Lighting systems and illumination conditions

Two supplemental LED lighting systems from FUTURELED GmbH, Berlin, Germany (Apollo R1 and Lumitronics Air) were used to set up three spectral lighting conditions (RB = Red/Blue, RGB = Red/Green/Blue, SUN = artificial sunlight) at equal photon flux density (PFD). At start, all plants were illuminated with a PFD of $150 \mu\text{mol m}^{-2} \text{s}^{-1}$ (at plant pot level). Under exclusion of natural daylight, plants were subjected to LED lighting in a growth room from 6:00 a.m. to 10:00 p.m. for a daily photoperiod of 16 h during the experiment.

2.5 Irradiance measurements

Irradiance measurements were taken using a spectral PAR meter (PG200N, UPRtek, Aachen, Germany). Spectral composition, light intensities and photon distribution were measured and recorded at plant pot level under trial conditions prior to the experiment (Figure 15; Table 15).

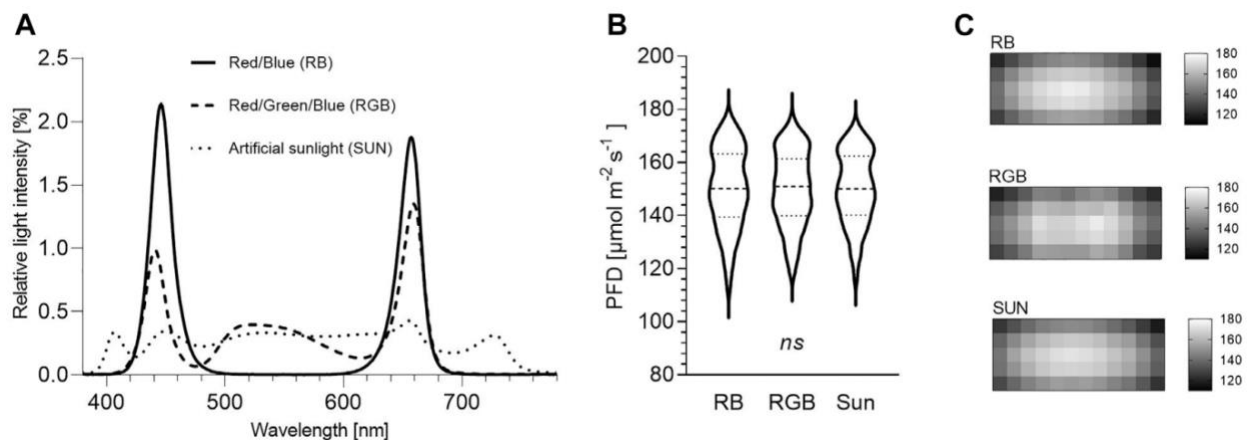


Figure 15 – Irradiance measurements of three light spectra between 380 and 780 nm at plant pot level. RB = Red/Blue, RGB = Red/Green/Blue, SUN = artificial sunlight spectra. **(A)** Relative spectral composition.¹ **(B)** Light intensity.² **(C)** Photon distribution.³

¹ Depicted are the relative light intensities [%] per wavelength [nm] between 380 and 780 nm of the RB, RGB and SUN light spectra used during the experiment.

² Presented are photon flux densities (PFD) [$\mu\text{mol m}^{-2} \text{s}^{-1}$] measured every 100 cm^2 within each cultivation shelf underneath RB, RGB and SUN light spectra ($n = 60$ per light spectra). The violin plot represents median (dashed line) and quartiles (dotted lines). Ordinary one-way ANOVA did not detect significant differences among means of light treatments ($p > 0.99$).

³ Visualized are light distribution patterns measured every 100 cm^2 within each cultivation shelf underneath RB, RGB and SUN light spectra ($n = 60$ per light spectra). Each heat map depicts the photon flux densities (PFD) [$\mu\text{mol m}^{-2} \text{s}^{-1}$].

Table 15 – Spectral composition of three LED light spectra and solar spectrum between 380 and 780 nm.

Parameter ¹	RB ²		RGB		SUN		Solar spectrum ³
	PFD ⁴	%	PFD	%	PFD	%	%
PFD (380-780nm)	150 ± 14.9	100 ± 9.9	150 ± 13.8	100 ± 9.2	150 ± 13.4	100 ± 8.9	100
PPFD (400-700nm)	149.1 ± 9.8	99.4 ± 9.9	148.8 ± 9.1	99.2 ± 9.2	125.9 ± 6.3	83.9 ± 7.5	80.5
UV (380-400nm)	0.15 ± 0.0	0.1 ± 0.0	0.15 ± 0.0	0.1 ± 0.0	1.2 ± 0.0	0.8 ± 0.1	2.5
B (400-500nm)	64.1 ± 2.8	42.7 ± 4.4	33 ± 0.8	22.0 ± 2.3	30.2 ± 0.5	20.1 ± 1.8	26.0
G (500-600nm)	0.8 ± 0.0	0.5 ± 0.0	46.8 ± 1.3	31.2 ± 2.8	45.3 ± 1.2	30.2 ± 2.7	28.2
R (600-700nm)	84.3 ± 4.7	56.2 ± 5.6	69 ± 2.9	46.0 ± 4.2	50.4 ± 1.5	33.6 ± 3.0	26.0
FR (700-780nm)	0.8 ± 0.0	0.5 ± 0.0	1.1 ± 0.0	0.7 ± 0.1	23 ± 0.3	15.3 ± 1.3	17.2
B:R ratio	~ 0.8		~ 0.5		~ 0.6		~ 1.0
B:G ratio	~ 80		~ 0.7		~ 0.7		~ 0.9
R:FR ratio	~ 105.4		~ 62.7		~ 2.2		~ 1.5

¹ PFD = photon flux density, PPFD = photosynthetic photon flux density, UV = ultraviolet, B = blue, G = green, R = red, FR, far-red, B:R = blue-to-red ratio, B:G = blue-to-green ratio, R:FR, red-to-far-red ratio.

² Light treatments: RB = Red/Blue, RGB = Red/Green/Blue, SUN = artificial sunlight spectra.

³ Terrestrial solar spectrum at global tilt (ASTM G173-03 Reference Spectra; data courtesy of the U.S. National Renewable Energy Laboratory (NREL 2020).

⁴ PFD presents mean photon flux density [expressed in $\mu\text{mol m}^{-2} \text{s}^{-1}$ and in percent (%)] \pm standard deviation from 60 measurements per light treatment within a cultivation shelf measured every 100 cm^2 .

The software package of the spectrometer (uSpectrum PC laboratory software) automatically calculated electromagnetic parameters including photon flux density (PFD in $\mu\text{mol m}^{-2} \text{s}^{-1}$) between 380 and 780 nm, photosynthetic photon flux density (PPFD in $\mu\text{mol m}^{-2} \text{s}^{-1}$) between 400 and 700 nm, amounts of ultraviolet (380–400 nm), blue (400–500 nm), green (500–600 nm), red (600–700 nm) and far-red (700–780 nm) radiation (in $\mu\text{mol m}^{-2} \text{s}^{-1}$) and the ratios of blue-to-green and red-to-far-red light. Additionally, red-to-blue light ratio was calculated.

2.6 Crop measurements and harvest

After the beginning of the light experiment, plant height (measured from top of soil to tip of apical bud) and number of leaf pairs (≥ 1 cm) were assessed weekly in 7-day intervals at 41, 48, 55, 62 and 69 days of culture (DOC). Side shoot lengths were also assessed weekly in 7-day intervals at 55, 62 and 69 DOC by continuously measuring the lengths of the first fully developed side branches. For data analysis, these two side branch measurements were averaged per peppermint plant. Before harvest on 69 DOC, four peppermint leaves from 10 randomly selected plants per replicate ($N = 90$, $n = 30$ per light treatment) were scanned (CanoScan LiDE 400) to measure the leaves' width and length via ImageJ software (Version 1.52a). Thereby, the first, third, fifth and seventh peppermint leaf from the apex was removed. Additionally, all 270 experimental peppermint plants were harvested separately under each treatment and replication to analyze the effects of treatments on biomass yields. Therefore, fresh matter of aerial plant parts was individually recorded at harvest and total dry matter was measured after drying the samples in a circulated drying oven at 30° C for ≤ 7 days until stable mass was attained (optimal drying method was chosen and standardized as it highly influences peppermints' EO yields (Beigi et al., 2018). After removal of shoots, leaf dry matter (L_{DM}) was determined for all plants. Dried leaf samples were vacuum-sealed (V.300®, Landig + Lava GmbH & Co. KG, Bad Saulgau, Germany) and stored in the dark at 4°C until further processing.

2.7 Essential oil isolation

Five gram of air-dried peppermint leaves (combining L_{DM} of three to four plant samples of the same spatial replication) were ground and hydrodistilled for 60 min using a clevenger-type apparatus. Volume (ml) of the isolated EO were recorded and stored at -70 °C in sealed glass vials for further processing. The EO volume was density-corrected according to the European Pharmacopoeia with factor 0.908 (Schmiedel 2008). EO content and yield, expressed on a dry weight basis, were calculated according to the following equations: EO content (%) = (distilled EO (g)/5 g) x 100; EO yield ($\text{mg g leaf dry matter}^{-1}$ (L_{DM})) = mean of

EO yield ($\text{mg g L}_{\text{DM}}^{-1}$) ($n = 8$ per spatial replication) \times total L_{DM} (g). To determine a possible influence of the temporary aphid infestation on the chemical composition of the monoterpenes, volatiles were extracted according to the procedure described in Tabbert et al., 2021.

2.8 GC-FID and GC-MS analysis

1 μl of EOs was diluted in isooctane (1:1,000) [containing 1: 40,000 (v/v) carvacrol as internal standard] and transferred into GC-vials. 3 μl of each sample was analyzed by GC-FID using an Agilent gas chromatograph 6890N fitted with an HP-Innowax column (30 m \times 250 μm \times 0.5 μm) in split mode (split ratio 10:1). Detector and injector temperatures were set to 250 $^{\circ}\text{C}$. The following oven temperature program was used: 50 $^{\circ}\text{C}$ for 2 min, heating from 50 to 210 $^{\circ}\text{C}$ at a rate of 3 $^{\circ}\text{C min}^{-1}$. The final temperature was held for 6 min. Hydrogen was used as carrier gas with a constant flow rate of 1.2 ml min^{-1} . GC-MS was performed using an Agilent 5,973 Network mass spectrometer, on an HP-Innowax column (see GC), operating at 70 eV ionization energy, using the same temperature program as above. Helium was used as carrier gas with a constant flow rate of 1.2 ml min^{-1} . Retention indices were calculated by using retention times of C7-C40-saturated alkanes (Merck KGaA, Darmstadt, Germany) that were injected under the same chromatographic conditions.

2.9 Identification and quantification of essential oil compounds

All main compounds of the EOs were identified by comparing their mass spectra with those of the National Institute of Standards and Technology (NIST) mass spectral library and confirmed by comparing their retention indices. Additionally, identification of 1-octen-3-ol, 1,8-cineole, 3-octanol, α -pinene, α -terpineol, β -caryophyllene, β -farnesene, β -myrcene, β -pinene, γ -terpinene, caryophyllene oxide, limonene, germacrene D, iso-menthone, linalool, menthofuran, menthol, menthone, menthyl acetate, neo-menthol, ocimene, piperitenone, piperitone, pulegone, sabinene, terpinen-4-ol and viridiflorol was affirmed by authentic reference materials (RMs) with a purity of at least 95%. For compounds not verified by RMs (*cis*-isopulegone, *trans*-isopulegone, δ -terpineol and *trans*-verbenol), accuracy of internal reference library identification was $\geq 78\%$. EO compounds were quantified based on the known concentration of the internal standard (carvacrol).

2.10 Statistical analysis

Statistical analyses were performed using GraphPad Prism 8.4.3.686 (San Diego, United States). Spectral light distribution data passed normality via D'Agostino & Pearsons omnibus normality test, and thus were

analyzed via ordinary one-way ANOVA ($p > 0.99$, not significant). Collected data sets of plant height, side branch length, total plant fresh and dry weight, leaf and shoot dry weight ($N = 270$, $n = 30$ peppermint plants per replication, respectively) as well as of leaf length and leaf area ($N = 90$, $n = 30$ peppermint plants per replication, respectively) and data sets of EO compounds as well as of EO contents ($N = 72$, $n = 8$ EOs per replication, respectively) and data sets of EO yields ($N = 9$, $n = 3$ per light treatment) of each spatial replication ($n = 3$) and light treatment ($n = 3$) were tested for normality via D'Agostino & Pearsons omnibus normality and Shapiro-Wilk test. If the normality test failed, outliers were identified via ROUT method ($Q \leq 10\%$) and removed to establish normality of all data sets. Plant height, side branch length, length and width of fresh leaves, EO compounds and contents: Nested one-way ANOVA was used to detect differences between light treatments (nested factor: spatial replications per light treatment ($n = 3$). When significant ($p \leq 0.05$), Tukey's multiple comparisons test at 95 % confidence interval was applied. Equal variances of data sets were visually checked by graphing homoscedasticity plots. Fresh matter, dry matter and leaf dry matter yields: Due to significant differences between spatial replications ($p \leq 0.05$), means of each spatial replication and light treatment ($N = 9$, $n = 3$ per light treatment) were used to conduct an ordinary one-way ANOVA. Number of leaf pairs: Means of each spatial replication per light treatment ($n = 3$) were analyzed via Kruskal–Wallis nonparametric test. (Additionally, amounts of main volatiles (menthone, pulegone, menthofuran) of uninfested and temporarily aphid-infested peppermint plants ($N = 58$) were compared via unpaired t-test and did not differ ($p \geq 0.8$), ruling out an influence of aphids on EO composition.)

3. Results

3.1 Plant height

After 2 weeks, peppermint grown under SUN and RGB exceeded plant heights reached under RB ($p = 0.03$ respectively), averaging 19.4 ± 1.0 , 22.2 ± 0.6 and 23.5 ± 1.6 cm under RB, RGB and SUN, respectively. With average plant heights of 33.0 ± 0.7 and 34.5 ± 1.3 cm, peppermints grown under RGB and SUN were significantly taller than peppermints grown under RB (27.2 ± 1.2 cm) after 3 weeks of cultivation ($p = 0.01$). Difference in plant height further increased between aforementioned light spectra after 4 weeks of the experiment ($p \leq 0.01$). While peppermints grown under RGB and SUN reached average plant heights of 44.2 ± 1.0 and 47.0 ± 0.3 cm respectively, peppermints grown under RB remained significantly shorter with average heights of 35.1 ± 1.2 cm (Figure 16A).

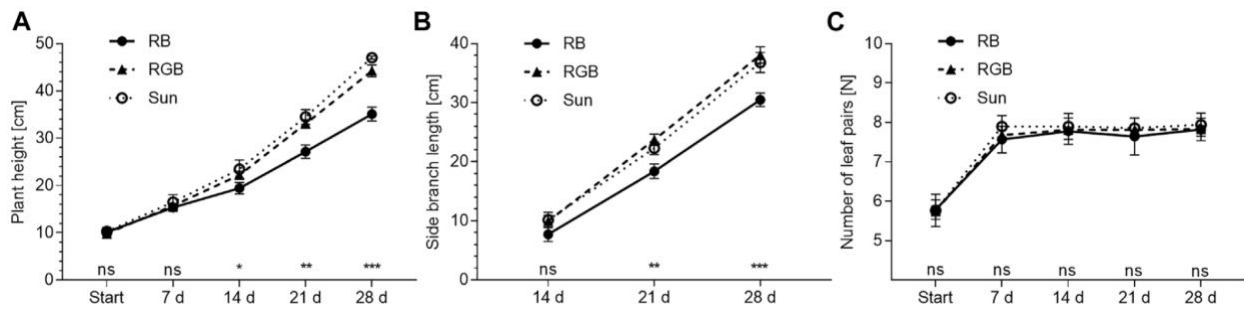


Figure 16 – Morphological characteristics of *Mentha x piperita* var. *piperita* cv. *Multimentha* as effected by light spectra over time. RB = Red/Blue, RGB = Red/ Green/Blue, SUN = artificial sunlight spectrum. **(A)** Plant height.¹ **(B)** Side branch length.¹ **(C)** Number of leaf pairs.²

¹ Presented are mean plant heights and side branch lengths of three independent spatial replications ($n = 3$) \pm standard deviation (SD) of 25–30 assessed peppermint plants per spatial replication and light treatment (N of plant height = 267; N of side branch length = 253). Significant differences between light treatments were determined according to nested one-way ANOVA (*: $p \leq 0.05$, **: $p \leq 0.01$, ***: $p \leq 0.001$, ns: not significant) followed by Tukey's multiple comparison test at 95 % confidence level.

² Presented are mean numbers of leaf pairs of three independent spatial replications ($n = 3$) \pm SD of 30 assessed peppermint plants per spatial replication and light treatment ($N = 270$). Nonparametric Kruskal–Wallis tests ($p \geq 0.9$) were used to test for significant differences between light treatments (ns: not significant) at each time point.

3.2 Branch Length

Three weeks after start of the experiment, side branches were elongated under RGB and SUN as compared to branches grown under RB ($p = 0.01$ respectively). Branch lengths under RGB, SUN and RB averaged 23.7 ± 0.8 , 22.3 ± 0.9 and 18.4 ± 1.0 cm. After 4 weeks, differences in branch elongation further increased ($p \leq 0.01$) between RB- and RGB-illuminated as well as between RB- and SUN-illuminated plants, and averaged 30.5 ± 0.9 , 38.1 ± 1.1 and 36.8 ± 1.4 cm under RB, RGB and SUN respectively (Figure 16B).

3.3 Number of leaf pairs

Number of fully developed leaf pairs along the stem did not differ between peppermints illuminated with RB, RGB or SUN light spectra ($p \geq 0.44$). While all plants averaged six fully developed leaf pairs at the beginning of the experiment, the peppermints averaged eight leaf pairs along the main stem for the remaining study time (Figure 16C).

3.4 Length and width of leaves

The top leaves of the peppermint canopy were affected by light treatment (Figure 17). Top leaves under RB were shorter (6.8 ± 0.1 cm) and narrower (4.4 ± 0.2 cm) than those under RGB (length = 7.4 ± 0.1 cm, width = 5.1 ± 0.1 cm) ($p \leq 0.001$, $p \leq 0.01$ respectively). Similarly, length and width of top leaves under RB

remained shorter and narrower than under SUN (length = 7.3 ± 0.2 cm, width = 4.9 ± 0.1 cm) ($p \leq 0.01$, respectively). Clearly, no differences in peppermint leaves' length and width between top leaves under RGB und SUN light spectra were detected ($p \geq 0.72$). Leaves deeper within the canopy remained indifferent in size after light treatment ($p \geq 0.13$).

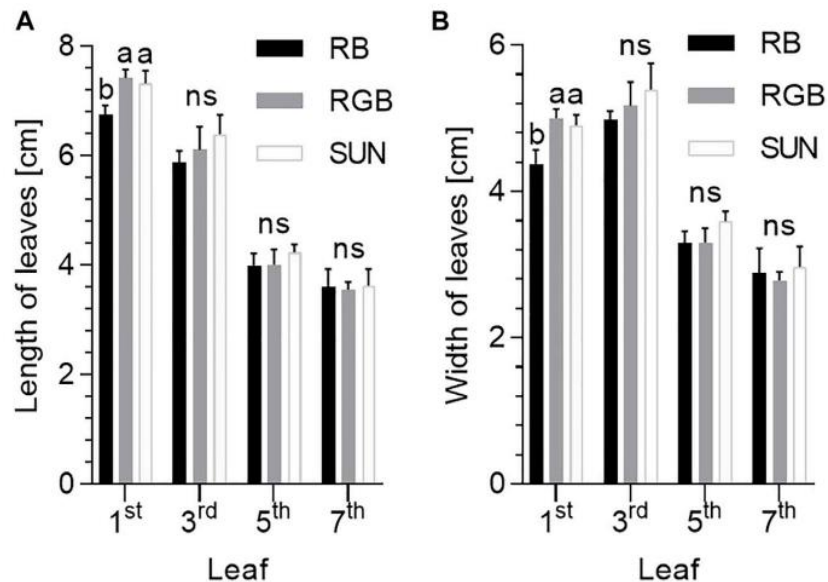


Figure 17 – Length and width of fresh leaves of *Mentha x piperita* var. *piperita* cv. *Multimentha* as effected by different light spectra. RB = Red/Blue, RGB = Red/ Green/Blue, SUN = artificial sunlight spectrum, first, third, fifth and seventh leaf on x-axes represent measurements of the top leaf (first) to the bottom leaf (seventh) along the shoot. **(A)** Length of peppermint leaves as effected by light treatment ($N = 74-89$, $n = 5-10$ leaves per spatial replication and light treatment).¹ **(B)** Width of peppermint leaves as effected by light treatment ($N = 74-89$, $n = 5-10$ leaves per spatial replication and light treatment).¹

¹ For each leaf position (1–4), significant differences between light treatments were determined according to nested one-way ANOVA test (*ns*: not significant). When significant differences were determined, Tukey's multiple comparisons test followed (different letters indicate significant differences between light treatments at 95 % confidence level).

3.5 Biomass yields

Total fresh and dry matter yields of peppermints cultivated under RB, RGB and SUN light spectra did not differ at the end of the experiment ($p = 0.76$ and $p = 0.87$, respectively). On average, peppermints under RB, RGB and SUN accumulated a fresh weight of 31.7 ± 7.0 , 32.7 ± 6.2 and 30.1 ± 6.5 g per plant, respectively (Figure 18A). Dry weights per plant under the same light spectra (RB, RGB, SUN) averaged 3.5 ± 0.9 , 3.5 ± 0.7 and 3.4 ± 0.9 g per plant (Figure 18B). No differences in total leaf dry matter per plant was observed ($p = 0.20$), averaging 2.0 ± 0.4 , 1.9 ± 0.4 and 1.7 ± 0.4 g per plant for RB-, RGB- and SUN-treated peppermints (Figure 18C).

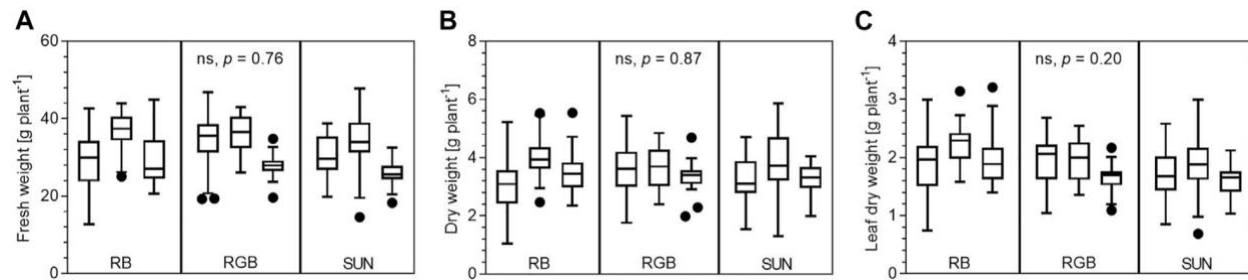


Figure 18 – Biomass yields of *Mentha x piperita* var. *piperita* cv. *Multimentha* as effected by different light spectra. RB = Red/Blue, RGB = Red/Green/Blue, SUN = artificial sunlight spectrum. **(A)** Fresh matter yields in gram plant⁻¹ per light spectra and spatial replication ($N = 269$).¹ **(B)** Dry matter yields in gram plant⁻¹ per light spectra and spatial replication ($N = 270$).¹ **(C)** Leaf dry matter in gram plant⁻¹ per light spectra and spatial replication ($N = 266$).¹

¹ Presented are minimum, 25th percentile, median, 75th percentile and maximum yields as well as outliers (black dots) of all assessed peppermint plants per light treatment and spatial replication ($n = 29$ – 30 plants per replication). Ordinary one-way ANOVA with the means of each spatial replication was used to test for significant differences between light treatments (ns : not significant).

3.6 Composition, content and yield of essential oil

Analysis of peppermint oils enabled the identification of 24 EO compounds (Table 16). While EO yields remained unaffected, EO compositions significantly differed between the light treatments applied. While desired percentages of menthone and iso-menthone as well as piperitone and piperitenone were significantly greater under the SUN and RB light treatment, the percentages of the undesired compounds pulegone and menthofuran were significantly greater in peppermints grown under the RGB light treatment. Further, all LED light treated plants are characterized by an atypical EO composition for *Mentha x piperita* var. *piperita* cv. *Multimentha* when compared to its common EO composition detected under field conditions (Table 17; Schulz et al., 1999; Schulz and Krüger, 1999; Das Bundessortenamt, 2002; Pank et al., 2013). With pulegone and menthofuran as the dominating EO components (and only small amounts of menthone and menthol) detected under all three LED light conditions, their EO compositions differ significantly from the typically menthone and menthol enriched EOs of this cultivar under field conditions.

Table 16 – Effect of three light qualities on the chemical composition of 24 identified essential oil compounds, essential oil content and yield of *Mentha x piperita* var. *piperita* cv. *Multimentha*.

No.	Compound	RI Samples ¹	Identification	RB	RGB	SUN	p-value ²
				Percent (%) of total essential oil composition ³			
1	α -Pinene	1030	RM, MS	0.45 ± 0.03 ^a	0.48 ± 0.04 ^b	0.45 ± 0.06 ^{ab}	0.03
2	β -Pinene	1120	RM, MS	0.73 ± 0.03 ^a	0.77 ± 0.04 ^b	0.73 ± 0.06 ^a	0.01
3	Sabinene	1132	RM, MS	0.38 ± 0.02 ^a	0.40 ± 0.02 ^b	0.40 ± 0.03 ^{ab}	0.01
4	β -Myrcene	1175	RM, MS	0.42 ± 0.03 ^a	0.45 ± 0.03 ^b	0.45 ± 0.04 ^b	0.02
5	Limonene	1212	RM, MS	0.36 ± 0.06	0.42 ± 0.06	0.44 ± 0.06	0.06 (ns)
6	1,8-Cineole	1221	RM, MS	2.52 ± 0.18	2.54 ± 0.19	2.49 ± 0.23	0.91 (ns)
7	<i>Trans</i> - β -Ocimene	1248	RM, MS	0.15 ± 0.02	0.13 ± 0.02	0.14 ± 0.02	0.16 (ns)
8	3-Octanol	1404	RM, MS	0.18 ± 0.03	0.17 ± 0.02	0.16 ± 0.02	0.16 (ns)
9	Menthone	1480	RM, MS	26.57 ± 3.14 ^a	19.72 ± 3.94 ^b	28.87 ± 3.53 ^a	< 0.01
10	Menthofuran	1502	RM, MS	16.90 ± 1.25 ^{ab}	18.19 ± 1.06 ^a	15.20 ± 1.92 ^b	0.02
11	Iso-Menthone	1508	RM, MS	1.75 ± 0.18 ^a	1.39 ± 0.20 ^b	1.96 ± 0.21 ^a	< 0.01
12	Linalool	1561	RM, MS	0.26 ± 0.03	0.28 ± 0.03	0.33 ± 0.04	0.06 (ns)
13	<i>Cis</i> -Isopulegone	1591	MS	0.64 ± 0.08	0.75 ± 0.10	0.60 ± 0.08	0.07 (ns)
14	<i>Trans</i> -Isopulegone	1603	MS	0.38 ± 0.02	0.37 ± 0.02	0.37 ± 0.02	0.12 (ns)
15/16	β -Caryophyllene & Neo-Menthol	1611 1615	RM, MS RM, MS	1.09 ± 0.29 ^{ab}	0.89 ± 0.27 ^a	1.33 ± 0.32 ^b	0.05
	Menthol	1654	RM, MS	1.21 ± 0.31	0.85 ± 0.26	1.05 ± 0.25	0.07 (ns)
18	Pulegone	1665	RM, MS	43.06 ± 3.42 ^a	49.72 ± 4.36 ^b	41.41 ± 3.25 ^a	< 0.01
19	δ -Terpineol	1687	MS	0.16 ± 0.02	0.15 ± 0.02	0.17 ± 0.03	0.24 (ns)
20	<i>Trans</i> -Verbenol	1693	MS	0.09 ± 0.06	0.11 ± 0.04	0.09 ± 0.06	0.30 (ns)
21	α -Terpineol	1712	RM, MS	0.15 ± 0.01	0.17 ± 0.01	0.17 ± 0.01	0.06 (ns)
22	Germacrene D	1724	RM, MS	0.95 ± 0.27 ^{ab}	0.79 ± 0.29 ^a	1.12 ± 0.26 ^b	0.05
23	Piperitone	1745	RM, MS	0.24 ± 0.04 ^a	0.17 ± 0.04 ^b	0.26 ± 0.05 ^a	< 0.01
24	Piperitenone	1941	RM, MS	0.24 ± 0.03 ^a	0.26 ± 0.03 ^{ab}	0.27 ± 0.03 ^b	< 0.01
TOTAL [%] ⁴				98.89 ± 0.34	99.19 ± 0.45	98.66 ± 1.03	
EO content [%] ⁵				3.21 ± 0.55	3.20 ± 0.54	3.21 ± 0.55	0.99 (ns)
EO yield [mg shelf ⁻¹] ⁶				65.45 ± 9.63	59.85 ± 6.78	55.83 ± 8.37	0.42 (ns) ⁷

RI = Retention index, RM = Reference material, MS = Mass spectra, RB = Red/Blue, RGB = Red/Green/Blue, SUN = artificial sunlight spectrum

¹ Presented are mean RIs of samples under GC-FID conditions (deviation of RIs under GC-MS conditions were ≤ 0.5 %).

² Significant differences between light treatments were determined according to nested one-way ANOVA test (*ns* = not significant). When significant, Tukey's multiple comparisons test followed (different letters within a row indicate significant differences between light treatments at 95 % confidence interval) ($N = 72$, $n = 8$ essential oils per spatial replication and light treatment).

³ Presented are mean percentages of essential oil compounds \pm their standard deviations of all analyzed peppermint oils per light treatment ($N = 72$, $n = 24$ essential oils per light treatment).

⁴ Percentage represents total of identified compounds. (Traces of eight unidentified and traces of ten identified compounds (namely γ -Terpinene (RI 1258, RM, MS (90%)^{1,2}), 1-Octen-3-ol (RI 1463, RM, MS (42%)), Methyl acetate (RI 1578, RM, MS (76%)), Terpinen-4-ol (RI 1618, RM, MS (96%)), *Trans*- β -Farnesene (RI 1679, RM, MS (42 %)), Isopiperitenone & Carvone (co-eluded: MS (38%) and MS (59%) respectively), Caryophyllene oxide (RI 1999, RM, MS (41%)), Viridiflorol (RI 2098, RM, MS (93%)), Spathulenol (RI 2141, MS (86%))) are excluded from the table.)

⁵ EO content = Essential oil content; percentage (%) is based on hydro-distilled leaf dry matter (w/w).

⁶ EO yield = Essential oil yield; EO yield represents the calculated essential oil (mg) per shelf (0.6 m²).

⁷ Significant differences between light treatments were determined according to ordinary one-way ANOVA test (*ns* = not significant) ($N = 9$, $n = 3$ per light treatment).

Table 17 – Essential oil composition of *Mentha x piperita* L. var. *piperita* cv. *Multimentha*¹ detected under field conditions at Julius Kühn Institute, Berlin, Germany².

No.	Compound	RI Samples ³	Percent (%) of total EO composition ⁴
1	α -Pinene	1028	0.34 \pm 0.07
2	β -Pinene	1116	0.51 \pm 0.06
3	Sabinene	1129	0.33 \pm 0.03
4	β -Myrcene	1174	0.38 \pm 0.04
5	Limonene	1209	0.41 \pm 0.18
6	1,8-Cineole	1216	3.13 \pm 0.35
7	<i>Trans</i> - β -Ocimene	1246	0.50 \pm 0.06
8	3-Octanol	1406	0.32 \pm 0.02
9	Menthone	1476	51.53 \pm 4.40
10	Menthofuran	1497	2.42 \pm 0.90
11	Iso-Menthone	1503	3.83 \pm 0.01
12	Linalool	1563	0.23 \pm 0.06
13/14	β -Caryophyllene &	1611	2.57 \pm 0.33
	Neo-Menthol	1615	
15	Menthol	1655	25.78 \pm 5.01
16	Pulegone	1659	1.33 \pm 0.89
17	Germacrene D	1717	1.32 \pm 0.07
18	Piperitone	1739	1.30 \pm 0.14
TOTAL [%] ⁵			96.22 \pm 0.003

RI = Retention index, EO = Essential oil.

¹ The field-grown peppermint is genetically identical to the *Mentha x piperita* L. var. *piperita* cv. *Multimentha* used during the LED light experiment.

² The test site is located at 52.5°N, 13.3°E and 45 meters above sea level. The soil (loamy sand with partly chromic luvisols over a thick layer of clay in two-meter depth) has a soil quality of 36-46 ground points. The average annual temperature and precipitation are 8.8 °C and ~600 millimeters, respectively.

³ Presented are mean RIs of samples under GC-FID conditions (deviation of RIs under GC-MS conditions were \leq 0.72 %).

⁴ Presented are mean percentages of essential oil compounds \pm their standard deviations of four analyzed peppermint oils grown under field conditions at Julius Kühn Institute, Berlin, Germany.

⁵ Percentage represents total of identified compounds (traces of eight unidentified and traces of ten identified compounds, namely γ -terpinene (RI 1256), *cis*-3-hexenal (RI 1400), β -bourbonene (RI 1526), methyl acetate (RI 1574), β -elemene (RI 1605), terpinen-4-ol (RI 1617), neo-iso-menthol (RI 1644), δ -terpineol (RI 1687), bicyclogermacrene (RI 1743) and viridiflorol (RI 2096) are excluded from the table).

4. Discussion

As known from recent studies on the impact of G wavelengths inducing stem elongations and leaf expansions in basil and tomato (Kaiser et al., 2019; Schenkels et al., 2020), RB resulted in a compact peppermint growth, whereas both G-containing light conditions induced stem and side branch elongations as well as significant expansion of top leaves in *Mentha x piperita*. Contrary to our expectations, these profound morphological differences were not accompanied with biomass and EO yield increases at the time of harvest. However, the broad SUN spectrum as well as the RB spectrum significantly affected the

composition of the EOs by accelerating the reduction of pulegone to menthone (and iso-menthone), representing an important quality-determining transformation step during menthol biosynthesis.

4.1 Plant height

It is well documented that B light inhibits hypocotyl growth and stem elongation (Sellaro et al., 2010; Pedmale et al., 2016), independent of different R light proportions (Hernandez and Kubota 2016; Spalholz et al., 2020). These observations coincide with our findings as the peppermints developed a more compact phenotype under RB in comparison to RGB and SUN. To the contrary, low B/G ratios as well as low R/FR ratios are both independently known to elongate stems in a variety of plants, representing a typical plant adaptation known as shade avoidance symptom in order to increase light capture (Franklin 2008; Zhang et al., 2011; Smith et al., 2017). For example, G induced extreme stem and branch elongations under low B/G ratios in *Arabidopsis*, basil, tomato and different lettuce cultivars (Sellaro et al., 2010; Zhang et al., 2011; Kaiser et al., 2019; Schenkels et al., 2020; Spalholz et al., 2020). Also, low R/FR ratios have been reported to induce stem elongations e.g. in *Arabidopsis*, basil and squash (Yang et al., 2012; Carvalho et al., 2016; Pedmale et al., 2016). In our study however, the excessive stem and side branch elongations detected under RGB and SUN compared to RB are likely a result of the high G fluence rates the peppermints were exposed to (likely by strongly stimulating the expression of hypocotyl growth-promoting genes as proposed by Pedmale et al., 2016). That the supplied FR light under SUN had no additional stem- or branch-elongating effect on the peppermints when compared to RGB lacking FR can be attributed to the specific R/FR ratio of 2.2 used in our study. Based on the phytochrome-mediated model, the SUN-treated peppermints absorbed more R than FR photons. Thus, the involved phytochrome-photoreceptor (PhyB) remained in its active R-absorbing form, which restricts elongation (by inhibiting phytochrome-interacting factor (PIF) activity required for the biosynthesis of the elongation-promoting phytohormone auxin (Frankhauser and Batschauer 2016)).

4.2 Leaf growth and expansion

Peppermint leaves of the upper canopy level (first to third leaf pairs from the top) reached lengths between 5.7 and 7.5 cm under all light treatments, which represents the upper size range described for peppermint. As reviewed by Mahendran and Rahman (2020), leaves of *Mentha x piperita* L. are usually between 2 and 7 cm long. This indicates leaf expansion responses due to the light treatments applied, and represents another typical shade avoidance response of the young peppermints (Franklin 2008; Zhang et al., 2011; Smith et al., 2017).

Furthermore, significant treatment differences were observed on the fully expanded top leaves, as the peppermints' top leaves under RGB and SUN were significantly longer and wider than the top leaves exposed to RB. This outcome is in agreement with multiple studies that reported increased leaf areas when RB spectra were either partially replaced with G light or compared to broad white lighting conditions for a variety of plant species (Zhang et al., 2011; Lin et al., 2013; Carvalho et al., 2016; Kaiser et al., 2019; Schenkels et al., 2020; Spalholz et al., 2020). Thus, the greater leaf expansions detected under RGB and SUN compared to expansions detected under RB can be attributed to the low B/G ratios supplied by RGB and SUN.

To investigate, if the leaf expansions also take place deeper within the canopy of the peppermints, we additionally measured the lengths and widths from the third, fifth and seventh leaf pair underneath. Contrary to our expectation, an increase in leaf size under the G-containing light treatments deeper within the canopy (as G can penetrate deeper into leaves and canopies than R and B (Smith et al., 2017; Saengtharatip et al., 2020; Schenkels et al., 2020)) was not observed.

4.3 Biomass accumulation

G has the potential to drive photosynthesis more effectively than R and B by increasing carbon fixation under PPFs greater than $200 \mu\text{mol m}^{-2} \text{s}^{-1}$ in spinach leaves (Terashima et al., 2009). Thus, scientists increasingly recommend the investigation and implementation of G light in order to increase biomass accumulations and yields under LED-based lighting systems (Folta 2004; Smith et al., 2017). However, studies describing yield increases due to incorporation of G light are scarce and were only focused on a few plant species (Novičkovas et al., 2012; Lin et al., 2013; Schenkels et al., 2020). For other plants, biomass increases were not observed (Spalholz et al., 2020), supporting our findings. Neither the peppermints' excessive stem elongations nor the partial leaf expansions in the upper canopy observed in our study resulted in significant increases of fresh or dry mass accumulations during the peppermints' early vegetative phase in the automated vertical cultivation system.

Most likely, the received light intensity as well as the early time of harvest constrained the detection of possible differences in biomass yields. However, it is also possible that the high variabilities in the light distribution patterns within each cultivation shelf (as depicted in Figures 15B,C) increased the variance of biomasses per plant and thus, hindered the detection of statistical effects.

4.4 Essential oil

Peppermints' EO content increases rapidly with leaf development and reaches its maximum when the leaf is fully expanded. Thus, EO formation of peppermint is under pronounced endogenous control (Gershenzon et al., 2000; McConkey et al., 2000). As the peppermints' leaf development as well as biomasses remained indifferent between the light qualities, it was not surprising that total EO yields remained unaffected under the applied light treatments.

Nevertheless, the light treatments significantly influenced the composition of the obtained EOs. The biosynthetic pathway of the quality-determining EO constituent menthol is characterized by a series of well-described transformation reactions (Croteau et al., 2005). With percentages of 41–50 % and 20–29 %, pulegone and menthone are the two main EO constituents detected during the early vegetative phase of *Mentha x piperita* L. in our study, and represent the last two central intermediates during menthol biosynthesis. The metabolite pulegone becomes reduced to menthone by pulegone reductase. To a smaller extent, the same enzyme reduces pulegone to iso-menthone. Then, menthone and iso-menthone are finally reduced to menthol and iso-menthol by menthone reductase (Croteau et al., 2005). As percentages of pulegone decreased and percentages of menthone and iso-menthone significantly increased under RB and SUN, our results indicate an accelerated conversion of pulegone to menthone and iso-menthone in comparison to RGB.

As R light has been shown to promote EO content in *Mentha x piperita* (Sabzalian et al., 2014), the accelerated conversion detected under RB may be explained by the elevated R fluence rate in comparison to the rate of R supplied by the RGB treatment during the trial period. However, as the amounts of R, B and G light between RGB and SUN were almost identical, the flanking regions including UV-A and/or FR light must have contributed to the enhanced conversion from pulegone to menthone (and iso-menthone) under SUN as well. As FR light actually suppresses terpene production (Tanaka et al., 1989; Yamaura et al., 1991), and partially reduces volatile emissions under low R/FR ratios (Kegge et al., 2013), it appears that the FR light fraction under the SUN treatment (with a high R/FR ratio) was not involved in the observed maturation process. Thus, the SUNs' proportion of UV-A must have expedited the conversion under our experimental conditions, which is further supported by findings of Behn et al. (Behn et al., 2010), who reported an accelerated monoterpene transformation during flowering of *Mentha x piperita* exposed to low solar radiation including UV-B (as compared to low solar radiation excluding UV-B).

With a percentage of 15–18 %, menthofuran is the third most abundant EO component detected under all supplied light qualities. As menthofuran synthesis represents a diversion from the desired

menthol biosynthetic pathway at the branch point metabolite pulegone (Croteau et al., 2005), all three light treatments severely reduced menthol production potential.

According to the European Pharmacopoeia (Schmiedel 2008), the detected percentages of pulegone (41–50 %) and menthofuran (15–18 %) highly exceeded the legal limits of 4 and 9 %, as both compounds have shown to be hepatotoxic (Malekmohammad et al., 2019). As menthofuran and pulegone productions have been shown to be favored under continuous low light intensities and short day lengths (Burbott and Loomis 1967; Clark and Menary 1980; Voirin et al., 1990; Croteau et al., 2005), the low light intensities at the bottom of the shelves received by the peppermints ($\sim 200 \mu\text{mol m}^{-2} \text{s}^{-1}$) were far too low for obtaining an EO of desired compositional quality. As shown in Figure 19, LED light intensities decrease tremendously with increasing distance to the LED light source (e.g., light intensity 5 cm from the light source: $\sim 1,150 \mu\text{mol m}^{-2} \text{s}^{-1}$; light intensity 10 cm from the light source: $\sim 650 \mu\text{mol m}^{-2} \text{s}^{-1}$). Thus, most of the plant was cultivated under low light intensities of $\geq 150 \mu\text{mol m}^{-2} \text{s}^{-1}$. As our results indicate, these light intensities lead to the divergence from and incompleteness of menthol biosynthesis and thus—from a consumer safety perspective—to non-marketable peppermint plants. The drastically increasing light intensity (up to $\sim 1,200 \mu\text{mol m}^{-2} \text{s}^{-1}$) with decreasing plant distance to the LED light source in the vertical cultivation system could not change the direction of the biosynthetic pathway during the trial period. The impact of these steep light intensity gradients of LED systems needs to receive more attention in future plant-dependent light studies, including a stronger focus on EO composition. So far, most published studies addressing the effects of LED lighting on plant performance have focused on morphological traits and EO contents, however, as shown in this study, the complex interaction of LED light spectrum and intensity also affect the composition of EOs—a research question that has received too little attention yet.

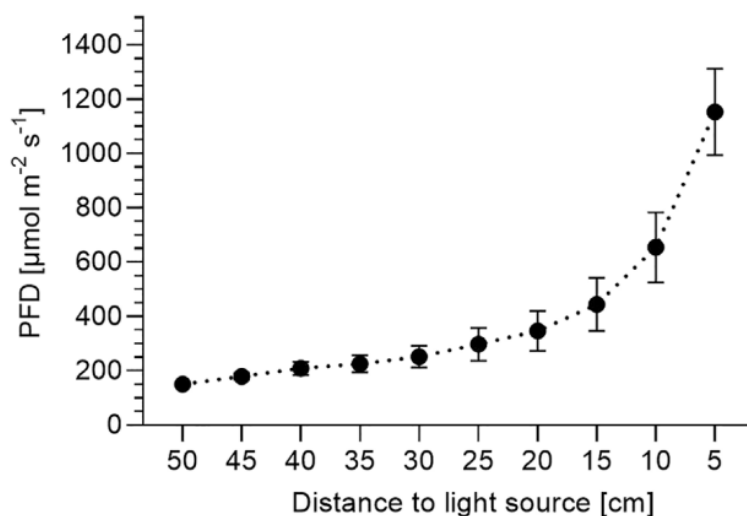


Figure 19 – Photon flux density depending on distance to light source.

Presented are average photon flux densities (PFD) [$\mu\text{mol m}^{-2} \text{s}^{-1}$] \pm SD between 380 and 780 nm recorded in 5 cm intervals starting at plant pot level 50 cm from the light source) from nine representative positions across the cultivation shelf per light treatment ($N = 27$) at each distance.

5. Conclusion

Despite substantial light intensity increases with decreasing distance to LED-light sources in the vertical cultivation systems (up to $\sim 1,200 \mu\text{mol m}^{-2} \text{s}^{-1}$), the G-containing treatments RGB and SUN with their low B/G ratios induced such excessive stem and branch elongations, that peppermint cultivation remained constrained to the vegetative phase. In contrast, RB with its high B fluence rate induced compact growth (appropriate for prolonged space-limited cultivation of peppermint). The impact of G light on peppermints' stem and branch elongation in this study has been shown for the first time and thus, supports the G-induced elongations revealed recently in other plant species. Further, our study supports the potential of G light to induce leaf expansions as recently shown by other authors. However, the expected leaf expansion deeper within the canopy was not observed in the young peppermint plants at the time of harvest. In the future, further trials with more mature peppermint plants and thus with more mature leaves deeper within the canopy should be conducted, in order to assess the G light potential for leaf expansions deeper within the canopy. The extreme elongations and partial leaf expansions did not result in the expected biomass and EO yield increases, and may again be attributed to the short trial period due to the peppermints' excessive stem elongations in the vertical cultivation system.

Further, the pronounced vertical loss of light intensity in the vertical cultivation system resulted in insufficient photosynthetic conditions and crucially determined the direction of monoterpene transformation reactions in peppermint. The low light intensities led to unwanted high pulegone contents and triggered the undesired synthesis of menthofuran under all light qualities. Thus, the light intensities perceived by the peppermint plants are not suitable for obtaining peppermint oil of quality as specified by the European Pharmacopoeia. Nevertheless, R as well as UV-A represent promising spectral light regions for accelerating the peppermints' EO maturation process as reductions of pulegone to menthone appeared significantly enhanced.

Subsequent studies with light intensities near the light saturation point of peppermint should be conducted, with special emphasis on high proportions of R, B and UV-A. Further fundamental studies, including the impact of specific G narrow wavebands, of G light at different PPFDs and of different B/G and R/G ratios are necessary to improve horticultural applicability of G light. In addition, uniformity of LED light distribution patterns remains a focal point for technical improvements to ensure uniform plant growth in vertical cultivation systems.

Facing energy limitations – approaches to increase basil (*Ocimum basilicum* L.) growth and quality by different increasing light intensities emitted by a broadband LED spectrum (400-780 nm)

Abstract: Based on the current trend towards broad-bandwidth LED light spectra for basil productions in multi-tiered controlled-environment horticulture, a recently developed white broad-bandwidth LED light spectrum (400-780 nm) including far-red wavelengths with elevated red and blue light fractions was employed to cultivate basil. Four *Ocimum basilicum* L. cultivars (cv. Anise, cv. Cinnamon, cv. Dark Opal and cv. Thai Magic) were exposed to two different rising light intensity conditions (I_{Low} and I_{High}). In dependence of the individual cultivar-specific plant height increase over time, basil cultivars were exposed to light intensities increasing from ~ 100 to $\sim 200 \mu\text{mol m}^{-2} \text{s}^{-1}$ under I_{Low} , and from 200 to $400 \mu\text{mol m}^{-2} \text{s}^{-1}$ under I_{High} (due to the exponential light intensity increases with decreasing proximity to the LED light fixtures). Within the first experiment, basil's morphological developments, biomass yields and time to marketability under both light conditions were investigated and the energy consumptions were determined to calculate the basil's light use efficiencies. In detail, cultivar-dependent differences in plant height, leaf and branch pair developments over time are described. In comparison to the I_{Low} light conditions, I_{High} resulted in accelerated developments and greater yields of all basil cultivars and expedited their marketability by 3-5 days. However, exposure to light intensities above $\sim 300 \mu\text{mol m}^{-2} \text{s}^{-1}$ induced light avoidance responses in the green-leafed basil cultivars cv. Anise, cv. Cinnamon and cv. Thai Magic. In contrast, I_{Low} resulted in consumer-preferred visual qualities and greater biomass efficiencies of the green-leafed basil cultivars and are discussed as a result of their ability to adapt well to low light conditions. Contrarily to the green-leafed cultivars, purple-leafed cv. Dark Opal developed insufficiently under I_{Low} , but remained light-tolerant under I_{High} , which is related to its high anthocyanin contents. In a second experiment, cultivars' volatile organic compound (VOC) contents and compositions over time were investigated. While VOC contents per gram of leaf dry matter gradually decreased in purple-leafed cv. Dark Opal between seedling stage to marketability, their contents gradually increased in the green cultivars. Regardless of the light treatment applied, cultivar-specific VOC compositions changed tremendously in a developmental stage-dependent manner.

Keywords: light-emitting diode (LED), morphology, essential oil, volatile organic compound (VOC), energy use efficiency (EUE)

1. Introduction

Basil (*Ocimum basilicum* L.) is by far one of the most popular culinary herbs worldwide and is highly appreciated for its medicinal and aromatic properties. As reviewed by Filip (2017), basil essential oils have antiviral, antioxidant, anti-inflammatory, antidiabetic and antimicrobial properties. Prominent levels of phenolic acids (Jayasinghe et al., 2003; Kwee and Niemeyer, 2011), as well as substantial amounts of anthocyanins found specifically in purple basil varieties (Flanigan and Niemeyer, 2014) further contribute to basil's potent antioxidant capacities. Besides its health-promoting properties, basil is cherished for its distinct aroma and pleasant taste. Within the species, some of the most important aroma compounds are 1,8-cineole, linalool, β -caryophyllene, estragole (methyl chavicol), eugenol, methyl eugenol and methyl cinnamate (Makri and Kintzios, 2008; Schulz et al., 2003). Each compound imparts a distinct aroma (Patel et al., 2021), and their varying amounts strongly influence the basil's flavor and consumer preferences (Walters et al., 2021).

However, the progressing climatic changes and extreme weather conditions continue to result in variable field-grown basil qualities and yields (Barut et al., 2021). To still meet the incessant consumer demand of fresh basil (Market Research Report, 2022), stakeholders are increasingly considering the implementation of environmental-friendly vertical farms and plant factories including light-emitting diodes (e.g., Kozai, 2019; Benke and Tomkins, 2018) for the production of this high-value crop. By conducting a comprehensive economic evaluation, Liaros et al. (2016) showed that basil cultivations in plant factories are principally feasible. However, the fixtures' light intensity settings were among the most influential factors impacting its profitability. Thus, the scientific community is currently in search of minimal light intensity requirements and optimal light qualities to increase the viability of LED-based indoor basil productions.

Although lighting strategies for commercial indoor plant productions are typically adjusted during different plant stages (Currey et al., 2017) and help in reducing energy costs (Lopez and Runkle, 2008), constant (spectrum-dependent) light intensities between 180 and 545 $\mu\text{mol m}^{-2} \text{s}^{-1}$ are currently recommended for indoor basil cultivations (Park et al., 2016; Sipos et al., 2021). Pennisi et al. (2020), who employed five different light intensities between 100 and 300 $\mu\text{mol m}^{-2} \text{s}^{-1}$ emitted by narrow blue (B) and red (R) LEDs with main peaks at 463 and 657 nm, concluded that a constant light intensity of 250 $\mu\text{mol m}^{-2} \text{s}^{-1}$ optimizes basil yield and as well as water and energy use efficiencies. However, an increase in basil yield of 20 % was recently observed when shifting the narrow B wavelength from 450 to 435 nm (Rihan et al., 2020). While basil's optimal RB ratios are still under extensive investigation (Rihan et al., 2020; Pennisi et al., 2019; Naznin et al., 2019), inclusions of other wavelengths increasingly show great

potentials for improving basil yields and qualities as well. A partial replacement of B and R with green (G) light (500-600 nm) resulted in higher basil productions by inducing stem and leaf elongations (Schenkels et al., 2020). Additions of far-red (FR) light (700-750 nm) have shown to increase basil's canopy photosynthesis (Zhen and Bugbee, 2020), and explain the increased basil yields observed by Rahman et al. (2021) in comparison to broad white (400-700 nm) and narrow RB spectra under equal light intensity conditions. Increased fresh weights, leaf areas as well as total antioxidant capacities of basil seedlings were found under any RB spectrum that included either yellow (Y, main peak at 600 nm), G (main peak at 520 nm) or FR (main peak at 735 nm) wavelengths when compared to RB alone (Carvalho et al., 2016). However, Lin et al. (2021) demonstrated enhanced photosynthetic activities and growth of green and purple basil varieties when the proportion of R was increased in an RGB spectrum, and Song et al. (2020) showed that the inclusion of B increased the accumulation and antioxidant activity of polyphenols and essential oil content in basil when compared to different combinations of B, R and W LED light. Thus, a growing body of research suggests light spectra that consist of elevated R and B LEDs, supplemented with broad W LEDs including FR wavelengths (Sipos et al., 2021).

Based on this current trend towards broad-bandwidth LED light spectra for basil productions in controlled-environment horticulture, a white broad-bandwidth LED light spectrum (400-780 nm) with elevated R and B light fractions was developed. It could be assumed that basil plants develop more rapidly under increasing high light conditions. Reaching market maturity earlier allows for higher plant production per cultivation unit and leads to higher profitability due to higher throughput. At the same time, basil developing under rising low light conditions with the same light composition could use light more efficiently, ultimately resulting in greater profitability due to lower energy costs. Since not only morphology but also sensory quality aspects have to be taken into account for the evaluation of profitability, the contents and compositions of essential oil (influencing aroma and flavor), which change considerably over time (i.e., Lewinsohn et al., 2000), also have to be considered.

Therefore, the aim of this study was to explore the photo-morphological development as well as the content and composition of volatile organic compounds (VOS) of four basil cultivars (cv. Anise, cv. Cinnamon, cv. Dark Opal and cv. Thai Magic) over time (from seed to common marketability) under two different rising light intensity conditions (I_{Low} and I_{High}). We further aimed at investigating the basil's biomass efficiencies under both light conditions to determine the basil's light use efficiencies under these prototype LED light fixtures.

2. Materials and methods

2.1 Experimental design

Using a randomized block design, a three-factorial experiment (including two light intensities (I_{Low} ; I_{High}), four basil cultivars ('Anise', 'Cinnamon', 'Dark Opal', 'Thai Magic') and four non-destructive weekly plant assessments (at 14, 21, 28 and 35 days after sowing (DAS)) with four spatially independent replications (= experimental blocks) per light treatment was conducted ($N = 576$ plant pots, $n = 72$ pots per experimental block with $n = 18$ pots per basil cultivar). To weekly collect plant material for volatile organic compound analyses, the experiment was repeated under identical conditions.

2.2 Plant material and growth conditions

Seeds of four basil cultivars, namely *Ocimum basilicum* cv. 'Anise', *O. basilicum* cv. 'Cinnamon', *O. basilicum* L. cv. 'Dark Opal' and *O. basilicum* L. var. *thyrsoiflorum* cv. 'Thai Magic' were purchased from Rühlemann's Kräuter- und Duftpflanzen, Horstedt, Germany. In 32 seed boxes, ~ 150 seeds of each basil cultivar were sown on the surface of moist potting substrate (Fruhstorfer Einheitserde Typ P, Hawita, Vechta, Germany). Four seed boxes (each containing the seeds of one basil cultivar respectively) were placed in the center of each experimental block at equal PFD (photon flux density) of ~ 150 $\mu\text{mol m}^{-2} \text{s}^{-1}$ and misted daily to allow for optimal light- and moisture-dependent germination. Seven days after sowing, four representative basil seedlings per cultivar were transplanted into pots ($\varnothing = 9$ cm, height 6.8 cm, volume 0.28 L) (MXC 9, Kausek, Mittenwalde, Germany). Each of the 576 pots contained a mixture of 0.28 L potting substrate (Fruhstorfer Einheitserde Typ P, Hawita, Vechta, Germany) and 560 mg of a slow-release fertilizer (15-9-11+2MgO +TE (trace elements)) (Osmocote Exact Mini 3-4M, Hermann Meyer KG, Rellingen, Germany) to ensure identical nutrient contents in all plant pots. Eight perforated propagation trays (50 x 32 x 6 cm) (CRP Import – Export GmbH, Hamburg, Germany) equipped with nine equally spaced basil pots were placed evenly under each experimental block within 1.2 m^2 under the two different light intensity treatments. To ensure uniform watering, perforated propagation trays were submerged in unperforated propagation trays filled with equal amounts of water for 30 minutes daily. Due to inhomogeneous light intensity distributions underneath each experimental block (Figure 20), propagation trays were rotated and re-positioned daily to minimize positional effects. To prevent sciarid fly (*Sciaridae*) infestations during experiments, nematodes (*Steinernema feltiae*) (Katz BiotechAG, Baruth, Germany) were preventively applied weekly as recommended by the supplier. At all eight experimental blocks, data loggers (EL-USB-2, Lascar, Conrad, Hirschau, Germany) continuously measured climatic conditions including temperature and relative humidity. With average temperatures ($^{\circ}\text{C} \pm$ standard deviation (SD)) of

21.6 ± 2.8 and 21.2 ± 2.6 (with a measuring accuracy of $1\text{ }^{\circ}\text{C}$) and average humidities (%rh \pm SD) of 68.9 ± 13.4 and 70.8 ± 13.02 (with a measuring accuracy of 2.25%) under both light treatments, climatic conditions did not differ between light treatments.

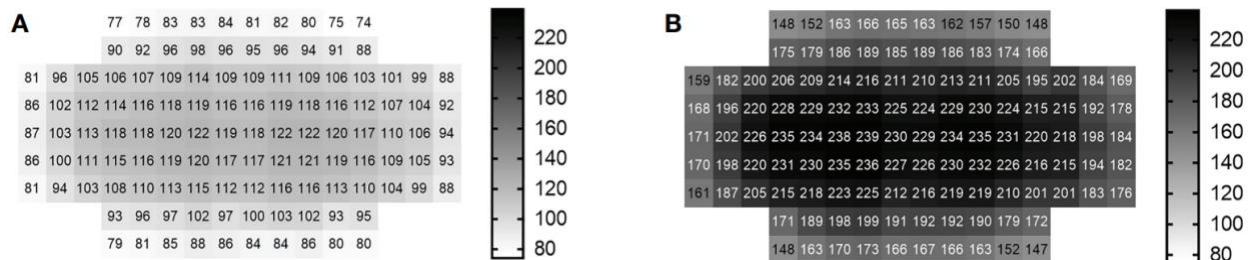


Figure 20 – Light intensity distribution underneath each LED light treatment.¹ (A) Low light intensity treatment (I_{Low}), (B) High light intensity treatment (I_{High})

¹ Each heat map depicts the photon flux densities (PFDs) between 400 and 780 nm [$\mu\text{mol m}^{-2} \text{s}^{-1}$] measured every 100 cm² within one experimental block (1.2 m²) underneath the light treatments at cultivation table level ($n = 120$ measurements). Gray scales to the right of each light distribution pattern are scaled from minimum to maximum PFDs (74-239 $\mu\text{mol m}^{-2} \text{s}^{-1}$) measured across both light treatments.

2.3 Lighting systems and illumination conditions

Light experiments were conducted in climate-controlled cultivation rooms. Each of the eight experimental blocks per experiment consisted of two prototype LED lamps (Apollo R1, FUTURELED®, Berlin, Germany) which were mounted 0.67 m apart from another and mounted onto given steel frames resulting in 1.00 m between the cultivation table and the bottom of the LED lights. The illuminated area of 1.2 m² underneath these two multispectral LED lamps represented one of eight experimental blocks per experiment. Plastic sheeting extending from above the light fixtures to below the cultivation tables eliminated neighboring light pollution from other experimental blocks. Light intensity distributions, broad LED light spectra and spectral compositions during the experiments are depicted in Figures 20, 21 and Table 18, and were measured with an Ocean FX-UV-VIS spectrometer (Ocean Insight, Ostfildern, Germany).

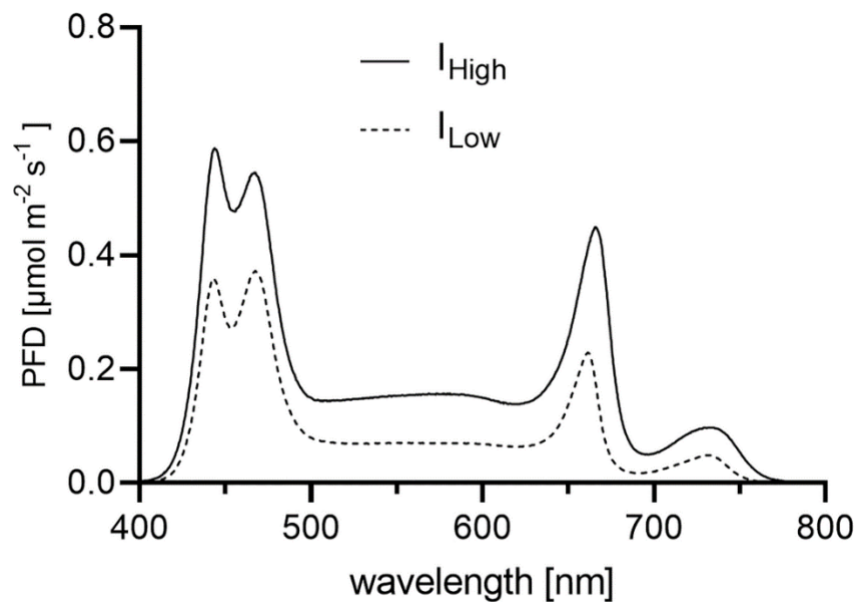


Figure 21 – White broad-band LED light spectra applied during the experiments.

Depicted are the LED light spectra as PFDs (photon flux densities) [$\mu\text{mol m}^{-2} \text{s}^{-1}$] per wavelength [nm] between 400 and 780 nm. Each LED light spectrum (I_{Low} light treatment = dashed line; I_{High} light treatment = solid line) represents the average PFDs per wavelength obtained from 120 measurements across the entire experimental block (1.2 m²).

Table 18 – Spectral compositions of the white broad-band LED light spectra.¹

	I_{Low}	I_{High}
	(Photosynthetic) photon flux densities [$\mu\text{mol m}^{-2} \text{s}^{-1}$] ¹	
<i>PFD</i> (400~780nm)	102 ± 14	200 ± 26
<i>PPFD</i> (400~700nm)	96 ± 13	185 ± 24
B (400~500nm)	50 ± 7	82 ± 11
G (500~600nm)	21 ± 3	44 ± 6
R (600~700nm)	25 ± 4	59 ± 8
FR (700~780nm)	6 ± 1	14 ± 3

I_{Low} = Low light intensity treatment, I_{High} = High light intensity treatment, *PFD* = Total photon flux density (400-780 nm), *PPFD* = photosynthetic photon flux density (400-700 nm), B = blue photons, G = green photons, R = red photons, FR = far-red photons

¹ Presented are mean photon flux densities ± standard deviations (SD) expressed in $\mu\text{mol m}^{-2} \text{s}^{-1}$ from 120 measurements taken every 100 cm² across an experimental block under each light treatment at cultivation table level.

All basil seeds and seedlings were subject to a broad LED light spectrum (400-780 nm) with elevated (R) and blue (B) wavelength proportions under a PFD of $\sim 150 \mu\text{mol m}^{-2} \text{s}^{-1}$ during germination. Starting seven days after sowing, basil plants were then subject to either a PFD of $\sim 102 \mu\text{mol m}^{-2} \text{s}^{-1}$ (= I_{Low}) or a PFD of $\sim 200 \mu\text{mol m}^{-2} \text{s}^{-1}$ (= I_{High}) at cultivation table level for the remainder of the light experiments. Over time, PFDs increased with increasing height of basil cultivars (as the distance of the canopy to the LED light sources decreased) (Figure 22). Plants were subject to artificial lighting from 6.00 am to 10.00 pm for a photoperiod of 16 hours per day during the experiments (duration 35 days).

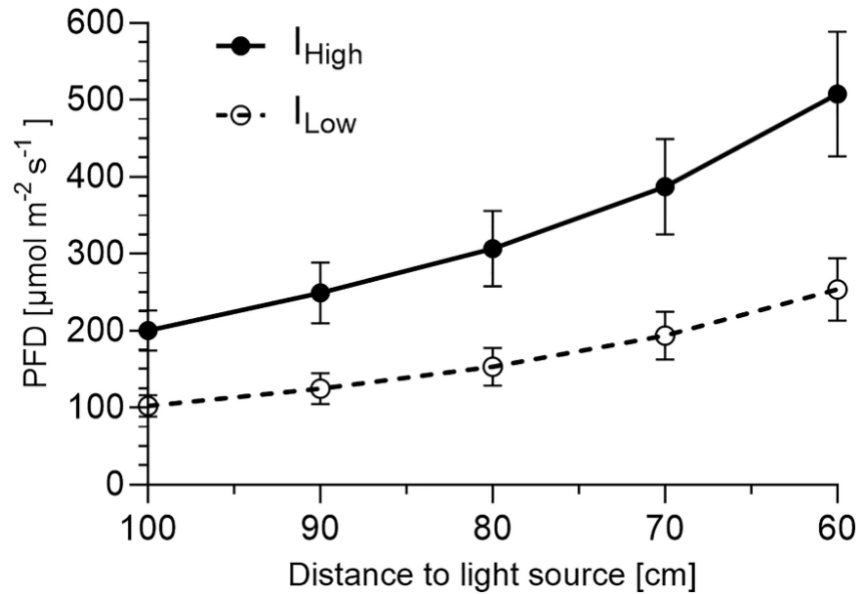


Figure 22 – Photon flux density depending on distance to light source.

Presented are average photon flux densities (PFD) [$\mu\text{mol m}^{-2} \text{s}^{-1}$] \pm SD between 400 and 780 nm recorded in 10 cm intervals (starting at cultivation table level 100 cm from the light source) from nine representative positions across the cultivation area (1.2 m²) at each distance.

2.4 Energy measurements

The power draw of current (A) and voltage (V) from representative lamps of each light treatment were measured using a power meter (ENERGY MONITOR 3000, Voltcraft®, Wernberg-Köblitz, Germany) to estimate the yield efficacy of the LED light treatments for each basil cultivar. Electrical consumptions were calculated by multiplying the power consumptions with the running hours of the LED light fixtures (16 hours per day, 35 days in total). Biomass efficacy (total fresh yields per kWh and cultivation area (1.2 m²)) as well as VOC efficacy (volatile organic compound yields per kWh and cultivation area) were calculated by multiplying the cultivars' average yields per experimental area with 72 (= maximum number of pots per experimental block) and dividing these yields by the total kilowatt hours used per experimental block.

2.5 Extraction of volatiles

After samples were gently air-dried in a drying oven at 30 °C for \leq 7 days until stable mass was attained and shortly stored under cool, dry and dark conditions, volatile compounds of basil leaves were extracted according to the following procedure: 100 mg (\pm 2 %) of dried and powdered (3 intervals of 10 seconds at 15,000 rpm via Tube Mill control, IKA®, Staufen, Germany) basil leaves from two basil pots (of the same

cultivar, light treatment, harvest date and experimental block) were transferred into 2 mL screw cap micro tubes (Sarstedt AG & Co. KG, Nümbrecht, Germany) including two steel grinding balls (\varnothing 2 mm) and homogenized in 1.0 mL of high-performance liquid chromatography grade isooctane (Th. Geyer, Renningen, Germany) [containing 1:2000 (v/v) carvacrol as internal standard] for 10 minutes at 30 rps with a ball mill (MM400, Retsch®, Haan, Germany). After 10 minutes of ultra-sonification (Sonorex RK 106, Bandelin electronic GmbH & Co. KG, Berlin, Germany) and 10 minutes of centrifugation at 13,000 rpm (Heraeus™ Labofuge™ 400 R, Thermo Scientific™, Osterode, Germany) at 22 °C respectively, the supernatants were transferred into GC-vials and stored at -70 °C until analysis ($N = 256$ samples).

2.6 GC-FID and GC-MS analysis

1 μ L of the obtained extracts of volatiles were analyzed by GC–FID using an Agilent gas chromatograph 6890N fitted with a HP-5MS column (30 m \times 250 μ m \times 0.5 mm) in split mode (1:20). Detector and injector temperatures were set to 250 °C. The following oven temperature program was used: 50 °C for 2 min, heating from 50 to 320 °C at a rate of 5 °C min^{-1} . The final temperature was held for 6 min. Hydrogen was used as carrier gas with a constant flow rate of 1.2 mL min^{-1} . GC-MS was performed using an Agilent 5975 Network mass spectrometer, on a HP-5MS column (see GC), operating at 70 eV ionization energy, using the same temperature program as above. Helium was used as carrier gas with a constant flow rate of 1.2 mL min^{-1} . Retention indices were calculated by using retention times of C6- C24-alkanes (Merck KGaA, Darmstadt, Germany) that were injected under the same chromatographic conditions.

2.7 Identification and quantification of volatile compounds

All main compounds of the volatile extracts were identified by comparing their mass spectra with those of internal reference libraries (Adams, NIST). Additionally, identification of 1,8- cineole, α -pinene, α -terpineol, β -elemene, β -myrcene, β -pinene, borneol, camphor, carvacrol, eugenol, β -farnesene, limonene, linalool, methyl chavicol, methyl cinnamate, methyl eugenol, ocimene and sabinene was affirmed by pure standard substances (purchased as analytical standards with a purity ≥ 95 % for GC reference analysis from Abcam (Cambridge, United Kingdom), Alfa Aesar (Kandel, Germany), Carl Roth (Karlsruhe, Germany), Fluka (Seelze, Germany), Merck KGaA (Darmstadt, Germany) and TCI GmbH (Eschborn, Germany)) and

confirmed by comparing their retention indices. Volatile compounds were quantified based on the known concentration of the internal standard carvacrol.

2.8 Statistics and calculations

GraphPad Prism (version 9.3.1.471, San Diego, USA) was used for statistical analyses and graphical representations of all data sets. Plant heights, fresh/dry weights, VOC contents and compositions: Normality of data sets were tested via Shapiro-Wilk or D'Agostino & Pearson tests within and across spatial replications at $\alpha < 0.05$. When distributions deviated from normality, outliers were identified via ROUT method at $Q = 10\%$ and removed to obtain normality. When standard deviations (SDs) of data sets passed Brown-Forsythe and Bartlett's tests at $\alpha < 0.05$, ordinary one-way ANOVAs followed by Tukey's multiple comparisons test at 95 % confidence level ($\alpha < 0.05$) were applied; when SDs were not equal between light treatments and cultivars, Brown-Forsythe and Welch ANOVAs followed by Dunnett's T3 multiple comparisons test at 95 % confidence level ($\alpha < 0.05$) were applied to analyze differences between light treatments and cultivars. (Data set of plant height: $N = 566-575$, $n = 14-18$ average plant heights per basil cultivar, light treatment and spatial replication: each n used for statistical analysis represents the average plant height of all four measured basil plants per pot; data sets of fresh/dry weights: $N = 570/567$, $n = 15-18$ values per cultivar, light treatment and spatial replication; data sets of volatile organic compound (VOC) content and composition: $N = 32-64$, $n = 4-8$ values per cultivar and light treatment). Number of leaf and branch pairs: As no differences within light treatments across spatial replications were observed after applying a Kruskal-Wallis test followed by Dunn's multiple comparisons test at confidence level 95 % ($P < 0.05$) for basil plants at each time point ($p > 0.99$), data sets of all four spatial replications per light treatment and cultivar were combined for further statistical analysis. To analyze differences between light treatments and cultivars at each time point, Kruskal-Wallis tests followed by Dunn's multiple comparisons test at 95 % confidence level ($P < 0.05$) were conducted, respectively (Data set: $N = 576$, $n = 72$ assessed pots per light treatment, cultivar and time point; each n used for statistical analysis represents the average number of leaf pairs/side branches from all four assessed basil plants per pot). Principal component regressions (PCRs) were performed to determine the predictive power of morphological parameters (plant height, number of leaf and branch pairs) on the basil's VOC compositions by including the average values of all morphological observations (dependent variables) and of all detected VOCs (independent variables) per light treatment and DAS. Thus, data sets of each cultivar consisted of eight average values per each of the three dependent variables (as each value represents the average morphological observation per time (14, 21, 28, 35 DAS) and light treatment (I_{High} , I_{Low}) and eight values per each of the 21-25 independent

variables (as we detected 21, 22, 23 and 25 VOCs in cv. Anise, Dark Opal, Cinnamon and Thai Magic, respectively). Yield efficacy: The average fresh weights and leaf dry weights from 15-18 harvested basil pots per cultivar and spatial replication were multiplied by factor 72 to approximate the basil cultivars' fresh weight and VOC productions for the entire illuminated experimental area. Approximated production yields were then divided by the calculated kilowatt hours consumed under the experimental area of 1.2 m² by the end of the trial period to determine biomass and VOC efficacies. When data sets passed normality via Shapiro-Wilk test at $\alpha < 0.05$, data sets were analyzed via unpaired t test, otherwise via non-parametric Kolmogorov-Smirnov test at 95 % confidence level ($P < 0.05$), respectively.

3. Results and discussion

3.1 Cultivar-dependent morphological differences

The species *Ocimum basilicum* L. exhibits an immense variety of different cultivars and is characterized by a high intra-specific diversity in morphological traits, and the specific appearances of each cultivar observed in our study coincide with their typical phenotypes described by Carović -Stanko et al. (2011) and Lin et al. (2021). For example, basil cultivars cv. Anise, cv. Cinnamon and cv. Thai Magic were characterized by green leaves with purple stems and flowers, while basil cv. Dark Opal was characterized by the purple color of all its aerial parts and its compact growth (Figure 23).

With an average plant height of ~ 25 and ~ 27 cm and an average of four and five leaf pairs as well as branch pairs by the end of the trial period (35 days after sowing (DAS)) under I_{Low} and I_{High} light conditions, respectively, basil cv. Cinnamon grew the tallest and developed the most leaf and branch pairs from all investigated cultivars (Table 19; Figure 24). In addition, while ~ 43 % of all investigated cv. Cinnamon basil plants had developed flower buds by the end of the experiment under I_{High} , no flower buds had formed under I_{Low} (Table 19).

Though basil cv. Anise showed the most homogeneous development (lowest variance) of all investigated basil cultivars, cv. Anise and cv. Thai Magic developed very similarly under both LED light conditions (Table 19; Figure 24). While both cultivars reached a plant height of ~ 20 cm under I_{Low} , the cultivars grew significantly taller under I_{High} and reached heights of ~ 23 cm by the end of the trial period. In addition, both cultivars developed the same number of leaf pairs along the main stem during the experiment and had developed an average of four leaf pairs along the main stem under both light conditions by the end of the experiment. Further, all cv. Anise basil plants and ~ 93 % of the cv. Thai Magic basil plants had formed flower buds under I_{High} , whereas no flower bud formation was detected under I_{Low} .

Though branching of cv. Anise progressed faster, both cultivars averaged three and four branch pairs at the end of the trial period under I_{Low} and I_{High} , respectively.

With heights of ~ 10 and ~ 16 cm, and an average of one and two branch pairs per basil plant under I_{Low} and I_{High} at harvest, respectively, the purple-leaved cv. Dark Opal remained the shortest and least branched of the four investigated cultivars (Table 19; Figure 24). Though cv. Dark Opal developed the fewest leaf pairs under the I_{Low} light conditions, its leaf pairs developed rapidly under I_{High} by growing an average of ~ 5 leaf pairs per basil plant.

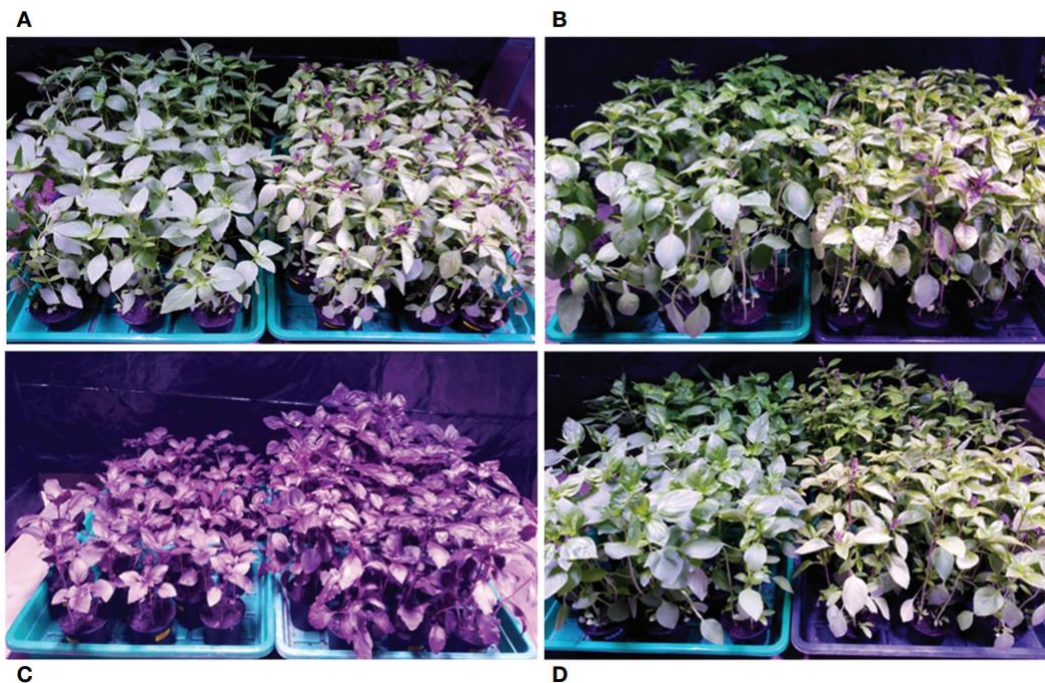


Figure 23 – Visual appearance of four *Ocimum basilicum* L. cultivars at harvest. (A) *O. basilicum* L. cv. ‘Anise’, (B) *O. basilicum* L. cv. ‘Cinnamon’, (C) *O. basilicum* L. cv. ‘Dark Opal’, (D) *O. basilicum* L. cv. ‘Thai Magic’ under the low (left) and high (right) light intensity, respectively, 35 days after sowing.

Table 19 – Summarized plant characteristics of four basil cultivars grown under two LED light intensities over time (including light intensities at plant canopy levels).

Basil cultivar		‘Anise’		‘Cinnamon’		‘Dark Opal’		‘Thai Magic’	
Parameter	DAS	I _{Low}	I _{High}	I _{Low}	I _{High}	I _{Low}	I _{High}	I _{Low}	I _{High}
Plant height [cm] ¹	14	1.2 ± 0.2 ^c	1.7 ± 0.3 ^b	2.0 ± 0.3 ^b	2.8 ± 0.4 ^a	1.8 ± 0.4 ^b	2.0 ± 0.4 ^b	1.2 ± 0.3 ^c	1.7 ± 0.4 ^b
	21	3.8 ± 0.4 ^c	5.9 ± 0.8 ^b	6.7 ± 0.8 ^b	8.5 ± 1.0 ^a	3.9 ± 0.6 ^c	5.7 ± 0.8 ^b	4.3 ± 0.8 ^c	6.3 ± 1.1 ^b
	28	9.4 ± 1.2 ^c	14.8 ± 1.3 ^b	14.4 ± 1.6 ^b	17.4 ± 2.0 ^a	6.0 ± 0.9 ^d	9.6 ± 1.1 ^c	9.8 ± 1.4 ^c	14.5 ± 1.7 ^b
	35	19.8 ± 1.4 ^c	22.9 ± 1.4 ^b	25.3 ± 2.2 ^a	26.8 ± 2.3 ^a	10.0 ± 1.3 ^e	15.9 ± 1.2 ^d	19.9 ± 2.5 ^c	22.6 ± 2.1 ^b
Light intensity at canopy level [μmol m ⁻² s ⁻¹] ²	14	115 ± 17	230 ± 33	117 ± 17	236 ± 34	117 ± 17	232 ± 34	115 ± 17	230 ± 33
	21	122 ± 18	254 ± 38	130 ± 20	270 ± 40	122 ± 18	253 ± 37	123 ± 19	256 ± 38
	28	138 ± 21	312 ± 48	155 ± 24	331 ± 51	128 ± 19	276 ± 41	140 ± 21	309 ± 47
	35	175 ± 28	376 ± 60	198 ± 32	411 ± 66	140 ± 21	320 ± 49	176 ± 28	373 ± 59
Leaf pairs [n] ¹	14	1.0 ± 0.0 ^b	1.0 ± 0.0 ^b	1.0 ± 0.0 ^b	1.0 ± 0.1 ^a	1.0 ± 0.1 ^b	1.0 ± 0.1 ^b	1.0 ± 0.0 ^b	1.0 ± 0.0 ^b
	21	2.0 ± 0.0 ^c	2.9 ± 0.3 ^a	2.0 ± 0.1 ^c	3.0 ± 0.2 ^a	1.6 ± 0.3 ^d	2.4 ± 0.3 ^b	2.0 ± 0.2 ^c	2.3 ± 0.4 ^b
	28	3.0 ± 0.0 ^e	4.0 ± 0.1 ^{ab}	3.2 ± 0.3 ^{de}	4.1 ± 0.2 ^a	2.5 ± 0.3 ^f	3.4 ± 0.4 ^{cd}	2.9 ± 0.2 ^e	3.7 ± 0.3 ^{bc}
	35	4.0 ± 0.2 ^{de}	4.0 ± 0.1 ^{de}	4.4 ± 0.3 ^{bc}	5.1 ± 0.4 ^a	3.5 ± 0.3 ^f	4.6 ± 0.4 ^b	3.8 ± 0.3 ^e	4.1 ± 0.3 ^{cd}
Branch pairs [n] ¹	21	0.7 ± 0.5 ^b	2.0 ± 0.1 ^a	0.8 ± 0.5 ^b	2.0 ± 0.1 ^a	0.0 ± 0.0 ^c	0.0 ± 0.1 ^c	0.6 ± 0.5 ^b	1.9 ± 0.2 ^a
	28	3.0 ± 0.1 ^b	3.7 ± 0.4 ^a	2.0 ± 0.2 ^c	3.0 ± 0.1 ^b	0.0 ± 0.0 ^e	1.1 ± 0.6 ^d	1.9 ± 0.3 ^{cd}	2.9 ± 0.2 ^b
	35	3.0 ± 0.0 ^d	4.0 ± 0.1 ^c	4.3 ± 0.3 ^b	5.0 ± 0.4 ^a	0.5 ± 0.5 ^f	2.2 ± 0.7 ^e	2.8 ± 0.3 ^e	3.7 ± 0.4 ^d
Flower buds [%] ³	35	0	100	0.0	43.1	0.0	0.0	0.0	93.1
Fresh weight [g] ¹	35	13.4 ± 1.2 ^e	18.9 ± 1.6 ^{cd}	24.0 ± 2.3 ^b	28.7 ± 3.0 ^a	7.1 ± 1.3 ^f	18.5 ± 2.6 ^{cd}	16.4 ± 2.0 ^{de}	21.6 ± 2.7 ^{bc}
Dry weight [g] ¹	35	1.2 ± 0.2 ^d	3.0 ± 0.3 ^b	2.1 ± 0.3 ^c	3.7 ± 0.5 ^a	0.5 ± 0.1 ^e	1.6 ± 0.3 ^d	1.5 ± 0.3 ^d	3.2 ± 0.4 ^{ab}
Leaf dry weight [g] ¹	35	0.7 ± 0.1 ^{de}	1.9 ± 0.2 ^{ab}	1.4 ± 0.3 ^{bc}	2.1 ± 0.6 ^a	0.3 ± 0.1 ^e	1.1 ± 0.2 ^{cd}	0.9 ± 0.2 ^{cd}	2.2 ± 0.3 ^a
VOC concentration [mg g L _{DM} ⁻¹] ⁴	14	4.0 ± 1.0 ^{de}	5.4 ± 1.2 ^{cde}	4.2 ± 0.9 ^e	5.4 ± 1.6 ^{cde}	8.6 ± 0.5 ^{bc}	14.8 ± 3.2 ^a	9.6 ± 2.2 ^b	7.6 ± 2.1 ^{bcd}
	21	7.6 ± 0.9 ^{bc}	7.3 ± 1.4 ^{bc}	6.1 ± 0.8 ^c	6.9 ± 2.7 ^{bc}	11.8 ± 1.6 ^a	11.3 ± 2.3 ^a	9.0 ± 1.9 ^{ab}	7.4 ± 1.9 ^{bc}
	28	8.1 ± 1.5 ^{bc}	9.1 ± 1.8 ^{bc}	7.0 ± 1.6 ^c	7.8 ± 2.3 ^{bc}	8.5 ± 2.2 ^{bc}	8.0 ± 1.8 ^{bc}	11.6 ± 1.9 ^{ab}	13.8 ± 4.3 ^a
	35	9.9 ± 1.7 ^{ab}	9.7 ± 1.3 ^{ab}	11.4 ± 3.5 ^{ab}	8.8 ± 2.4 ^b	7.9 ± 1.0 ^b	8.0 ± 2.3 ^b	13.1 ± 2.3 ^a	9.1 ± 3.2 ^b
VOC yield [mg total L _{DM} ⁻¹] ⁵	35	7.2 ± 0.1 ^d	18.6 ± 0.9 ^a	15.6 ± 1.2 ^b	17.8 ± 2.0 ^a	2.6 ± 0.2 ^e	8.5 ± 0.6 ^{cd}	10.5 ± 0.5 ^c	19.2 ± 0.5 ^a

DAS: days after sowing; I_{Low}: Low light intensity treatment; I_{High}: High light intensity treatment; VOC: volatile organic compounds; L_{DM}: leaf dry matter; Different letters within a row indicate significant differences at $P \leq 0.05$.

¹ Presented are average values ± SD of four spatial replications (each spatial replication per basil cultivar consists of $n = 14$ -18 plant pots, each n represents the mean value of four assessed basil plants per pot).

² Presented are calculated photon flux densities (*PFDs*) \pm *SD* at canopy level based on the exponential growth rate calculated in Excel via GROWTH function from the measured data points depicted in Figure 22.

³ Presented are percentage values across all four spatial replications.

⁴ Presented are average VOC contents \pm *SD* in mg g L_{DM}^{-1} (leaf dry matter) (w/w) across all four spatial replications.

⁵ Presented are calculated average total VOC quantities \pm *SD* in mg total L_{DM}^{-1} (leaf dry matter) across four spatial replications.

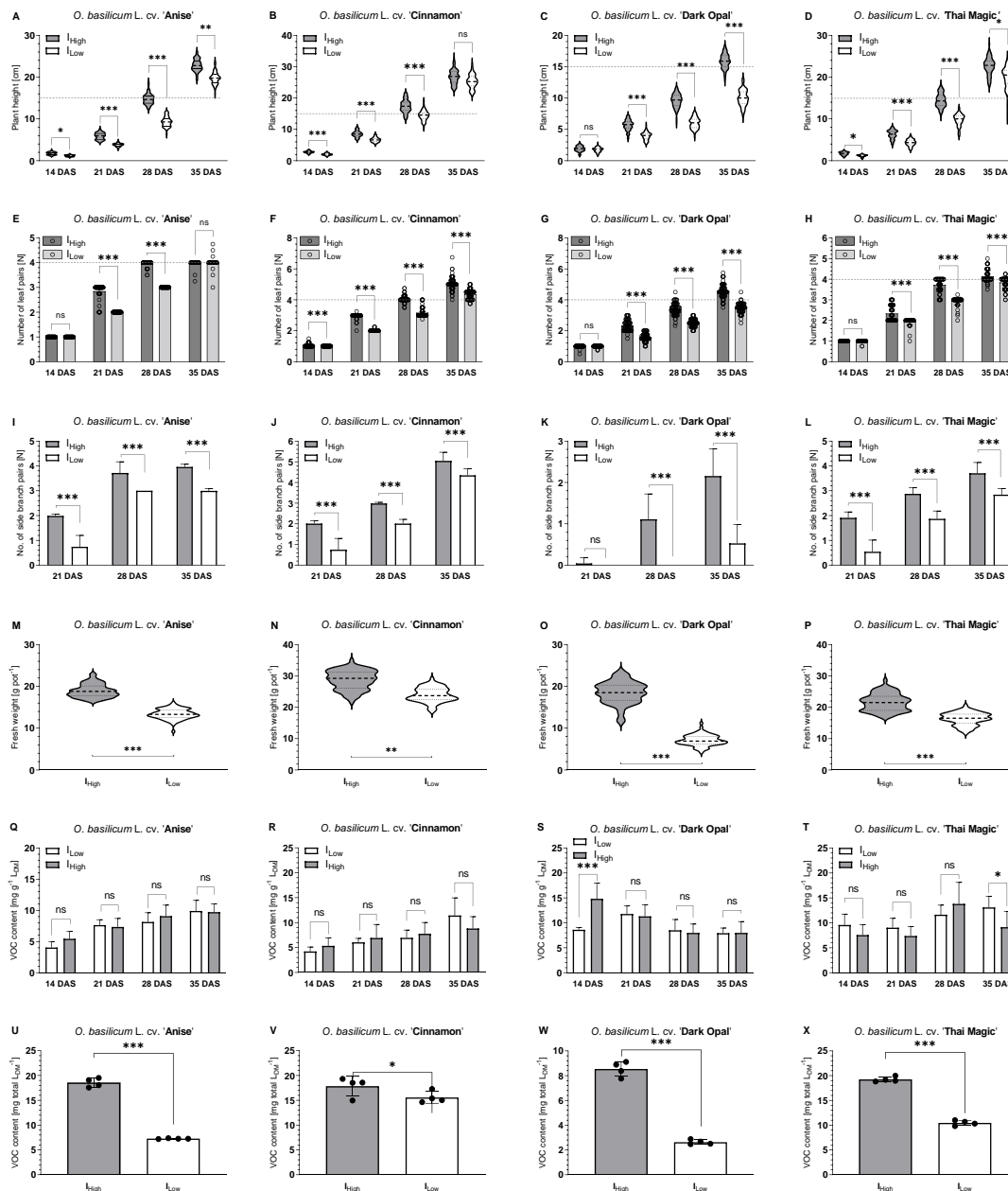


Figure 24 – Characteristics of four *Ocimum basilicum* L. cultivars under two different broad-bandwidth LED light intensities over time.¹ I_{High}: High light intensity treatment; I_{Low}: Low light intensity treatment; DAS: days after sowing; dashed horizontal lines represent marketability (defined as plant height \geq 15cm and/or number of leaf pairs \geq 4); L_{DM}: leaf dry matter; VOC: volatile organic compound; significance levels: ns = not significant, * \leq 0.05, ** \leq 0.02, *** \leq 0.01; please note the differently scaled Y-axes between cultivars.

¹ A-D: Plant height development of basil cultivar 'Anise' (A), 'Cinnamon' (B), 'Dark Opal' (C) and 'Thai Magic' (D) over time (dashed and dotted lines within violin plots represent medians and quartiles (25th and 75th percentile) of the data set, respectively; dashed lines horizontally across the graph represent

marketability at height ≥ 15 cm); **E-H**: Leaf pair development of basil cultivar ‘Anise’ (**E**), ‘Cinnamon’ (**F**), ‘Dark Opal’ (**G**) and ‘Thai Magic’ (**H**) over time (dashed lines represent marketability at a number of leaf pairs ≥ 4); **I-L**: Branch pair development of basil cultivar ‘Anise’ (**I**), ‘Cinnamon’ (**J**), ‘Dark Opal’ (**K**) and ‘Thai Magic’ (**L**) over time; **M-P**: Fresh weight per pot of basil cultivar ‘Anise’ (**M**), ‘Cinnamon’ (**N**), ‘Dark Opal’ (**O**) and ‘Thai Magic’ (**P**) 35 days after sowing (at harvest; dashed and dotted lines within violin plots represent medians and quartiles (25th and 75th percentile) of the data set, respectively); **Q-T**: Volatile organic compound content per gram of leaf dry matter of basil cultivar ‘Anise’ (**Q**), ‘Cinnamon’ (**R**), ‘Dark Opal’ (**S**) and ‘Thai Magic’ (**T**) over time; **U-X**: Total volatile organic compound content per total leaf dry matter of basil cultivar ‘Anise’ (**U**), ‘Cinnamon’ (**V**), ‘Dark Opal’ (**W**) and ‘Thai Magic’ (**X**) 35 days after sowing (at harvest).

3.2 Enhanced basil development under I_{High} results in earlier marketability than under I_{Low}

All four investigated *Ocimum basilicum* L. cultivars developed more rapidly under I_{High} than under I_{Low} light conditions. During all weekly assessments, basil heights as well as the number of leaf and branch pairs were mostly greater under I_{High} when compared to the developmental stages reached under I_{Low} during the same assessment week. Further, while basil flower buds developed under I_{High} in all three green-leafed basil cultivars during the last week of the trial period, no flower bud formations were observed under I_{Low} . Accordingly, all cultivars had accumulated greater total fresh and dry weights as well as leaf dry weights per basil pot under I_{High} at the end of the experiment than under I_{Low} (Table 19; Figures 24A–P). Thus, marketability based on morphological criteria (defined as basil height ≥ 15 cm and/or number of leaf pairs along the main stem ≥ 4) of cv. Cinnamon, cv. Anise, cv. Thai Magic and cv. Dark Opal was reached 27, 29, 30 and 32 DAS under the I_{High} light treatment, respectively (Figures 24A–H). Though the light intensity of I_{Low} represented $\sim 50\%$ of I_{High} (Table 18), green-leafed cultivars were marketable only 3-4 days later than under I_{High} conditions: While marketability of the cultivars cv. Cinnamon and cv. Thai Magic was reached three days later (30 and 33 DAS, respectively), cv. Anise reached marketability under I_{Low} four days later than under I_{High} (33 DAS). Cultivar Dark Opal did not reach the defined marketable stage under I_{Low} during the 35 days of cultivation. However, based on cv. Dark Opals’ growth function, its marketability under I_{Low} can be expected 37 DAS (5 days later than under I_{High}) as the leaf pair criterium (≥ 4 leaf pairs along the main stem) should be reached.

3.3 I_{High} induced light avoidance responses in green basil cultivars while purple basil remained ‘light-tolerant’

As evident in Figure 24, undesirable morphological and anatomical leaf adaptations to I_{High} became clearly visible at the top canopy of the green-leafed cultivars cv. Anise, cv. Cinnamon and cv. Thai Magic during

the last week of the trial period when PFDs exceeded an average of $300 \mu\text{mol m}^{-2} \text{s}^{-1}$ at canopy level (Table 19). In addition to purple pigment productions observed in some leaves of cv. Anise and cv. Cinnamon, all three green-leafed cultivars displayed leaf curling, reduced and dehydrated leaf blades and a pale green leaf color under the I_{High} light treatment, which are associated with reduced consumer preferences (Walters et al., 2021).

These leaf alterations exemplify typical light avoidance responses (Logan et al., 2015). To protect themselves from irreversible damages caused by excessive light (such as loss of oxygen evolution and loss of electron transfer activity of photosystem II (Tyystjärvi, 2013), sessile plants have evolved sophisticated signaling and protective mechanisms such as anthocyanin biosynthesis (Ma et al., 2021), chloroplast avoidance response (Wada, 2013) and thermal energy dissipation (Garcia-Plazaola et al., 2012).

The visible purple pigmentations in cv. Anise and cv. Cinnamon at the end of the trial period result from the biosynthesis of non-photosynthetic anthocyanins. Anthocyanin accumulations were proven to be stimulated by high light intensities to shield photosynthetic apparatuses from exceeding light conditions (Gould et al., 2018; Stetsenko et al., 2020; Ma et al., 2021). In example, anthocyanin contents increased by more than 20 % after LED light exposure to $\geq 300 \mu\text{mol m}^{-2} \text{s}^{-1}$ in a green-leafed lemon basil (*O. basilicum* x *O. americanum*) (Stetsenko et al., 2020), and their presence has been shown previously for both cultivars (Kwee and Niemeyer, 2011; Carović -Stanko et al., 2011). Thus, the anthocyanin formations observed in some leaves of cv. Anise and cv. Cinnamon under I_{High} (but not under I_{Low}) are obviously a light-induced photoprotective mechanism.

In addition, comparative studies investigating high light responses in acyanic (green-leafed) and cyanic (purple-leafed) basil varieties (Landi et al., 2014; Tattini et al., 2014; Logan et al., 2015; Stetsenko et al., 2020) prove and support that the constitutively high anthocyanin concentrations in purple basil varieties are responsible for mitigating light stress responses (while their green basil counterparts start to downregulate their photochemical efficiency under equal light stress conditions). Their findings explain the absence of visible photomorphogenic responses and thus, the 'light-tolerance' of purple-leafed 'Dark Opal' under I_{High} in our study, which represents a cultivar with very high anthocyanin contents (Lin et al., 2021).

The pale green color of leaves observed in all green cultivars under I_{High} is a typical sign of a chloroplast avoidance response: While the green color-giving chloroplasts distribute across the upper and lower sides of each palisade cell to achieve maximal light absorption under low to optimal light conditions (explaining the characteristic green leaf colors present under I_{Low} (Figure 23), chloroplasts gather at the side walls of each palisade cell to minimize the damages associated with the absorption of excessive light energy by chlorophyll pigments (Kagawa et al., 2001; Wada, 2013).

Additionally, comparable to our observations, leaves of green basil cultivars tend to reduce in size when exposed to a constant PPFD of $300 \mu\text{mol m}^{-2} \text{s}^{-1}$, which was associated with decreased chlorophyll contents, stomatal conductance, stomatal size and density in the green basil cultivar 'Genovese' (Pennisi et al., 2020). Reduced leaf sizes were also observed in the green cultivar 'Tigullio' under full sunlight when compared to leaves grown under 30 % sunlight (Tattini et al., 2014).

All described light avoidance responses of the green basil cultivars under I_{High} during the last week of the trial period are unmistakable signs of non-photochemical quenching (NPQ), a fundamental physiological photoprotective mechanism which involves the conversion and dissipation of excess excitation energy into heat. As NPQ represents a plants' shift from a photosynthetically efficient state to a state in which a fraction of photosynthetic reaction centers is non-functional, NPQ always occurs at the expense of photosynthetic efficiency and results in limited growth and reduced crop yields (García-Plazaola et al., 2012; Logan et al., 2015).

In addition, I_{High} conditions accelerated flower initiation in green basil cultivars. Based on the seed supplier, cv. Anise, cv. Cinnamon and cv. Thai Magic are endogenously programmed to initiate flowering after eight, seven and six nodes have been developed, respectively. However, under I_{High} these cultivars initiated flowering after developing only five, six and five nodes (including cotyledons), respectively (Table 19; Figure 24), which is a phenomenon that has recently been categorized as stress-induced flowering in angiosperms (Takeno, 2016). Although stress-induced flowering has received little attention so far, previous studies of *Salvia*, *Calendula*, and *Pharbitis* have shown that intense light stress triggers an earlier flowering pulse (Moccaldi and Runkle, 2007; Hirai et al., 1994).

3.4 I_{Low} resulted in beneficial acclimation responses in green basil cultivars while purple basil performed insufficiently

In contrast to the undesirable light-avoiding leaf adaptations and flower initiations detected under I_{High} (as described in the section above), the light-orientated leaves of the green cultivars cv. Anise, cv. Cinnamon and cv. Thai Magic were fully expanded, thin and displayed typical green leaf colors under I_{Low} (Figure 24), which represent decisive external quality attributes for consumers (Rouphael et al., 2012). As investigated by Walters et al. (2021), consumers prefer big, fresh basil leaves without detectable discolorations and damages as well as 'soft' leaf textures. Consequently, all visual traits detected under I_{Low} supersede the unsatisfactory visual attributes identified under I_{High} and translate into highly desirable basil products by meeting the consumers' basil preferences.

These favored basil leaf qualities under I_{Low} represent acclimation responses often found in green leaves exposed to low light levels to increase light capture and photosynthetic efficiency (Nemali and van Iersel, 2004; Wada, 2013; Stagnari et al., 2018), and are to be ascribed to the great plasticity in morpho-anatomical, physiological and biochemical traits of green basil: As shown by Tattini et al. (2014), the capability of green basil cv. Tigullio to increase its leaf area, photosynthetic pigment concentrations and CO₂ assimilation rates under 30 % sunlight resulted in greater net photosynthesis and net daily carbon gains than detected in cv. Tigullio under full sunlight. The greater leaf sizes, the evenly distributed chloroplasts across the leaves of cv. Anise, cv. Cinnamon and cv. Thai Magic (Figure 24) as well as the fact that the marketability criteria were reached just 3-4 days later under I_{Low} (as described in section 3.2) are robust signs that very similar (beneficial) low light acclimation responses took place in the green cultivars investigated in our study.

To the contrary, the comparatively small leaf sizes (as evident in Figure 23C) and the slow development of cv. Dark Opal under I_{Low} (as evident by the great differences in plant height, number of developed leaf and branch pairs and thus biomass yields (Table 19, Figures 24C, G, K, O) in comparison to I_{High} show clearly, that cv. Dark Opal was not able to adjust as well as its green basil counterparts to the given low light conditions. The reason for cv. Dark Opals poor performance under I_{Low} can be ascribed to its high content of leaf anthocyanins (Lin et al., 2021), which proved to translate into an intrinsically low ability to maximize light interception and transmission in the similar anthocyanin-rich purple leaves of basil cultivar 'Red Rubin' under low light conditions (Tattini et al., 2014). The anthocyanins' role in the observed insufficient I_{Low} performance is further strengthened by Misyura et al. (2013) who showed that anthocyanin-rich *Arabidopsis thaliana* mutants grew worse compared to the wild type under equal light conditions.

3.5 Cultivar-dependent light intensity requirements under increasing light intensity conditions

Providing photon fluxes that surpass the plants' ability to absorb the supplied energy decrease photosynthetic rates and consequently result in decreasing photosynthate accumulations and biomass productions (Tyystjärvi, 2013). Hence, plants' light saturation points (the intensity at which additional increases in light do not increase photosynthesis) should not be exceeded for optimal (and cost-effective) plant development.

The light saturation point of *Ocimum basilicum* L. was recently determined [under an RB spectrum with narrow peaks at 660 and 445 nm, ratio 7:3, utilized cultivar not provided] to be between 420 and 545 $\mu\text{mol m}^{-2} \text{s}^{-1}$ (Park et al., 2016). Also, Beaman et al. (2009) determined [under cool white fluorescent and

incandescent lamps] high light intensity requirements of $500 \mu\text{mol m}^{-2} \text{s}^{-1}$ for optimal cultivation of green basil cultivars 'Italian Large Leaf', 'Genovese' and 'Nufar'. In contrast, a current review by Sipos et al. (2021) concluded constant spectrum-dependent PFDs of only 180 to $300 \mu\text{mol m}^{-2} \text{s}^{-1}$ to be adequate for basil cultivation. However, the review does not take cultivar-dependent differences into account, even though optimal light intensities are known to vary among cultivars. (Lee et al., 2019; Viršilė et al., 2019). In our investigation, basil plants developed under rising (not constant) photon fluxes as the basil grew towards the LED light sources in proximity (Figure 22).

If not constantly adjusted manually, increasing light intensity gradients are common under space-limited growing conditions e.g., in vertical farms and plant factories (Tabbert et al., 2022a), and could be used strategically since light requirements and the ability to absorb light energy generally increases during plant development until saturation is reached (Currey et al., 2017). For example, providing increasing light intensities resulted in shoot dry weights and leaf numbers alike those generated under constantly high light intensities (Lopez and Runkle, 2008; Oh et al., 2010) but under reduced energy costs (Poulet et al., 2014).

In general, all four of our investigated basil cultivars developed well under rising light intensity conditions which is in accordance with Solis-Toapanta and Gómez (2019), who evaluated growths and photosynthetic capacities of green basil cultivar 'Genovese Compact' and purple cultivar 'Red Rubin' under increasing and constant light intensities.

However, (as described in section 3.3) the light intensities reached under I_{High} during the last week of our experiment (28- 35 DAS) led to adverse, quality-reducing effects in the investigated green basil cultivars. Average PFDs above 312, 331 and $309 \mu\text{mol m}^{-2} \text{s}^{-1}$ under I_{High} became detrimental and should therefore not be exceeded under the applied spectral composition (and growing conditions). In contrast, cv. Anise, cv. Cinnamon and cv. Thai Magic indicated no unfavorable signs under average PFDs of 175, 198 and $176 \mu\text{mol m}^{-2} \text{s}^{-1}$ under I_{Low} by the end of the experiment (Table 19). Hence, even under the increasing light intensity conditions applied in our study, the recommended upper limit of $300 \mu\text{mol m}^{-2} \text{s}^{-1}$ for commercial basil production under artificial lighting by Sipos et al. (2021) holds true for the investigated cultivars 'Anise', 'Cinnamon' and 'Thai Magic'. In contrast, the light-tolerant purple basil cultivar 'Dark Opal' could be grown under artificial PFDs greater than $320 \mu\text{mol m}^{-2} \text{s}^{-1}$ as no obvious negative effects were detected at this light intensity during harvest, and could generate higher yields than measured in our study.

However, with the high-quality market-ready basil within 30-37 DAS (Figures 24A–H) detected under I_{Low} under increasing light intensities (between ~ 100 and $200 \mu\text{mol m}^{-2} \text{s}^{-1}$ (Table 19)) mostly below the lowest recommended constant light intensity of $180 \mu\text{mol m}^{-2} \text{s}^{-1}$ as recently reviewed by Sipos et al.

(2021), the increasing light conditions applied in this study show that even with lower than previously assumed light requirements, high-quality basil productions under artificial light conditions are possible.

3.6 Cultivar-specific VOC concentrations change over time

The gas chromatographic analyses of basil leaf extracts resulted in the identification of 37 volatile organic compounds (VOCs), representing more than 96 % of all detected compounds. All investigated cultivars showed compositional similarities as many VOC compounds (e.g., 1,8-cineole, β -elemene and methyl eugenol) were found in all four basil cultivars. Nevertheless, cultivars cv. Anise and cv. Thai Magic were characterized by high concentrations of methyl chavicol (Tables 20, 21), whereas linalool, methyl chavicol, *trans*-methyl cinnamate and methyl eugenol were the major compounds of cultivar 'Cinnamon' (Table 22). Leaf extracts of the cultivar 'Dark Opal' were characterized by high concentrations of methyl eugenol, as well as 1,8-cineole, linalool and eugenol (Table 23). Thus, each cultivars' VOC compositions as affected by the artificial light conditions applied in this study are in good agreement with published VOC compositions identified under greenhouse and field conditions (Elansary and Mahmoud, 2014; Wesolowska and Jadczyk, 2016; Maggio et al., 2016; Varga et al., 2017; Dehsheikh et al., 2020).

Table 20 – Relative abundance of major volatile organic compounds identified in the leaves of *O. basilicum* L. cv. ‘Anise’ as affected by LED light intensity treatments over time.

No.	Compound	RI ¹	I _{Low}				I _{High}			
			DAS 14	DAS 21	DAS 28	DAS 35	DAS 14	DAS 21	DAS 28	DAS 35
Percent (%) of total volatile organic compound composition ²										
1	<i>α</i> -pinene	938	-	-	0.3±0.0 ^{bc}	0.3±0.0 ^c	-	0.4±0.0 ^{ab}	0.4±0.0 ^{abc}	0.4±0.0 ^a
2	sabinene	978	-	-	0.3±0.0 ^c	0.3±0.0 ^c	-	0.4±0.0 ^{abc}	0.3±0.0 ^{bc}	0.4±0.0 ^a
3	<i>β</i> -pinene	982	0.9±0.1 ^a	0.7±0.0 ^c	0.7±0.1 ^c	0.7±0.1 ^c	0.9±0.0 ^a	0.8±0.0 ^{ab}	0.7±0.1 ^{bc}	0.9±0.0 ^a
4	<i>β</i> -myrcene	992	-	-	-	0.3±0.0 ^b	-	-	0.4±0.1 ^b	0.5±0.0 ^a
5	limonene	1033	-	-	-	0.3±0.0 ^b	-	-	0.3±0.0 ^{ab}	0.3±0.0 ^a
6	1,8-cineole	1036	8.2±0.5^{bc}	7.0±0.4^d	6.8±0.5^d	7.2±0.5^{cd}	8.4±0.2^b	8.2±0.3^b	7.9±0.8^{bc}	9.3±0.3^a
7	<i>trans</i> - <i>β</i> -ocimene	1050	-	0.5±0.0 ^d	0.7±0.1 ^c	0.9±0.1 ^b	-	0.7±0.1 ^c	1.0±0.1 ^b	1.3±0.1 ^a
8	camphor	1154	1.5±0.1 ^a	1.3±0.1 ^b	1.3±0.1 ^b	1.4±0.1 ^{ab}	1.4±0.0 ^{ab}	1.5±0.1 ^a	1.5±0.2 ^a	1.3±0.1 ^b
9	<i>α</i> -terpineol	1197	-	0.7±0.0 ^{cd}	0.7±0.0 ^d	0.8±0.0 ^{bc}	0.8±0.0 ^{bc}	0.8±0.0 ^b	0.8±0.1 ^b	1.0±0.1 ^a
10	methyl chavicol	1204	76.9±1.4^{abc}	78.5±0.7^a	77.4±1.0^{ab}	74.5±1.2^{cd}	76.2±1.1^{bc}	75.4±1.1^{cd}	74.0±1.9^d	68.9±0.8^e
11	<i>cis</i> -methyl cinnamate	1294	-	-	-	0.3±0.1 ^b	-	-	0.4±0.1 ^b	0.5±0.1 ^a
12	<i>trans</i> -methyl cinnamate	1390	0.9±0.1 ^a	0.5±0.0 ^c	0.4±0.0 ^{cd}	0.3±0.0 ^{de}	0.6±0.0 ^b	0.4±0.0 ^{cde}	0.3±0.0 ^e	0.3±0.0 ^e
13	<i>β</i> -elemene	1402	-	-	-	0.4±0.1 ^{ab}	-	-	0.4±0.1 ^b	0.5±0.0 ^a
14	methyl eugenol	1407	-	0.5±0.0 ^c	0.5±0.0 ^c	0.5±0.0 ^c	0.7±0.0 ^a	0.6±0.0 ^b	0.6±0.1 ^{abc}	0.5±0.0 ^c
15	aromadendrene	1446	2.4±0.4 ^{abcde}	1.6±0.2 ^{bcd}	1.4±0.1 ^{de}	1.3±0.2 ^e	2.1±0.1 ^a	1.8±0.1 ^b	1.4±0.1 ^{de}	0.9±0.1 ^f
16	<i>β</i> -farnesene	1461	6.2±0.8 ^a	4.7±0.3 ^b	4.2±0.5 ^{bc}	3.4±0.3 ^{de}	4.6±0.2 ^b	4.0±0.2 ^{cd}	3.3±0.4 ^e	2.2±0.3 ^f
17	<i>α</i> -amorphene	1471	1.6±0.2 ^{ab}	1.1±0.1 ^{abc}	0.9±0.0 ^{bcd}	0.9±0.1 ^{cd}	1.2±0.1 ^a	0.9±0.1 ^{bcd}	0.9±0.1 ^{bcd}	0.8±0.1 ^d
18	bicyclogermacrene	1498	2.6±0.5 ^{bcd}	2.1±0.2 ^d	2.8±0.3 ^c	3.6±0.2 ^b	2.1±0.1 ^d	2.5±0.4 ^{cd}	3.7±0.5 ^b	4.4±0.2 ^a
19	<i>δ</i> -cadinene ³	1521	-	-	-	0.3±0.0 ^b	-	-	-	0.5±0.1 ^a
20	<i>cis</i> -nerolidol	1529	-	0.4±0.0 ^d	0.7±0.1 ^c	1.0±0.1 ^b	-	0.7±0.1 ^c	1.1±0.2 ^b	1.5±0.1 ^a
21	<i>α</i> -cadinol	1657	-	0.6±0.1 ^d	1.2±0.1 ^c	1.8±0.1 ^b	0.6±0.0 ^d	1.2±0.2 ^c	2.1±0.4 ^{ab}	2.6±0.2 ^a
TOTAL [%] ⁴			100±0.0	100.0±0.0	100.0±0.0	99.8±0.2	99.8±0.2	99.7±0.2	99.8±0.2	98.6±0.3
VOC content [%] ⁵			0.4±0.1 ^e	0.8±0.1 ^{bcd}	0.8±0.1 ^{abc}	1.0±0.2 ^a	0.5±0.1 ^{de}	0.7±0.1 ^{cd}	0.9±0.2 ^{abc}	1.0±0.1 ^{ab}
VOC content [mg total L _{DM} ⁻¹] ⁶							7.3±0.1 ^b			

RI = retention index; DAS = days after sowing; different letters within a row indicate significant differences at $p \leq 0.5$.

¹ Presented are mean RIs of samples under GC-FID conditions on an HP-5MS column relative to a series of n-alkanes.

² Presented are mean percentages \pm SD of volatile organic compounds of all analyzed basil leaf extracts ($n = 8$ leaf extracts per light treatment and DAS).

³ Data set was analyzed via unpaired t-test with p -value ≤ 0.05 .

⁴ Percentage [%] \pm SD represents total of listed volatile organic compounds. (Traces of eight identified compounds (namely *cis*-sabinene hydrate (RI 1072), borneol (RI 1174), chavicol (RI 1253), eugenol (RI1364), *α*-humulene (RI 1452), germacrene D (RI 1480), spathulenol (RI 1578) *epi-α*-cadinol (RI 1633) are excluded from the table.

⁵ Presented are average VOC contents \pm SD in percent [%] per gram of leaf dry matter (w/w) from four independent experimental replications per light treatment.

⁶ Presented are calculated average total VOC contents \pm SD in mg total L_{DM}⁻¹ (leaf dry matter) across four spatial replications at harvest (35 DAS) per basil pot.

Table 21 – Relative abundance of major volatile organic compounds identified in the leaves of *O. basilicum* L. cv. ‘Thai Magic’ as affected by LED light intensity treatments over time.

No.	Compound	RI ¹	I _{Low}				I _{High}			
			DAS 14	DAS 21	DAS 28	DAS 35	DAS 14	DAS 21	DAS 28	DAS 35
Percent (%) of total volatile organic compound composition ²										
1	α -pinene	938	-	-	0.3 \pm 0.0	0.2 \pm 0.0	-	-	0.2 \pm 0.0	0.2 \pm 0.0
2	β -pinene	982	-	0.4 \pm 0.0	0.3 \pm 0.0	0.3 \pm 0.0	-	0.4 \pm 0.0	0.4 \pm 0.1	0.4 \pm 0.0
3	β -myrcene	992	-	-	0.3 \pm 0.0	0.3 \pm 0.0	-	-	0.4 \pm 0.1	0.3 \pm 0.0
4	limonene	1033	0.7 \pm 0.2 ^{abc}	0.7 \pm 0.1 ^a	0.6 \pm 0.0 ^{ab}	0.5 \pm 0.1 ^{bc}	0.7 \pm 0.0 ^a	0.7 \pm 0.1 ^{ab}	0.6 \pm 0.1 ^{abc}	0.5 \pm 0.0 ^c
5	1,8-cineole	1036	2.5 \pm 0.5 ^d	3.4 \pm 0.4 ^c	3.4 \pm 0.4 ^c	3.6 \pm 0.3 ^{bc}	3.9 \pm 0.5 ^{abc}	4.4 \pm 0.5 ^a	4.2 \pm 0.6 ^{ab}	3.9 \pm 0.4 ^{abc}
6	<i>trans</i> - β -ocimene	1050	0.7 \pm 0.1 ^e	0.8 \pm 0.1 ^{de}	1.1 \pm 0.1 ^c	1.4 \pm 0.2 ^b	1.0 \pm 0.1 ^c	0.9 \pm 0.1 ^{cd}	1.7 \pm 0.3 ^{ab}	1.8 \pm 0.2 ^a
7	terpinolene	1095	2.9 \pm 0.9 ^a	2.4 \pm 0.6 ^a	1.8 \pm 0.2 ^b	1.2 \pm 0.3 ^c	3.1 \pm 0.8 ^a	2.2 \pm 0.6 ^a	1.3 \pm 0.3 ^c	0.8 \pm 0.1 ^c
8	linalool	1100	-	0.4 \pm 0.1 ^c	0.6 \pm 0.1 ^{bc}	0.9 \pm 0.3 ^{ab}	-	1.2 \pm 0.8 ^{abc}	1.3 \pm 0.4 ^a	1.2 \pm 0.3 ^a
9	camphor	1154	1.1 \pm 0.1 ^c	1.3 \pm 0.3 ^{bc}	1.3 \pm 0.1 ^{bc}	1.5 \pm 0.2 ^b	1.7 \pm 0.4 ^{ab}	2.0 \pm 0.3 ^a	1.9 \pm 0.2 ^a	1.4 \pm 0.2 ^{bc}
10	borneol	1174	-	0.4 \pm 0.1	0.5 \pm 0.1	0.7 \pm 0.1	-	0.5 \pm 0.1	0.8 \pm 0.2	1.4 \pm 0.3
11	α -terpineol	1197	0.4 \pm 0.0 ^c	0.4 \pm 0.0 ^c	0.5 \pm 0.1 ^{bc}	0.5 \pm 0.0 ^b	0.5 \pm 0.1 ^{bc}	0.5 \pm 0.0 ^b	0.7 \pm 0.1 ^a	0.7 \pm 0.1 ^a
12	methyl chavicol	1204	69.7\pm1.9^{abcde}	73.0\pm2.6^{abc}	73.5\pm2.0^a	71.7\pm1.1^{abcd}	68.7\pm4.2^{cde}	68.6\pm1.8^{de}	66.4\pm3.3^e	70.1\pm2.3^{abcde}
13	<i>trans</i> -methyl cinnamate	1390	1.1 \pm 0.1 ^a	0.7 \pm 0.1 ^b	0.6 \pm 0.1 ^c	0.3 \pm 0.0 ^{de}	0.8 \pm 0.1 ^b	0.4 \pm 0.1 ^{cd}	0.2 \pm 0.0 ^e	-
14	β -elemene	1403	-	-	0.3 \pm 0.0 ^b	0.4 \pm 0.1 ^b	-	-	0.4 \pm 0.1 ^b	0.7 \pm 0.1 ^a
15	methyl eugenol	1406	7.2 \pm 1.8 ^a	3.0 \pm 0.4 ^{bc}	2.2 \pm 0.6 ^{cd}	1.4 \pm 0.2 ^d	4.2 \pm 0.6 ^{ab}	2.0 \pm 0.4 ^d	1.1 \pm 0.1 ^e	0.9 \pm 0.2 ^e
16	α - <i>trans</i> -bergamotene	1437								
17	aromadendrene	1446	4.6 \pm 0.1 ^b	4.4 \pm 0.8 ^b	4.3 \pm 0.3 ^b	5.2 \pm 0.8 ^{ab}	5.4 \pm 0.5 ^{ab}	5.7 \pm 0.8 ^{ab}	6.5 \pm 1.1 ^a	5.3 \pm 1.1 ^{ab}
18	β -farnesene	1460	3.8 \pm 0.7 ^a	2.6 \pm 0.3 ^b	2.6 \pm 0.4 ^b	2.2 \pm 0.3 ^{bc}	3.5 \pm 0.6 ^a	2.1 \pm 0.3 ^{bc}	2.0 \pm 0.5 ^{bc}	1.6 \pm 0.4 ^c
19	bicyclogermacrene	1497	1.0 \pm 0.2 ^{de}	0.8 \pm 0.0 ^e	1.1 \pm 0.2 ^{bcd}	1.4 \pm 0.1 ^{ab}	1.2 \pm 0.2 ^{bcd}	1.1 \pm 0.2 ^{cde}	1.6 \pm 0.4 ^{abc}	1.8 \pm 0.3 ^a
20	γ -cadinene	1514	-	-	0.3 \pm 0.1 ^c	0.4 \pm 0.1 ^{bc}	-	-	0.5 \pm 0.1 ^{ab}	0.5 \pm 0.1 ^a
21	δ -cadinene	1521	-	-	0.3 \pm 0.1 ^c	0.5 \pm 0.2 ^{bc}	-	-	0.7 \pm 0.1 ^{ab}	0.9 \pm 0.2 ^a
22	<i>cis</i> -nerolidol	1529	-	0.4 \pm 0.0 ^d	0.6 \pm 0.1 ^c	0.8 \pm 0.1 ^b	-	0.8 \pm 0.2 ^{bc}	1.1 \pm 0.2 ^{ab}	1.3 \pm 0.2 ^a
23	spathulenol	1578	0.5 \pm 0.1 ^c	1.2 \pm 0.5 ^{ab}	0.7 \pm 0.4 ^{bc}	0.6 \pm 0.2 ^{bc}	1.0 \pm 0.2 ^b	2.0 \pm 0.5 ^a	0.6 \pm 0.2 ^{bc}	0.6 \pm 0.1 ^{bc}
24	<i>epi</i> - α -cadinol	1633	-	-	-	0.3 \pm 0.0 ^b	-	-	0.3 \pm 0.0 ^a	0.4 \pm 0.1 ^a
25	α -cadinol	1657	0.4 \pm 0.1 ^f	0.7 \pm 0.1 ^e	1.1 \pm 0.2 ^{cd}	1.5 \pm 0.2 ^{bc}	0.8 \pm 0.2 ^{def}	1.3 \pm 0.3 ^{bcd}	1.9 \pm 0.4 ^{ab}	2.3 \pm 0.3 ^a
TOTAL [%] ³			96.7 \pm 0.7	97.5 \pm 0.6	97.9 \pm 0.4	97.6 \pm 0.4	97.2 \pm 0.6	96.6 \pm 0.2	96.5 \pm 1.1	97.6 \pm 0.9
VOC content [%] ⁴			0.9 \pm 0.1 ^{bc}	0.9 \pm 0.2 ^{bc}	1.2 \pm 0.2 ^{abc}	1.3 \pm 0.2 ^{ab}	0.8 \pm 0.2 ^c	0.7 \pm 0.2 ^c	1.4 \pm 0.4 ^a	0.9 \pm 0.3 ^{bc}
VOC content [mg total L _{DM} ⁻¹] ⁵						10.5 \pm 0.5 ^b				19.2 \pm 0.5 ^a

RI = retention index; DAS = days after sowing; different letters within a row indicate significant differences at $p \leq 0.5$.

¹ Presented are mean RIs of samples under GC-FID conditions on an HP-5MS column relative to a series of n-alkanes.

² Presented are mean percentages \pm SD of volatile organic compounds of all analyzed basil leaf extracts ($n = 8$ leaf extracts per light treatment and DAS)

³ Percentage [%] \pm SD represents total of listed volatile organic compounds. (Traces of nine identified compounds (namely camphene (RI 954), sabinene (RI 978), *cis*-sabinene hydrate (RI 1072), chavicol (RI 1253), nerol (RI 1227), *cis*-methyl cinnamate (RI 1294), eugenol (RI 1364), α -humulene (RI 1452), α -amorphene (RI 1471), germacrene D (RI 1479), *trans*-cadina-1,4-diene (RI 1534), viridiflorol (RI 1596) and traces of four unidentified compounds (RI 1015, RI 1120, RI 1261, RI 1557) are excluded from the table.)

⁴ Presented are average VOC contents \pm SD in percent [%] per gram of leaf dry matter (w/w) from four independent experimental replications per light treatment.

⁵ Presented are calculated average total VOC contents \pm SD in mg total L_{DM}^{-1} (leaf dry matter) across four spatial replications at harvest (35 DAS) per basil pot.

Table 22 – Relative abundance of major volatile organic compounds identified in the leaves of *O. basilicum* L. cv. ‘Cinnamon’ as affected by LED light intensity treatments over time.

No.	Compound	RI ¹	I _{Low}				I _{High}			
			DAS 14	DAS 21	DAS 28	DAS 35	DAS 14	DAS 21	DAS 28	DAS 35
Percent (%) of total volatile organic compound composition ²										
1	1,8-cineole	1036	3.0 \pm 0.7 ^{ab}	2.5 \pm 0.6 ^{ab}	2.4 \pm 0.8 ^b	3.4 \pm 0.7 ^a	3.3 \pm 0.7 ^{ab}	3.1 \pm 0.5 ^{ab}	2.7 \pm 0.4 ^{ab}	2.6 \pm 0.6 ^{ab}
2	<i>trans</i> - β -ocimene	1049	0.6 \pm 0.0	0.6 \pm 0.1	0.5 \pm 0.2	0.5 \pm 0.1	0.6 \pm 0.3	0.7 \pm 0.1	0.5 \pm 0.0	0.6 \pm 0.3
3	terpinolene	1094	1.6 \pm 0.4 ^a	0.9 \pm 0.3 ^{bc}	0.6 \pm 0.2 ^{bc}	0.4 \pm 0.1 ^c	1.6 \pm 0.4 ^a	1.0 \pm 0.4 ^b	0.5 \pm 0.1 ^{bc}	0.5 \pm 0.1 ^{bc}
4	linalool	1101	7.9\pm2.2^e	13.8\pm2.5^d	18.8\pm1.8^c	23.7\pm3.1^{ab}	13.6\pm3.0^d	20.1\pm2.8^{bc}	27.2\pm3.1^a	23.5\pm5.0^{abc}
5	camphor	1153	0.8 \pm 0.1	0.6 \pm 0.1	0.6 \pm 0.2	0.5 \pm 0.2	0.8 \pm 0.1	0.8 \pm 0.3	0.5 \pm 0.2	0.5 \pm 0.2
6	α -terpineol	1184	0.9 \pm 0.1	0.8 \pm 0.2	0.9 \pm 0.3	0.7 \pm 0.2	0.7 \pm 0.1	0.9 \pm 0.2	0.7 \pm 0.3	0.7 \pm 0.5
7	methyl chavicol	1203	26.8\pm11.3^a	20.5\pm5.4^{ab}	15.3\pm7.1^{bc}	8.7\pm5.0^c	17.7\pm10.0^{abc}	12.0\pm4.8^{bc}	9.1\pm6.5^{bc}	9.8\pm4.2^{bc}
9	eugenol	1364	1.7 \pm 1.1	1.6 \pm 0.5	3.1 \pm 1.6	5.2 \pm 4.8	3.8 \pm 2.2	1.5 \pm 0.7	5.9 \pm 5.1	2.1 \pm 2.5
10	<i>trans</i>-methyl cinnamate	1391	8.7\pm3.8^d	30.2\pm6.0^{abc}	35.1\pm8.2^a	33.3\pm8.4^a	20.2\pm6.4^{bcd}	34.4\pm6.2^a	27.5\pm5.6^{ab}	36.9\pm12.1^a
11	β -elemene	1403	0.7 \pm 0.0	0.5 \pm 0.1	0.6 \pm 0.2	0.9 \pm 0.3	0.4 \pm 0.0	0.6 \pm 0.2	0.7 \pm 0.2	0.9 \pm 0.3
12	methyl eugenol	1406	27.5\pm10.8^a	13.2\pm3.7^{abc}	6.7\pm1.9^{def}	4.0\pm2.9^{efg}	18.2\pm8.9^{abcd}	7.5\pm1.6^{cde}	3.3\pm2.2^{fg}	0.9\pm0.2^g
13	aromadendrene	1446	2.2 \pm 0.6 ^{abc}	1.4 \pm 0.5 ^{abcd}	1.3 \pm 0.2 ^d	1.3 \pm 0.4 ^{cd}	2.3 \pm 0.6 ^{ab}	1.9 \pm 1.1 ^{bcd}	2.0 \pm 1.2 ^{bcd}	0.9 \pm 0.3 ^d
14	α -humulene	1451	-	-	0.4 \pm 0.1 ^b	0.6 \pm 0.2 ^{ab}	-	0.4 \pm 0.0 ^b	0.8 \pm 0.3 ^a	0.7 \pm 0.2 ^{ab}
15	β -farnesene	1460	5.6 \pm 0.7 ^b	4.3 \pm 0.5 ^c	3.0 \pm 0.5 ^{de}	2.2 \pm 0.5 ^{ef}	6.7 \pm 1.0 ^a	3.5 \pm 0.5 ^{cd}	2.5 \pm 0.5 ^{def}	1.6 \pm 0.5 ^f
16	α -amorphene	1471	3.1 \pm 1.0 ^a	1.2 \pm 0.3 ^{bc}	0.8 \pm 0.1 ^d	-	1.6 \pm 0.3 ^{ab}	1.0 \pm 0.2 ^{cd}	1.0 \pm 0.0 ^c	0.6 \pm 0.2 ^d
17	germacrene D	1479	-	-	-	0.4 \pm 0.0 ^b	-	0.3 \pm 0.0 ^c	0.5 \pm 0.0 ^a	0.4 \pm 0.1 ^{ab}
18	bicyclogermacrene	1497	4.3 \pm 0.6 ^{ab}	3.6 \pm 0.3 ^b	3.8 \pm 0.2 ^{ab}	4.3 \pm 0.3 ^a	4.0 \pm 0.5 ^{ab}	3.8 \pm 0.2 ^{ab}	5.0 \pm 0.7 ^a	4.9 \pm 0.7 ^{ab}
19	γ -cadinene	1513	0.8 \pm 0.2 ^b	1.0 \pm 0.2 ^{ab}	1.1 \pm 0.1 ^{ab}	1.4 \pm 0.2 ^a	1.1 \pm 0.2 ^{ab}	1.2 \pm 0.1 ^{ab}	1.6 \pm 0.6 ^{ab}	1.5 \pm 0.5 ^{ab}
20	δ -cadinene	1521	-	0.5 \pm 0.0 ^b	0.5 \pm 0.3 ^b	1.0 \pm 0.4 ^{ab}	-	0.6 \pm 0.1 ^b	1.3 \pm 0.3 ^a	1.0 \pm 0.3 ^{ab}
21	<i>cis</i> -nerolidol	1529	1.3 \pm 0.3 ^c	1.3 \pm 0.1 ^c	1.6 \pm 0.2 ^{bc}	2.1 \pm 0.2 ^a	1.4 \pm 0.2 ^c	1.8 \pm 0.3 ^b	2.5 \pm 0.1 ^a	2.5 \pm 0.4 ^a
22	<i>epi</i> - α -cadinol	1633	-	-	0.4 \pm 0.1 ^c	0.6 \pm 0.1 ^{bc}	-	0.5 \pm 0.1 ^c	0.7 \pm 0.1 ^{ab}	0.7 \pm 0.1 ^a
23	α -cadinol	1657	2.4 \pm 0.6 ^d	2.5 \pm 0.2 ^d	3.2 \pm 0.6 ^{cd}	4.2 \pm 0.5 ^{ab}	2.6 \pm 0.7 ^d	3.4 \pm 0.8 ^{bcd}	5.1 \pm 0.8 ^a	5.1 \pm 1.0 ^{ab}
TOTAL [%] ³			99.6 \pm 0.5	100.0 \pm 0.0	99.7 \pm 0.5	98.4 \pm 0.6	99.6 \pm 0.7	99.2 \pm 0.8	98.6 \pm 0.6	97.8 \pm 1.0

VOC content [%] ⁴	0.4±0.1 ^d	0.6±0.1 ^{ab}	0.7±0.2 ^{ab}	1.1±0.4 ^a	0.5±0.2 ^{bcd}	0.7±0.3 ^{abcd}	0.8±0.2 ^{abcd}	0.9±0.2 ^{ab}
VOC content [mg total L _{DM} ⁻¹] ⁵	15.6±1.2 ^b							17.8±2.0 ^a

RI = retention index; DAS = days after sowing; different letters within a row indicate significant differences at $p \leq 0.5$.

¹ Presented are mean RIs of samples under GC-FID conditions on an HP-5MS column relative to a series of n-alkanes.

² Presented are mean percentages \pm SD of volatile organic compounds of all analyzed basil leaf extracts ($n = 8$ leaf extracts per light treatment and DAS)

³ Percentage [%] \pm SD represents total of listed volatile organic compounds. (Traces of eight identified compounds (namely β -pinene (RI 982), limonene (RI 1033), *cis*-linalool oxide (RI 1071), borneol (RI 1174), α -terpineol (RI 1196), chavicol (RI 1253), *cis*-methyl cinnamate (RI 1293), viridiflorol (RI 1596) and traces of two unidentified compounds (RI 1569, RI 1574) are excluded from the table.)

⁴ Presented are average VOC contents \pm SD in percent [%] per gram of leaf dry matter (w/w) from four independent experimental replications per light treatment.

⁵ Presented are calculated average total VOC contents \pm SD in mg total L_{DM}⁻¹ (leaf dry matter) across four spatial replications at harvest (35 DAS) per basil pot.

Table 23 – Relative abundance of major volatile organic compounds identified in the leaves of *O. basilicum* L. cv. ‘Dark Opal’ as affected by LED light intensity treatments over time.

No.	Compound	RI ¹	I _{Low}				I _{High}			
			DAS 14	DAS 21	DAS 28	DAS 35	DAS 14	DAS 21	DAS 28	DAS 35
Percent (%) of total volatile organic compound composition ²										
1	α -pinene	938	0.4±0.0 ^{cd}	0.4±0.0 ^{cd}	0.4±0.0 ^{cd}	0.4±0.1 ^{bcd}	0.4±0.0 ^{cd}	0.4±0.1 ^{cd}	0.5±0.0 ^{ab}	0.5±0.1 ^{abc}
2	β -pinene	982	0.5±0.0 ^c	0.6±0.1 ^{bc}	0.6±0.1 ^{bc}	0.7±0.1 ^b	0.7±0.0 ^b	0.6±0.1 ^{bc}	0.9±0.1 ^a	0.9±0.1 ^a
3	β -myrcene	992	-	0.4±0.1 ^f	0.4±0.1 ^{def}	0.5±0.1 ^{bcd}	0.5±0.0 ^{ef}	0.5±0.1 ^{def}	0.6±0.0 ^{ab}	0.7±0.1 ^a
4	limonene	1033	0.7±0.1 ^{abc}	0.6±0.1 ^{abc}	0.6±0.1 ^{bc}	0.6±0.1 ^{abc}	0.7±0.0 ^a	0.6±0.1 ^c	0.7±0.1 ^{ab}	0.6±0.1 ^{abc}
5	1,8-cineole	1036	4.4±0.3^d	5.2±0.5^d	5.6±0.7^d	6.6±0.8^{bcd}	6.0±0.0^{abcd}	6.3±0.8^d	8.2±1.0^{abcd}	9.5±1.1^a
6	terpinolene	1095	3.3±0.7 ^{abcd}	2.6±0.3 ^a	2.3±0.2 ^{abc}	2.2±0.1 ^{abc}	2.9±0.3 ^a	2.1±0.2 ^{bc}	2.0±0.2 ^{bc}	1.3±0.2 ^d
7	linalool	1101	1.6±0.7^e	2.7±0.4^e	4.5±0.8^d	8.8±1.5^c	5.4±0.4^d	8.3±1.2^c	16.0±2.3^b	28.4±5.0^a
8	α -terpineol	1197	-	0.3±0.0 ^f	0.4±0.0 ^e	0.5±0.0 ^{cd}	0.5±0.0 ^{de}	0.6±0.1 ^c	0.7±0.1 ^b	1.0±0.1 ^a
9	nerol	1227	0.9±0.1 ^b	0.9±0.2 ^b	0.9±0.1 ^b	0.9±0.1 ^b	0.9±0.1 ^b	1.0±0.1 ^b	1.5±0.2 ^a	1.7±0.2 ^a
10	eugenol	1364	-	0.6±0.2^g	1.0±0.3^{fg}	3.2±0.8^{cd}	2.1±0.9^{defg}	4.9±1.0^{bc}	4.6±0.3^b	9.0±2.5^a
11	β -elemene	1403	-	0.4±0.1 ^d	0.3±0.2 ^{cd}	0.3±0.2 ^{cd}	0.3±0.0 ^d	0.5±0.1 ^c	0.5±0.1 ^{bcd}	0.8±0.1 ^a
12	methyl eugenol	1408	75.7±3.2^{ab}	74.2±1.7^a	72.3±2.2^a	63.0±3.9^{cd}	66.3±1.5^{bc}	61.0±2.7^d	48.4±3.8^f	25.2±4.3^g
13	α - <i>trans</i> -bergamotene	1437	1.9±0.1 ^a	1.7±0.1 ^{bc}	1.7±0.1 ^{bc}	1.7±0.1 ^{abc}	1.5±0.1 ^c	1.7±0.0 ^{abc}	1.7±0.1 ^{abc}	1.9±0.2 ^{ab}
14	aromadendrene	1446	0.4±0.1 ^{bcd}	0.3±0.0 ^f	0.3±0.0 ^{ef}	0.3±0.0 ^{def}	0.5±0.1 ^{ab}	0.4±0.1 ^{bcd}	0.4±0.1 ^{cde}	0.4±0.1 ^{bcd}
15	α -humulene	1451	0.4±0.0 ^{de}	0.3±0.0 ^{ef}	0.3±0.0 ^{ef}	0.4±0.0 ^{cde}	0.2±0.0 ^f	0.4±0.0 ^e	0.5±0.1 ^{bc}	0.8±0.1 ^a
16	β -farnesene	1461	4.4±0.8 ^{ab}	3.2±0.3 ^{ab}	3.2±0.2 ^b	3.4±0.3 ^{ab}	4.0±0.5 ^{ab}	3.7±0.2 ^a	3.9±0.4 ^a	3.3±0.3 ^{ab}
17	α -amorphene	1471	0.8±0.1 ^a	0.5±0.0 ^{cd}	0.5±0.0 ^{de}	0.5±0.0 ^e	0.6±0.0 ^{bcd}	0.5±0.0 ^{bcd}	0.6±0.1 ^{bcd}	0.6±0.0 ^{bcd}
18	bicyclogermacrene	1498	1.8±0.2 ^f	1.8±0.1 ^f	2.0±0.1 ^{cdef}	2.1±0.1 ^{bc}	1.9±0.1 ^{cdef}	2.1±0.2 ^{bcd}	2.3±0.2 ^b	3.1±0.2 ^a
19	γ -cadinene	1513	0.5±0.0 ^e	0.5±0.0 ^e	0.7±0.1 ^d	1.0±0.1 ^b	0.8±0.1 ^{cd}	0.9±0.1 ^{bc}	1.2±0.2 ^{abc}	1.3±0.2 ^a
20	δ -cadinene	1521	-	0.1±0.1 ^f	0.4±0.0 ^e	0.6±0.0 ^{bc}	0.3±0.0 ^f	0.5±0.1 ^{de}	0.8±0.1 ^b	1.4±0.1 ^a
21	<i>cis</i> -nerolidol	1529	0.6±0.0 ^{fg}	0.6±0.1 ^{fg}	0.6±0.1 ^{efg}	0.7±0.0 ^{de}	0.6±0.0 ^g	0.7±0.0 ^{de}	0.8±0.1 ^{bcd}	1.2±0.1 ^a

22	α -cadinol	1657	1.1±0.1 ^{fg}	1.1±0.1 ^g	1.2±0.2 ^{efg}	1.1±0.0 ^g	1.1±0.0 ^g	1.3±0.1 ^{def}	1.5±0.2 ^{bcde}	2.3±0.1 ^a
	TOTAL [%] ³		99.4±0.4	99.4±0.2	99.4±0.1	99.1±0.3	98.8±0.3	98.3±0.4	98.8±0.4	98.3±0.3
	VOC content [%] ⁴		0.9±0.0 ^{bcd}	1.2±0.2 ^{ab}	0.9±0.2 ^{cd}	0.8±0.1 ^d	1.5±0.3 ^a	1.1±0.2 ^{abc}	0.8±0.2 ^d	0.8±0.2 ^d
	VOC content [mg total L _{DM} ⁻¹] ⁵					2.6±0.2 ^b				8.5±0.6 ^a

RI = retention index; DAS = days after sowing; different letters within a row indicate significant differences at $p \leq 0.5$.

¹ Presented are mean RIs of samples under GC-FID conditions on an HP-5MS column relative to a series of n-alkanes.

² Presented are mean percentages \pm SD of volatile organic compounds of all analyzed basil leaf extracts ($n = 8$ leaf extracts per light treatment and DAS)

³ Percentage [%] \pm SD represents total of listed volatile organic compounds. (Traces of ten identified compounds (namely sabinene (RI 978), *cis*-linalool oxide (RI 1071), borneol (RI 1174), methyl chavicol (RI 1203), chavicol (RI 1256), β -cubebene (RI 1384), *trans*-methyl cinnamate (RI 1390), germacrene D (RI 1479), viridiflorol (RI 1596), *epi*- α -cadinol (RI 1633) and traces of three unidentified compounds (RI 1015, RI 1120, RI 1548) are excluded from the table.)

⁴ Presented are average VOC contents \pm SD in percent [%] per gram of leaf dry matter (w/w) from four independent experimental replications per light treatment.

⁵ Presented are calculated average total VOC contents \pm SD in mg total L_{DM}⁻¹ (leaf dry matter) across four spatial replications at harvest (35 DAS) per basil pot.

The complexity of VOC profiles increased with the basil's progressing development. In example, while leaf extracts of 14-day-old cv. Anise seedlings were characterized by nine and twelve major volatiles under I_{Low} and I_{High} , respectively, the total of detected VOCs increased weekly and reached their highest total in 35-day-old basil plants (Table 20).

Regardless of the light intensities applied, each cultivar underwent analogous compositional changes throughout the trial period. In example, under both light intensity treatments, percentages of linalool and *trans*-methyl cinnamate increased and percentages of methyl chavicol and methyl eugenol decreased in the developing 'Cinnamon' cultivar (Table 22).

However, in comparison to the compositional changes observed in the cultivars under I_{High} , the same directional changes occurred time-delayed under I_{Low} . In example, while the percentage of methyl chavicol reduced from ~ 17.7 % at 14 DAS to ~ 12.0 % at 21 DAS and ~ 9.1 % at 28 DAS under I_{High} in the basil cultivar 'Cinnamon', a comparable drop was observed one week later under I_{Low} as the percentage of methyl chavicol decreased from ~ 20.5 % at 21 DAS to ~ 15.3 % at 28 DAS and finally ~ 8.7 % at 35 DAS (Table 22). In the same manner, the percentage of linalool increased from ~ 5.4 % at 14 DAS to ~ 8.3 % at 21 DAS under I_{High} , while linalool increased in the same way (from ~ 4.5 to ~ 8.8 %) two weeks later between 28 DAS and 35 DAS under I_{Low} in the cultivar 'Dark Opal', (Table 23).

So far, not many studies have investigated compositional differences in *Ocimum basilicum* L. under different (LED) light intensities, but their outcomes are highly consistent with our findings. In example, Chang et al. (2008) and Walters et al. (2021) reported increasing linalool concentrations in the green basil cultivars 'Genovese' and 'Nufar', respectively, with increasing light intensities, which agrees with our findings in the linalool-containing cultivars 'Cinnamon', 'Dark Opal' and 'Thai Magic'. Also, the observed relative decrease of methyl eugenol with increasing light intensities in cv. Genovese (Chang et al., 2008) was observed in the three cultivars that were characterized by elevated concentrations of methyl eugenol (cv. Cinnamon, cv. Dark Opal and cv. Thai Magic). The authors also described fairly constant as well as slightly increasing relative concentrations of 1,8-cineole in cv. Genovese and cv. Nufar, respectively. This is also congruent with the indifferent relative concentrations of 1,8-cineole in the cultivars 'Anise', 'Cinnamon' and 'Thai Magic, and the slight upwards trend of 1,8-cineole concentrations detected in cv. Dark Opal with increasing light intensity. In addition, the fluctuating relative eugenol concentrations reported by Chang et al. (2008) and Walters et al. (2021) were also detected in our study in the eugenol-containing cultivars 'Cinnamon' and 'Dark Opal'. Alike the findings observed by Walters et al. (2021) in 14-day-old cv. Nufar seedlings, we observed no differences in relative methyl chavicol concentrations between both light treatments throughout the trial period in cv. Cinnamon and cv. Dark Opal and 14 DAS in cv.

Anise. In contrast, decreased relative methyl chavicol concentrations under I_{High} were observed in older cv. Anise at 21, 28 and 35 DAS.

During the last few years, great progress has been made in the elucidation of most of the genes, transcription factors, enzymes, and substrates involved in the biosynthesis of the individual terpenes and phenylpropenes detected in our study. This led to coherent proposals of their biosynthetic pathways in the peltate glands of basil (Gang et al., 2001; Iijima et al., 2004; Kapteyn et al., 2007; Zvi et al., 2012; Dhar et al., 2020). *In vivo* however, the individual VOC profiles depend greatly on enzyme abundance and activity, their substrate specificity and availability (Lewinsohn et al., 2000; Muñoz-Bertomeu et al., 2006; Xie et al., 2008; Singh et al., 2015b; Yahyaa et al., 2019), all of which can be highly affected by abiotic factors (including drought stress (Mandoulakani et al., 2017), carbon dioxide concentration and temperature (Chang et al., 2005; Tursun & Telci, 2020), nutrients and biofertilizers (Hanif et al., 2017, Dehsheikh et al., 2020), light quality (Carvalho et al., 2016; Hosseini et al., 2018; Milenković et al., 2019; Tabbert et al., 2022a) and elicitors (Deschamps & Simon, 2006; Loni et al., 2021)). The dynamics are further complicated as basil's VOC compositions do not only depend on individual leaf maturation (Lewinsohn et al., 2000) but also considerably on the position of the basil leaf along the stem (Fischer et al., 2011). Thus, the underlying processes that regulate these compositional changes are exceptionally complex.

Nevertheless, the weekly assessments of the basil's VOC compositions clearly show that each basil cultivar undergoes fundamentally well-coordinated compositional changes. As the detected compositional changes were identical under both light intensity treatments and occurred only time-delayed under I_{Low} in comparison to I_{High} , it becomes evident that the observed compositional differences in our study (as well as the differences observed by Chang et al., 2008 and Walters et al., 2021) are related to the cultivars' developmental stage and thus, growth rates. The high correlations between the basil's complex VOC profiles and their morphological stages as determined by principal component regressions (Table 24) strongly support this developmental stage-dependency.

Table 24 – Correlation between basil cultivars' complex VOC profiles over time and their morphological stage.

Dependent variable	Goodness of fit ¹			
	'Anise'	'Cinnamon'	'Dark Opal'	'Thai Magic'
Plant height	0.88	0.87	0.85	0.82
Number of leaf pairs	0.75	0.96	0.78	0.87
Number of branch pairs	0.76	0.90	0.90	0.92

¹ Summarized are the coefficients of determination (R^2) that describe the goodness of fit of the selected dependent variable on the basil cultivars' aroma profiles as determined by principal component regressions (PCRs).

Different VOC accumulation patterns were observed between the investigated basil cultivars (Figures 24Q–T). While VOC concentrations per gram of leaf dry matter (L_{DM}) gradually increased in the cultivars 'Anise', 'Cinnamon' and 'Thai Magic' under both light intensity treatments during the trial period, a decreasing trend in VOC concentrations was observed in cv. Dark Opal. That VOC accumulation patterns strongly deviate within the species *Ocimum basilicum* has already been demonstrated by Macchia et al., 2006 and Szabó & Bernáth, 2002.

Within each cultivar, VOC concentrations generally did not differ between I_{Low} and I_{High} during each investigated time point, however, exceptions were observed in the cultivars 'Dark Opal' and 'Thai Magic' (Figures 24Q–T). The reason for the indifferent VOC concentrations observed under both light intensity treatments at each time point are likely to be attributed to the fact that the examined leaf extracts contained all developed leaves per basil plant irrespective of leaf age and maturation: Generally, glandular trichome densities decline while leaves age and expand. Though young leaves generally contain lower VOC quantities than older leaves, younger leaves tend to have higher VOC concentrations due to their lower weight (Fischer et al., 2011). The significantly lower VOC concentration detected under I_{Low} in comparison to I_{High} at 14 DAS in 'Dark Opal' (Figure 24S) may be ascribed to the cultivars' limited photosynthetic capabilities under low light conditions as discussed before in section 3.4 and hence, a presumably lower availability of photosynthates for secondary metabolism. The slightly increased VOC concentration observed under I_{Low} in comparison to I_{High} at 35 DAS in cv. Thai Magic (Figure 24T) may indicate that this cultivar reaches its maximum VOC accumulation before flower buds arise (Figure 23D) after which VOC concentrations decrease – an accumulation pattern that has previously been described for the *Ocimum basilicum* cultivars 'Rit-Sat' and 'Lengyel' (Szabó & Bernáth, 2002) as well as for *Ocimum ciliatum* (Moghaddam et al., 2015). However, further experiments are needed to prove these hypotheses.

When comparing total VOC yields produced at the end of the experiment (35 DAS), all cultivars had accumulated substantially greater VOC quantities under I_{High} than basil of the same age under I_{Low} due to the cultivars' overall greater leaf biomasses accumulated under I_{High} (Table 19, Figures 24U–X). In

comparison to VOC yields under I_{Low} , yields were elevated by ~ 12.4, ~ 45.6, ~ 60.8 and ~ 69.2 % under I_{High} in cultivars 'Cinnamon', 'Thai Magic', 'Anise' and 'Dark Opal', respectively.

It is well known that the flavor of basil is due to the presence and individual concentration of specific terpenes and phenylpropenes (for basil aroma descriptions see Patel et al., 2021). As the leaf extracts of the cultivars 'Anise' and 'Thai Magic' contained high concentrations of methyl chavicol throughout the investigation, both cultivars should be characterized by strong anise-like/licorice flavors regardless of their developmental stage and light intensity treatment applied (Tables 20, 21). With relative concentrations of 1,8-cineole between 6.8 and 9.3 %, 'Anise' should also include a noticeable eucalyptus aroma (Table 20). However, as shown by Lee et al. (2017), a trained panel was able to clearly discriminate between two basil cultivars that contained the same array of flavoring volatiles in different relative ratios. That indicates that the specific flavors of the cultivars 'Cinnamon' and 'Dark Opal' may tremendously change over time: While relatively high concentrations of methyl chavicol (imparting an anise-like/ licorice aroma) and methyl eugenol (imparting a weak clove-like aroma) were detected during 'Cinnamons' early development, more mature 'Cinnamon' basil was characterized by relatively high concentrations of linalool (imparting a sweet floral aroma) and *trans*-methyl cinnamate (imparting a cinnamon-like aroma) (Table 22). Similarly, while methyl eugenol (weak clove-like aroma) clearly dominated in young 'Dark Opal', the relative abundances of linalool (sweet floral aroma), eugenol (clove-like aroma) and 1,8-cineole (eucalyptus aroma) increased greatly over time (Table 23).

Though concrete health risks for humans have not been confirmed, methyl chavicol (estragole) and methyl eugenol have shown to induce dose-dependent genotoxic and carcinogenic effects in multiple independent animal trials (NTP, 2000; Martins et al., 2012) which raised toxicological concerns of these naturally occurring substances. On grounds of the preventive protection of public health, legislators banned the addition of methyl chavicol and methyl eugenol as food additives and set maximum levels of these substances if naturally present in flavorings and food ingredients (Regulation No 1334, 2008). Consequently, basil producers and food processing industries are obligated to exploit possibilities to largely lower these two critical constituents.

As the main VOC in cv. Anise and cv. Thai Magic, methyl chavicol was found in consistently high percentages regardless of DAS and light intensity treatment (Table 20, 21). However, independent of the light intensity treatment, the percentages of methyl chavicol and methyl eugenol continuously decreased during ontogenesis of cv. Cinnamon (Table 22). Thus, by thoughtfully managing the time of harvest, levels of both critical constituents can be significantly reduced. Further, with 75.5 % under I_{Low} and 66.3 % under I_{High} at DAS 14, the percentages of methyl eugenol are indifferently high under both light treatments in cv.

Dark Opal (Table 23). While the percent share reduces only to 63 % under I_{Low} , the percent share significantly drops to 25.2 % under I_{High} by the end of the experiment. Hence, cultivating cv. Dark Opal under low light intensities is not only unsuitable in terms of low yield and insufficient morphological development, but also with regard to methyl eugenol as a compound of toxicological concern.

In addition, as observed in cv. Dark Opal, via suitable light intensity settings, contents of (critical) compounds can be controlled and significantly reduced.

3.7 In contrast to purple basil, green basil cultivars use energy more efficiently under I_{Low}

Despite the accelerated basil development observed under I_{High} , the green-leafed cultivars ‘Anise’, ‘Cinnamon’ and ‘Thai Magic’ converted the available light energy more effectively into biomass under I_{Low} than the basil plants that were cultivated under I_{High} (Table 25). If these three cultivars were to be grown until marketability (based on the morphological criteria described in section 3.2), more than 50 % of electrical energy could be saved under I_{Low} in comparison to I_{High} , while cultivar-dependent yields would only be decreased by approximately 3- 11 % (Table 26). In theory, a little more than one additional crop cycle per year could be generated under I_{High} .

Table 25 – Biomass efficacy of four *Ocimum basilicum* L. cultivars grown under two different light intensity treatments.

Basil cultivar	Biomass efficiency [g kWh ⁻¹] ¹		
	I_{Low}	I_{High}	<i>P</i>
‘Anise’	5.6 ± 0.1 ^a	3.4 ± 0.6 ^b	0.03
‘Cinnamon’	10.0 ± 1.3 ^a	5.2 ± 0.8 ^b	0.01
‘Dark Opal’	2.9 ± 0.1 ^{ns}	3.4 ± 0.6 ^{ns}	<i>ns</i>
‘Thai Magic’	6.7 ± 0.6 ^a	3.9 ± 0.2 ^b	0.01

Different letters within a row indicate significant differences at $p \leq 0.05$; *P* = significance level; *ns* = not significant.

¹ Presented are calculated average basil fresh weights ± *SD* ($n = 4$) produced per kilowatt hour consumed under the experimental area of 1.2 m² by the end of the trial period (35 days after sowing) from four independent spatial replications per light treatment.

In contrast, year-round basil cultivations under I_{Low} would save ~ 57 % in energy usage while cultivar-dependent productivity losses would be between 15-19 % (Table 27). Hence, the great low light adaptability of the green basil cultivars (as described in section 3.4) ultimately resulted in improved biomass efficiencies under I_{Low} when compared to the biomass efficiencies reached under I_{High} . In contrast, biomass efficiencies of cv. Dark Opal were statistically indifferent between the two light intensity

treatments (Table 25). Because cv. Dark Opal did not reach the marketability threshold under I_{Low} during the trial period, a cultivation under I_{Low} light conditions would result in the lowest number of crop cycles per year and the greatest productivity losses of all investigated cultivars (Tables 26, 27).

Table 26 – Energy consumption and biomass at marketability of four *Ocimum basilicum* L. cultivars grown under two different light intensities.

Basil cultivar	Marketability ¹ [DAS]		Energy consumption [kWh] at marketability		Energy savings [%]	FW [g pot ⁻¹] at marketability ²		Productivity loss [%]
	I_{High}	I_{Low}	I_{High}	I_{Low}		I_{High}	I_{Low}	
'Anise'	29	33	327.9	161.1	50.9	~ 11.9	~ 11.5	~ 9.1
'Cinnamon'	27	30	305.3	146.4	52.4	~ 18.7	~ 17.0	~ 3.4
'Dark Opal'	32	<i>na</i>	361.8	<i>na</i>	<i>na</i>	~ 14.9	<i>na</i>	<i>na</i>
'Thai Magic'	30	33	339.2	161.1	52.5	~ 15.0	~ 13.4	~ 10.7

DAS = days after sowing; FW = fresh weight; I_{High} = High light intensity; I_{Low} = Low light intensity; *na* = not available.

¹ Marketability is defined as plant height ≥ 15 cm and/or number of leaf pairs ≥ 4 [by our cooperation partners Oderbruch Müller, an organic nursery in Bad Freienwalde, Germany]; see also Figures 24A-H.

² Basil fresh weights [g pot⁻¹] at marketability were calculated using each cultivars' polynomial biomass rates under each light treatment ($R^2 > 0.99$).

Table 27 – Achievable crop cycles, biomass production, and its energy consumption per year when grown until marketability.

Basil cultivar	Crop cycles per year ¹		FW [kg area ⁻¹ y ⁻¹] ²		Productivity loss [%]	Energy consumption [kWh y ⁻¹]		Energy savings [%]
	I_{High}	I_{Low}	I_{High}	I_{Low}		I_{High}	I_{Low}	
'Anise'	12.6	11.1	~ 10.8	~ 9.2	~ 14.8			
'Cinnamon'	13.5	12.2	~ 18.2	~ 14.9	~ 18.1	4126.6	1781.7	56.8
'Dark Opal'	11.4	<i>na</i>	~ 12.2	<i>na</i>	<i>na</i>			
'Thai Magic'	12.2	11.1	~ 13.2	~ 10.7	~ 18.9			

FW = Fresh weight

¹ From seed to marketability (see also Table 26).

² Fresh weight [kg] per experimental area (1.2 m²) and year were calculated by multiplying the calculated average fresh weights at marketability with the number of possible plant pots ($n = 72$) and the number of possible crop cycles per year.

3.8 Improvement of basil production via eustress management

In general, beneficial effects induced by small doses and/or durations of stress factors are called eustressor effects (Vázquez-Hernández et al., 2019), and basil producers may be encouraged to provoke slight light and/or shade stresses in basil to stimulate different beneficial effects on their performance and/or human health: Even though the observed accumulations of anthocyanins in the top leaves of cv. Anise, cv. Cinnamon and cv. Thai Magic under I_{High} represent direct stress responses triggered by the intense light

conditions they grew into to protect their chloroplasts from photoinhibitory and photooxidative effects (as described in section 3.3), other diverse protective roles are ascribed to anthocyanins as members of the flavonoid group (Lila, 2004). These phytochemicals are known to enhance the plants' resistance to the effects of chilling and freezing and increase their resistance to herbivores and pathogens (Gould, 2004). In addition, numerous protective roles to human health (from antioxidative and free-radical scavenging capabilities, obesity prevention, amelioration of hyperglycemia, neuroprotective effects to positive influences on vascular functions) have been attributed to anthocyanins (well summarized by Lila, 2004). In addition, the light stress under I_{High} resulted in accelerated basil growths, accompanied with enhanced VOC maturations and high yields (as described in sections 3.1, 3.2 and 3.6). On the other hand, the shade stress under I_{Low} resulted in consumer-preferred leaf appearances and producer-preferred biomass efficiencies (as described in sections 3.4 and 3.7). Hence, basil producers may be interested in carefully managing light and/or shade stresses to stimulate specific positive effects of interest in basil and/or to improve their production efficiencies (Vázquez-Hernández et al., 2019).

4. Conclusion

From seed to marketability, the broad-bandwidth LED light spectrum including FR light with elevated R and B light fractions enabled an adequate growth and development of all four investigated basil cultivars ('Anise', 'Cinnamon', 'Dark Opal' and 'Thai Magic') under both rising light intensity conditions applied in this study.

In comparison to the I_{Low} light conditions, I_{High} resulted in an accelerated development and thus expedited marketability of all investigated basil cultivars. However, exposure to light intensities above $300 \mu\text{mol m}^{-2} \text{s}^{-1}$ caused adverse quality-reducing effects in the green-leafed cultivars 'Anise', 'Cinnamon' and 'Thai Magic' and should therefore not be exceeded.

In contrast, the applied I_{Low} light conditions resulted in consumer-preferred appearances and greater biomass efficiencies and appear to be the result of a great low light adaptability of green-leafed basil cultivars. Despite the time-delayed marketability (based on morphological criteria) under I_{Low} in comparison to I_{High} , the superior visual quality of the green-leafed cultivars in combination with the significantly reduced energy consumptions under I_{Low} can ultimately result in greater revenues for basil producers.

Though purple-leafed cultivar 'Dark Opal' was able to mitigate high intensity light stress responses under I_{High} in comparison to the green-leafed cultivars, its indoor production until the common marketability criteria (plant height ≥ 15 cm and/or leaf pairs ≥ 4) are reached remains the least economical

due to the high energy consumptions necessary, the comparatively low yields and number of annual crop cycles possible.

However, basil cultivar-specific VOC contents and profiles proved to change tremendously over time in a developmental stage-correlated manner. Thus, consumer flavor preferences of differently aged basil plants should be further explored, and time of harvest should be individually reconsidered [especially as the demand and popularity of microgreens is on the rise (Kyriacou et al., 2016; Mir et al., 2016)].

1. General Discussion

1.1 Effectiveness of the developed broadband LED lighting systems and some technological challenges to overcome.

Besides the light fixtures' inherent photosynthetic photon efficacies (pertaining to the lamp systems' ability to convert electrical energy into photosynthetic photon fluxes), light spectrum and intensity settings, photoperiods and the accompanying horticultural yields, as well as light distribution patterns generally influence the usefulness of the photon delivery systems in horticultural applications.

The conducted greenhouse experiment demonstrated a remarkable potential of the applied broadband LED system for increasing the horticultural yields of *Thymus vulgaris* L. while reducing the energy consumed during the naturally light-insufficient fall and winter months of Germany in comparison to the commercial HPS and FL lighting systems. Due to the high photosynthetic photon output, the correlated fast growth and the low energy demand, the implementation of the investigated broadband LED system could not only make profitable use of the highly under-utilized greenhouse capacities during low light seasons in northern regions of the world. It could also enable a greater variety of horticultural productions as greater DLI requirements can be reached which cannot be attained by the HPS and FL light sources.

Also, the study of *Ocimum basilicum* L. cultivars in the absence of natural light revealed that the applied broadband LED system (with elevated R and B wavebands) can quickly yield basil plants of marketable quality. Further, the investigation highlighted electrical saving potentials when applying low light intensities (even below recommended levels) as improved light use efficiencies in three of four basil cultivars came to light. Optimizing light intensity settings towards high light use efficiencies is thus a viable approach to increase the feasibility of LED-based indoor horticultural crop productions.

However, unpublished calculations of the photon efficiencies of the dichromatic RB, trichromatic RGB and the broadband LED light spectra applied in the vertical cultivation system during the *Mentha x piperita* L. cultivation indicate that the broadband LED light spectrum is currently not the most efficient LED lighting system (Table 28): Between the wavelength range of 380 and 780 nm, the greatest output of photons per electrical input was achieved by the RGB-emitting lighting system with a photon efficiency of $1.25 \mu\text{mol J}^{-1}\text{s}$, followed by the RB-emitting light fixture with an efficiency of $1.16 \mu\text{mol J}^{-1}\text{s}$ – an outcome that contrasts Kusuma et al. (2020), who stated that photon efficiencies of R and B LEDs are currently greater than photon efficiencies of G LEDs (and points out the importance of comparing the LED systems' specific photon efficiencies under identical and standardized conditions). The lowest number of emitted photons per electrical input was calculated for the broadband LED light system with a photon

efficiency of $0.99 \mu\text{mol J}^{-1} \text{s}$, which coincides with Kusuma et al. (2020), who stated that “white” LED systems are currently the least photon efficient systems²¹. All three LED lightings enabled similar fresh weights and essential oil contents per kilowatt-hour. However, leaf dry weight efficacy was significantly reduced under the broadband LED light system compared to the RB and RGB lighting.

Table 28 – Photon efficiency, biomass and essential oil efficiency of LED-lighting fixtures for the production of peppermint at equal photon flux density (PPFD) in the vertical cultivation system.

	RB ¹	RGB	SUN	<i>p</i> -value ⁴
Photon efficiency [$\mu\text{mol J}^{-1} \text{s}$] ²	1.16	1.25	0.99	<i>not applicable</i>
Fresh weight [g kWh^{-1}] ³	13.03 ± 1.73	13.62 ± 1.85	10.44 ± 1.43	0.98 (<i>ns</i>)
Leaf dry weight [mg kWh^{-1}] ³	$834.8 \pm 76.11^{\text{a}}$	$772.4 \pm 74.71^{\text{a}}$	$601.6 \pm 42.11^{\text{b}}$	0.01
Essential oil [mg kWh^{-1}] ³	21.53 ± 3.16	19.76 ± 2.30	15.52 ± 2.33	0.58 (<i>ns</i>)

¹ RB = Red/blue, RGB = Red/green/blue, SUN = Artificial sunlight spectrum.

² Mean photon output based on PPFDs²² per electrical input of light fixture expressed in μmol of photons per second divided by joules per second.

³ Presented are total fresh weight, leaf dry weight and essential oil productions \pm SD of *Mentha x piperita* var. *piperita* ‘Multimentha’ based on the power consumptions of each LED-lighting system within a shelf of three independent spatial replications per light treatment ($n = 3$) of 30 harvested plants per spatial replication and light treatment ($N = 270$, $n = 90$ plants per light treatment, $n = 30$ plants per spatial replication). Significant differences ($p \leq 0.05$) were determined according to Tukey’s multiple comparisons test after ordinary one-way ANOVA (fresh weight: $p = 0.98$, leaf dry weight: $p = 0.01$, essential oil yield: $p = 0.07$). Different letters within a row indicate significant differences between light treatments.²³

⁴ Significant differences between light treatments were determined according to ordinary one-way ANOVA test (*ns* = not significant). When significant, Tukey’s multiple comparisons test followed (different letters within a row indicate significant differences between light treatments at 95 % confidence interval) ($N = 9$, $n = 3$ samples per light treatment).²⁴

²¹ Detailed information on LEDs’ photon efficiencies can be reviewed in section 1.2.

²² Please bear in mind that LED photon efficiency values highly depend on the proximity to the LED light source at which the measurement is taken as the photon output (light intensity) increases greatly with decreasing proximity to the light source. Please also keep in mind that photon efficiencies are currently based on photons within what is currently defined as PAR which excludes UV and FR light ranges. For these calculations, average PPFDs across the whole spectrum (380-780 nm) at plant pot level were used (which allows a fair assessment and better comparison of the LED systems’ photon efficiencies).

²³ In contrast to the thyme and basil studies in which LED exposure began after sowing, the peppermint study began 36 days after stolon segments were cultivated under greenhouse conditions. Hence, the efficacy calculations do not account for the biomasses that were accumulated prior to the LED exposure.

²⁴ The power draw of current (I) and voltage (U) as well as electrical characteristics including real power (P) and apparent power (S) from representative lamps of each lighting treatment were measured using a power meter (ENERGY MONITOR 3000, VOLT-CRAFT®, Wernberg-Köblitz, Germany) in order to estimate photon efficiency and biomass efficacy of LED-lighting fixtures. To correct for detected differences between P and S of the LED-systems, the measured *cos phi* of each lighting condition was incorporated into the power consumption calculations. Final electrical consumptions were then calculated by multiplying the power consumptions with the hours fixtures were turned on (16 hours per day; 33 days in total). Photon efficiency of the light fixtures, meaning light output per unit electricity ($\mu\text{mol J}^{-1}$), were estimated based on average PPFD. Biomass efficacy (total fresh or leaf dry weights per kWh and shelf) as well as essential oil efficacy (essential oil content (EO) per kWh and shelf) were calculated by dividing

Hence, the energy efficiency of broadband LED lighting systems needs improvement to increase their cost effectiveness and to better meet sustainability goals in terms of minimizing resource inputs. One improvement effect could result from excluding wavebands greater than 750 nm in future broadband LED light fixtures as wavebands greater than 750 nm have shown to be useless for a variety of horticulturally relevant plant species (as just recently explored by Zhen & Bugbee, 2020a) (Figure 25). In addition, peak wavelengths of FR should shift towards 700 nm as FR effects decreased with increasing FR wavelength (Zhen & Bugbee, 2020a). In other words, by reducing and improving broadband LED spectra towards the photosynthetically and photobiologically relevant photons that can be fixed as chemical energy and/or that can be used to improve morphological traits of interest by activating the plants' photosensory systems, the photon efficiencies, the plants' light use efficacies and ultimately the cost effectiveness of broadband LED light fixtures can be improved.

Which of the three applied broadband LED light systems is the best in terms of photon efficiency cannot be answered concretely in retrospect, but due to the currently low efficiency of UV light-emitting diodes and the high efficiency of red and blue light-emitting diodes (e.g., Kusuma et al., 2020), the broadband LED system without UV wavelengths and with the elevated R and B wavebands applied in the basil study may be the most photon efficient broad white LED light spectrum of the three. Following the same argumentation, the least photon efficient system is probably the UV-containing white LED system applied in the vertical cultivation system (Figure 25).

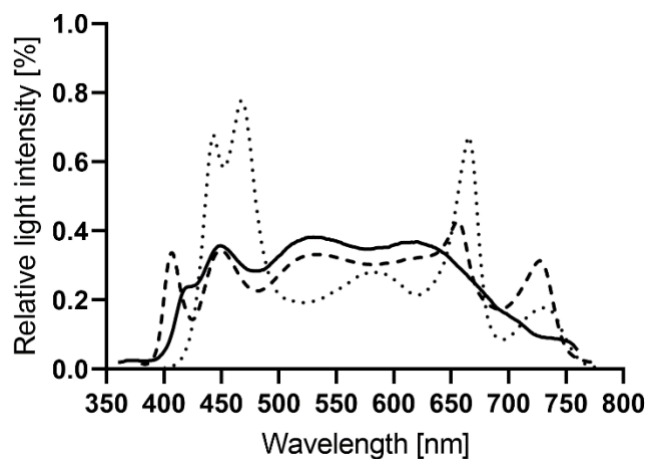


Figure 25 – Reducing FR emissions to 750 nm can improve the plants' light use efficacies and the LEDs' cost effectiveness.

Solid line: Broadband LED light spectrum applied in the greenhouse experiment with *Thymus vulgaris* L.

Dashed line: Broadband LED light spectrum applied in the vertical cultivation system with *Mentha x piperita* L.

Dotted line: Broadband LED light spectrum applied in the growth room in the absence of natural light with cultivars of *Ocimum basilicum* L.

the cumulative fresh weight or the cumulative leaf dry weights per shelf with total kilowatt-hours per shelf as well as EO per shelf with total kilowatt-hours per shelf.

Overall, photon efficiencies across the plants' entire photobiologically relevant wavelength range and the plants' light use efficiencies must receive much greater attention in future LED studies in search of feasible LED lighting strategies.

In addition, the research community must emphasize on describing "white" LED light spectra more precisely. Though all three broadband LED light spectra applied in this dissertation appear "white" to the human eye, these "white" spectra differ significantly from one another (Figure 25) and can have various impacts on plant development (as already summarized in section 1.5).

More attention must also be given to the light distribution patterns emitted by (broadband) LED light systems. As depicted in Figure 26, light distribution patterns differ significantly between HPS, FL and LED light fixtures (Figure 26A) as well as between different LED light systems (Figure 26B).

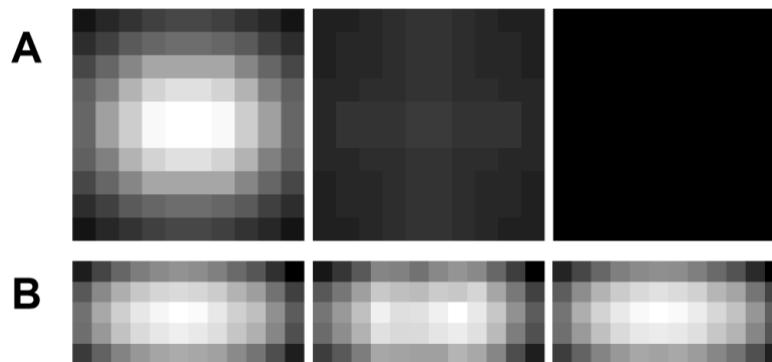


Figure 26 – Light distribution patterns of (broadband) LED systems must be improved.²⁵

A: Light distribution patterns of broadband LED (left), HPS (middle) and FL system (right) during the greenhouse experiment with *Thymus vulgaris* L.

B: LED light distribution patterns of dichromatic RB (left), trichromatic RGB (middle) and broadband white spectrum (right) during the vertical cultivation experiment with *Mentha x piperita* L.

While HPS and especially FL lamps deliver a high light uniformity across a given area, the applied LED systems (as well as LED systems in general) are presently characterized by inhomogeneous light distributions, that may result in undesired heterogeneous plant growth. As increasing the number of LED light fixtures per area to achieve greater light uniformity inevitably increases power consumptions and biomass efficacies, using light reflectors inside of cultivation spaces (especially in closed CEA applications) may be a more cost-effective way to improve these LED light distributions.

²⁵ Light intensity decreases from white to black. Illuminated areas and light intensity scales are not depicted to scale between Figure 26A and Figure 26B.

Finally, LED light sources are increasingly applied in very close proximity to plants (e.g., in space-limited multi-tiered vertical farms, plant factories and during photobiological research investigations). This form of light application is accompanied by steep light intensity increases with the plants' declining proximity to the light sources due to their growth over time (as shown in both the basil and the peppermint investigation). These existing light intensity gradients under space-limited growing conditions must therefore be described in more detail in upcoming research investigations, especially as these gradients can be used strategically for plant growth (since light requirements and the ability to absorb light energy generally increase during plant development until saturation is reached).

1.2 Are broadband LED light spectra photosynthetically efficient?

Since the late 1970s, the conception hardened, that blue and red light combinations optimally drive plant photosynthesis, because maximal light absorptions by the plants' chlorophyll pigments were found in these two spectral regions²⁶. This prevalent view was further reinforced by the often-cited action spectra of photosynthesis published by McCree (1972a) and Inida (1976)²⁷. In consequence, narrow dichromatic blue and red light-emitting diode systems with peak wavelengths around 450 and 660 nm represent the prevailing LED lighting strategy in horticultural applications today²⁸. Nevertheless, as described thoroughly in the introduction, a growing body of research indicates that inclusions of modest levels of ultraviolet radiation (especially λ 369-400 nm), green wavelengths (particularly λ 500-580 nm) and far-red illuminations (solely λ 700-750 nm) can improve the plants' photosynthetic efficiencies and biomass yields²⁹.

All in all, high biomass yields were achieved under all three investigated broadband LED light spectra in all three investigated Lamiaceae species. As a brief reminder, the broadband LED lighting system applied in the greenhouse resulted in highly apparent yield increases in *T. vulgaris* in comparison to the HPS and FL systems. However, if the high biomass yields observed under the white LED light spectrum partly resulted from the applied light quality (which spanned across the photosynthetically relevant spectral range) remains speculative, as the applied LED lighting system also emitted higher light intensities

²⁶ Review chapter 1- section 1.3.1.3 for details.

²⁷ McCrees' and Inidas' well-known action spectra of photosynthesis are depicted and addressed in chapter 1 - section 1.3.1.4.

²⁸ Review chapter 1 - section 1.4.1 for details.

²⁹ Review chapter 1 - sections 1.4.2.1, 1.4.2.2, 1.4.2.3 and 1.5 for plant responses to ultraviolet, green, far-red and broadband white lighting, respectively.

than the other two lighting systems, which resulted in greater daily light integrals available to the *T. vulgaris* plants.

A bit more indicative of broadband spectra potentials to improve photosynthetic assimilation rates may be a comparison of biomass yields achieved by the investigated basil cultivars under the broadband LED spectra with published basil yields achieved under dichromatic RB light spectra (e.g., as investigated by Pennisi et al. (2019, 2020)): Under five different RB light treatments (with peak wavelengths at 669 and 465 nm and RB ratios of 1:2, 1:1, 2:1, 3:1 and 4:1), constant light intensity of $215 \mu\text{mol m}^{-2} \text{s}^{-1}$ and a daily photoperiod of 16 hours, green basil cultivar 'Superbo' achieved 12.5 to 21 gram of fresh basil per plant, respectively, after 39 days of cultivation (Pennisi et al., 2019). In the following year, Pennisi et al. (2020) published 7.4, 9.3, 14.1, 25.0 and 21.0 gram of fresh basil per plant (cv. 'Suberbo') after 39 days of cultivation under an RB spectrum (with peak wavelengths at 669 and 465 nm and an RB ratio of 3:1), five different constant light intensity settings ($100, 150, 200, 250$ and $300 \mu\text{mol m}^{-2} \text{s}^{-1}$, respectively) and daily photoperiods of 16 hours. The fact that we observed similar and higher fresh green basil yields under partly significantly lower light intensities (100 to $\leq 175, 176$ and $198 \mu\text{mol m}^{-2} \text{s}^{-1}$, respectively) and fewer days of cultivation (35 DAS)³⁰ certainly points towards greater photosynthetic assimilation rates accomplishable via broadband LED light spectra. Nevertheless, direct comparisons of light quality effects remain indispensable as cultivars and cultivation conditions significantly influence the outcome.

Therefore, the peppermint study may represent the most revelatory investigation in the pursuit to answer whether or not broadband LED light spectra can improve photosynthesis and biomass yields in comparison to narrow LED light spectra. In brief, not only the number of leaf pairs (as an indicator of growth rate) but also the biomass yields per peppermint plant remained identical between the narrow dichromatic RB spectrum (with main peak wavelengths at 657 and 446 nm), the trichromatic RGB spectrum and the broad LED spectrum (SUN). As growth rates and biomass yields were indifferent between RB and RGB even though the green color fraction increased from almost non-existent under RB (0.5 %) to 31.2 % under RGB, it certainly appears that the applied green light fraction enabled efficient photosynthetic assimilations. Similarly, despite reduced red and blue light fractions and increased ultraviolet A (0.8 %), green (30.2 %) and far-red (15.3 %) light fractions of the applied broad LED spectrum, growth rates and biomass yields remained indifferent between RB and SUN. Hence, the potential of ultraviolet A, green and far-red to be photosynthetically efficient is – carefully speaking – not groundless. However, due to the excessive stem elongations induced by the RGB and SUN light treatment, the

³⁰ Under the I_{low} light treatment of our study, the green basil cultivars 'Anise', 'Thai Magic' and 'Cinnamon' achieved 13.4, 16.4 and 24.0 gram of fresh basil per plant, respectively, after 35 days of cultivation.

peppermint plants reached greater photon fluxes as they rapidly grew closer to the light source than the compact peppermints that were exposed to RB. So again, the influence of light quality and light intensity cannot be considered decoupled from one another, which manifests the importance of experimental designs that highly control the incident light intensity that reaches plant leaves and canopies throughout the duration of light quality experiments.

Hence, forthcoming research is still absolutely needed to determine light scenarios that most efficiently drive photosynthesis of individual plant species and cultivars. I suppose one way to improve the photosynthetic lighting efficiency is to provide a full light spectrum with a spectral distribution that matches the quantum yield pattern of a plant leaf. In a first step, quantum yields of representative plant leaves across the entire photobiologically relevant spectrum (e.g., 280-750 nm) should be determined via fluorescence spectrometers under controlled and specified conditions (similarly to the method applied by McCree (1972a)). Since LEDs with a wide range of peak wavelengths are available today³¹, LED spectra depicting these determined quantum yield curves should then be tailored. The plants' development and its photochemistry should then be investigated under such a customized LED spectrum (and compared to results obtained under e.g., the commonly applied RB spectrum, greenhouse and/or field conditions at equal light intensity settings). Especially chlorophyll fluorescence and gas exchange measurements should be taken to obtain a full picture of the plants' photochemical responses. Though such an LED spectrum may not be the most electrically efficient lighting strategy today³², it should in theory result in the most photosynthetically efficient light spectrum.

As factors such as light intensity, temperature and CO₂ concentration influence the quantum yields of plants (McCree, 1972a), these important conditions (which are (highly) controllable in CEAs) should be optimized towards high quantum yields as well. Multifactorial experimental designs that account for these as well as other environmental factors (such as humidity, nutrition and pH level) will help to identify lighting strategies – and cultivation conditions in general – that allow efficient conversions of light energy into chemical energy and high photosynthetic assimilation rates.

³¹ Review Figure 2 in chapter 1 - section 1.2 for an overview of the diverse LEDs and their peak wavelengths currently available.

³² Review chapter 1 - section 1.2 for the technological details.

1.3 Broadband LED light spectra can expand morphological plant trait manipulations.

As evident in all three conducted studies, the applied broadband LED spectra resulted in long stems and internodes. In brief, thyme³³ and peppermint³⁴ stems were extensively elongated in both the greenhouse and the vertical cultivation study when exposed to the broadband lightings. In addition, noticeable leaf expansions became evident in both species. To a lesser extent, yet clearly visible by the eye, also the basil cultivars³⁵ grew lengthy stems under the applied white LED light spectrum. These observations are in strong agreement with many recent studies which found that green and far-red wavelengths induce stem elongations and leaf expansions independently from one another³⁶.

However, the recent finding from Zhang et al. (2022), that G and FR wavelengths have an additive effect on plant height (as a partial replacement of RB with G in the presence of FR enhanced tomato plant heights more than a partial replacement of RB with G alone) contrasts the finding of our peppermint study in which peppermint plant heights remained indifferent between the SUN treatment which included FR and the RGB treatment that excluded FR. The contradictory result may just simply be a result of the short cultivation time of the peppermint plants in the vertical cultivation system which may have limited the detection of this suggested additive effect. However, as both study designs did not keep the photon fluxes of B light constant (which is known to suppress stem elongation under high fluence rates, but which is also known to enhance stem elongations under low fluence rates (e.g. Pedmale et al., 2016, Mizuno et al., 2011)), further investigations that include treatments with constant blue photon fluxes (similar to the study design applied by Zhang et al. (2011)) are required to conclusively investigate this suggested additive effect of G and FR wavebands on plant heights.

Further, it remains to be thoroughly investigated which specific green wavelengths, intensities and photoreceptor(s) are responsible for these shade avoidance symptoms and which color ratios represent the thresholds for these responses (e.g., blue-to-green, red-to-green ratios).

Nevertheless, the results strongly suggest that green and/or far-red light can be strategically added to increase light capture as a consequence of stem elongations and leaf expansions under cultivation conditions in which compact growth is not a necessary trade (as it is under space-limited growth conditions such as vertical farms and plant factories, or as it is for the majority of ornamentals). For example,

³³ Review Figure 2 – Visual appearance of *Thymus vulgaris* L. at harvest cultivated under different supplemental lighting systems during fall and winter of Berlin, Germany in Tabbert et al. (2021).

³⁴ Review Figure 2A – Morphological characteristics of *Mentha x piperita* var. *piperita* cv. *Multimentha* as effected by light spectra over time in Tabbert et al. (2022a).

³⁵ Review Figure 4 – Visual appearance of *Ocimum basilicum* L. cultivars at harvest in Tabbert et al. (2022b)

³⁶ Review chapter 1 - sections 1.4.2.2 and 1.4.2.3 for details.

greenhouse cultivations of tall-growing horticultural crops such as tomatoes, cucumbers and bell peppers under LED lighting systems that are mounted inflexibly far away from the crops, could benefit from quickly growing tall towards the LED light source as it is concomitant with greater light intensities. The morphological expansion and elongation effects that result from G and FR supplementations can clearly be used to increase light capture capacities.

In other words, the absence of G and FR in narrow-bandwidth LED light applications leaves a clear opportunity to control plant behaviors or product qualities essentially unexploited. Widening the range of color LEDs will allow growers to promote and repress plant traits of interest to much greater extents than RB light spectra.

1.4 Multidisciplinary research efforts are required to advance essential oil regulations under LED-based CEAs.

Research efforts on essential oil plants aiming at increased productions and quality enhancements of essential oils are not only needed for their many medicinal and culinary purposes and for the many agro-industrial applications³⁷. In addition, European legislators have set maximum levels of certain aromatic essential oil constituents in specific foods, if they are naturally present in flavorings and food ingredients to protect public health (Table 29).

In addition, these aromatic essential oil constituents shall not be added as such (e.g., as a pure substance) to foods (Regulation No 1334, 2008) to avoid potential health risks related to them (e.g., methyl chavicol and methyl eugenol are suspected to be carcinogenic (De Vincenci et al., 2000; NTP, 2000; EMA, 2005); pulegone and menthofuran can be hepatotoxic (Khojasteh et al., 2010; Khojasteh-Bakht et al., 1999).

While the addition of fresh, dried and frozen basil (as one of the herbs rich in the aromatic yet health-concerning phenylpropanoids methyl chavicol and methyl eugenol³⁸) to compound foods is unrestricted, basil extracts intended as flavorings have to meet the set maximum levels since 2021 (Regulation No 1334, 2008). Though higher concentration levels of menthofuran and pulegone (which are commonly found in peppermint³⁹) are allowed in processed foods, these monoterpenoids are restricted

³⁷ Review chapter 1 - section 1.6 for details.

³⁸ Review Tables 3-6 – Relative abundances of major volatile organic compounds identified in the leaves of *O. basilicum* L. cultivars as affected by LED light intensity treatments over time (cultivar ‘Anise’ - Table 3, cultivar ‘Dark Opal’ - Table 4, cultivar ‘Thai Magic’ - Table 5, cultivar ‘Cinnamon’ – Table 6) in Tabbert et al. (2022b).

³⁹ Review Table 2 – Effects of three light qualities on the chemical composition of 24 identified essential oil compounds, essential oil content and yield of *Mentha x piperita* L. var. *piperita* cv. *Multimentha* after 69 days of cultivation in Tabbert et al. (2022a).

regardless of being added as part of raw herb materials or as part of extracts to meet consumer safety requirements.

Table 29 – Selection of essential oil constituents used as food flavorings, the foods in which their presence is restricted and the set maximum levels.¹

Essential oil constituent	Food in which the constituent is restricted	Maximum level [mg/kg]
Methyl chavicol ²	Dairy products	50
	Processed fruits, vegetables (incl. mushrooms, fungi, roots, tubers, pulses and legumes), nuts and seeds	50
	Fish products	50
	Non-alcoholic beverages	10
Methyl eugenol ²	Dairy products	20
	Meat preparations and meat products, including poultry and game	15
	Fish preparations and fish products	10
	Soups and sauces	60
	Ready-to-eat savories	20
	Non-alcoholic beverages	1
Menthofuran	Mint/peppermint containing confectionery, except micro breath freshening confectionery	500
	Micro breath freshening confectionery	3000
	Chewing gum	1000
	Mint/peppermint containing alcoholic beverages	200
Pulegone	Mint/peppermint containing confectionery, except micro breath freshening confectionery	250
	Micro breath freshening confectionery	2000
	Chewing gum	350
	Mint/Peppermint containing non-alcoholic beverages	20
	Mint/Peppermint containing alcoholic beverages	100

¹ Data retrieved from Regulation No 1334, 2008.

² Maximum levels do not apply if the food ingredient is added as a fresh, dried or frozen herb.

Hence, herb growers and processing industries are in need of strategies to lower these naturally occurring substances in these globally consumed medicinal and aromatic crop species and in their essential oil extracts before further processing. And today, LED-based CEAs are (rightfully) seen as a promising strategy to produce medicinal and aromatic plants with continuously high essential oil qualities and quantities.

Though numerous alterations in essential oil compositions and contents upon different LED light exposures have been described⁴⁰, the underlying causes are rarely discussed and remain poorly

⁴⁰ Review Table 10 – Essential oil contents and compositions of aromatic and medicinal plants as affected by LED lighting (λ 100-800 nm) in chapter 1 - section 1.6.

understood today. In addition, differences in experimental approaches and contradicting reports complicate the identification of commonalities⁴¹.

Also our investigations remained mainly descriptive in nature, and may be repeated hereafter in a highly condensed manner.

The investigation of *T. vulgaris* L. revealed similar essential oil compositions between the three diverse broadband lighting systems (LED, HPS and FL) after a cultivation period of four months in a greenhouse setting. However, the essential oil yields were significantly increased under the LED treatment and to a lesser extent under the HPS treatment compared to the FL treatment. This outcome was found to be correlated with the high, medium and low daily light integrals received by the thyme plants under the respective lighting systems and the concomitantly high, medium and low leaf productions, respectively. To which extent the different light spectra contributed to the outcomes remained speculative, however (Tabbert et al., 2021). That essential oil yields increase with increasing light intensity was substantiated by the investigation of *O. basilicum* L. cultivars in the growth chambers as the higher light intensity treatment accelerated the production of the essential oil-containing basil leaves. Additionally, the basil investigation showed that the compositional changes of the volatile extracts were highly dependent on the basil's developmental stages (Tabbert et al., 2023). And the peppermint experiment revealed compositional differences under three different light qualities. However, possible impacts of the diverging light intensities as a result of the differing morphological responses of the peppermint plants to the applied light qualities under the space-limited vertical cultivation conditions cannot be ruled out entirely (Tabbert et al., 2022a).

Hence, while choice of cultivar, time of harvest as well as light conditions can significantly contribute to meeting specific demands on essential oil qualities and quantities (as evident in all three published articles), a range of research efforts remain pivotal to advance our ability to tailor essential oils in LED-based CEAs:

For instance, photoreceptor mutant studies could be employed to find out if and to which extent specific photoreceptors are involved in the biosynthesis of essential oils and/or in the development of essential oil-containing structures. For example, an involvement of phytochrome photoreceptors in the production of terpenoids has already been suggested over 30 years ago by Yamaura et al. (1991) and Tanaka et al. (1989) but has not been verified. In addition, UVR8 and cryptochrome photoreceptors are known to be involved in the production of flavonoids which originate from the phenylpropanoid pathway.

⁴¹ Review chapter 1 - section 1.6 for details.

Hence, I hypothesize that UVR8 and cryptochromes are also involved in the production of the aromatic phenylpropanoids found in essential oils. Concomitantly, I propose that the light regions these photoreceptors are sensitive to⁴² can be used to regulate the biosynthesis of aromatic terpenes and phenylpropenes, respectively. That additions of approximately $25 \mu\text{mol m}^{-2} \text{s}^{-1}$ of narrow UV-A (peak wavelength $368 \pm 10 \text{ nm}$) and broad B (400-500 nm) to I_{High} respectively (Figure 27) resulted in an increase of methyl eugenol by more than 2-fold in the purple basil cultivar ‘Dark Opal’ in one of our unpublished experiments⁴³ certainly hints towards an involvement of cryptochrome in the regulation of aromatic phenylpropanoids.

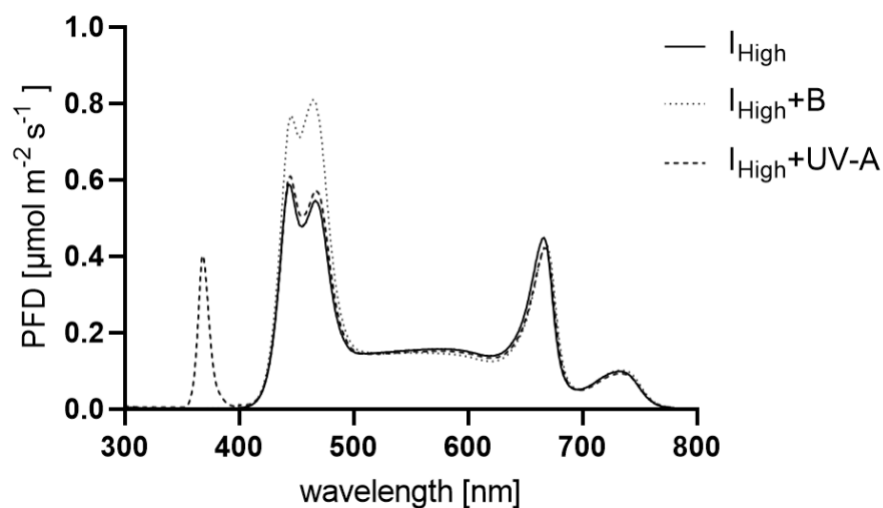


Figure 27 – White broad-band LED light spectra with additional UV-A or B applied in the unpublished experiment. Depicted are the LED light spectra as PFDs (photon flux densities [$\mu\text{mol m}^{-2} \text{s}^{-1}$] per wavelength [nm] between 300 and 800 nm. Each LED light spectrum represents the average PFDs per wavelength obtained from 120 measurements across the entire experimental block (1.2 m^2).

While the VOC contents per gram of leaf dry matter were found to be the same between the published I_{High} light treatment and the unpublished $I_{\text{High}}+\text{UV-A}$ and $I_{\text{High}}+\text{B}$ light treatments, the relative contents of methyl eugenol more than doubled (Table 30). And the low relative contents of eugenol, being

⁴² Review Figure 6 – Absorption spectra of photoreceptors in chapter 1 - section 1.3.2.1 for a general overview of the photoreceptors’ light absorption spectra.

⁴³ The experiment was conducted under identical conditions as described in Tabbert et al. (2022b) with the differences that either narrow UV-A ($368 \pm 10 \text{ nm}$) or broad B (400-500 nm) photons ($25 \pm 5 \mu\text{mol m}^{-2} \text{s}^{-1}$ at plant pot level) were added to the described I_{High} light treatment, and that the plant material for VOC analyses was only collected at the end of the experiment (35 days after sowing).

the direct metabolic precursor of methyl eugenol⁴⁴, could indicate a high enzymatic conversion rate of eugenol to methyl eugenol under the additional UV-A and B photon fluxes.

Table 30 – Volatile organic compound (VOC) content and relative abundance of major volatile organic compounds identified in the leaves of *O. basilicum* L. cv. ‘Dark Opal’ as affected by three different LED light treatments 35 days after sowing.

No.	Compound	RI ¹	Experiment A		Experiment B	
			I _{High}	I _{High+UV-A}	I _{High+B}	
VOC content [mg g L _{DM} ⁻¹] ²			8.0 ± 2.3 ^{ns}	7.2 ± 1.1 ^{ns}	7.0 ± 1.1 ^{ns}	
Percent (%) of total volatile organic compound composition ³						
1	α -pinene	938	0.5±0.1 ^a	0.5±0.1 ^a	0.5±0.1 ^a	
2	β -pinene	982	0.9±0.1 ^a	0.9±0.1 ^a	0.9±0.1 ^a	
3	β -myrcene	992	0.7±0.1 ^a	0.5±0.2 ^b	0.5±0.2 ^b	
4	limonene	1033	0.6±0.1 ^a	0.7±0.1 ^a	0.7±0.1 ^a	
5	1,8-cineole	1036	9.5±1.1^a	8.8±0.9^a	9.1±1.0^a	
6	terpinolene	1095	1.3±0.2 ^c	2.3±0.2 ^a	2.1±0.2 ^b	
7	linalool	1101	28.4±5.0^a	12.5±2.6^b	13.5±1.7^b	
8	α -terpineol	1197	1.0±0.1 ^a	0.7±0.1 ^b	0.8±0.1 ^b	
9	nerol	1227	1.7±0.2 ^a	1.7±0.2 ^a	1.8±0.1 ^a	
10	eugenol	1364	9.0±2.5^a	1.2±0.7^c	2.0±0.5^b	
11	β -elemene	1403	0.8±0.1 ^a	0.6±0.2 ^b	0.6±0.1 ^b	
12	methyl eugenol	1408	25.2±4.3^b	55.3±5.2^a	53.2±3.8^a	
13	α - <i>trans</i> -bergamotene	1437	1.9±0.1 ^a	1.7±0.2 ^a	1.7±0.1 ^a	
14	aromadendrene	1446	0.4±0.1 ^a	0.5±0.1 ^a	0.5±0.1 ^a	
15	α -humulene	1451	0.8±0.1 ^a	0.5±0.0 ^b	0.5±0.1 ^b	
16	β -farnesene	1461	3.3±0.3 ^a	3.3±0.3 ^a	3.4±0.3 ^a	
17	α -amorphene	1471	0.6±0.0 ^a	0.5±0.0 ^a	0.6±0.0 ^a	
18	bicyclogermacrene	1498	3.1±0.2 ^a	1.9±0.1 ^b	1.9±0.2 ^b	
19	γ -cadinene	1513	1.3±0.2 ^a	0.8±0.1 ^b	0.8±0.1 ^b	
20	δ -cadinene	1521	1.4±0.1 ^a	0.5±0.1 ^b	0.6±0.0 ^b	
21	<i>cis</i> -nerolidol	1529	1.2±0.1 ^a	0.9±0.1 ^c	1.0±0.1 ^b	
22	α -cadinol	1657	2.3±0.1 ^a	1.7±0.2 ^c	1.8±0.2 ^b	
TOTAL [%] ⁴			98.3±0.3	98.7±0.7	98.3±0.8	

RI = Retention index; VOC = volatile organic compounds; L_{DM} = leaf dry matter; different letters within a row indicate significant differences at $p \leq 0.05$; *ns* = not significant (Statistical tests are described in Tabbert et al. (2022b).)

¹ Presented are mean Ris of samples under GC-FID conditions on an HP-5MS column relative to a series of n-alkanes.

² Presented are average VOC contents ± SD in mg g L_{DM}⁻¹ (w/w) across four independent experimental replications per light treatment. ³ All VOCs were extracted from leaf dry matter of two basil plant pots from the same experimental block; Experiment A: $n = 8$ extracts per light treatment; Experiment B: $n = 32$ extracts per light treatment.

⁴⁴ Review Figure 8 – Biosynthesis of major volatile aromatic compounds in plants in chapter 1 - section 1.6.

³ Presented are mean percentages \pm SD of volatile organic compounds of all analyzed basil leaf extracts (I_{High} : $n = 8$ leaf extracts per light treatment; $I_{\text{High}}+\text{UV-A}$ and $I_{\text{High}}+\text{B}$: $n = 32$ leaf extracts per light treatment).

⁴ Percentage [%] \pm SD represents total listed volatile organic compounds. Traces of 14 compounds are excluded from the table.

Another focal point of research could be the micromorphology of leaves: As observed in all three publications, leaves show a great phenotypic plasticity due to the light conditions available to them. If and to which extent the secretory structures (which are responsible for the biosynthesis and storage of essential oils (Rehman et al., 2016)) on these leaves are affected in shape, number, size and density as well as in essential oil content and composition by different light qualities could be insightful for tailoring light conditions for medicinal and aromatic plants.

Also, genetic and enzymatic studies will deepen the present understanding of light signals on biosynthetic pathways (as recently shown and suggested by Sankhuan et al., 2021). As peppermints' monoterpenoid biosynthetic pathway, its involved genes and enzymes are already well-known (thanks to the works of Croteau and his colleagues (e.g., Croteau et al., 2005)), *Mentha x piperita* L. represents a great model plant for further photobiological studies that aim at interpreting the influence of light on terpenoid productions.

In addition, as terpene biosynthesis partly depends on primary metabolites from the MEP pathway which takes place in chloroplasts (e.g., Ahmadi et al., 2021), it would be interesting to study whether or not an increase in chloroplast concentrations correlates with increased terpenoid productions. If so, long UV-A, B, short G as well as R wavelengths should be useful light regions for increased terpenoid productions due to their tendency to increase chlorophyll concentrations in many plant species⁴⁵.

Finally, it remains to be determined to which extent changes of other abiotic factors (such as temperature, humidity and fertilization) affect the contents and compositions of the essential oils. Thus far, none of the published LED studies have incorporated these highly influential factors⁴⁶.

⁴⁵ Not only are phytochromes and cryptochromes known to be involved in chlorophyll biosynthesis upon R and B light exposures (chapter 1 - sections 1.3.2.2.1 and 1.3.2.2.2), UV-A, B and short G LED wavelengths have often been correlated with increased chlorophyll concentrations (chapter 1 - sections 1.4.1, 1.4.2.1 and 1.4.2.2).

⁴⁶ Review chapter 1 - section 1.6 for details.

References

- Ahmad, M., Grancher, N., Heil, M., Black, R.C., Giovani, B., Galland, P., Lardemer, D. (2002) *Action spectrum for cryptochrome-dependent hypocotyl growth inhibition in Arabidopsis*. Plant Physiol. 129:774-785. <https://doi.org/10.1104/pp.010969>
- Ahmad, M., Jarillo, J.A., Smirnova, O., Cashmore, A.R. (1998) *The cry1 blue light photoreceptor of Arabidopsis interacts with phytochrome A in vitro*. Mol. Cell. 1(7):939-948. [https://doi.org/10.1016/S1097-2765\(00\)80094-5](https://doi.org/10.1016/S1097-2765(00)80094-5)
- Ahmad, M., Lin, C., Cashmore, A.R. (1995) *Mutations throughout an Arabidopsis blue-light photoreceptor impair blue-light-responsive anthocyanin accumulation and inhibition of hypocotyl elongation*. Plant J. 8(5):653-658. <https://doi.org/10.1046/j.1365-313X.1995.08050653.x>
- Ahmadi, T., Shabani, L., Sabzalian, M.R. (2021) *LED light sources improved the essential oil components and antioxidant activity of two genotypes of lemon balm (Melissa officinalis L.)* Bot. Stud. 62:9. <https://doi.org/10.1186/s40529-021-00316-7>
- Aldarkazali, M., Rihan, H.Z., Carne, D., Fuller, M.P. (2019) *The growth and development of sweet basil (Ocimum basilicum) and bush basil (Ocimum minimum) grown under three light regimes in a controlled environment*. Agronomy. 9(11):743. <https://doi.org/10.3390/agronomy9110743>
- Ali, F., Falaq, R.N., Jyoti, S., Siddique, Y.H. (2017) *Health functionality of apigenin: A review*. Int. J. Food Prop. 20(6):1197-1238. <https://doi.org/10.1080/10942912.2016.1207188>
- Alvarenga, I.C.A., Pacheco, F.V., Silva, S.T., Bertolucci, S.K.V., Pinto, J.E.B.P. (2015) *In vitro culture of Achillea millefolium L.: quality and intensity of light on growth and production of volatiles*. PCTOC. 122:299-308. <https://doi.org/10.1007/s11240-015-0766-7>
- Amaki, W., Yamazaki, N., Ichimura, M., Watanabe, H. (2011) *Effects of light quality on the growth and essential oil content in sweet basil*. Acta Hortic. 907:91-94. <https://doi.org/10.17660/ActaHortic.2011.907.9>
- Andrade, H.B., Braga, A.F., Bertolucci, S.K.V., Hsie, B.S., Silva, S.T., Pinto, J.E.B.P. (2017) *Effect of plant growth regulators, light intensity and LED on growth and volatile compound of Hyptis suaveolens (L.) Poit in vitro plantlets*. Acta Hortic. 1155:277-284. <https://doi.org/10.17660/ActaHortic.2017.1155.40>
- Araújo, D.X., Rocha, T.T., de Carvalho, A.A., Bertolucci, S.K.V., Medeiros, A.P.R., Ribeiro, F.N.S., Barbos, S.M., Pinto, J.E.B.P. (2021) *Photon flux density and wavelength influence on growth, photosynthetic*

- pigments and volatile organic compound accumulation in *Aeollanthus suaveolens* (Catinga-de-mulata) under in vitro conditions. *Ind. Crop Prod.* 168:113597. <https://doi.org/10.1016/j.indcrop.2021.113597>
- Arrow (2022) <https://lh3.googleusercontent.com/-7DhSgeE3fkw/YRnA1wWqGvI/AAAAAACZIo/134Cw7B68MwxSKsluheITE7uAy13B1UyACLcBGAsYHQ/image.png> (accessed September 20, 2022)
- Ascrizzi, R., Fraternali, D., Flamini, G. (2018) *Photochemical response of parsley (Petroselinum crispum (Mill.) Fuss) grown under red light: The effect on the essential oil composition and yield.* *J. Photochem. Photobiol.* 185:185-191. <https://doi.org/10.1016/j.jphotobiol.2018.06.006>
- Ballard, C.R., Maróstica, M.R. (2019) *Chapter 10 - Health benefits of flavonoids.* pp. 185-201. In: *Bioactive compounds*, Campos, M.R.S. (ed.), Woodhead Publishing. <https://doi.org/10.1016/B978-0-12-814774-0.00010-4>
- Ballaré, C.L., Pierik, R. (2017) *The shade-avoidance syndrome: multiple signals and ecological consequences.* *Plant Cell Environ.* 40(11):2530-2543. <https://doi.org/10.1111/pce.12914>
- Banerjee, R., Schleicher, E., Meier, S., Viana, R.M., Pokorny, R., Ahmad, R.B., Batschauer, A. (2007) *The signaling state of Arabidopsis cryptochrome 2 contains flavin semiquinone.* *J. Biol. Chem.* 282(20):14916-14922. <https://doi.org/10.1074/jbc.M700616200>
- Bantis, F., Smirnakou, S., Ouzounis, T., Koukounaras, A., Ntagkas, N., Radoglou, K. (2018) *Current status and recent achievements in the field of horticulture with the use of light-emitting diodes (LEDs).* *Sci. Hortic.* 235:437-451. <https://doi.org/10.1016/j.scienta.2018.02.058>
- Barta, D.J., Tibbitts, T.W., Bula, R.J., Morrow, R.C. (1992) *Evaluation of light emitting diode characteristics for a space-based plant irradiation source.* *Adv. Space. Res.* 12(5):141-149. [https://doi.org/10.1016/0273-1177\(92\)90020-x](https://doi.org/10.1016/0273-1177(92)90020-x)
- Barut, M., Tansi, L. S., Akyuz, A. M., Karaman, S. (2021) *Quality and yield of different basil (Ocimum basilicum L.) cultivars with various planting and cutting times under hot Mediterranean climate.* *Appl. Ecol. Environ. Res.* 19(4):3115– 3136. https://doi.org/10.15666/aeer/1904_31153136
- Batista, D.S., de Castro, K.M., da Silva, A.R., Teixeira, M.L., Sales, T.A., Soares, L.I., Cardoso, M. das G., Santos, M. de O., Viccini, L.F., Otoni, W.C. (2016) *Light quality affects in vitro growth and essential oil profile in Lippia alba (Verbenaceae).* *In vitro Cell. Dev. Biol. – Plant.* 52:276-282. <https://doi.org/10.1007/s11627-016-9761-x>

- Battle, M.W., Vegliani, F., Jones, M.A. (2020) *Shades of green: untying the knots of green photoreception*. J. Exp. Bot. 71(19):5764-5770. <https://doi.org/10.1093/jxb/eraa312>
- Beaman, A. R., Gladon, R. J., Schrader, J. A. (2009) *Sweet basil requires an irradiance of 500 $\mu\text{mol m}^{-2} \text{s}^{-1}$ for greatest edible biomass production*. HortSci. 44(1):64–67. <https://doi.org/10.21273/HORTSCI.44.1.64>
- Behn, H., Albert, A., Marx, F., Noga, G., Ulbrich, A. (2010) *Ultraviolet-B and photosynthetically active radiation interactively affect yield and pattern of monoterpenes in leaves of peppermint (*Mentha × piperita* L.)*. J. Agric. Food Chem. 58(12):7361–7367. <https://doi.org/10.1021/jf9046072>
- Beigi, M., Toriki-Harchegani, M., Ghasemi Pirbalouti, A. (2018) *Quantity and chemical composition of essential oil of peppermint (*Mentha × piperita* L.) leaves under different drying methods*. Int. J. Food Prop. 21(1):267–276. <https://doi.org/10.1080/10942912.2018.1453839>
- Benke, K., Tomkins, B. (2018) *Future food-production systems: vertical farming and controlled-environment agriculture*. Sustain.: Sci. Pract. Policy. 13(1):13-26. <https://doi.org/10.1080/15487733.2017.1394054>
- Bian, Z., Yang, Q., Li, T., Cheng, R., Barnett, Y., Lu, C. (2018) *Study of the beneficial effects of green light on lettuce grown under short-term continuous red and blue light-emitting diodes*. Physiol. Plant. 164(2):226-240. <https://doi.org/10.1111/ppl.12713>
- Björn, L.O., Papageorgiou, G.C., Blankenship, R.E., Govindje (2009) *A viewpoint: Why Chlorophyll a?* Photosynt. Res. 99:85-98. <https://doi.org/10.1007/s11120-008-9395-x>
- Boliki, M.C. (2019) *FAO and the situation of food security and nutrition in the world*. J. Nutr. Sci. Vitaminol. 65:S4-S8. <https://doi.org/10.3177/jnsv.65.S4>
- Borthwick, H.A., Hendricks, S.B., Parker, M.W., Toole, E.H., Toole, V.K. (1952) *A reversible photoreaction controlling seed germination*. Proc. Natl. Acad. Sci., USA 38:662-666. <https://doi.org/10.1073/pnas.38.8.662>
- Botto, J.F., Smith, H. (2002) *Differential genetic variation in adaptive strategies to a common environmental signal in Arabidopsis accessions: phytochrome-mediated shade avoidance*. Plant Cell Environ. 25(1):53-63. <https://doi.org/10.1046/j.0016-8025.2001.00812.x>
- Bouly, J.-P., Schleicher, E., Dionisio-Sese, M., Vandenbussche, F., Van der Straeten, D., Bakrim, N., Meier, S., Batschauer, A., Galland, P., Bittl, R., Ahmad, M. (2007) *Cryptochrome blue light photoreceptors are*

- activated through interconversion of flavin redox states. *J. Biol. Chem.* 282(13):9383-9391. <https://doi.org/10.1074/jbc.M609842200>
- Bourget, C.M. (2008) *An introduction to light-emitting diodes*. *HortSci.* 43(7):1944-1946. <https://doi.org/10.21273/HORTSCI.43.7.1944>
- Brazaitytė, A., Viršile, A., Samoulienė, G., Vaštakaitė-Kairienė, V., Jankauskienė, J., Miliauskienė, J., Novičkovas, A., Duchovskis, P. (2019) *Response of mustard microgreens to different wavelengths and durations of UV-A LEDs*. *Front. Plant Sci.* 10:1153. <https://doi.org/10.3389/fpls.2019.01153>
- Britton, G., Liaaen-Jensen, S., Pfander, H. (eds.) (2008) *Carotenoids*. Birkhäuser Verlag, Basel, Switzerland.
- Brown, C.S., Schuerger, A.C., Sager, J.C. (1995) *Growth and Photomorphogenesis of pepper plants under red light-emitting diodes with supplemental blue or far-red lighting*. *J. Amer. Soc. Hort. Sci.* 120(5):808-813. <https://doi.org/10.21273/JASHS.120.5.808>
- Bugbee, B. (2016) *Toward an optimal spectral quality for plant growth and development: The importance of radiation capture*. *Acta Hortic.* 1134:1-12. <https://doi.org/10.17660/ActaHortic.2016.1134.1>
- Bunse, M., Daniels, R., Gründemann, C., Heilmann, J., Kammerer, D.R., Keusgen, M., Lindequist, U., Melzig, M.F., Morlock, G.E., Schulz, H., Schweiggert, R., Simon, M., Stintzing, F.C., Wink, M. (2022) *Essential oils as multicomponent mixtures and their potential for human health and well-being*. *Front Pharmacol.* 13:956541. <https://doi.org/10.3389/fphar.2022.956541>
- Burattini, C., Mattoni, B., Bisegna, F. (2017) *The impact of spectral composition of white LEDs on spinach (Spinacia oleracea) growth and development*. *Energies.* 10(9):1383. <https://doi.org/10.3390/en10091383>
- Burbott, A. J., Loomis, W. D. (1967) *Effects of light and temperature on the monoterpenes of peppermint*. *Plant Physiol.* 42(1):20–28. <https://doi.org/10.1104/pp.42.1.20>
- Cao, K., Yan, F., Xu, D., Ai, K., Yu, J., Bao, E., Zou, Z. (2018) *Phytochrome B1-dependent control of SP5G transcription is the basis of the night break and red to far-red light ratio effects in tomato flowering*. *BMC Plant Biol.* 18:158. <https://doi.org/10.1186/s12870-018-1380-8>
- Canamero, R.C., Bakrim, N., Bouly, J.-P., Garay, A., Dudkin, E.E., Habricot, Y., Ahmad, M. (2006) *Cryptochrome photoreceptors cry1 and cry2 antagonistically regulate primary root elongation in Arabidopsis thaliana*. *Planta.* 224:995-1003. <https://doi.org/10.1007/s00425-006-0280-6>

- Carović -Stanko, K., Šalinović , A., Grdiša, M., Liber, Z., Kolak, I., Satovic, Z. (2011) *Efficiency of morphological trait descriptors in discrimination of Ocimum basilicum l. accessions*. Plant Biosyst. 145(2): 298–305. <https://doi.org/10.1080/11263504.2011.558677>
- Carvalho, S.D., Schieterman, M.L., Abrahan, C.E., Colquhoun, T.A., Folta, K.M. (2016) *Light quality dependent changes in morphology, antioxidant capacity, and volatile production in sweet basil (Ocimum basilicum)*. Front. Plant Sci. 7:1328. <https://doi.org/10.3389/fpls.2016.01328>
- Casal, J.J. (2000) Phytochromes, cryptochromes, phototropin: *Photoreceptor interactions in plants*. Photochem. Photobiol. 71(1):1-11. [https://doi.org/10.1562/0031-8655\(2000\)0710001PCPPII2.0.CO2](https://doi.org/10.1562/0031-8655(2000)0710001PCPPII2.0.CO2)
- Casal, J.J. (2012) Shade avoidance. ASPB. 10:e0157. <https://doi.org/10.1199/tab.0157>
- Casal, J.J., Mazzella, M.A. (1998) *Conditional synergism between cryptochrome 1 and phytochrome B is shown by the analysis of phyA, phyB, and hy4 simple, double, and triple mutants in Arabidopsis*. Plant Physiol. 118(1):19-25. <https://doi.org/10.1104/pp.118.1.19>
- Casamayor, J., Su, D., Sarshar, M. (2015) *Extending the lifespan of LED-lighting products*. Archit. Eng. Des. Manag. 11(2):105-122. <https://doi.org/10.1080/17452007.2013.834813>
- Casson, S.A., Hetherington, A.M. (2014) *Phytochrome B is required for light-mediated systemic control of stomatal development*. Cur. Biol. 24(11):1216-1221. <https://doi.org/10.1016/j.cub.2014.03.074>
- Cerdán, P.D., Chory, J. (2003) *Regulation of flowering time by light quality*. Nature. 423:881-885. <https://doi.org/10.1038/nature01636>
- Chang, X., Alderson, P., Wright, C. (2005) *Effect of temperature integration on the growth and volatile oil content of basil (Ocimum basilicum l.)*. J. Hortic. Sci. Biotechnol. 80(5):593–598. <https://doi.org/10.1080/14620316.2005.11511983>
- Chang, X., Alderson, P. G., Wright, C. J. (2008). *Solar irradiance level alters the growth of basil (Ocimum basilicum l.) and its content of volatile oils*. Environ. Exp. Bot. 63(1-3):216–223. <https://doi.org/10.1016/j.envexpbot.2007.10.017>
- Chaves, M.C., Freitas, J.C.E., Nery, F.C., Paiva, R., Prudente, D. de O., Costa, B.G.P., Daubermann, A.G., Bernardes, M.M., Grazul, R.M. (2020) *Influence of colorful light-emitting diodes on growth, biochemistry, and production of volatile organic compounds in vitro of Lippia filifolia (Verbenaceae)* J. Photochem. Photobiol. 212:112040. <https://doi.org/10.1016/j.jphotobiol.2020.112040>

- Chen, S., Marcelis, L.F.M., Heuvelink, E. (2022) *Far-red radiation increases flower and fruit abortion in sweet pepper (Capsicum annuum L.)* Sci. Hortic. 305:111386.
<https://doi.org/10.1016/j.scienta.2022.111386>
- Chen, X.-L., Xue, X.-Z., Guo, W.-Z., Wang, L.-C., Qiao, X.-J. (2016) *Growth and nutritional properties of lettuce affected by mixed irradiation of white and supplemental light provided by light-emitting diode.* Sci. Hortic. 200:111-118. <https://doi.org/10.1016/j.scienta.2016.01.007>
- Chen, Y., Li, T., Ynag, Q., Zhang, Y., Zou, J., Bian, Z., Wen, X. (2019) *UVA radiation is beneficial for yield and quality of indoor cultivated lettuce.* Front. Plant Sci. 10:1563. <https://doi.org/10.3389/fpls.2019.01563>
- Chia, Po-Lung, Kubota, C. (2010) *End-of-day far-red light quality and dose requirements for tomato rootstock hypocotyl elongation.* HortSci. 45(10):1501-1506.
<https://doi.org/10.21273/HORTSCI.45.10.1501>
- Choi, D.-S., Nguyen, T.K.L., Oh, M.-M. (2022) *Growth and biochemical responses of kale to supplementary irradiation with different peak wavelengths of UV-A light-emitting diodes.* Hortic. Environ. Biotechnol. 63:65-76. <https://doi.org/10.1007/s13580-021-00377-4>
- Choudhury, F.K., Rivero, R.M., Blumwald, E., Mittler, R. (2017) *Reactive oxygen species, abiotic stress, and stress combination.* Plant J. 90(5):856-867. <https://doi.org/10.1111/tpj.13299>
- Clark, R., Menary, R. (1980) *Environmental effects on peppermint (Mentha piperita L.). I. effect of daylength, photon flux density, night temperature and day temperature on the yield and composition of peppermint oil.* Funct. Plant Biol. 7(6):685-692. <https://doi.org/10.1071/PP9800685>
- Colquhoun, T.A., Schwieterman, M.L., Gilbert, J.L., Jaworski, E.A., Langer, K.M., Jones, C.R., Rushing, G.V., Hunter, T.M., Olmstead, J., Clark, D.G., Folta, K.M. (2013) *Light modulation of volatile organic compounds from petunia flowers and select fruits.* Postharvest Biol. Technol. 86:37-44.
<https://doi.org/10.1016/j.postharvbio.2013.06.013>
- Coman, V., Vodnar, D.C. (2019) *Hydroxycinnamic acids and human health: recent advances.* J. Sci. Food Agric. 100(2):483-499. <https://doi.org/10.1002/jsfa.10010>
- Cope, K.R., Bugbee, B. (2013) *Spectral effects of three types of white light-emitting diodes on plant growth and development: Absolute versus relative amounts of blue light.* HortSci. 48(4):504-509.
<https://doi.org/10.21273/HORTSCI.48.4.504>

- Cordeiro, A.M., Andrade, L., Monteiro, C.C., Leitão, G., Wigge, P.A., Saibo, N.J.M. (2022) *Phytochrome-interacting factors: a promising tool to improve crop productivity*. J. Exp. Bot. 73(12):3881-3897. <https://doi.org/10.1093/jxb/erac142>
- Craver, J.K., Boldt, J.K., Lopez, R.G. (2018) *Radiation intensity and quality from sole-source light-emitting diodes affect seedling quality and subsequent flowering of long-day bedding plants*. Hort. Sci. 53(10):1407-1415. <https://doi.org/10.21273/HORTSCI13228-18>
- Craver, J.K., Boldt, J.K. and Lopez, R.G. (2019) *Comparison of supplemental lighting provided by high-pressure sodium lamps or light-emitting diodes for the propagation and finishing of bedding plants in a commercial greenhouse*. HortSci. 54(1):52-59. <https://doi.org/10.21273/HORTSCI13471-18>
- Croteau, R. (1977) *Site of monoterpene biosynthesis in majorana hortensis leaves*. Plant Physiol. 59(3):519-520. <https://doi.org/10.1104/pp.59.3.519>
- Croteau, R. B., Davis, E. M., Ringer, K. L., Wildung, M. R. (2005) (-)-Menthol Biosynthesis and Molecular Genetics. Naturwissenschaften 92(12):562–577. <https://doi.org/10.1007/s00114-005-0055-0>
- Croteau, R., Felton, M., Karp, F., Kjonaas, R. (1981) *Relationship of camphor biosynthesis to leaf development in sage (Salvia officinalis)*. Plant Physiol. 67(4):820-824. <https://doi.org/10.1104/pp.59.3.519>
- Currey, C. J., Kopsell, D. A., Mattson, N. S., Craver, J. K., Lopez, R. G., Erwin, J. E., et al. (2017) *“Supplemental and sole-source lighting of leafy greens, herbs and microgreens”* in Light management in controlled environments. Eds. R. Lopez and E. Runkle (Willoughby, Ohio, USA: Meister Media Worldwide), 170–175.
- Darko, E., Heydarizadeh, P., Schoefs, B., Sabzalian, M.R. (2014) *Photosynthesis under artificial light: the shift in primary and secondary metabolism*. Phil. Trans. R. Soc. B. 369(1640):20130243. <https://doi.org/10.1098/rstb.2013.0234>
- Das Bundessortenamt (BSA) (2002). *“Multimentha,”* in Beschreibende Sortenliste Arznei- und Gewürzpflanzen. 1st ed (Hannover, Germany: Deutscher Landwirtschaftsverlag GmbH), 121.
- Dedino, D.B., Destro de Lima, J., Bortolucci, W. de C., Rivadavea, W.R., Lovato, E.C.W., Gazim, Z.C., Gonçalves, J.E., Monzon, D.L.R., da Silva, G.J. (2022) *Red LED light and different cultivation methods changed the essential oil composition of Acmella oleracea*. PCTOC. 151:511-520. <https://doi.org/10.1007/s11240-022-02367-5>

- Dehsheikh, A. B., Sourestani, M. M., Zolfaghari, M., Enayatizamir, N. (2020) *Changes in soil microbial activity, essential oil quantity, and quality of Thai basil as response to biofertilizers and humic acid*. J. Clean Prod. 256:120439. <https://doi.org/10.1016/j.jclepro.2020.120439>
- Demkura, P.V., Ballaré (2012) *UVR8 mediates UV-B-induced Arabidopsis defense responses against Botrytis cinerea by controlling sinapate accumulation*. Mol. Plant. 5(3):642-652. <https://doi.org/10.1093/mp/sss025>
- Demotes-Mainard, S., Péron, T., Corot, A., Bertheloot, J., Le Gourrierec, J., Pelleschi-Travier, S., Crespel, L., Morel, P., Huché-Thélier, L., Boumaza, R., Vian, A., Guérin, V., Leduc, N., Sakr, S. (2016) *Plant responses to red and far-red lights, applications in horticulture*. Env. Exp. Bot. 121:4-21. <https://doi.org/10.1016/j.envexpbot.2015.05.010>
- Deng, Y., Lu, S. (2017) *Biosynthesis and regulations of phenylpropanoids in plants*. Crit. Rev. Plant Sci. 36(4):257-290. <https://doi.org/10.1080/07352689.2017.1402852>
- Deschamps, C., Simon, J. E. (2006) *Terpenoid essential oil metabolism in basil (Ocimum basilicum L.) following elicitation*. J. Essent. Oil Res. 18(6):618–621. <https://doi.org/10.1080/10412905.2006.9699183>
- Despommier, D. (2011) *Advantages of the vertical farm*. p. 259-275. In: Sustainable Environmental Design in Architecture: Impacts on Health, Pardalos, P.M., Rassia, S.T. (eds.), Springer Optimization and its applications. https://doi.org/10.1007/978-1-4419-0745-5_16
- De Vincenci, M., Silano, M., Maialetti, F., Scazzocchio, B. (2000) *Safety data review. Constituents of aromatic plants: II. Estragole*. Fitoterapia. 71(6):725-729. [https://doi.org/10.1016/s0367-326x\(00\)00153-2](https://doi.org/10.1016/s0367-326x(00)00153-2)
- Devlin, P.F., Kay, S.A. (2000) *Cryptochromes are required for phytochrome signaling to the circadian clock but not for rhythmicity*. Plant Cell. 12(12):2499-2509. <https://doi.org/10.1105/tpc.12.12.2499>
- Dhar, N., Sarangapani, S., Reddy, V. A., Kumar, N., Panicker, D., Jin, J., Chua, N.-H., Sarojam, R. (2020) *Characterization of a sweet basil acyltransferase involved in eugenol biosynthesis*. J. Exp. Bot. 71(12):3638–3652. <https://doi.org/10.1093/jxb/eraa142>
- Dieleman, J.A., de Visser, P.H.B., Vermeulen, P.C.M. (2016) *Reducing the carbon footprint of greenhouse grown crops: re-designing LED-based production systems*. Acta Hort. 1134:395-402 <https://doi.org/10.17660/ActaHortic.2016.1134.51>

- Dmello, J.R., Chandekar, L.P., Bavadekar, T.A., Buttar, H.S., Kaur, G. (2023) Quercetin: A promising flavonoid for the therapy of cardiac hypertrophy and heart failure mediated by the renin angiotensin system. In: The renin angiotensin system in cardiovascular disease. Advances in biochemistry in health and disease, Dhalla, N.S., Bhullar, S.K. (eds.), Springer, Cham. https://doi.org/10.1007/978-3-031-14952-8_23
- Döös, B.R. (2002) *Population growth and loss of arable land*. Glob. Environ. Change. 12(4):303-311. [https://doi.org/10.1016/s0959-3780\(02\)00043-2](https://doi.org/10.1016/s0959-3780(02)00043-2)
- Dougher, T.A.O., Bugbee, B. (2001) Evidence for yellow light suppression of lettuce growth. Photochem. Photobiol. 73(2):208-212. [https://doi.org/10.1562/0031-8655\(2001\)0730208EFYLSO2.0.CO2](https://doi.org/10.1562/0031-8655(2001)0730208EFYLSO2.0.CO2)
- Duriyaprapan, S., Britten, E.J. (1982). *The effect of age and location of leaf on quantity and quality of Japanese mint oil production*. J. Exp. Bot. 33(4):810-814. <https://doi.org/10.1093/jxb/33.4.810>
- Eichhorn Bilodeau, S., Wu, B.-S., Rufyikiri, A.-S., MacPherson, S., Lefsrud, M. (2019) *An update on plant photobiology and implications for cannabis production*. Front. Plant Sci. 10:296. <https://doi.org/10.3389/fpls.2019.00296>
- Eisinger, W.R., Bogomolni, R.A., Taiz, L. (2003) *Interactions between a blue-green reversible photoreceptor and a separate UV-B receptor in stomatal guard cells*. Am. J. Bot. 90(11):1560-1566. <https://doi.org/10.3732/ajb.90.11.1560>
- Elansary, H. O., Mahmoud, E. A. (2014) *Basil cultivar identification using chemotyping still favored over genotyping using core barcodes and possible resources of antioxidants*. J. Essent. Oil Res. 27(1):82–87. <https://doi.org/10.1080/10412905.2014.982874>
- EMA – European Medicines Agency (2005) *Committee on herbal medicinal products. Final public Statement on the use of herbal medicinal products containing estragole*. https://www.ema.europa.eu/docs/en_GB/document_library/Scientific_guideline/2010/4/WC500089960.pdf
- Emerson, R., Chalmers, R., Cederstrand, C. (1957) *Some factors influencing the long-wave limit of photosynthesis*. PNAS. 43(1):133-143. <https://doi.org/10.1073/pnas.43.1.133>
- Esteban, R., Barrutia, O., Artetxe, U., Fernández-Marín, B., Hernández, A., García-Plazaola, J.I. (2014) *Internal and external factors affecting photosynthetic pigment composition in plants: a meta-analytical approach*. New Phytol. 206(1):268-280. <https://doi.org/10.1111/nph.13186>

- Evans, J.R. (1987) *The dependence of quantum yield on wavelength and growth irradiance*. Aust. J. Plant Physiol. 14(1):69-79. <https://doi.org/10.1071/PP9870069>
- Fanwoua, J., Vercambre, G., Buck-Sorlin, G., Dieleman, J.A., de Visser, P., Génard, M. (2019) *Supplemental LED lighting affects the dynamics of tomato fruit growth and composition*. Sci. Hortic. 256:108571. <https://doi.org/10.1016/j.scienta.2019.108571>
- Faust, J.E. (2020) *First research report. Light management in greenhouses. I. Daily light integral: A useful tool for the U.S. floriculture industry*. <https://www.specmeters.com/assets/1/7/A051.pdf>. (accessed April 17, 2020)
- Faust, J.E., Logan, J. (2018) *Daily light integral: A research review and high-resolution maps of the United States*. HortSci. 53(9):1250-1257. <https://doi.org/10.21273/HORTSCI13144-18>
- Fedoroff, N. (2015) *Food in a future of 10 billion*. Agric. Food Secur. 4:11. <https://doi.org/10.1186/s40066-015-0031-7>
- Feher, B., Kozma-Bognar, L., Kevei, E., Hajdu, A., Binkert, M., Davis, S.J., Schäfer, E., Ulm, R., Nagy, F. (2011) *Functional interaction of the circadian clock and UV resistance locus 8-controlled UV-B signalling pathways in Arabidopsis thaliana*. Plant J. 67(1):37-48. <https://doi.org/10.1111/j.1365-313X.2011.04573.x>
- Fiorucci, A.-S., Frankhauser, C. (2017) *Plant strategies for enhancing access to sunlight*. Curr. Biol. 27(17):931-940. <https://doi.org/10.1016/j.cub.2017.05.085>
- Fischer, R., Nitzan, N., Chaimovitsh, D., Rubin, B., Dudai, N. (2011) *Variation in essential oil composition within individual leaves of sweet basil (Ocimum basilicum L.) is more affected by leaf position than by leaf age*. J. Agric. Food Chem. 59(9):4913–4922. <https://doi.org/10.1021/jf200017h>
- Flanigan, P. M., Niemeyer, E. D. (2014) *Effect of cultivar on phenolic levels, anthocyanin composition, and antioxidant properties in purple basil (Ocimum basilicum L.)*. Food Chem. 164:518–526. <https://doi.org/10.1016/j.foodchem.2014.05.061>
- Folta, K.M. (2004) *Green light stimulates early stem elongation, antagonizing light-mediated growth inhibition*. Plant Physiol. 135(3):1407-1416. <https://doi.org/10.1104/pp.104.038893>
- Folta, K.M., Carvalho, S.D. (2015) *Photoreceptors and control of horticultural plant traits*. HortSci. 50(9):1274-1280. <https://doi.org/10.21273/hortsci.50.9.1274>

- Folta, K.M., Maruhnich, S.A. (2007) *Green light: A signal to slow down or stop*. J. Exp. Bot. 58(12):3099-3111. <https://doi.org/10.1093/jxb/erm130>
- Folta, K.M., Spalding, E.P. (2001) *Unexpected roles for cryptochrome 2 and phototropin revealed by high-resolution analysis of blue light-mediated hypocotyl growth inhibition*. Plant J. 26(5):471-478. <https://doi.org/10.1046/j.1365-313x.2001.01038.x>
- Frank, H.A., Brudvig, G.W. (2014) *Redox functions of carotenoids in photosynthesis*. 43(27):8607-8615. Biochem. <https://doi.org/10.1021/bi0492096>
- Frankhauser, C., Batschauer, A. (2016) *Shadow on the plant: a strategy to exit*. Cell. 164(1-2):15-17. <https://doi.org/10.1016/j.cell.2015.12.043>
- Franklin, K.A. (2008) *Shade avoidance*. New Phytol. 179:930-944. <https://doi.org/10.1111/j.1469-8137.2008.02507.x>
- Franklin, K.A., Quail, P.H. (2010) *Phytochrome functions in Arabidopsis development*. J. Exp. Bot. 61(1):11-24. <https://doi.org/10.1093/jxb/erp304>
- Franklin, K.A., Whitelam, G.C. (2007) *Red:far-red ratio perception and shade avoidance*. In: Light and Plant Development. P. 211-234. Whitelam, G.C., Halliday, K.J. (eds.), Blackwell Publishing, Oxford, UK. <https://doi.org/10.1002/9780470988893.ch9>
- Fraser, D.P., Hayes, S., Franklin, K.A. (2016) *Photoreceptor crosstalk in shade avoidance*. Curr. Opin. Plant Biol. 33:1-7. <https://doi.org/10.1016/j.pbi.2016.03.008>
- Frechilla, S., Talbott, L.D., Bogomolni, R.A., Zeiger, E. (2000) *Reversal of blue light-stimulated stomatal opening by green light*. Plant Physiol. 41(2):171-176. <https://doi.org/10.1093/pcp/41.2.171>
- Fu, X., Chen, Y., Mei, X., Katsuno, T., Kobayashi, E., Dong, F., Watanabe, N., Yang, Z. (2015) *Regulation of formation of volatile compounds of tea (Camellia sinensis) leaves by single light wavelength*. Sci. Rep. 5:16858. <https://doi.org/10.1038/srep16858>
- Fuglevand, G., Jackson, J.A., Jenkins, G.I. (1996) *UV-B, UV-A and blue light signal transduction pathways interact synergistically to regulate chalcone synthase gene expression in Arabidopsis*. Plant Cell. 8(12):2347-2357. <https://doi.org/10.1105/tpc.8.12.2347>
- Gang, D. R., Wang, J., Dudareva, N., Simon, J. E., Lewinsohn, E., Pichersky, E. (2001) *An investigation of the storage and biosynthesis of phenylpropenes in sweet basil*. Plant Physiol. 125(2):539-555. <https://doi.org/10.1104/pp.125.2.539>

- Gao, M., Li, Y., Jiang, H., He, R., Shi, R., Song, S., Liu, H. (2022) *UVA-radiation exposure of different durations promoted the growth, phytochemicals and glucosinolate biosynthesis of Chinese kale*. Int. J. Mol. Sci. 23(14):7619. <https://doi.org/10.3390/ijms23147619>
- Gao, S. et al. (2020) *Photosynthetic characteristics and chloroplast ultrastructure of welsh onion (*Allium fistulosum* L.) grown under different LED wavelengths*. BMC Plant Biol. 20(1):78. <https://doi.org/10.1186/s12870-020-2282-0>
- Garcia-Plazaola, J. I., Esteban, R., Fernandez-Marin, B., Kranner, I., Porcar-Castell, A. (2012) *Thermal energy dissipation and xanthophyll cycles beyond the Arabidopsis model*. Photosynth. Res. 113:89–103. <https://doi.org/10.1007/s11120-012-9760-7>
- Gershenzon, J., McConkey, M. E., Croteau, R. B. (2000). *Regulation of monoterpene accumulation in leaves of peppermint*. Plant Physiol. 122(1):205–214. <https://doi.org/10.1104/pp.122.1.205>
- Ghaffari, Z., Rahimmalek, M., Sabzalian, M.R. (2019) *Variation in the primary and secondary metabolites derived from the isoprenoid pathway in the Perovskia species in response to different wavelengths generated by light emitting diodes (LEDs)* Ind. Crop Prod. 140:111592. <https://doi.org/10.1016/j.indcrop.2019.111592>
- Giliberto, L., Perrotta, G., Pallara, P., Weller, J.L., Fraser, P.D., Bramley, P.M., Fiore, A., Tavazza, M., Giuliano, G. (2005) *Manipulation of the blue light photoreceptor cryptochrome 2 in tomato affects vegetative development, flowering time, and fruit antioxidant content*. Plant Physiol. 137(1):199-208. <https://doi.org/10.1104/pp.104.051987>
- Gleizes, M., Pauly, G., Bernard-Dagan, C., Jacques, P. (1980) *Effects of light on terpene hydrocarbon synthesis in Pinus pinaster*. Physiol. Plant. 50:16-20. <https://doi.org/10.1111/j.1399-3054.1980.tb02676.x>
- Goins, G.D., Yorio, N.C., Sanwo, M.M., Brown, C.S. (1997) *Photomorphogenesis, photosynthesis, and seed yield of wheat plants grown under red light-emitting diodes (LEDs) with and without supplemental blue lighting*. J. Exp. Bot. 48(7):1407-1413. <https://doi.org/10.1093/jxb/48.7.1407>
- Goins, G.D., Yorio, N.C., Sanwo-Lewandowski, M.M., Brown, C.S. (1998) *Life cycle experiments with Arabidopsis grown under red light-emitting diodes (LEDs)*. Life Support Biosph. Sci. 5(2):143-149.
- Gómez, C., Izzo, L.G. (2018) *Increasing efficiency of crop production with LEDs*. AIMS. 3(2):135-153. <https://doi.org/10.3934/agrfood.2018.2.135>

- Gómez, C., Morrow, R.C., Bourget, C.M., Massa, G.D., Mitchell, C.A. (2013) Comparison of intrac canopy light-emitting diode towers and overhead high-pressure sodium lamps for supplemental lighting of greenhouse-grown tomatoes. *HortTechnology*. 23(1):93-98. <https://doi.org/10.21273/horttech.23.1.93>
- Gomiero, T. (2016) *Soil degradation, land scarcity and food security: Reviewing a complex challenge*. *Sustainability*. 8(3):281. <https://doi.org/10.3390/su8030281>
- Goto, E. (2012) *Plant production in a closed plant factory with artificial lighting*. *Acta Hortic*. 956:37-49. <https://doi.org/10.17660/actahortic.2012.956.2>
- Gouinguene, S.P., Turlings, T.C.J. (2002) *The effects of abiotic factors on induced volatile emissions in corn plants*. *Plant Physiol*. 129(3):1296-1307. <https://doi.org/10.1104/pp.001941>
- Gould, K. S. (2004) *Nature's Swiss army knife: The diverse protective roles of anthocyanins in leaves*. *J. Biomed. Biotech*. 5:314–320. <https://doi.org/10.1155/S1110724304406147>
- Gould, K. S., Jay-Allemand, C., Logan, B. A., Baissac, Y., Bidel, L. P. R. (2018) *When are foliar anthocyanins useful to plants? Re-evaluation of the photoprotection hypothesis using Arabidopsis thaliana mutants that differ in anthocyanin accumulation*. *Environ. Exp. Bot*. 154, 11–22. <https://doi.org/10.1016/j.envexpbot.2018.02.006>
- Guo, H., Yang, H., Mockler, T.C., Lin, C. (1998) *Regulation of flowering time by Arabidopsis photoreceptors*. *Sci*. 279(5355):1360-1363. <https://doi.org/10.1126/science.279.5355.1360>
- Han, T., Vaganov, V., Cao, S., Li, Q., Ling, L., Cheng, X., Peng, L., Zhang, C., Yakovlev, A.N., Zhong, Y., Tu, M. (2017) *Improving 'color rendering' of LED lighting for the growth of lettuce*. *Sci. Rep*. 7:45944. <https://doi.org/10.1038/srep45944>
- Hanif, M. A., Nawaz, H., Ayub, M. A., Tabassum, N., Kanwal, N., Rashid, N., Saleem, M., Ahmad, M. (2017) *Evaluation of the effects of zinc on the chemical composition and biological activity of basil essential oil by using raman spectroscopy*. *Ind. Crop Prod*. 96:91–101. <https://doi.org/10.1016/j.indcrop.2016.10.058>
- Harbick, K., Albright, L.D., Mattson, N.S. (2016) *Electrical savings comparison of supplemental lighting control systems in greenhouse environments*. ASABE Annual International Meeting. <https://doi.org/10.13031/aim.20162460478>
- Hart, J.W. (1988) *Light and Plant Growth*. p. 1-17. Black, M., Chapman, J. (eds.), Unwin Hyman Ltd. <https://doi.org/10.1007/978-94-011-5996-8>

- Hashimoto, H., Uagami, C., Cogdell, R.J. (2016) *Carotenoids and Photosynthesis*. pp. 111-139. In: *Carotenoids in Nature. Subcellular Biochemistry*, vol. 79, Stange, C. (eds.), Springer, Cham, Switzerland. https://doi.org/10.1007/978-3-319-39126-7_4
- Hayes, S., Velanis, C.N., Jenkins, G.I., Franklin, K.A. (2014) *UV-B detected by the UVR8 photoreceptor antagonizes auxin signaling and plant shade avoidance*. PNAS. 111(32):11894-11899. <https://doi.org/10.1073/pnas.1403052111>
- Heffer, P., Prud'homme, M. (2013) *Nutrients as limited resources: global trends in fertilizer production and use*. p. 57-78. In: *Improving water and nutrient-use efficiency in food production systems*, Rengel, Z. (eds.), John Wiley & Sons.
- Hernandez, E., Timmons, M.B. and Mattson, N.S. (2020) *Quality, yield, and biomass efficacy of several hydroponic lettuce (*Lactuca sativa* L.) cultivars in response to high pressure sodium lights of light emitting diodes for greenhouse supplemental lighting*. Horticulturae. 6(1):7. <https://doi.org/10.3390/horticulturae6010007>
- Hernández, R., Kubota, C. (2016) *Physiological responses of cucumber seedlings under different blue and red photon flux ratios using LEDs*. Environ. Exp. Bot.121:66-74 <https://doi.org/10.1016/j.envexpbot.2015.04.001>
- Hideg, É., Jansen, M.A.K., Strid, Å. (2013) *UV-B exposure, ROS, and stress: inseparable companions or loosely linked associates?* Trends Plant Sci. 18(2):107-115. <https://doi.org/10.1016/j.tplants.2012.09.003>
- Hikosaka, S., Moriyama, F., Goto, E. (2021) *Effects of photosynthetic photon flux density and red/blue ratio on the leaf shape and concentrations of functional and aromatic compounds in sweet basil (*Ocimum basilicum* L.)* Jap. Soc. Hortic. Sci. 90(4):357-364. <https://doi.org/10.2503/hortj.UTD-273>
- Hirai, N., Yamamuro, M., Koshimizu, K., Shinozaki, M., Takimoto, A. (1994) *Accumulation of phenylpropanoids in the cotyledons of morning glory (*Pharbitis nil*) seedlings during the induction of flowering by low temperature treatment, and the effect of precedent exposure to high-intensity light*. Plant Cell Physiol. 35(4):691–695. <https://doi.org/10.1093/oxfordjournals.pcp.a078644>
- Hoenecke, M.E., Bula, R.J., Tibbitts, T.W. (1992) *Importance of 'blue' photon levels for lettuce seedlings grown under red-light-emitting diodes*. HortSci. 27(5):427-430. <https://doi.org/10.21273/HORTSCI.27.5.427>

- Hogewoning, S.W., Wientjes, E., Douwstra, P., Trouborst, G., van Ieperen, W., Croce, R., Harbinson, J. (2012) *Photosynthetic quantum yield dynamics: from photosystems to leaves*. *Plant Cell*. 24(5):1921-1935. <https://doi.org/10.1105/tpc.112.097972>
- Hollósy, F. (2002) *Effects of ultraviolet radiation on plant cells*. *Micron*. 33(2):179-197. [https://doi.org/10.1016/s0968-4328\(01\)00011-7](https://doi.org/10.1016/s0968-4328(01)00011-7)
- Hosseini, A., Mehrjerdi, M.Z., Aliniaefard, S. (2018) *Alteration of bioactive compounds in two varieties of basil (*Ocimum basilicum*) grown under different light spectra*. *J. Essent. Oil Bear. Plants*. 21(4):913-923. <https://doi.org/10.1080/0972060X.2018.1526126>
- Hsie, B.S., Bueno, A., I.S., Bertolucci, S.K.V., Carvalho, A.A., Cunha, S.H.B., Martins, E.R., Pinto, J.E.B.P. (2019) *Study of the influence of wavelength and intensities of LEDs on the growth, photosynthetic pigment, and volatile compounds production of *Lippia rotundifolia* Cham in vitro*. *J. Photochem. Photobiol*. 198:111577. <https://doi.org/10.1016/j.jphotobiol.2019.111577>
- Huché-Thélier, L., Crespel, L., Le Gourrierec, J., Morel, P., Sakr, S., Leduc, N. (2016) *Light signaling and responses to blue and UV radiations – perspectives for applications in horticulture*. *Env. Exp. Bot*. 121:22-38. <https://doi.org/10.1016/j.envexpbot.2015.06.009>
- Humphrey, J.M., Chapple, C. (2002) *Rewriting the lignin roadmap*. *Curr. Opin. Plant Biol*. 5(1):224-229. [https://doi.org/10.1016/s1369-5266\(02\)00257-1](https://doi.org/10.1016/s1369-5266(02)00257-1)
- Huq, E., Al-Sady, B., Hudson, M., Kim C., Apel, K., Quail, P.H. (2004) *Phytochrome-interacting factor 1 is a critical bHLH regulator of chlorophyll biosynthesis*. *Sci*. 305(5692):1937-1941. <https://doi.org/10.1126/science.1099728>
- Hyun, M.W., Yun, Y.H., Kim, J. Y., Kim, S.H. (2011) *Fungal and plant phenylalanine ammonia-lyase*. *Mycobiol*. 39(4):257-265. <https://doi.org/10.5941/MYCO.2011.39.4.257>
- Iijima, Y., Davidovich-Rikanati, R., Fridman, E., Gang, D. R., Bar, E., Lewinsohn, E., Pichersky, E. (2004) *The biochemical and molecular basis for the divergent patterns in the biosynthesis of terpenes and phenylpropenes in the peltate glands of three cultivars of basil*. *Plant Physiol*. 136(3):3724–3736. <https://doi.org/10.1104/pp.104.051318>
- Imran, M., Rauf, A., Abuo-Izneid, T., Nadeem, M., Shariati, M.A., Khan, I.A., Imran, A., Orhan, I.E., Rizwan, M., Atif, M., Gondal, T.A., Mubarak, M.S. (2019) *Luteolin, a flavonoid, as an anticancer agent: A review*. *Biomed. Pharmacother*. 112:108612. <https://doi.org/10.1016/j.biopha.2019.108612>

- Imran, M., Rauf, A., Shah, Z., A., Saeed, F., Imran, A., Arshad, M.U., Ahmad, B., Bawazeer, S., Atif, M., Peters, D.G., Mubarak, M.S. (2018) *Chemo-preventive and therapeutic effect of the dietary flavonoid kaempferol: A comprehensive review*. *Phytother. Res.* 33(2):2633-275. <https://doi.org/10.1002/ptr.6227>
- Inada, K. (1976) *Action spectra for photosynthesis in higher plants*. *Plant Cell Physiol.* 17(2):355-365. <https://doi.org/10.1093/oxfordjournals.pcp.a075288>
- Inoue, S.-I., Kinoshita, T., Takemiya, A., Doi, M., Shimazaki, K.-I. (2008) *Leaf positioning of Arabidopsis in response to blue light*. *Mol. Plant.* 1(1):15-26. <https://doi.org/10.1093/mp/ssm001>
- Jang, S., Marchal, V., Panigrahi, K.C.S., Wenkel, S., Soppe, W., Deng, X.-W., Valverde, F., Coupland, G. (2008) *Arabidopsis COP1 shapes the temporal pattern of CO accumulation conferring a photoperiodic flowering response*. *EMBO J.* 27(8):1277-1288. <https://doi.org/10.1038/emboj.2008.68>
- Janoudi, A.-K., Gordon, W.R., Wagner, D., Quail, P., Poff, K.L. (1997a) *Multiple phytochromes are involved in red-light-induced enhancement of first-positive phototropism in Arabidopsis thaliana*. *Plant Physiol.* 113(3):975-979. <https://doi.org/10.1104/pp.113.3.975>
- Janoudi, A.-K., Konjevic, R., Whitelam, G., Gordon, W., Poff, K.L. (1997b) *Both phytochrome A and phytochrome B are required for the normal expression of phototropism in Arabidopsis thaliana seedlings*. *Physiol. Plant.* 101(2):278-282. <https://doi.org/10.1111/j.1399-3054.1997.tb00997.x>
- Jaramillo, P., Coutinho, K., Cabral, B.J.C., Canuto, S. (2011) *Explicit solvent effects on the visible absorption spectrum of a photosynthetic pigment: chlorophyll-c₂ in methanol*. *Chem. Phys. Lett.* 516(4-6):250-253. <https://doi.org/10.1016/j.cplett.2011.10.016>
- Jarillo, J.A., Gabrys, H., Capel, J., Alonso, J.M., Ecker, J.R., Cashmore, A.R. (2001) *Phototropin-related NPL1 controls chloroplast relocation induced by blue light*. *Nature.* 410:952-954. <https://doi.org/10.1038/35073622>
- Jayasinghe, C., Gotoh, N., Aoki, T., Wada, S. (2003) *Phenolics composition and antioxidant activity of sweet basil (Ocimum basilicum L.)*. *J. Agric. Food Chem.* 51(15):4442-4449. <https://doi.org/10.1021/jf034269o>
- Jenkins, G.I. (2014) *The UV-B photoreceptor UVR8: From structure to physiology*. *Plant Cell.* 26(1):21-37. <https://doi.org/10.1105/tpc.113.119446>

- Jenkins, G.I., Long, J.C., Wade, H.K., Shenton, M.R., Bibikova, T.N. (2001) *UV and blue light signalling: pathways regulating chalcone synthase gene expression in Arabidopsis*. *New Phytol.* 151(1):121-131. <https://doi.org/10.1046/j.1469-8137.2001.00151.x>
- Ji, Y., Ocaña, D.N., Choe, D., Larsen, D.H., Marcelis, L.F.M., Heuvelink, E. (2020) *Far-red radiation stimulates dry mass partitioning to fruits by increasing fruit sink strength in tomato*. *New Phytol.* 228(6):1914-1925. <https://doi.org/10.1111/nph.16805>
- Ji, Y., Ouzounis, T., Courbier, S., Kaiser, E., Nguyen, P.T., Schouten, H.J., Visser, R.G.F., Pierik, R., Marcelis, L.F.M., Heuvelink, E. (2019) *Far-red radiation increases dry mass partitioning to fruits but reduces Botrytis cinerea resistance in tomato*. *Env. Exp. Bot.* 168:103889. <https://doi.org/10.1016/j.envexpbot.2019.103889>
- Jin, W., Urbina, J.L., Heuvelink, E., Marcelis, L.F.M. (2021) *Adding far-red to red-blue light-emitting diode light promotes yield of lettuce at different planting densities*. *Front. Plant Sci.* 11:609977. <https://doi.org/10.3389/fpls.2020.609977>
- Jing, Y., Lin, R. (2020) *Transcriptional regulatory network of the light signaling pathways*. *New Phytol.* 227(3):683-697. <https://doi.org/10.1111/nph.16602>
- Johkan, M., Shoji, K., Goto, F., Hahida, S., Yoshihara, T. (2012) *Effect of green light wavelength and intensity on photomorphogenesis and photosynthesis in Lactuca sativa*. *Environ. Exp. Bot.* 75:128-133. <https://doi.org/10.1016/j.envexpbot.2011.08.010>
- Jones, M.A. (2018) *Using light to improve commercial value*. *Hortic. Res.* 5:47. <https://doi.org/10.1038/s41438-018-0049-7>
- Joshi, N.C., Ratner, K., Eidelman, O., Bednarczuk, D., Zur, N., Many, Y., Shahak, Y., Aviv-Sharon, E., Achiam, M., Gilad, Z., Charuvi, D. (2019) *Effects of daytime intra-canopy LED illumination on photosynthesis and productivity of bell pepper grown in protected cultivation*. *Sci. Hortic.* 250:81-88. <https://doi.org/10.1016/j.scienta.2019.02.039>
- Kagawa, T., Sakai, T., Suetsugu, N., Oikawa, K., Ishiguro, S., Kato, T., Tabata, S., Okada, K., Wada, M. (2001) *Arabidopsis NPL1: A phototropin homolog controlling the chloroplast high-light avoidance response*. *Sci.* 2138-2141. <https://doi.org/10.1126/science.291.5511.2138>

- Kaiser, E., Weerheim, K., Schipper, R., Dieleman, J.A. (2019) *Partial replacement of red and blue by green light increases biomass and yield in tomato*. *Sci. Hortic.* 249:271-279.
<https://doi.org/10.1016/j.scienta.2019.02.005>
- Kalaitzoglou, P., van Ieperen, W., Harbinson, J., van der Meer, M., Martinakos, S., Weerheim, K., Nicole, C.C.S., Marcelis, L.F.M. (2019) *Effects of continuous or end-of-day far-red light on tomato plant growth, morphology, light absorption, and fruit production*. *Front. Plant Sci.* 10:322.
<https://doi.org/10.3389/fpls.2019.00322>
- Kang, S., Zhang, Y., Zhang, Y., Zou, J., Yang, Q., Li, T. (2018) *Ultraviolet-A radiation stimulates growth of indoor cultivated tomato (*Solanum lycopersicum*) seedlings*. *Hort. Sci.* 53(10):1429-1433.
<https://doi.org/10.21273/hortsci13347-18>
- Kang, W.H., Park, J.S., Park, K.S., Son, J.E. (2016) *Leaf photosynthetic rate, growth, and morphology of lettuce under different fractions of red, blue, and green light from light-emitting diodes (LEDs)*. *Hortic. Environ. Biotechnol.* 57(6):573-579. <https://doi.org/10.1007/s13580-016-0093-x>
- Kapteyn, J., Qualley, A. V., Xie, Z., Fridman, E., Dudareva, N., Gang, D. R. (2007) *Evolution of cinnamate/p-coumarate carboxyl methyltransferase and their role in the biosynthesis of methylcinnamate*. *Plant Cell.* 19(10):3212–3229. <https://doi.org/10.1105/tpc.107.054155>
- Karousou, R., Grammatikopoulos, G., Lanaras, T., Manetas, Y., Kokkini, S. (1998) *Effects of enhanced UV-B radiation on *Mentha spicata* essential oils*. *Phytochem.* 49(8):2273-2277. [https://doi.org/10.1016/S0031-9422\(98\)00385-9](https://doi.org/10.1016/S0031-9422(98)00385-9)
- Kasperbauer, M.J. (1987) *Far-red light reflection from green leaves and effects on phytochrome-mediated assimilate partitioning under field conditions*. *Plant Physiol.* 85(2):350-354.
<https://doi.org/10.1104/pp.85.2.350>
- Katzin, D., Marcelis, L.F.M., van Mourik, S. (2021) *Energy savings in greenhouses by transition from high-pressure sodium to LED lighting*. *Appl. Energy.* 281:116019.
<https://doi.org/10.1016/j.apenergy.2020.116019>
- Kaur, C., Kapoor, H.C. (2001) *Antioxidants in fruits and vegetables – the millennium’s health*. *Int. J. Food Sci. Tech.* 36(7):703-725. <https://doi.org/10.1111/j.1365-2621.2001.00513.x>

- Ke, X., Yoshida, H., Hikosaka, S., Goto, E. (2021) *Optimization of photosynthetic photon flux density and light quality for increasing radiation-use efficiency in dwarf tomato under LED light at the vegetative growth stage*. *Plants*. 11(1):121. <https://doi.org/10.3390/plants11010121>
- Kegge, W., Weldegergis, B.T., Soler, R., Vergeer-Van Eijk, M., Dicke, M., Voeselek, L.A.C., Pierik, R. (2013) *Canopy light cues affect emission of constitutive and methyl jasmonate-induced volatile organic compounds in Arabidopsis thaliana*. *New Phytologist*. 200:861-874. <https://doi.org/10.1111/nph.12407>
- Khojasteh, S.C., Oishi, S., Nelson, S.D. (2010) *Metabolism and toxicity of menthofuran in rat liver slices and in rats*. *Chem. Res. Toxicol.* 23(11):1824-1832. <https://doi.org/10.1021/tx100268g>
- Kohjasteh-Bakht, S.C., Chen, W., Koenigs, L.L., Peter, R.M., Nelson, S.D. (1999) *Metabolism of (R)-(+)-pulegone and (R)-(+)-menthofuran by human liver cytochrome P-450s: evidence for formation of a furan epoxide*. *Drug Metab. Dispos.* 27(5):574-580.
- Kim, H.-H., Goins, G.D., Wheeler, R.M., Sager, J.C. (2004) *Green-light supplementation for enhanced lettuce growth under red- and blue-light-emitting diodes*. *Hort. Sci.* 39(7):1617-1622. <https://doi.org/10.21273/HORTSCI.39.7.1617>
- Kim, H.-J., Lin, M.-Y., Mitchell, C.A. (2019) *Light spectral and thermal properties govern biomass allocation in tomato through morphological and physiological changes*. *Env. Exp. Bot.* 157:228-240 <https://doi.org/10.1016/j.envexpbot.2018.10.019>
- Kim, J., Yi, H., Choi, G., Shin, B., Song, P.-S., Choi, G. (2003) *Functional characterization of phytochrome interacting factor 3 in phytochrome-mediated light signal transduction*. *Plant Cell*. 15(10):2399-2407. <https://doi.org/10.1105/tpc.014498>
- Kim, J., Song, K., Park, E., Kim, K., Bae, G., Choi, G. (2016) *Epidermal phytochrome B inhibits hypocotyl negative gravitropism non-cell-autonomously*. *Plant Cell*. 28(11):2770-2785. <https://doi.org/10.1105/tpc.16.00487>
- Kinoshita, T., Doi, M., Suetsugu, N., Kagawa, T., Wada, M., Shimazaki, K.-I. (2001) *Phot1 and phot2 mediate blue light regulation of stomatal opening*. *Nat.* 414:656-660. <https://doi.org/10.1038/414656a>
- Kivimäenpää, M., Mofikoya, A., El-Raheem, A.M.A., Riikonen, J., Julkunen-Tiitto, R., Holopainen, J.K. (2022) *Alteration in light spectra causes opposite responses in volatile phenylpropanoids and terpenoids compared with phenolic acids in sweet basil (Ocimum basilicum L.) leaves*. *J. Agric. Food Chem.* 70(39):12287-12296. <https://doi.org/10.1021/acs.jafc.2c03309>

- Kong, S.-W., Chung, H.-Y., Chang, M.-Y., Fang, W. (2015) *The contribution of different spectral sections to increase fresh weight of boston lettuce*. HortSci. 50(7):1006-1010.
<https://doi.org/10.21273/HORTSCI.50.7.1006>
- Kong, Y., Llewellyn, D., Zheng, Y. (2017) *Response of growth, yield, and quality of pea shoots to supplemental light-emitting diode lighting during winter greenhouse production*. Can. J. Plant Sci. 98(3):732-740. <https://doi.org/10.1139/cjps-2017-0276>
- Kontor (2018). Available online:
<https://www.wetterkontor.de/de/wetter/deutschland/rueckblick.asp?id=20&datum0=09.10.2018&datum1=31.12.2018&jr=2021&mo=3&datum=08.03.2021&t=8&part=0> (accessed March 10, 2021)
- Kontor (2021). Available online:
<https://www.wetterkontor.de/de/wetter/deutschland/rueckblick.asp?id=20&datum0=10.04.2019&datum1=06.05.2019&jr=2021&mo=3&datum=08.03.2021&t=8&part=0> (accessed October 25, 2021)
- Köppe, J.M., von Studzinski, C., Mewis, I., Arnold, O., Schulz, H. (2018) *Basil cultivation without sunlight*. Braunschweig. In: Proceedings of the Young Scientists Meeting. [YSM Poster Tabbert \(maiden name Koeppe\) et al.pdf](#)
- Köppe, J.M., Riewe, D., von Studzinski, C., Mewis, I., Arnold, O., Schulz, H. (2019) *Basil cultivation without sunlight: Proceedings in LED technology*. Quedlinburg. In: OpenAgrar Repository.
https://www.openagrar.de/receive/openagrar_mods_00086027
- Korczyński, P.C., Logan, J., Faust, J.E. (2002) *Mapping monthly distribution of daily light integrals across the contiguous United States*. HortTechnology. 12(1):12-16. <https://doi.org/10.21273/HORTTECH.12.1.12>
- Kozai, T. (2019) *Towards sustainable plant factories with artificial lighting (PFALs) for achieving SDGs*. Int. J. Agric. Biol. Eng. 12(5):28-37. <https://doi.org/10.25165/j.ijabe.20191205.5177>
- Kume, A., Akitsu, T., Nasahara, K.N. (2018) *Why is chlorophyll b only used in light-harvesting systems?* J. Plant Res. 131:961-972. <https://doi.org/10.1007/s10265-018-1052-7>
- Kusuma, P., Bugbee, B. (2021) *Improving the predictive value of phytochrome photoequilibrium: Consideration of spectral distortion within a leaf*. Front. Plant Sci. 12:596943.
<https://doi.org/10.3389/fpls.2021.596943>
- Kusuma, P., Pattison, M., Bugbee, B. (2020) *From physics to fixtures to food: current and potential LED efficacy*. Hort. Res. 7:56. <https://doi.org/10.1038/s41438-020-0283-7>

- Kusuma, P., Pattison, M., Bugbee, B. (2022) *Chapter 7 - Photon efficacy in horticulture: turning LED packages into LED luminaires*. p. 115-128. In: *Plant factory basics, applications and advances*, Kozai, T., Niu, G., Masabni, J. (eds.), Academic Press. <https://doi.org/10.1016/B978-0-323-85152-7.00006-9>
- Kwee, E. M., Niemeyer, E. D. (2011) *Variations in phenolic composition and antioxidant properties among 15 basil (*Ocimum basilicum* L.) cultivars*. *Food Chem.* 128(4):1044–1050.
<https://doi.org/10.1016/j.foodchem.2011.04.011>
- Kyriacou, M. C., Roupshael, Y., Di Gioia, F., Kyratzis, A., Serio, F., Renna, M., De Pascale, S., Santamaria, P. (2016) *Micro-scale vegetable production and the rise of microgreens*. *Trends Food Sci. Technol.* 57(A):103–115. <https://doi.org/10.1016/j.tifs.2016.09.005>
- Łabuz, J., Hermanowicz, P., Gabryś, H. (2015) *The impact of temperature on blue light induced chloroplast movements in *Arabidopsis thaliana**. *Plant Sci.* 239:238-249.
<https://doi.org/10.1016/j.plantsci.2015.07.013>
- Łabuz, J., Sztatelman, O., Hermanowicz, P. (2022) *Molecular insights into the phototropin control of chloroplast movements*. *J. Exp. Bot.* 73(18):6034-6051. <https://doi.org/10.1093/jxb/erac271>
- Landi, M., Guidi, L., Pardossi, A., Tattini, M., Gould, K. S. (2014) *Photoprotection by foliar anthocyanins mitigates effects of boron toxicity in sweet basil (*Ocimum basilicum*)*. *Planta.* 240:941–953.
<https://doi.org/10.1007/s00425-014-2087-1>
- Landi, M., Zivcak, M., Sytar, O., Brestic, M., Allakhverdiev, S.I. (2020) *Plasticity of photosynthetic processes and the accumulation of secondary metabolites in plants in response to monochromatic light environments*. *BBA.* 1861(2):148131. <https://doi.org/10.1016/j.bbabi.2019.148131>
- Lanoue, J., Little, C., Hao, X. (2022) *The power of far-red light at night: photomorphogenic, physiological, and yield response in pepper during dynamic 24 hour lighting*. *Front. Plant Sci.* 13:857616.
<https://doi.org/10.3389/fpls.2022.857616>
- Lazzarini, L.E.S., Bertolucci, S.K.V., Pacheco, F.V., dos Santos, J., Silva, S.T., Carvalho, A.A., Pinto, J.E.B.P. (2018) *Quality and intensity of light affect *Lippia gracilis* Schauer plant growth and volatile compounds in vitro*. *PCTOC.* 135:367-379. <https://doi.org/10.1007/s11240-018-1470-1>
- Leduc, N., Roman, H., Barbier, F., Péron, T., Huché-Thélier, L., Lothier, J., Demotes-Mainard, S., Sakr, S. (2014) *Light signaling in bud outgrowth and branching in plants*. *Plants.* 3(2):223-250.
<https://doi.org/10.3390/plants3020223>

Lee, J.-H., Oh, M.-M., Son, K.-H. (2019) *Short-term ultraviolet (UV)-A light-emitting diode (LED) radiation improves biomass and bioactive compounds in kale*. *Front. Plant Sci.* 10:1042.

<https://doi.org/10.3389/fpls.2019.01042>

Lee, J.-W., Park, S.-Y., Oh, M.-M. (2021) *Supplemental radiation of ultraviolet-A light-emitting diode improves growth, antioxidant phenolics, and sugar alcohols of ice plant*. *Hortic. Environ. Biotechnol.*

62:559-570. <https://doi.org/10.1007/s13580-021-00340-3>

Lee, M., Rivard, C., Pliakoni, E., Wang, W., Rajashekar, C.B. (2021a) *Supplemental UV-A and UV-B affect the nutritional quality of lettuce and tomato: health-promoting phytochemicals and essential nutrients*.

Am. J. Plant Sci. 12(1):104-126. <https://doi.org/10.4236/ajps.2021.121007>

Lee, R. J., Bhandari, S. R., Lee, G., Lee, J. G. (2019) *Optimization of temperature and light, and cultivar selection for the production of high-quality head lettuce in a closed-type plant factory*. *Hortic. Environ. Biotechnol.* 60:207– 216. <https://doi.org/10.1007/s13580-018-0118-8>

Lee, R., Simon, J. E., Reichert, W., Juliani, H. R., Tepper, B. J. (2017) *A fresh language*. *Perfum Flavor.* 42:36–50.

Legendre, R., van Iersel, M.W. (2021) *Supplemental far-red light stimulates lettuce growth: disentangling morphological and physiological effects*. *Plants.* 10(1):166. <https://doi.org/10.3390/plants10010166>

Leonardo, E.D., Ma, X., Lanoue, J., Grodzinski, B. (2019) *Leaf and whole plant gas exchange and water-use efficiency of chrysanthemum under HPS and LEDs during vegetative and flower-induction stages*.

Can. J. Plant Sci. 99(5):639-653. <https://doi.org/10.1139/cjps-2018-0245>

Lewinsohn, E., Ziv-Raz, I., Dudai, N., Tadmor, Y., Lastochkin, E., Larkov, O., Chaimovitsh, D., Ravid, U., Putievsky, E., Pichersky, E., Shoham, Y. (2000) *Biosynthesis of estragole and methyleugenol in sweet basil (Ocimum basilicum L.). developmental and chemotypic association of allylphenol O-methyltransferase activities*. *Plant Sci.* 160(1):27–35. [https://doi.org/10.1016/S0168-9452\(00\)00357-5](https://doi.org/10.1016/S0168-9452(00)00357-5)

Li, D., Wang, P., Luo, Y., Zhao, M., Chen, F. (2017) *Health benefits of anthocyanins and molecular mechanisms: Update from recent decade*. *Crit. Rev. Food Sci. Nutr.* 57(8):1729-1741.

<https://doi.org/10.1080/10408398.2015.1030064>

Li, D., Rui, Y.-X., Guo, S.-D., Luan, F., Liu, R., Zeng, N. (2021) *Ferulic acid: A review of its pharmacology, pharmacokinetics and derivatives*. *Life Sci.* 284:119921. <https://doi.org/10.1016/j.lfs.2021.119921>

- Li, J., Ou-Lee, T.-M., Raba, R., Amundson, R.G., Last, R.L. (1993) *Arabidopsis flavonoid mutants are hypersensitive to UV-B radiation*. Plant Cell. 5(2):171-179. <https://doi.org/10.1105/tpc.5.2.171>
- Li, Q.-H., Yang, H.-Q. (2007) *Cryptochrome signaling in plants*. Photochem. Photobiol. 83(1):94-101. <https://doi.org/10.1562/2006-02-28-IR-826>
- Li, Q., Kubota, C. (2009) *Effects of supplemental light quality on growth and phytochemicals of baby leaf lettuce*. Env. Exp. Bot. 67(1):59-64. <https://doi.org/10.1016/j.envexpbot.2009.06.011>
- Li, W., Tan, L., Zou, Y., Tan, X., Huang, J., Chen, W., Tang, Q. (2020) *The effects of ultraviolet A/B treatments on anthocyanin accumulation and gene expression in dark-purple tea cultivar 'Ziyan' (Camellia sinensis)*. Molecules. 25(2):354. <https://doi.org/10.3390/molecules25020354>
- Li, Y.-L., Craker, L.E., Potter, T. (1996) *Effect of light level on essential oil production of sage (Salvia officinalis) and thyme (Thymus vulgaris)*. Acta Hort. 426:419-426. <https://doi.org/10.17660/actahortic.1996.426.46>
- Li, Y., Zheng, Y., Zheng, D., Zhang, Y., Song, S., Su, W., Liu, H. (2020a) *Effects of supplementary blue and UV-A LED lights on morphology and phytochemicals of Brassicaceae baby-leaves*. Molecules. 25(23):5678. <https://doi.org/10.3390/molecules25235678>
- Liaros, S., Botsis, K., Xydis, G. (2016) *Technoeconomical evaluation of urban plant factories: The case of basil (Ocimum basilicum)*. Sci. Total Environ. 554-555:218–227. <https://doi.org/10.1016/j.scitotenv.2016.02.174>
- Lila, M.A. (2004) *Anthocyanins and human health: An in vitro investigative approach*. J. Biomed. Biotech. 5:306-313.
- Lin, C., Ahmad, M., Gordon, D., Cashmore, A.R. (1995) *Expression of an Arabidopsis cryptochrome gene in transgenic tobacco results in hypersensitivity to blue, UV-A, and green light*. PNAS. 92(18):8423-8427. <https://doi.org/10.1073/pnas.92.18.8423>
- Lin, K.-H., Huang, M.-Y., Huang, W.-D., Hsu, M.-H., Yang, Z.-W., Yang, C.-M. (2013) *The effects of red, blue, and white light-emitting diodes on the growth, development, and edible quality of hydroponically grown lettuce (Lactuca sativa L. var. capitata)*. Sci. Hortic. 150: 86–91. <https://doi.org/10.1016/j.scienta.2012.10.002>

- Liu, H., Fu, Y., Wang, M., Liu, H. (2017) *Green light enhances growth, photosynthetic pigments and CO₂ assimilation efficiency of lettuce as revealed by 'knock out' of the 480-560 nm spectral waveband.* Photosyn. 55(1):144-152. <https://doi.org/10.1007/s11099-016-0233-7>
- Liu, J., van Iersel, M.W. (2022) *Far-red light effects on lettuce growth and morphology in indoor production are cultivar specific.* Plants. 11(20):2714. <https://doi.org/10.3390/plants11202714>
- Liu, Z., Wang, H., Xie, J., Lv, J., Zhang, G., Hu, L., Luo, S., Li, L., Yu, J. (2021) *The roles of cruciferae glucosinolates in disease and pest resistance.* Plants. 10(6):1097. <https://doi.org/10.3390/plants10061097>
- Lee, K.P., Pisurewicz, U., Turečková, V., Carat, S., Chappuis, R., Strnad, M., Frankhauser, C., Lopez-Molina, L. (2012) *Spatially and genetically distinct control of seed germination by phytochromes A and B.* Genes Dev. 26:1984-1996. <https://doi.org/10.1101/gad.194266.112>
- Legris, M., Ince, Y.Ç., Frankhauser, C. (2019) *Molecular mechanisms underlying phytochrome-controlled morphogenesis in plants.* Nat. Commun. 10:5219. <https://doi.org/10.1038/s41467-019-13045-0>
- Lobiuc, A., Vasilache, V., Pintilie, O., Stoleru, T., Burducea, M., Oroian, M., Zamfirache, M.-M. (2017) *Blue and red LED illumination improves growth and bioactive compounds contents in acyanic and cyanic Ocimum basilicum L. microgreens.* Molecules. 22(12):2111. <https://doi.org/10.3390/molecules22122111>
- Logan, B. A., Stafstrom, W. C., Walsh, M. J. L., Reblin, J. S., Gould, K. S. (2015) *Examining the photoprotection hypothesis for adaxial foliar anthocyanin accumulation by revisiting comparisons of green- and red-leafed varieties of coleus (Solenostemon scutellarioides).* Photosynth. Res. 124:267–274. <https://doi.org/10.1007/s11120-015-0130-0>
- Loni, A., Saadatmand, S., Yazdi, H. L., Iranbakhsh, A. (2021) *Application of nano-β-cyclodextrin to induce biosynthesis of phenylpropanoids and antioxidant activity in basil.* Iran. J. Sci. Technol. Trans. Sci. 45:1951–1962. <https://doi.org/10.1007/s40995-021-01163-8>
- Lopez, R. G., Runkle, E. S. (2008) *Photosynthetic daily light integral during propagation influences rooting and growth of cuttings and subsequent development of new guinea impatiens and petunia.* HortScience. 43(7):2052– 2059. <https://doi.org/10.21273/HORTSCI.43.7.2052>
- Luesse, D.R., DeBlasio, S.L., Hangarter, R.P. (2010) *Integration of phot1, phot2, and phyB signaling in light-induced chloroplast movements.* J. Exp. Bot. 61(15):4387-4397. <https://doi.org/10.1093/jxb/erq242>

- Ma, D., Li, X., Guo, Y., Chu, J., Fang, S., Yan, C., Noel, J.P., Liu, H. (2016) *Cryptochrome 1 interacts with PIF4 to regulate high temperature-mediated hypocotyl elongation in response to blue light*. PNAS. 113(1):224-229. <https://doi.org/10.1073/pnas.1511437113>
- Ma, Y., Ma, X., Gao, X., Wu, W., Zhou, B. (2021) *Light induced regulation pathway of anthocyanin biosynthesis in plants*. Int. J. Mol. Sci. 22:11116. <https://doi.org/10.3390/ijms222011116>
- Macchia, M., Pagano, A., Ceccarini, L., Benvenuti, S., Cioni, P. L., Flamini, G. (2006) *Agronomic and phytochemic characteristics in some genotypes of Ocimum basilicum L.* Acta Hort. 723:143–150. <https://doi.org/10.17660/ActaHortic.2006.723.15>
- Maeda, H., Dudareva, N. (2012) *The shikimate pathway and aromatic amino acid biosynthesis in plants*. Annu. Rev. Plant Biol. 63:73-105. <https://doi.org/10.1146/annurev-arplant-042811-105439>
- Maffei, M., Scannerini, S. (1999) *UV-B effects on photomorphogenesis and essential oil composition in peppermint (Mentha piperita L.)*. J. Essen. Oil Res. 12(5):523-529. <https://doi.org/10.1080/10412905.2000.9712150>
- Maffei, M., Scannerini, S. (1999) *Photomorphogenic and chemical responses to blue light in Mentha piperita*. J. Essent. Oil Res. 11(6):730–738. <https://doi.org/10.1080/10412905.1999.9712007>
- Maggio, A., Roscigno, G., Bruno, M., De Falco, E., Senatore, F. (2016) *Essential oil variability in a collection of Ocimum basilicum L. (Basil) cultivars*. Chem. Biodivers. 13(10):1357–1368. <https://doi.org/10.1002/cbdv.201600069>
- Mahendran, G., Rahman, L. U. (2020) *Ethnomedicinal, phytochemical and pharmacological updates on peppermint (Mentha × piperita L.) - A review*. Phytotherapy Res. 34(9):2088–2139. <https://doi.org/10.1002/ptr.6664>
- Makri, O., Kintzios, S. (2008) *Ocimum sp (Basil): Botany, cultivation, pharmaceutical properties, and biotechnology*. J. Herbs Spices Med. Plants. 13(3):123–150. https://doi.org/10.1300/J044v13n03_10
- Malekmohammad, K., Rafieian-Kopaei, M., Sardari, S., Sewell, R. D. E. (2019) *Toxicological effects of Mentha x piperita (Peppermint): a review*. Toxin Rev. 40:445–459. <https://doi.org/10.1080/15569543.2019.1647545>
- Mandoulakani, B. A., Eyvazpour, E., Ghadimzadeh, M. (2017) *The effect of drought stress on the expression of key genes involved in the biosynthesis of phenylpropanoids and essential oil components in basil (Ocimum basilicum L.)*. Phytochem. 139:1–7. <https://doi.org/10.1016/j.phytochem.2017.03.006>

- Mao, J., Zhang, Y.-C., Sang, Y., Li, Q.-H., Yang, H.-Q. (2005) *A role for Arabidopsis cryptochromes and COP1 in the regulation of stomatal opening*. PNAS. 102(34):12270-12275.
<https://doi.org/10.1073/pnas.0501011102>
- Mao, P., Duan, F., Zheng, Y., Yang, Q. (2020) *Blue and UV-A light wavelengths positively affected accumulation profiles of healthy compounds in pak-choi*. J. Sci. Food Agri. 101(4):1676-1684.
<https://doi.org/10.1002/jsfa.10788>
- Maoka, T. (2020) *Carotenoids as natural functional pigments*. J. Nat. Med. 74:1-16.
<https://doi.org/10.1007/s11418-019-01364-x>
- Market Research Report (2022) *Basil leaves market – global industry analysis, size and forecast-2027*. Available at: <https://www.futuremarketinsights.com/reports/basil-leaves-market> (accessed August 10, 2022)
- Martineau, V., Lesrud, M., Naznin, M.T., Kopsell, D.A. (2012) *Comparison of light-emitting diode and high-pressure sodium light treatments for hydroponics growth of boston lettuce*. HortSci. 47(4):477-482.
<https://doi.org/10.21273/HORTSCI.47.4.477>
- Martins, C., Cação, R., Cole, K. J., Phillips, D. H., Laires, A., Rueff, J., Rodrigues, A.S. (2012) *Estragole: A weak direct-acting food-borne genotoxin and potential carcinogen*. Mutat. Res. 747(1):86–92.
<https://doi.org/10.1016/j.mrgentox.2012.04.009>
- Mas, P., Devlin, P.F., Panda, S., Kay, S.A. (2000) *Functional interaction of phytochrome B and cryptochrome 2*. Nature. 408:207-211. <https://doi.org/10.1038/35041583>
- Massa, G.D., Kim, H.-H., Wheeler, R.M., Mitchell, C.A. (2008) *Plant productivity in response to LED lighting*. Hort. Sci. 43(7):1951-1956. <https://doi.org/10.21273/hortsci.43.7.1951>
- Mathew, S. (2006) *Phytochrome-mediated development in land plants: red light sensing evolves to meet the challenges of changing light environments*. Mol. Ecol. 15(12):3482-3503.
<https://doi.org/10.1111/j.1365-294X.2006.03051.x>
- Matysiak, B., Kowalski, A. (2019) *White, blue and red LED lighting on growth, morphology and accumulation of flavonoid compounds in leafy greens*. Zemdirbyste-Agriculture. 106(3):281-286.
<https://doi.org/10.13080/z-a.2019.106.036>

- McConkey, M.E., Gershenzon, J., Croteau, R.B. (2000) *Developmental regulation of monoterpene biosynthesis in the glandular trichomes of peppermint*. *Plant Physiol.* 122(1):215-223.
<https://doi.org/10.1104/pp.122.1.215>
- McCree, K.J. (1972a) *The action spectrum absorptance and quantum yield of photosynthesis in crop plants*. *Agric. Meteorol.* 10:191-216. [https://doi.org/10.1016/0002-1571\(72\)90045-3](https://doi.org/10.1016/0002-1571(72)90045-3)
- McCree, K.J. (1972b) *Test of current definitions of photosynthetically active radiation against leaf photosynthesis data*. *Agric. Meteorol.* 10:443-453. [https://doi.org/10.1016/0002-1571\(72\)90045-3](https://doi.org/10.1016/0002-1571(72)90045-3)
- Mehldau, K. (2020) *Studies on greenhouse cultivation of turmeric (Curcuma longa L.) – Effects of supplemental LED lighting on yield and secondary metabolites*. [Master thesis, Humboldt-Universität zu Berlin, Thae-Institute of Agricultural and Horticultural Science]
- Meng, Q., Kelly, N., Runkle, E.S. (2019) *Substituting green or far-red radiation for blue radiation induces shade avoidance and promotes growth in lettuce and kale*. *Env. Exp. Bot.* 162:383-391.
<https://doi.org/10.1016/j.envexpbot.2019.03.016>
- Meng, Q., Runkle, E.S. (2019) *Regulation of flowering by green light depends on its photon flux density and involves cryptochromes*. *Physiol. Plant.* 166(3):762-771. <https://doi.org/10.1111/ppl.12832>
- Meng, Q., Runkle, E.S. (2019a) *Far-red radiation interacts with relative and absolute blue and red photon flux densities to regulate growth, morphology, and pigmentation of lettuce and basil seedlings*. *Sci. Hortic.* 255:269-280. <https://doi.org/10.1016/j.scienta.2019.05.030>
- Mickens, M.A., Skoog, E.J., Reese, L.E., Barnwell, P.L., Spencer, L.E., Massa, G.D., Wheeler, R.M. (2018) *A strategic approach for investigating light recipes for 'Outredgeous' red romaine lettuce using white and monochromatic LEDs*. *Life Sci. Space Res.* 19:53-62. <https://doi.org/10.1016/j.lssr.2018.09.003>
- Mickens, M.A., Torralba, M., Robinson, S.A., Spencer, L.E., Romeyn, M.W., Massa, G.D., Wheeler, R.M. (2019) *Growth of red pak choi under red and blue, supplemented white, and artificial sunlight provided by LEDs*. *Sci. Hortic.* 245:200-209. <https://doi.org/10.1016/j.scienta.2018.10.023>
- Milenković, L., Stanojević, J., Cvetković, D., Stanojević, L., Lalević, D., Šunić, L., Fallik, E., Ilić, Z.S. (2019) *New technology in basil production with high essential oil yield and quality*. *Ind. Crops Prod.* 140:111718.
<https://doi.org/10.1016/j.indcrop.2019.111718>

- Millar, A.J., Straume, M., Chory, J., Chua, N.-H., Kay, S.A. (1995) *The regulation of circadian period by phototransduction pathways in Arabidopsis*. *Sci.* 267(5201):1163-1166.
<https://doi.org/10.1126/science.7855596>
- Mir, S. A., Shah, M. A., Mir, M. M. (2016) *Microgreens: Production, shelf life, and bioactive components*. *Crit. Rev. Food Sci. Nutr.* 57(12):2730–2736. <https://doi.org/10.1080/10408398.2016.1144557>
- Misyura, M., Colasanti, J., Rothstein, S. J. (2013) *Physiological and genetic analysis of Arabidopsis thaliana anthocyanin biosynthesis mutants under chronic adverse environmental conditions*. *J. Exp. Bot.* 64(1):229–240. <https://doi.org/10.1093/jxb/ers328>
- Mitchell, C.A., Dzakovich, M.P., Gómez, C., Lopez, R., Burr, J.F., Hernández, R., Kubota, C., Currey, C.J., Meng, Q., Runkle, E.S. (2015) *Light-emitting diodes in horticulture*. In *Horticultural Reviews*, 1st ed., Janick, J., Ed., Wiley-Blackwell: Hoboken, NJ, USA, Volume 43.
- Mizuno, T., Amaki, W. (2011) *Effects of monochromatic light irradiation by LED on the growth and anthocyanin contents in leaves of cabbage seedlings*. *Acta. Hort.* 907:179-184.
<https://doi.org/10.17660/ActaHortic.2011.907.25>
- Moccaldi, L. A., Runkle, E. S. (2007) *Modeling the effects of temperature and photosynthetic daily light integral on growth and flowering of Salvia splendens and Tagetes patula*. *J. Amer. Soc Hortic. Sci.* 123(3):283–288. <https://doi.org/10.21273/JASHS.132.3.283>
- Mockler, T.C., Guo, H., Yang, H., Duong, H., Lin, C. (1999) *Antagonistic actions of Arabidopsis cryptochromes and phytochrome B in the regulation of floral induction*. *Dev.* 126(10):2073-2082.
<https://doi.org/10.1242/dev.126.10.2073>
- Moghaddam, M., Pirbalouti, A. G., Mehdizadeh, L., Pirmoradi, M. R. (2015) *Changes in composition and essential oil yield of Ocimum ciliatum at different phenological stages*. *Eur. Food Res. Technol.* 240:199-204. <https://doi.org/10.1007/s00217-014-2320-y>
- Morales, L.O., Brosché, M., Vainonen, J., Jenkins, G.I., Wargent, J.J., Sipari, N., Strid, Å., Lindfors, A.V., Tegelberg, R., Aphalo, P.J. (2013) *Multiple roles for UV resistance locus8 in regulating gene expression and metabolite accumulation in Arabidopsis under solar ultraviolet radiation*. *Plant Physiol.* 161(2):744-759. <https://doi.org/10.1104/pp.112.211375>
- Morgan, K. (2009) *Feeding the city: The challenge of urban food planning*. *Int. Plan. Stud.* 14(4): 341-348.
<https://doi.org/10.1080/13563471003642852>

- Morrow, R.C. (2008) *LED lighting in horticulture*. Hort. Sci. 43(7):1947-1950.
<https://doi.org/10.21273/hortsci.43.7.1947>
- Muñoz-Bertomeu, J., Arrillaga, I., Ros, R., Segura, J. (2006) *Up-regulation of 1-deoxy-D-xylulose-5-phosphate synthase enhances production of essential oils in transgenic spike lavender*. Plant Physiol. 142(3):890–900. <https://doi.org/10.1104/pp.106.086355>
- Nabors, M.W. (2007) *Photosynthese*. In: Botanik. p. 207-226. Cummings, B. (eds.), Pearson Education.
- Nakamura, S., Mukai, T., Senoh, M. (1994) *Candela-class high-brightness InGaN/AlGaIn double-heterostructure blue-light-emitting diodes*. App. Phys. Lett. 64:1687. <https://doi.org/10.1063/1.111832>
- National Renewable Energy Laboratory (NREL). (2020) Reference Air Mass 1.5 Spectra. Available online: <https://www.nrel.gov/grid/solar-resource/spectra-am1.5.html> (accessed March 24, 2020)
- Naveed, M., Hejazi, V., Abbas, M., Kamboh, A.A., Khan, G.J., Shumzaid, M., Ahmad, F., Babazadeh, D., FangFang, X., Modarresi-Ghazani, F., WenHua, L., XiaoHui, Z. (2018) *Chlorogenic acid (CGA): A pharmacological review and call for further research*. Biomed. Pharmacother. 97:67-74.
<https://doi.org/10.1016/j.biopha.2017.10.064>
- Naznin, M.T., Lefsrud, M., Gravel, V., Azad, M.O.K. (2019) *Blue light added with red LEDs enhance growth characteristics, pigments content, and antioxidant capacity in lettuce, spinach, kale, basil, and sweet pepper in controlled environment*. Plants. 8(4):93. <https://doi.org/10.3390/plants8040093>
- Neff, M.M., Chory, J. (1998) *Genetic interactions between phytochrome A, phytochrome B, and cryptochrome 1 during Arabidopsis development*. Plant Physiol. 118(1):27-35.
<https://doi.org/10.1104/pp.118.1.27>
- Nelson, J.A., Bugbee, B. (2014) *Economic analysis of greenhouse lighting: light emitting diodes vs. high intensity discharge fixtures*. PLoS ONE. 9(6):e99010. <https://doi.org/10.1371/journal.pone.0099010>
- Nemali, K. S., van Iersel, M. W. (2004) *Acclimation of wax begonia to light intensity: changes in photosynthesis, respiration, and chlorophyll concentration*. J. Amer. Soc Hort. Sci. 129(5):745–751.
<https://doi.org/10.21273/jashs.129.5.0745>
- Neugart, S., Schreiner, M. (2018) *UVB and UVA as eustressors in horticultural and agricultural crops*. Sci. Hortic. 234:370-381. <https://doi.org/10.1016/j.scienta.2018.02.021>

- Nguyen, T.L., Saleh, M.A. (2019) *Effect of exposure to light emitting diode (LED) lights on essential oil composition of sweet mint plants*. J. Environ. Sci. Part A. 54(5):435-440.
<https://doi.org/10.1080/10934529.2018.1562810>
- Nichia. (2019a) *Specifications for UV LED. Part No. NCSU334A(T)*.
<https://www.ledsupply.com/content/pdf/NCSU334A-E.pdf> (accessed September 19, 2022)
- Nichia. (2019b) *Specifications for UV LED. Part No. NVSU119CT*. <https://led-ld.nichia.co.jp/api/data/spec/tech/NVSU119C-E.pdf> (accessed September 19, 2022)
- Noguchi, A., Amaki, W. (2016) *Effects of light quality on the growth and essential oil production in Mexican mint*. Acta Hortic. 1134:239-244. <https://doi.org/10.17660/ActaHortic.2016.1134.32>
- Noreen, H., Semmar, N., Farman, M., McCullagh, J.S.O. (2017) *Measurement of total phenolic content and antioxidant activity of aerial parts of medicinal plant Coronopus didymus*. Asian Pac. J. Trop. Med. 10(8):792-801. <https://doi.org/10.1016/j.apjtm.2017.07.024>
- Novičkovas, A., Brazaityte, A., Duchovskis, P., Jankauskienė, J., Samuolienė, G., Viršilė, A., Sirtautas, R., Bliznikas, Z., Žukauskas, A. (2012) *Solid-state lamps (LEDs) for the short-wavelength supplementary lighting in greenhouses: experimental results with cucumber*. Acta Hortic. 927:723-730.
<https://doi.org/10.17660/ActaHortic.2012.927.90>
- NTP – National Toxicology Program (2000) *NTP toxicology and carcinogenesis studies of methyleugenol (CAS NO. 93-15-2) in F344/N rats and B6C3F1 mice (gavage studies)*. Natl. Toxicol. Program Tech. Tech. Ser. 491:1-412.
- Oh, J., Park, E., Song, K., Bae, G., Choi, G. (2020) *Phytochrome interacting factor 8 inhibits phytochrome A-mediated far-red light responses in Arabidopsis*. Plant Cell. 32(1):186-205.
<https://doi.org/10.1105/tpc.19.00515>
- Oh, W., Runkle, E. S., Warner, R. M. (2010) *Timing and duration of supplemental lighting during the seedling stage influence quality and flowering in petunia and pansy*. HortScience 45(9):1332–1337.
<https://doi.org/10.21273/HORTSCI.45.9.1332>
- Ohgishi, M., Saji, K., Okada, K., Sakai, T. (2004) *Functional analysis of each blue light receptor, cry1, cry2, phot1, and phot2, by using combinatorial multiple mutants in Arabidopsis*. PNAS. 101(8):2223-2228.
<https://doi.org/10.1073/pnas.0305984101>

- Orsini, F., Pennisi, G., Pennisi, G., Zulfiqar, F., Gianquinto, G. (2020) *Sustainable use of resources in plant factories with artificial lighting (PFALs)*. Eur. J. Hortic. Sci. 85(5):297–309.
<https://doi.org/10.17660/eJHS.2020/85.5.1>
- Ouzounis, T., Giday, H., Kjaer, K.H., Ottosen, C.-O. (2018) *LED or HPS in ornamentals? A case study in roses and campanulas*. Eur. J. Hortic. Sci. 83(3):166-172. <https://doi.org/10.17660/eJHS.2018/83.3.6>
- Ouzounis, T., Rosenqvist, E., Ottosen, C.-O. (2015) *Spectral effects of artificial lighting on plant physiology and secondary metabolism: A review*. Hort. Sci. 50(8):1128-1135.
<https://doi.org/10.21273/HORTSCI.50.8.1128>
- Palka, P., Cioć, M., Hura, K., Szewczyk-Taranek, B., Pawłowska, B. (2023) *Adventitious organogenesis and phytochemical composition of Madonna lily (Lilium candidum L.) in vitro modeled by different light quality*. PCTOC. 152:99-114. <https://doi.org/10.1007/s11240-022-02391-5>
- Pank, F., Blaschek, W., Bomme, U., Hammer, K., Schliephake, E., Schmatz, R. (2013). "Pfefferminze (*Mentha x piperita* L.)," in Handbuch des Arznei- und Gewürzpflanzenbaus. Band 5. Arznei- und Gewürzpflanzen L-Z. Editor B. Hoppe. 1st ed (Bernburg, Germany: Gartenbauwissenschaft), 316.
- Pantazopoulou, C.K., Bongers, F.J., Küpers, J.J., Reinen, E., Das, D., Evers, J.B., Anten, N.P.R., Pierik, R. (2017) *Neighbor detection at the leaf tip adaptively regulates upward leaf movement through spatial auxin dynamics*. PNAS. 114(28):7450-7455. <https://doi.org/10.1073/pnas.1702275114>
- Park, J.E., Park, Y.G., Jeong, B.R., Hwang, S.J. (2012) *Growth and Anthocyanin content of lettuce as affected by artificial light source and photoperiod in a closed-type plant production system*. Kor. J. Hort. Sci. Technol. 30(6):673-679. <https://doi.org/10.7235/hort.2012.12020>.
- Park, K. S., Bekhzod, K., Kwon, J. K., Son, J. E. (2016) *Development of a coupled photosynthetic model of sweet basil hydroponically grown in plant factories*. Hortic. Environ. Biotechnol. 57(1):20–26.
<https://doi.org/10.1007/s13580-016-0019-7>
- Park, Y., Runkle, E.S. (2017) *Far-red radiation promotes growth of seedlings by increasing leaf expansion and whole-plant net assimilation*. Env. Exp. Bot. 136:41-49.
<https://doi.org/10.1016/j.envexpbot.2016.12.013>
- Park, Y., Runkle, E.S. (2018) *Far-red and photosynthetic photon flux density independently regulate seedling growth but interactively regulate flowering*. Env. Exp. Bot. 155:206-216.
<https://doi.org/10.1016/j.envexpbot.2018.06.033>

- Park, Y., Runkle, E.S. (2018a) *Spectral effects of light-emitting diodes on plant growth, visual color quality, and photosynthetic photon efficiency: White versus blue plus red radiation*. PLoS ONE 13(8):e0202386. <https://doi.org/10.1371/journal.pone.0202386>
- Patel, M., Lee, R., Merchant, E. V., Juliani, H. R., Simon, J. E., Tepper, B. J. (2021) *Descriptive aroma profiles of fresh sweet basil cultivars (Ocimum spp.): Relationship to volatile chemical composition*. J. Food Sci. 86(7):3228–3239. <https://doi.org/10.1111/1750-3841.15797>
- Pedmale, U.V., Huang, S.-S.C., Zander, M., Cole, B.J., Hetzel, J., Ljung, K., Reis, P.A.B., Sridevi, P., Nito, K., Nery, J.R., Ecker, J.R., Chory, J. (2016) *Cryptochromes interact directly with PIFs to control plant growth in limiting blue light*. Cell. 164(1-2):1-13. <https://doi.org/10.1016/j.cell.2015.12.018>
- Pennisi, G., Blasioli, S., Cellini, A., Maia, L., Crepaldi, A., Braschi, I., Spinelli, F., Nicola, S., Fernandez, J.A., Stanghellini, C., Marcelis, L.F.M., Orsini, F., Gianquinto, G. (2019) *Unraveling the role of red:blue LED lights on resource use efficiency and nutritional properties of indoor grown sweet basil*. Front. Plant Sci. 10:305. <https://doi.org/10.3389/fpls.2019.00305>
- Pennisi, G., Pistillo, A., Orsini, F., Cellini, A., Spinelli, F., Nicola, S., Fernandez, J.A., Crepaldi, A., Gianquinto, G., Marcelis, L.F.M. (2020) *Optimal light intensity for sustainable water and energy use in indoor cultivation of lettuce and basil under red and blue LEDs*. Sci. Hortic. 272:109508. <https://doi.org/10.1016/j.scienta.2020.109508>
- Pettai, H., Oja, V., Freiberg, A., Laisk, A. (2005) *Photosynthetic activity of far-red light in green plants*. BBA. 1708(3):311-321. <https://doi.org/10.1016/j.bbabi.2005.05.005>
- Pérez-Urrestarazu, L., Lobillo-Eguíba, J., Fernández-Cañero, R., Fernández-Cabanás, V.M. (2019) *Food safety concerns in urban aquaponic production: nitrate contents in leafy vegetables*. UFUG. 44:126431. <https://doi.org/10.1016/j.ufug.2019.126431>
- Perrino, E.V., Valerio, F., Gannouchi, A., Trani, A., Mezzapesa, G. (2021) *Ecological and plant community implication on essential oils composition in useful wild officinal species: A pilot case study in Apulia (Italy)*. Plants. 10(3):574. <https://doi.org/10.3390/plants10030574>
- Pierik, R., de Wit, M. (2014) *Shade avoidance: phytochrome signalling and other aboveground neighbour detection cues*. J. Exp. Bot. 65(11):2815-2824. <https://doi.org/10.1093/jxb/ert389>
- Piovene, C. et al. (2015) *Optimal red:blue ratio in LED lighting for nutraceutical indoor horticulture*. Sci. Hortic. 193:202-208. <https://doi.org/10.1016/j.scienta.2015.07.015>

- Poel, B.R., Runkle, E.S. (2017) *Seedling growth is similar under supplemental greenhouse lighting from high-pressure sodium lamps or light-emitting diodes*. HortSci. 52(3):388-394.
<https://doi.org/10.21273/HORTSCI11356-16>
- Poulet, L., Massa, G., Morrow, R. C., Bourget, C. M., Wheeler, R. M., Mitchell, C. A. (2014) *Significant reduction in energy for plant-growth lighting in space using targeted LED lighting and spectral manipulation*. Life Sci. Space Res. 2:43–53. <https://doi.org/10.1016/j.lssr.2014.06.002>
- Pramuk, L.A. and Runkle, E.S. (2005) *Photosynthetic daily light integral during the seedling stage influences subsequent growth and flowering of Celosia, Impatiens, Salvia, Tagetes, and Viola*. HortSci. 40(5):1336-1339. <https://doi.org/10.21273/HORTSCI.40.5.1336>.
- Procko, C., Crenshaw, C.M., Ljung, K., Noel, J.P., Chory, J. (2014) *Cotyledon-generated auxin is required for shade-induced hypocotyl growth in Brassica rapa*. Plant Physiol. 165(3):1285-1301.
<https://doi.org/10.1104/pp.114.241844>
- Qian, M., Kalbina, I., Rosenqvist, E., Jansen, M.A.K., Teng, Y., Strid, Å. (2019) *UV regulates the expression of phenylpropanoid biosynthesis genes in cucumber (Cucumis sativus L.) in an organ and spectrum dependent manner*. Photochem. Photobiol. Sci. 18:424-433. <https://doi.org/10.1039/c8pp00480c>
- Qian, M., Rosenqvist, E., Flygare, A.-M., Kalbina, I., Teng, Y., Jansen, M.A.K., Strid, Å. (2020) *UV-A light induces a robust and dwarfed phenotype in cucumber plants (Cucumis sativus L.) without affecting fruit yield*. Sci. Hortic. 263:109110. <https://doi.org/10.1016/j.scienta.2019.109110>
- Rahman, M. M., Vasiliev, M., Alameh, K. (2021) *LED illumination spectrum manipulation for increasing the yield of sweet basil (Ocimum basilicum L.)*. Plants 10(2):344.
<https://doi.org/10.3390/plants10020344>
- Rai, N., Neugart, S., Yan, Y., Wang, F., Siipola, S.M., Lindfors, A.V., Winkler, J.B., Albert, A., Brosché, M., Lehto, T., Morales, L.O., Aphalo, P.J. (2019) *How do cryptochromes and UVR8 interact in natural and simulated sunlight?* J. Exp. Bot. 70(18):4975-4990. <https://doi.org/10.1093/jxb/erz236>
- Rechner, O., Neugart, S., Schreiner, M., Wu, S., Poehling, H.-M. (2017) *Can narrow-bandwidth light from UV-A to green alter secondary plant metabolism and increase brassica plant defenses against aphids?* PLoS ONE 12(11):e0188522. <https://doi.org/10.1371/journal.pone.0188522>

- Regulation No 1334 (2008) *European Parliament and of the Council on flavourings and certain food ingredients with flavouring properties for use in and on foods*. Annex III. Presence of certain substances. <https://www.legislation.gov.uk/eur/2008/1334/annex/III> (accessed April 4, 2023)
- Rehman, R., Hanif, M.A., Mushtaq, Z., Al-Sadi, A. (2015) *Biosynthesis of essential oils in aromatic plants: A review*. *Food Rev. Int.* 32(2):117-160. <https://doi.org/10.1080/87559129.2015.1057841>
- Rehman, R., Hanif, M.A., Mushtaq, Z., Mochona, B., Qi, X. (2016) *Biosynthetic factories of essential oils: the aromatic plants*. *Nat. Prod. Chem. Res.* 4(4):1000227. <https://doi.org/10.4172/2329-6836.1000227>
- Rihan, H.Z., Aldarkazali, M., Mohamed, S.J., McMulkin, N.B., Jbara, M.H., Fuller, M.P. (2020) *A novel new light recipe significantly increases the growth and yield of sweet basil (Ocimum basilicum) grown in a plant factory system*. *Agronomy*. 10(7):934. <https://doi.org/10.3390/agronomy10070934>
- Rihan, H.Z., Aljafer, N., Jbara, M., McCallum, L., Lengger, S., Fuller, M.P. (2022) *The impact of LED lighting spectra in a plant factory on the growth, physiological traits and essential oil content of lemon balm (Melissa officinalis)*. *Plants*. 11(3):342. <https://doi.org/10.3390/plants11030342>
- Rios-Esteva, R., Turner, G. W., Lee, J. M., Croteau, R. B., Lange, B. M. (2008). *A systems biology approach identifies the biochemical mechanisms regulating monoterpenoid essential oil composition in peppermint*. *Proc. Natl. Acad. Sci. U.S.A.* 105(8):2818–2823. <https://doi.org/10.1073/pnas.0712314105>
- Rota, M.C., Herrera, A., Martínez, R.M., Sotomayor, J.A., Jordán, M.J. (2008) *Antimicrobial activity and chemical composition of Thymus vulgaris, Thymus zygis and Thymus hyemalis essential oils*. *Food Control*. 19(7):681–687. <https://doi.org/10.1016/j.foodcont.2007.07.007>
- Rouphael, Y., Cardarelli, M., Bassal, A., Leonardi, C., Giuffrida, F., Colla, G. (2012) *Vegetable quality as affected by genetic, agronomic and environmental factors*. *J. Food Agric. Environ.* 10(3):680–688.
- Ruberti, I., Sessa, G., Ciolfi, A., Possenti, M., Carabelli, M., Morelli, G. (2012) *Plant adaptation to dynamically changing environment: The shade avoidance response*. *Biotechnol. Adv.* 30(5):1047-1058. <https://doi.org/10.1016/j.biotechadv.2011.08.014>
- Sabzalian, M.R., Heydarizadeh, P., Zahedi, M., Boroomand, A., Agharokh, M., Sahba, M.R., Schoefs, B. (2014) *High performance of vegetables, flowers, and medicinal plants in a red-blue LED incubator for indoor production*. *Agron. Sustain. Dev.* 34:879-886. <https://doi.org/10.1007/s13593-014-0209-6>

- Saengtharatip, S., Goto, N., Kozai, T., Yamori, W. (2020). *Green light penetrates inside crisp head lettuce leading to chlorophyll and ascorbic acid content enhancement*. *Acta Hort.* 1273:261–270. <https://doi.org/10.17660/ActaHortic.2020.1273.35>
- Sager, J.C., Smith, W.O., Edwards, J.L., Cyr, K.L. (1988) *Photosynthetic efficiency and phytochrome photoequilibria determination using spectral data*. *Trans. Am. Soc. Agric. Eng.* 31(6):1882-1889. <https://doi.org/10.13031/2013.30952>
- Sakai, T., Kagawa, T., Kasahara, M., Swartz, T.E., Christie, J.M., Briggs, W.R., Wada, M., Okada, K. (2001) *Arabidopsis nph1 and npl1: Blue light receptors that mediate both phototropism and chloroplast relocation*. *PNAS.* 98(12):6969-6974. <https://doi.org/10.1073/pnas.101137598>
- Salehi, B., Mishra, A.P., Shukla, I., Sharifi-Rad, M., Contreras, M., Segura-Carretero, A., Fathi, H., Nasrabadi, N.N., Kobarfard, F., Sharifi-Rad, J. (2018) *Thymol, thyme, and other plant sources: Health and potential uses*. *Phytother Res.* 32:1688-1706. <https://doi.org/10.1002/ptr.6109>
- Salehi, B., Stojanović-Radić, Z., Matejić, J., Sharopov, F., Antolak, H., Kręgiel, D., Sen, S., Sharifi-Rad, M., Acharya, K., Sharifi-Rad, R., Martorell, M., Sureda, A., Martins, N., Sharifi-Rad, J. (2018). *Plants of genus Mentha: from farm to food factory*. *Plants* 7(3):70. <https://doi.org/10.3390/plants7030070>
- Salehi, B., Venditti, A., Sharifi-Rad, M., Kręgiel, D., Sharifi-Rad, J., Durazzo, A., Lucarini, M., Santini, A., Souto, E.B., Novellino, E., Antolak, H., Azzini, E., Setzer, W.N., Martins, N. (2019) *The therapeutic potential of agpigenin*. *Int. J. Mol. Sci.* 20:1305. <https://doi.org/10.3390/ijms20061305>
- Samanta, A., Das, G., Das, S.K. (2011) *Roles of flavonoids in plants*. *Int. J. Pharm. Sci. Tech.* 6(1):12-35.
- Samuoliene, G., Virsile, A., Miliuskienė, J., Haimi, P., Laužikė, K., Jankauskienė, J., Novičkovas, A., Kupčinskienė, A., Brazaitytė, A. (2020) *The photosynthetic performance of red leaf lettuce under UV-A irradiation*. *Agronomy.* 10(6):761. <https://doi.org/10.3390/agronomy10060761>
- Sanchez, S.E., Rugnone, M.L., Kay, S.A. *Light perception: A matter of time*. *Mol. Plant.* 13(3):363-385. <https://doi.org/10.1016/j.molp.2020.02.006>
- Sangwan, N.S., Farooqui, A.H.A., Shabih, F., Sangwan, R.S. (2001) *Regulation of essential oil production in plants*. *Plant Growth Reg.* 34:3-21. <https://doi.org/10.1023/A:1013386921596>
- Sankhuan, D., Niramolyanun, G., Kangwanrangsang, N., Nakano, M., Supaibulwatana, K. (2022) *Variation in terpenoids in leaves of Artemisia annua grown under different LED spectra resulting in diverse*

- antimalarial activities against Plasmodium falciparum*. BMC Plant Biol. 22:128.
<https://doi.org/10.1186/s12870-022-03528-6>
- Sankhuan, D., Roytrakul, S., Nakano, M., Supaibulwatana, K. (2021) *Proteomic sensing associated with terpenoid biosynthesis of Artemisia annua L. in response to different artificial light spectra*. J. Plant Interact. 17(1):19-32. <https://doi.org/10.1080/17429145.2021.2009582>
- Schenkels, L., Saeys, W., Lauwers, A., De Proft, M.P. (2019) *Green light induces shade avoidance to alter plant morphology and increases biomass production in Ocimum basilicum L.* Sci. Hortic. 261:109002
<https://doi.org/10.1016/j.scienta.2019.109002>
- Schmiedel, R. (2008). *Europäisches Arzneibuch (Pharmacopoeia Europaea)*. 6th ed. Stuttgart, Germany: Deutscher Apotheker Verlag, 3633–3634.
- Schulz, H., Drews, H.-H., Krüger, H. (1999). *Rapid NIRS determination of quality parameters in leaves and isolated essential oils of Mentha species*. J. Essent. Oil Res. 11:185–190.
<https://doi.org/10.1080/10412905.1999.9701106>
- Schulz, H., Krüger, H. (1999). Zur Verbreitung, Züchtung und Verarbeitung von Pfefferminze und Krauseminze. Available at:
https://www.researchgate.net/publication/287643299_Zur_Verbreitung_Zuchtung_und_Verarbeitung_von_Pfefferminze_und_Krauseminze (accessed January 4, 2022)
- Schulz, H., Schrader, B., Quilitzsch, R., Pfeffer, S., Krüger, H. (2003) *Rapid classification of basil chemotypes by various vibrational spectroscopy methods*. J. Agric. Food Chem. 51(9):2475–2481.
<https://doi.org/10.1021/jf021139r>
- Sellaro, R., Crepy, M., Trupkin, S.A., Karayekov, E., Buchovsky, A.S., Rossi, C., Casal, J.J. (2010) *Cryptochrome as a sensor of the blue/green ratio of natural radiation in Arabidopsis*. Plant Physiol. 154(1):401-409. <https://doi.org/10.1104/pp.110.160820>
- Semenova, N.A., Smirnov, A.A., Ivanitskikh, A.S., Izmailov, A.Y., Dorokhov, A.S., Proshkin, Y.A., Yanykin, D.V., Sarimov, R.R., Gudkov, S.V., Chilingaryan, N.O. (2022) *Impact of ultraviolet radiation on the pigment content and essential oil accumulation in sweet basil (Ocimum basilicum L.)* Appl. Sci. 12:7190.
<https://doi.org/10.3390/app12147190>
- Shelford, T.J., Both, A.-J. (2021) *On the technical performance characteristics of horticultural lamps*. AgriEngineering. 3(4):716-727. <https://doi.org/10.3390/agriengineering3040046>

- Shen, H., Moon, J., Huq, E. (2005) *PIF1 is regulated by light-mediated degradation through the ubiquitin-26S proteasome pathway to optimize photomorphogenesis of seedlings in Arabidopsis*. Plant J. 44(6):1023-1035. <https://doi.org/10.1111/j.1365-313X.2005.02606.x>
- Simmonds, M.S.J. (2001) *Importance of flavonoids in insect-plant interactions: feeding and oviposition*. Phytochem. 56(3):245-252. [https://doi.org/10.1016/s0031-9422\(00\)00453-2](https://doi.org/10.1016/s0031-9422(00)00453-2)
- Singh, D., Basu, C., Meinhardt-Wollweber, M., Roth, B. (2015a) *LEDs for energy efficient greenhouse lighting*. Renew. Sustain. Energy Rev. 49:139-147. <https://doi.org/10.1016/j.rser.2015.04.117>
- Singh, P., Kalunke, R. M., Giri, A. P. (2015b) *Towards comprehension of complex chemical evolution and diversification of terpene and phenylpropanoid pathways in Ocimum species*. RSC Adv. 5(129):106886–106904. <https://doi.org/10.1039/C5RA16637C>
- Sipos, L., Balázs, L., Székely, G., Jung, A., Sárosi, S., Radácsi, P., Csambalik, L. (2021) *Optimization of basil (Ocimum basilicum L.) production in LED light environments – a review*. Sci. Horti. 289:110486. <https://doi.org/10.1016/j.scienta.2021.110486>
- Smith, H. (2000) *Phytochromes and light signal perception by plants – an emerging synthesis*. Nature. 407:585-591. <https://doi.org/10.1038/35036500>
- Smith, H.L., McAusland, L., Murchie, E.H. (2017) *Don't ignore the green light: exploring diverse roles in plant processes*. J. Exp. Bot. 68(9):2099-2110. <https://doi.org/10.1093/jxb/erx098>
- Snowden, M.C., Cope, K.R., Bugbee, B. (2016) *Sensitivity of seven diverse species to blue and green light: Interactions with photon flux*. PLoS ONE. 11(10):e0163121. <https://doi.org/10.1371/journal.pone.0163121>
- Solis-Toapanta, E., Gómez, C. (2019) *Growth and photosynthetic capacity of basil grown for indoor gardening under constant or increasing daily light integrals*. HortTechnology. 29(6):880–888. <https://doi.org/10.21273/HORTTECH04442-19>
- Son, K.-H., Oh, M.-M. (2015) *Growth, photosynthetic and antioxidant parameters of two lettuce cultivars as affected by red, green, and blue light-emitting diodes*. Hortic. Environ. Biotechnol. 56(6):639-653. <https://doi.org/10.1007/s13580-015-1064-3>
- Song, T.-E., Moon, J.-K., Lee, C. H. (2020) *Polyphenol content and essential oil composition of sweet basil cultured in a plant factory with light-emitting diodes*. Hortic. Sci. Technol. 38(5):620–630. <https://doi.org/10.7235/HORT.20200057>

- Spalholz, H., Perkins-Veazie, P., Hernández, R. (2020) *Impact of sun-simulated white light and varied blue:red spectrums on the growth, morphology, and phytochemical content of green- and red-leaf lettuce at different growth stages*. *Sci. Hortic.* 264:109195. <https://doi.org/10.1016/j.scienta.2020.109195>
- Spring, O., Priester, T. and Hager, A. (1986) *Light-induced accumulation of sesquiterpenes lactones in sunflower seedlings*. *J. Plant Physiol.* 123(1):79-89. [https://doi.org/10.1016/S0176-1617\(86\)80068-2](https://doi.org/10.1016/S0176-1617(86)80068-2)
- Stagnari, F., Di Mattia, C., Galieni, A., Santarelli, V., D'Egidio, S., Pagnani, G., Pisante, M. (2018) *Light quantity and quality supplies sharply affect growth, morphological, physiological and quality traits of basil*. *Ind. Crop Prod.* 122:277–289. <https://doi.org/10.1016/j.indcrop.2018.05.073>
- Stanghellini, C., Van 't Ooster, B., Heuvelink, E. (2019) *Greenhouse horticulture: technology for optimal crop production*. Stanghellini, C., Van 't Ooster, B., Heuvelink, E. (eds.) Wageningen Academic publishers. <https://doi.org/10.3920/978-90-8686-879-7>
- Stetsenko, L. A., Pashkovsky, P. P., Voloshin, R. A., Kreslavski, V. D., Kuznetsov, V. V., Allakhverdiev, S. I. (2020) *Role of anthocyanin and carotenoids in the adaptation of the photosynthetic apparatus of purple- and green-leaved cultivars of sweet basil (Ocimum basilicum) to high-intensity light*. *Photosynthetica.* 58(4):890–901. <https://doi.org/10.32615/ps.2020.048>
- Stober, K., Lee, K., Yamada, M., Pattison, M. (2017) *Energy savings potential of SSL in horticultural applications*. United States Department of Energy. <https://doi.org/10.2172/1418429> (accessed September 16, 2022)
- Stutte, G.W., Edney, S. (2009) *Photoregulation of bioprotectant content of red leaf lettuce with light-emitting diodes*. *HortSci.* 44(1):79-82. <https://doi.org/10.21273/HORTSCI.44.1.79>
- Sun, J., Nishio, J.N., Vogelmann, T.C. (1998) *Green light drives CO₂ fixation deep within leaves*. *Plant Cell Physiol.* 39(10):1020-1026. <https://doi.org/10.1093/oxfordjournals.pcp.a029298>
- Szabó, K., Bernáth, J. (2002) *Investigation of flowering dynamics of the basil (Ocimum basilicum L.) and its production consequences*. *Acta Hortic.* 576:105–112. <https://doi.org/10.17660/ActaHortic.2002.576.18>
- Tabbert, J.M. (2020) *Einsatz von LED-Technik im Gewächshausanbau von Arznei- und Gewürzpflanzen (AGP): Auswirkung auf Ertrag und Qualität von Echtem Thymian (Thymus vulgaris L.)*. Bernburg. In: Proceedings of the 30. Bernburger winter seminar for medicinal and spice plants. https://www.saluplanta.de/files/30_BWS.pdf

- Tabbert, J.M., Schulz, H., Krähmer, A. (2021) *Increased plant quality, greenhouse productivity and energy efficiency with broad-spectrum LED systems: A case study for thyme (Thymus vulgaris L.)* Plants. 10:960. <https://doi.org/10.3390/plants10050960>
- Tabbert, J.M., Schulz, H., Krähmer, A. (2022a) *Investigation of LED light qualities for peppermint (Mentha x piperita L.) cultivation focusing on plant quality and consumer safety aspects*. Front. Food Sci. Technol. 2:852155. <https://doi.org/10.3389/frfst.2022.852155>
- Tabbert, J.M., Riewe, D., Schulz, H., Krähmer, A. (2022b) *Facing energy limitations – Approaches to increase basil (Ocimum basilicum L.) growth and quality by different increasing light intensities emitted by a broadband LED light spectrum (400-780 nm)*. Front. Plant Sci. 13:1055352. <https://doi.org/10.3389/fpls.2022.1055352>
- Taherian, A.A., Babaei, M., Vafaei, A.A., Jarrahi, M., Jadidi, M., Sadeghi, H. (2009) *Antinociceptive effects of hydroalcoholic extract of thymus vulgaris*. Pak. J. Pharm. Sci. 22(1):83-89.
- Takeno, K. (2016) *Stress-induced flowering: the third category of flowering response*. J. Exp. Bot. 67(17):4925–4934. <https://doi.org/10.1093/jxb/erw272>
- Talbott, L.D., Nikolova, G., Ortiz, A., Shmayevich, I., Zeiger, E. (2002) *Green light reversal of blue-light-stimulated stomatal opening is found in a diversity of plant species*. Am. J. Bot. 89(2):366-368. <https://doi.org/10.3732/ajb.89.2.366>
- Takemiya, A., Inoue, S.-I., Doi, M., Kinoshita, T., Shimazaki, K.-I. (2005) *Phototropins promote plant growth in response to blue light in low light environments*. Plant Cell. 17(4):1120-1127. <https://doi.org/10.1105/tpc.104.030049>
- Tan, B., Soderstrom, D.N. (1988) *Qualitative aspects of UV-VIS spectrophotometry of β -carotene and lycopene*. J. Chem. Educ. 66(3): 258-260.
- Tanaka, S., Yamaura, T., Shigemoto, R., Tabata, M. (1989) *Phytochrome-mediated production of monoterpenes in thyme seedlings*. Phytochemistry. 28(11):2955-2957. [https://doi.org/10.1016/0031-9422\(89\)80260-2](https://doi.org/10.1016/0031-9422(89)80260-2)
- Tattini, M., Landi, M., Brunetti, C., Giordano, C., Remorini, D., Gould, K. S., Guidi, L. (2014) *Epidermal coumaroyl anthocyanins protect sweet basil against excess light stress: multiple consequences of light attenuation*. Physiol. Plant 152(3):585–598. <https://doi.org/10.1111/ppl.12201>

- Terashima, I., Fujita, T., Inoue, T., Chow, W.S., Oguchi, R. (2009) *Green light drives leaf photosynthesis more efficiently than red light in strong white light: Revisiting the enigmatic question of why leaves are green*. *Plant Cell Physiol.* 50(4):684-697. <https://doi.org/10.1093/pcp/pcp034>
- Tevini, M., Braun, J., Fieser, G. (1991) *The protective function of the epidermal layer of rye seedlings against ultraviolet-B radiation*. *Photochem. Photobiol.* 53(3):329-333. <https://doi.org/10.1111/j.1751-1097.1991.tb03636.x>
- Thompson, J.D., Chalchat, J.C., Michet, A., Linhart, Y.B., Ehlers, B. (2003) *Qualitative and quantitative variation in monoterpene co-occurrence and composition in the essential oil of Thymus vulgaris chemotypes*. *J. Chem. Ecol.* 29(4):859–880. <https://doi.org/10.1023/A:1022927615442>
- Tilbrook, K., Arongaus, A.B., Binkert, M., Heijde, M., Ruohe, Y. (2013) *The UVR8 UV-B photoreceptor: Perception, signaling and response*. *Arabidopsis Book*. 2013(11):1-21 <https://doi.org/10.1199/tab.0164>
- Tohidi, B., Rahimmalek, M., Arzani, A., Sabzalian, M.R. (2019) *Thymol, carvacrol, and antioxidant accumulation in Thymus species in response to different light spectra emitted by light-emitting diodes*. *Food Chem.* 307:125521. <https://doi.org/10.1016/j.foodchem.2019.125521>
- Touaibia, M., Jean-François, J., Doiron, J. (2011) *Caffeic acid, a versatile pharmacophore: An overview*. *Mini-Rev. Med. Chem.* 11(8):695-713. <https://doi.org/10.2174/138955711796268750>
- Trupkin, S.A., Legris, M., Buchovsky, A.S., Rivero, M.B.T., Casal, J.J. (2014) *Phytochrome B nuclear bodies respond to the low red to far-red ratio and to the reduced irradiance of canopy shade in Arabidopsis*. *Plant Physiol.* 165(4):1698-1708. <https://doi.org/10.1104/pp.114.242438>
- Tsao, J.Y., Han, J., Haitz, R.H., Pattison, P.M. (2015) *The blue LED nobel prize: Historical context, current scientific understanding, human benefit*. *Ann. Phys.* 527(5-6):A53-A61. <https://doi.org/10.1002/andp.201570058>
- Tursun, A. O., Telci, I. (2020) *The effects of carbon dioxide and temperature on essential oil composition of purple basil (Ocimum basilicum L.)*. *J. Essent. Oil Bear. Plants* 23(2):255–265. <https://doi.org/10.1080/0972060X.2020.1741452>
- Tyystjärvi, E. (2013) *Chapter seven - photoinhibition of photosystem II*. *Int. Rev. Cell Mol. Biol.* 300:243-303. <https://doi.org/10.1016/B978-0-12-405210-9.00007-2>

- UN - United Nations (2022) *Sustainable Development Goals*.
<https://www.un.org/sustainabledevelopment/news/communications-material/> (accessed September 2, 2022)
- Usami, T., Mochizuki, N., Kondo, M., Nishimura, M., Nagatani, A. (2004) *Cryptochromes and phytochromes synergistically regulate Arabidopsis root greening under blue light*. *Plant Cell Physiol.* 45(12):1798-1808. <https://doi.org/10.1093/pcp/pch205>
- USCB - United States Census Bureau (2021) *World population: 1950-2050*.
<https://www.census.gov/library/visualizations/2011/demo/world-population--1950-2050.html> (accessed August 28, 2022)
- Valverde, F., Mouradov, A., Soppe, W., Ravenscroft, D., Samach, A., Coupland, G. (2004) *Photoreceptor regulation of CONSTANS protein in photoperiodic flowering*. *Sci.* 303(5660):1003-1006.
<https://doi.org/10.1126/science.109161>
- Van Gelderen, K., Kang, C., Paalman, R., Keuskamp, D., Hayes, S., Pierik, R. (2018) Far-red light detection in the shoot regulates lateral root development through the HY5 transcription factor. *Plant Cell.* 30(1):101-116. <https://doi.org/10.1105/tpc.17.00771>
- Van Ieperen, W., Trouborst, G. (2008) *The application of LEDs as assimilation light source in greenhouse horticulture: a simulation study*. *Acta Hortic.* 801:1407-1414.
<https://doi.org/10.17660/actahortic.2008.801.173>
- Van Iersel, M.W., Gianino, D. (2017) *An adaptive control approach for light-emitting diode lights can reduce the energy costs of supplemental lighting in greenhouses*. *HortSci.* 52(1):72-77.
<https://doi.org/10.21273/HORTSCI11385-16>
- Varga, F., Carović-Stanko, K., Ristić, M., Grdiša, M., Liber, Z., Šatović, Z. (2017) *Morphological and biochemical intraspecific characterization of Ocimum basilicum L.* *Ind. Crop Prod.* 109:611–618.
<https://doi.org/10.1016/j.indcrop.2017.09.018>
- Vázquez-Hernández, M.C., Parola-Contreras, I., Montoya-Gómez, L.M., Torres-Pacheco, I., Schwarz, D., Guevara-González, R.G. (2019) *Eustressors: Chemical and physical stress factors used to enhance vegetable production*. *Sci. Hortic.* 250:223-229.
<https://doi.org/10.1016/j.scienta.2019.02.053>

- Verdaguer, D., Jansen, M.A.K., Llorens, L., Morales, L.O., Neugart, S. (2017) *UV-A radiation effects on higher plants: exploring the known unknown*. *Plant Sci.* 255:72-81.
<https://doi.org/10.1016/j.plantsci.2016.11.014>
- Viczián, A., Klose, C., Ádám, É., Nagy, F. (2017) *New insights of red light-induced development*. *Plant Cell Env.* 40(11):2457-2468. <https://doi.org/10.1111/pce.12880>
- Virsilė, A., Brazaitytė, A., Vaštakaite-Kairienė, V., Miliauskienė, J., Jankauskienė, J., Novičkovas, A., Samuolienė, G. (2019) *Lighting intensity and photoperiod serves tailoring nitrate assimilation indices in red and green baby leaf lettuce*. *J. Sci. Food Agr.* 99:6608–6619. <https://doi.org/10.1002/jsfa.9948>
- Vogt, T. (2010) *Phenylpropanoid biosynthesis*. *Mol. Plant.* 3(1):2-20. <https://doi.org/10.1093/mp/ssp106>
- Voirin, B., Brun, N., Bayet, C. (1990). *Effects of daylength on the monoterpene composition of leaves of Mentha x piperita*. *Phytochemistry* 29(3):749–755. [https://doi.org/10.1016/0031-9422\(90\)80012-6](https://doi.org/10.1016/0031-9422(90)80012-6)
- Wada, M. (2013) *Chloroplast movement*. *Plant Sci.* 210:177-182.
<https://doi.org/10.1016/j.plantsci.2013.05.016>
- Wade, H.K., Bibikova, T.N., Valentine, W.J., Jenkins, G.I. (2001) *Interactions within a network of phytochrome, cryptochrome and UV-B phototransduction pathways regulate chalcone synthase gene expression in Arabidopsis leaf tissue*. *Plant J.* 25(6):675-685. <https://doi.org/10.1046/j.1365-313x.2001.01001.x>
- Wallace, C. and Both, A.J. (2016) *Evaluating operating characteristics of light sources for horticultural applications*. *Acta Hort.* 1134:435-443. <https://doi.org/10.17660/ActaHortic.2016.1134.55>
- Walters, K. J., Lopez, R. G., Bridget, K. B. (2021) *Leveraging controlled-environment agriculture to increase key basil terpenoid and phenylpropanoid concentrations: The effects of radiation intensity and CO2 concentrations on consumer preference*. *Front. Plant Sci.* 11.
<https://doi.org/10.3389/fpls.2020.598519>
- Wang, P., Abid, M.A., Qanmber, G., Asari, M. Zhou, L., Song, Y., Liang, C., Meng, Z. Malik, W., Wei, Y., Wang, Y., Cheng, H., Zhang, R. (2022) *Photomorphogenesis in plants: The central role of phytochrome interacting factors (PIFs)*. *Environ. Exp. Bot.* 194:104704.
<https://doi.org/10.1016/j.envexpbot.2021.104704>
- Wang, Q., Liu, Q., Wang, X., Zuo, Z., Oka, Y., Lin, C. (2017) *New insights into the mechanism of phytochrome-cryptochrome coaction*. *New Phytol.* 217(2):547-551. <https://doi.org/10.1111/nph.14886>

- Wang, Y., Folta, K.M. (2013) *Contributions of green light to plant growth and development*. Am. J. Bot. 100(1):70-78. <https://doi.org/10.3732/ajb.1200354>
- Wargent, J.J., Gegas, V.C., Jenkins, G.I., Doonan, J.H., Paul, N.D. (2009) *UVR8 in Arabidopsis thaliana regulates multiple aspects of cellular differentiation during leaf development in response to ultraviolet B radiation*. New Phytol. 183:315-326. <https://doi.org/10.1111/j.1469-8137.2009.02855.x>
- Wesolowska, A., Jadczyk, D. (2016) *Composition of the essential oils from inflorescences, leaves and stems of Ocimum basilicum 'Cinnamon' cultivated in north-western Poland*. J. Essent. Oil Bear. Plants 19(4):1037-1042. <https://doi.org/10.1080/0972060X.2016.1197801>
- Whippo, C.W., Hangarter, R.P. (2003) *Second positive phototropism results from coordinated co-action of the phototropins and cryptochromes*. Plant Physiol. 132(3):1499-1507. <https://doi.org/10.1104/pp.102.018481>
- Wojciechowska, R., Dlugosz-Grochowska, O., Kolton, A., Żupnik, M. (2015) *Effects of LED supplemental lighting on yield and some quality parameters of lamb's lettuce grown in two winter cycles*. Sci. Hortic. 187:80-86. <https://doi.org/10.1016/j.scienta.2015.03.006>
- Wu, B.-S., Hitti, Y., MacPherson, S., Orsat, V., Lefsrud, M.G. (2020) *Comparison and perspective of conventional and LED lighting for photobiology and industry applications*. Environ. Exp. Bot. 171:103953. <https://doi.org/10.1016/j.envexpbot.2019.103953>
- Xiaoying, L., Shirong, G., Zhigang, X., Xuelei, J. (2011) *Regulation of chloroplast ultrastructure, cross-section anatomy of leaves, and morphology of stomata of cherry tomato by different light irradiations of light-emitting diodes*. Hort. Sci. 46(2):217-221. <https://doi.org/10.21273/HORTSCI.46.2.217>
- Xie, X., Shinomura, T., Inagai, N., Kiyota, S., Takano, M. (2007) *Phytochrome-mediated inhibition of coleoptile growth in rice: age-dependency and action spectra*. Photochem. Photobiol. 83(1):131-138. <https://doi.org/10.1562/2006-03-17-ra-850>
- Xie, Z., Kapteyn, J., Gang, D. R. (2008) *A systems biology investigation of the MEP/terpenoid and shikimate/phenylpropanoid pathways points to multiple levels of metabolic control in sweet basil glandular trichomes*. Plant J. 54(3):349-361. <https://doi.org/10.1111/j.1365-313X.2008.03429.x>
- Xu, Y. (2019) *Nature and source of light for plant factory*. p. 47-69. In: Plant factory using artificial light, Anpo, M., Fukuda, H., Wada, T. (eds.), Elsevier. <https://doi.org/10.1016/B978-0-12-813973-8.00002-6>

- Yahyaa, M., Berim, A., Nawade, B., Ibdah, M., Dudareva, N., Ibdah, M. (2019) *Biosynthesis of methyleugenol and methylisoeugenol in Daucus carota leaves: Characterization of eugenol/isoeugenol synthase and O-methyltransferase*. *Phytochem.* 159:179–189.
<https://doi.org/10.1016/j.phytochem.2018.12.020>
- Yamaura, T., Tanaka, S., Tabata, M. (1991) *Participation of phytochrome in the photoregulation of terpenoid synthesis in thyme seedlings*. *Plant Cell Physiol.* 32(5):603-607.
<https://doi.org/10.1093/oxfordjournals.pcp.a078122>
- Yan, Z., He, D., Niu, G., Zhou, Q., Qu, Y. (2020) *Growth, nutritional quality, and energy use efficiency in two lettuce cultivars as influenced by white plus red versus red plus blue LEDs*. *Int. J. Agric. Biol. Eng.* 13(2):33-40. <https://doi.org/10.25165/j.ijabe.20201302.5135>
- Yan, Z., He, D., Niu, G., Zhou, Q., Qu, Y. (2019) *Growth, nutritional quality, and energy use efficiency of hydroponic lettuce as influenced by daily light integrals exposed to white versus white plus red light-emitting diodes*. *HortSci.* 54(10):1737-1744. <https://doi.org/10.21273/hortsci14236-19>
- Yan, Z., Wang, C., Wang, L., Li, X., Wang, G., Yang, Y. (2022) *The combinations of white, blue, and UV-A light provided by supplementary light-emitting diodes promoted the quality of greenhouse-grown cucumber seedlings*. *Agriculture.* 12(10):1593. <https://doi.org/10.3390/agriculture12101593>
- Yan, Z., Wang, L., Wang, Y., Chu, Y., Lin, D., Yang, Y. (2021) *Morphological and physiological properties of greenhouse-grown cucumber seedlings as influenced by supplementary light-emitting diodes with same daily light integral*. *Horticulturae.* 7(10):361. <https://doi.org/10.3390/horticulturae7100361>
- Yang, Z.-C., Kubota, C., Chia, P.-L., Kacira, M. (2012) *Effect of end-of-day far-red light from a movable LED fixture on squash rootstock hypocotyl elongation*. *Sci. Hortic.* 136:81–86.
<https://doi.org/10.1016/j.scienta.2011.12.023>
- Yeh, N., Chung, J.P. (2009) *High-brightness LEDs – energy efficient lighting sources and their potential in indoor plant cultivation*. *Renew. Sust. Energ. Rev.* 13(8):2175-2180.
<https://doi.org/10.1016/j.rser.2009.01.027>
- Yorio, N.C., Goins, G.D., Kagie, H.R. (2001) *Improving spinach, radish, and lettuce growth under red light-emitting diodes (LEDs) with blue light supplementation*. *HortSci.* 36(2):380-383.
<https://doi.org/10.21273/HORTSCI.36.2.380>

- Zhang, T., Folta, K.M. (2012) *Green light signaling and adaptive response*. Plant Signal. Behav. 7(1):75-78. <https://doi.org/10.4161/psb.7.1.18635>
- Zhang, T., Maruhnich, S.A., Folta, K.M. (2011) *Green light induces shade avoidance symptoms*. Plant Physiol. 157(3):1528-1536. <https://doi.org/10.1104/pp.111.180661>
- Zhang, T., Shi, Y., Piao, F., Sun, Z. (2018) *Effects of different LED sources on the growth and nitrogen metabolism of lettuce*. PCTOC. 134:231-240. <https://doi.org/10.1007/s11240-018-1415-8>
- Zhang, X., Cai, X. (2011) *Climate change impacts on global agricultural land availability*. Environ. Res. Lett. 6(1):014014. <https://doi.org/10.1088/1748-9326/6/1/014014>
- Zhang, X., Heuvelink, E., Melegkou, M., Yuan, X., Jiang, W., Marcelis, L.F.M. (2022) *Effects of green light on elongation do not interact with far-red, unless the phytochrome photostationary state (PSS) changes in tomato*. Biology. 11(1):151. <https://doi.org/10.3390/biology11010151>
- Zhang, Y., Zhang, Y., Yang, Q., Li, T. (2019) *Overhead supplemental far-red light stimulates tomato growth under intra-canopy lighting with LEDs*. J. Integr. Agric. 18(1):62-69. [https://doi.org/10.1016/S2095-3119\(18\)62130-6](https://doi.org/10.1016/S2095-3119(18)62130-6)
- Zhen, S., Bugbee, B. (2020) *Far-red photons have equivalent efficiency to traditional photosynthetic photons: Implications for redefining photosynthetically active radiation*. Plant Cell Environ. 43(5):1259-1272. <https://doi.org/10.1111/pce.13730>
- Zhen, S., Bugbee, B. (2020a) *Substituting far-red for traditionally defined photosynthetic photons results in equal canopy quantum yield for CO₂ fixation and increased photon capture during long-term studies: implications for re-defining PAR*. Front. Plant Sci. 11:581156. <https://doi.org/10.3389/fpls.2020.581156>
- Zhen, S., Haidekker, M., van Iersel, M.W. (2018) *Far-red light enhances photochemical efficiency in a wavelength-dependent manner*. Physiol. Plant. 167(1):21-33. <https://doi.org/10.1111/ppl.12834>
- Zhen, S., van Iersel, M.W. (2017) *Far-red light is needed for efficient photochemistry and photosynthesis*. J. Plant Physiol. 209:115-122. <https://doi.org/10.1016/j.jplph.2016.12.004>
- Zheng, L., He, H., Song, W. (2019) *Application of light-emitting diodes and the effect of light quality on horticultural crops: A review*. Hort. Sci. 54(10):1656-1661. <https://doi.org/10.21273/hortsci14109-19>
- Zou, J., Zhang, Y., Zhang, Y., Bian, Z., Fanourakis, D., Yang, Q. (2019) *Morphological and physiological properties of indoor cultivated lettuce in response to additional far-red light*. Sci. Hortic. 257:108725. <https://doi.org/10.1016/j.scienta.2019.108725>

Zvi, M. M. B., Shklarman, E., Masci, T., Kalev, H., Debener, T., Shafir, S., Ovadis, M., Vainstein, A. (2012). *PAP1 transcription factor enhances production of phenylpropanoid and terpenoid scent compounds in rose flowers*. *New Phytol.* 195(2):335–345. <https://doi.org/10.1111/j.1469-8137.2012.04161.x>

Appendix

List of figures and tables

Figures

Figure 1 – Sustainable Development Goals (SDGs).

Figure 2 – Overview of the diverse light-emitting diodes and their peak wavelengths (nm).

Figure 3 – Schematic depiction of the heterogeneous light intensity and wavelength distributions of common LED luminaires.

Figure 4 – Absorption spectra of chlorophyll *a*, *b* and β -carotene within the visible light spectrum.

Figure 5 – Action spectra of photosynthesis from two different studies (McCree, 1972a & Inada, 1976).

Figure 6 – Absorption spectra of photoreceptors.

Figure 7 – Representation of monochromatic blue, green and red light penetrating through the vertical profile of a leaf illuminated from above the adaxial surface.

Figure 8 – Biosynthesis of major volatile aromatic compounds in plants.

Figure 9 – Project partners of LED4Plants.

Figure 10 – Light spectra of the three artificial light sources used during the greenhouse experiment.

Figure 11 – Irradiance profiles ($\text{W m}^{-2} \text{s}^{-1}$) of the experimental plots (1 m^2) underneath each supplemental lighting system.

Figure 12 – Biomass yields and partitioning of *Thymus vulgaris* L. cultivated under different supplemental lighting systems during fall and winter in Berlin, Germany.

Figure 13 – Visual appearance of *Thymus vulgaris* L. at harvest cultivated under different supplemental lighting systems during fall and winter of Berlin, Germany.

Figure 14 – Conceptual pictogram of the conducted LED light experiment.

Figure 15 – Irradiance measurements of three light spectra between 380 and 780 nm at plant pot level.

Figure 16 – Morphological characteristics of *Mentha x piperita* var. *piperita* cv. Multimentha as effected by light spectra over time.

Figure 17 – Length and width of fresh leaves of *Mentha x piperita* var. *piperita* cv. Multimentha as effected by different light spectra.

Figure 18 – Biomass yields of *Mentha x piperita* var. *piperita* cv. Multimentha as effected by different light spectra.

Figure 19 – Photon flux density depending on distance to light source.

Figure 20 – Light intensity distribution underneath each LED light treatment.

Figure 21 – White broad-band LED light spectra applied during the experiments.

Figure 22 – Photon flux density depending on distance to light source.

Figure 23 – Visual appearance of four *Ocimum basilicum* L. cultivars at harvest.

Figure 24 – Characteristics of four *Ocimum basilicum* L. cultivars under two different broad-bandwidth LED light intensities over time.

Figure 25 – Reducing FR emissions to 750 nm can improve the plants' light use efficiencies and the LEDs' cost effectiveness.

Figure 26 – Light distribution patterns of (broadband) LED systems must be improved.

Figure 27 – White broad-band LED light spectra with additional UV-A or B applied in the unpublished experiment.

Tables

Table 1 – Processes involving phytochrome actions.

Table 2 – Processes involving cryptochrome actions.

Table 3 – Processes involving phototropin actions.

Table 4 – Processes involving UV resistance locus 8 (UVR8) actions.

Table 5 – Effects of different red/blue LED ratios, intensities and peak wavelengths on selected horticultural crops published in recent years.

Table 6 – Morphological, physiological, phytochemical and genetic plant effects mediated by ultraviolet wavelengths (λ 280-400 nm).

Table 7 – Morphological, physiological and phytochemical plant effects mediated by green wavelengths (λ 500-600 nm).

Table 8 – Morphological, physiological and phytochemical plant effects mediated by far-red wavelengths (λ 700-800 nm).

Table 9 – Morphological, physiological and phytochemical plant effects mediated by broad white LED light spectra (λ 350-800 nm).

Table 10 – Essential oil contents and compositions of aromatic and medicinal plants as affected by LED lighting (λ 100-800)

Table 11 – Spectral composition of the supplemental lighting fixtures used in the greenhouse for the cultivation of thyme (*Thymus vulgaris* L.).

Table 12 – Effect of three different supplemental lighting systems on the chemical composition of 13 main volatile substances of *Thymus vulgaris* L. cultivated in the greenhouse during fall and winter of Berlin, Germany.

Table 13 – Fresh and dry plant productivity as well as content of volatile fraction of thyme (*Thymus vulgaris* L.) per m² under three supplemental lighting systems.

Table 14 – Power consumption of different supplemental lighting fixtures per square meter for the production of thyme (*Thymus vulgaris* L.) grown in a greenhouse during fall and winter of Berlin, Germany.

Table 15 – Spectral composition of three LED light spectra and solar spectrum between 380 and 780 nm.

Table 16 – Effect of three light qualities on the chemical composition of 24 identified essential oil compounds, essential oil content and yield of *Mentha x piperita* var. piperita cv. Multimentha.

Table 17 – Essential oil composition of *Mentha x piperita* L. var. piperita cv. Multimentha detected under field conditions at Julius Kühn Institute, Berlin, Germany.

Table 18 – Spectral compositions of the white broad-band LED light spectra.

Table 19 – Summarized plant characteristics of four basil cultivars grown under two LED light intensities over time (including light intensities at plant canopy levels).

Table 20 – Relative abundance of major volatile organic compounds identified in the leaves of *O. basilicum* L. cv. ‘Anise’ as affected by LED light intensity treatments over time.

Table 21 – Relative abundance of major volatile organic compounds identified in the leaves of *O. basilicum* L. cv. ‘Thai Magic’ as affected by LED light intensity treatments over time.

Table 22 – Relative abundance of major volatile organic compounds identified in the leaves of *O. basilicum* L. cv. ‘Cinnamon’ as affected by LED light intensity treatments over time.

Table 23 – Relative abundance of major volatile organic compounds identified in the leaves of *O. basilicum* L. cv. ‘Dark Opal’ as affected by LED light intensity treatments over time.

Table 24 – Correlation between basil’s complex VOC profiles over time and their morphological stage.

Table 25 – Biomass efficacy of four *Ocimum basilicum* L. cultivars grown under two different light intensity treatments.

Table 26 – Energy consumption and biomass at marketability of four *Ocimum basilicum* L. cultivars grown under two different light intensities.

Table 27 – Achievable crop cycles, biomass production, and its energy consumption per year when grown until marketability.

Table 28 – Photon efficiency, biomass and essential oil efficacy of LED lighting fixtures for the production of peppermint at equal photon flux density (PPFD) in the vertical cultivation system.

Table 29 – Selection of essential oil constituents used as food flavorings, the foods in which their presence is restricted and the set maximum levels.

Table 30 – Volatile organic compound (VOC) content and relative abundance of major volatile organic compounds identified in the leaves of *O. basilicum* L. cv. 'Dark Opal' as affected by three different LED light treatments 35 days after sowing.